Canadian Journal of Research

Issued by The National Research Council of Canada

VOLUME 5 AUGUST, 1931 NUMBER 2

LONGITUDINAL AND RADIAL VIBRATIONS IN LIQUIDS CONTAINED IN CYLINDRICAL TUBES[1]

By George S. Field[2]

Abstract

I. The boundary conditions at the tube wall are considered, taking into account the natural frequency of the wall itself. An expression is derived for the radial displacement of the wall due to the excess pressure acting in the liquid. II. A formula is developed for the resonant frequencies of radial vibration in the cylinder of liquid. For tubes of ordinary size these lie well up in the ultrasonic frequencies. III. The character of a longitudinal sound wave in tubes of liquid is analyzed. Selective absorption of the longitudinal vibration is found to occur at the natural frequency of the radial vibration of the column of liquid. Examination of the expression for particle velocities reveals that the vibration for low frequencies is of a different type from that for high.

Introduction

The following theoretical investigation is an attempt to explain certain experimental results which were observed by Boyle and Froman (1) while they were studying the propagation of sound through liquids contained in cylindrical tubes.

Although existing theory has explained fairly satisfactorily the diminution in wave velocity almost invariably observed by previous experimenters, an increased velocity such as was noted by Boyle and Froman seems to have been unaccounted for. In the following pages it will be shown that this phenomenon is due to selective absorption, caused by the energy of the longitudinal wave being absorbed by a radial vibration occurring at the natural frequency of this vibration.

In this discussion the case considered is that of an infinite cylinder of liquid. The viscosity of the liquid is neglected, and the walls of the tube are considered to be thin, though the effect of a thicker tube wall is discussed for approximate boundary conditions.

[1] *Manuscript received May 27, 1931.*
Contribution from the National Research Laboratories, Ottawa. Read before Section III of the Royal Society of Canada in May, 1931.

[2] *Junior Research Physicist, National Research Laboratories, Ottawa.*

Part I. Boundary Conditions at Wall of Tube

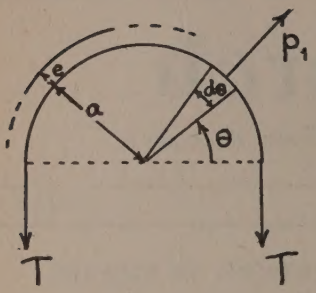

FIG. 1. *Half-section of tube wall showing pressure p_1 balanced by tension T.*

In Fig. 1, suppose the radius (a) of the tube increases by an amount e, on account of the excess pressure (δp) in the liquid at the boundary. Let the pressure necessary to produce the increase in radius be denoted by p_1.

If we consider a section of the tube, one unit long, we see that the pressure on one-half the tube is balanced by the tension (T) in the fibres of the tube wall (see Fig. 1).

Or, we have, $2T = 2\int_0^{\frac{\pi}{2}} a\, d\theta\, p_1 \sin\theta = 2ap_1$

Whence $T = ap_1$

Now the increase in circumference due to a tension T is given by, $\epsilon = \dfrac{Tl}{AE}$

Where T = force acting; l = original length $= 2\pi a$; A = cross-sectional area = $h \times 1$, where h = thickness of wall. E = Young's modulus.

In this relation, Young's modulus should be corrected to compensate for the fact that the stresses in the tube wall are rapidly alternating, so that the deformation of the wall does not quite attain the statical value corresponding to the instantaneous distribution of pressure in the liquid. Korteweg (3) suggests the following value be used,

$$E^1 = E\left(1 - \frac{5h}{6a}\right)$$

Our equation then becomes,

$$\epsilon = \frac{Tl}{AE^1}$$

Substitute $T = ap_1$, and $\epsilon = \dfrac{ap_1 \cdot 2\pi a}{hE^1} = \dfrac{2\pi a^2 p_1}{hE^1}$

Increase in radius $= e = \dfrac{\epsilon}{2\pi}$

$$= \frac{a^2 p_1}{hE^1}$$

We now have the relation, $e = \dfrac{a^2 p_1}{hE^1}$ or $p_1 = \dfrac{ehE^1}{a^2}$

Of the excess pressure at the boundary (δp), part is used up in producing the extension e, and part is used up in producing a change in momentum of the tube wall $\left(= m\dfrac{d^2e}{dt^2}\right)$ and also in opposing friction $\left(= r\dfrac{de}{dt}\right)$. In these relations m = mass of wall per unit area, corresponding to δp = force per unit area, and r = a constant of proportionality relating the frictional force opposing the

motion of the wall to the velocity of the latter. We here assume, as is usual, that the frictional force is directly proportional to the velocity.

Let ρ_1 = density of the material of the wall.

Then mass per unit area $(=m) = \rho_1 h$.

We now have the following equation, $\delta p = p_1 + m\frac{d^2e}{dt^2} + r\frac{de}{dt}$

$$\text{or, } \delta p = \frac{hE^1}{a^2}e + \rho_1 h\frac{d^2e}{dt^2} + r\frac{de}{dt} \tag{1}$$

But $\delta p = \rho\dot{\phi}$ (4)

Where ϕ = velocity potential existing for liquid, and $\dot{\phi} = \frac{\partial\phi}{\partial t}$

Hence, from equation (1), $\rho\dot{\phi} = \frac{hE^1}{a^2}e + \rho_1 h\frac{d^2e}{dt^2} + r\frac{de}{dt}$

$$\text{or, } \frac{d^2e}{dt^2} + \frac{r}{\rho_1 h}\frac{de}{dt} + \frac{E^1}{\rho_1 a^2}e = \frac{\rho}{\rho_1 h}\dot{\phi} \tag{2}$$

The general solution of equation (2) is,

$$e = \epsilon^{-\alpha t}\left[C\cos p_0 t + D\sin p_0 t\right] + \frac{\rho\dot{\phi}}{\rho_1 h[\beta^2 - \omega^2 + 2i\alpha\omega]} \tag{3}$$

Where, ϵ = base of Napierian logarithms; C and D are constants; $p_0 = \sqrt{\beta^2 - \alpha^2}$; $\beta^2 = \frac{E^1}{\rho_1 a^2}$; $2\alpha = \frac{r}{\rho_1 h}$; $\omega = 2\pi \times$ frequency.

Equation (3) represents the way the wall of the tube moves in and out with time. The first part of e is a transient solution, since the damping factor $(\epsilon^{-\alpha t})$ will soon damp out this part of the vibration.

Note that $\frac{p_0}{2\pi}$ is the frequency of the resonant vibration of the tube wall, and, $p_0 = \sqrt{\beta^2 - \alpha^2}$: α will be very small compared with β, and hence

$$p_0 \doteq \sqrt{\beta^2} = \beta = \frac{1}{a}\sqrt{\frac{E^1}{\rho_1}} \tag{4}$$

Equation (4) is the same as is given by Lamb*.

The steady state value of e is the one we need for our boundary conditions, *i.e.*,

$$e = \frac{\rho\dot{\phi}}{\rho_1 h[\beta^2 - \omega^2 + 2i\alpha\omega]}$$

But $\beta^2 = p_0^2 + \alpha^2$

Hence
$$e = \frac{\rho\dot{\phi}}{\rho_1 h[p_0^2 - \omega^2 + \alpha^2 + 2i\alpha\omega]} \tag{5}$$

Note that when the period of the pressure variations corresponds to that of the natural frequency of the tube wall, the displacement (e) becomes very large, limited only by the resistance factor $(\alpha^2 + 2i\alpha\omega)$.

**Reference (4, p. 138); for the case, $s = 0$.*

Part II. Resonant Frequencies of Radial Vibration in a Cylinder of Liquid

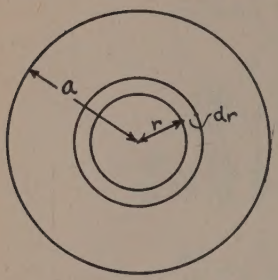

FIG. 2. *Section of cylinder of liquid.*

The method of developing the differential equation is similar to that adopted by Crandall (2, p. 87) in discussing *plane* waves of sound.

Consider a portion of the cylinder of unit length, radius a.

Take an annulus, width dr, at a distance r from the axis.

The flow into the annular ring is given by, $\rho\xi 2\pi r\, dt$

Where ρ = density of the liquid and ξ = particle velocity.

The flow out of the ring is, $2\pi\, dt \left\{ r\rho\xi + \frac{\partial}{\partial r}(r\rho\xi)\, dr \right\}$

Hence net flow in during time $dt = -2\pi\, dt \frac{\partial}{\partial r}(r\rho\xi) dr$

Also increase in fluid contained $= 2\pi r dr \frac{\partial \rho}{\partial t} \cdot dt$

And we have finally, $2\pi\, dr \cdot dt \frac{\partial}{\partial r}(r\rho\xi) dr + 2\pi r\, dr\, dt \frac{\partial \rho}{\partial t} = 0$

Or
$$r\frac{\partial \rho}{\partial t} + \frac{\partial}{\partial r}(r\rho\xi) = 0 \tag{6}$$

Which is the equation of continuity.

Consider a piece of the annular ring, of unit thickness, width dr one way and $rd\theta$ the other.

The force out due to harmonic pressure (p) is,

$$p \cdot r d\theta + \left[2 \frac{p + p + \frac{\partial p}{\partial r} \cdot dr}{2} \cdot \sin\frac{d\theta}{2} \right] dr$$
$$= p\, r\, d\theta + p\, dr\, d\theta$$

The force in $= \left(p + \frac{\partial p}{\partial r} \cdot dr \right) \left(r + dr \right) d\theta$

$$= p\, r\, d\theta + p\, dr\, d\theta + r\frac{\partial p}{\partial r} \cdot dr \cdot d\theta$$

Net force out $= -r\frac{\partial p}{\partial r} \cdot dr \cdot d\theta$

Rate of change of momentum $= \rho\, r d\theta\, dr \frac{\partial \xi}{\partial t}$

Hence we have, $r\frac{\partial p}{\partial r} + \rho r \frac{\partial \xi}{\partial t} = 0$

or,
$$\frac{\partial p}{\partial r} + \rho \frac{\partial \xi}{\partial t} = 0 \tag{7}$$

Which is the equation of motion.

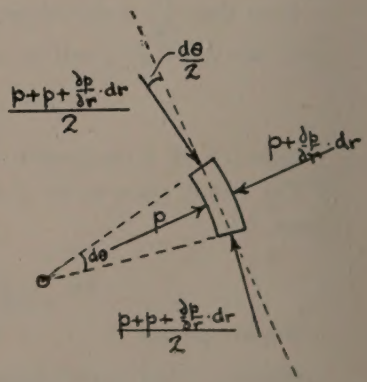

FIG. 3. *Element of liquid showing pressures acting.*

In Equation (6) substitute $\rho=\rho_0(1+s)$, where $s=$condensation.
In Equation (7) substitute $p=Ks$, where $K=$coefficient of cubic elasticity.
Neglect $s\xi$ compared with ξ (2, p. 87).

Then (6) leads to, $$r\frac{\partial s}{\partial t}+r\frac{\partial \xi}{\partial r}+\xi=0 \tag{8}$$

(7) leads to, $$K\frac{\partial s}{\partial r}+\rho\frac{\partial \xi}{\partial t}=0 \tag{9}$$

Differentiate (8) with respect to r.

$$\frac{\partial^2 s}{\partial r\cdot\partial t}+\frac{\partial^2\xi}{\partial r^2}+\frac{1}{r}\frac{\partial \xi}{\partial r}-\frac{\xi}{r^2}=0 \tag{10}$$

Differentiate (9) with respect to t.

$$K\frac{\partial^2 s}{\partial r\cdot\partial t}+\rho\frac{\partial^2\xi}{\partial t^2}=0 \tag{11}$$

Compare (10) and (11) and get,

$$\frac{\partial^2\xi}{\partial t^2}-\frac{K}{\rho}\left(\frac{\partial^2\xi}{\partial r^2}+\frac{1}{r}\frac{\partial \xi}{\partial r}-\frac{\xi}{r^2}\right)=0 \tag{12}$$

Suppose, $\xi=f(r)e^{ipt}$

Then, $\dfrac{\partial^2\xi}{\partial t^2}=-p^2 f(r)\,e^{ipt}$ $\qquad \dfrac{\partial \xi}{\partial r}=f'(r)\,e^{ipt}$

$$\frac{\partial^2\xi}{\partial r^2}=f''(r)\,e^{ipt}$$

Substitute in (12),

$$-p^2 f(r)-\frac{K}{\rho}\left\{\frac{\partial^2 f}{\partial r^2}+\frac{1}{r}\frac{\partial f}{\partial r}-\frac{f}{r^2}\right\}=0 \tag{13}$$

Let $\dfrac{K}{\rho}=c^2$

and we get, $$r^2\frac{\partial^2 f}{\partial r^2}+r\frac{\partial f}{\partial r}+(k^2r^2-1)\,f=0 \tag{14}$$

where $$k^2=\frac{p^2}{c^2} \tag{15}$$

The solution of (14) is $f=AJ_1(kr)+BK_1(kr)$ (16)
Where $J_1(kr)=$Bessel function of the first kind,
$K_1(kr)=$Bessel function of the second kind.
Now $K_1(kr)=\infty$ for $r=0$, and therefore this solution is not admissible.
Hence full solution of Equation (12) is,

$$\xi=AJ_1(kr)e^{ipt} \tag{17}$$

Approximate boundary conditions

(a) At $r=0$, $\xi=0$. This is satisfied by Equation (17). (b) At $r=a+t$, $\xi=0$. That is, the displacement (ξ) will not quite be zero at $r=a$, due to the non-rigidity of the wall. The effect will be the same, however, as if the displacement were zero at a point just greater than $r=a$, *i.e.*, at $r=a+t$. In other words, t is a wall correction. We here assume that t, which is related to e (Part I), is constant with frequency. This simplifies the results, and the more exact boundary condition at the wall will be discussed later.

Using condition (*b*), we have,

$$\xi_{r=a+t} = \int \dot{\xi}_{r=a+t}\, dt = \frac{A}{ip} J_1\{k(a+t)\} = 0$$

The first root for this function occurs at $k(a+t) = 1.22\pi$

$$k = \frac{p}{c} = \frac{2\pi n}{c} \quad \text{where } n = \text{frequency.}$$

$$n = \frac{1.22\pi \times c}{2\pi(a+t)} = \frac{1.22c}{2(a+t)}$$

$a+t$ might be called the "effective radius".

Then $2(a+t) =$ "effective diameter" $= d_0$

And
$$n = \frac{1.22c}{d_0} \tag{18}$$

This is the fundamental mode of radial vibration. The higher modes will have frequencies given by the higher roots of the Bessel function. It will be noted that n is inversely proportional to the diameter of the tube.

Effect of Changing Wall Thickness

Having in mind the results obtained by applying approximate boundary conditions, we can deduce the general effect on the natural frequencies produced by changing the thickness of the tube wall.

Suppose we keep a constant, but change the thickness of the wall.

We have $n = K.\frac{1}{a+t}$ where $K =$ a constant $= 1.22c$.

As the wall becomes more rigid, due to the increasing thickness, $\xi \rightarrow 0$ at $r = a$.

And as $\xi \rightarrow 0$ at $r = a$, $t \rightarrow 0$.

For an absolutely rigid wall, $n_r = \frac{K}{a}$, where $n_r =$ frequency for rigid wall, and $t = 0$.

In all practical cases, $t \neq 0$, though it may approach it very closely for a very thick wall. We note, however, that for thicker walls t is smaller, and hence n is greater than it is for thinner walls. That is, the frequencies of resonance are less for less rigid walls and greater for more rigid walls.

Exact Boundary Conditions

(a) At $r = 0$, $\xi = 0$. Satisfied by Equation (17). (b) At $r = a$, $\xi = e$, where $\xi =$ displacement of the fluid at the boundary; $e =$ change in radius of the tube wall, due to the harmonic pressure acting (see Part 1).

If ϕ is the velocity potential existing for the vibration in the liquid, we have,

$$-\frac{\partial \phi}{\partial r} = \xi^*$$

$$\text{or } \phi = -\int \xi dr$$

$$\dot{\phi} = \frac{\partial}{\partial t}\phi = -\frac{\partial}{\partial t}\int \xi dr = -\frac{\partial}{\partial t}\int A J_1(kr) e^{ipt} dr$$

$$\dot{\phi} = \frac{ip}{k} A J_0(kr) e^{ipt} \tag{19}$$

**Reference (2, p. 114)*

Since $$\frac{\partial}{\partial r} J_0(kr) = -kJ_1(kr)$$

Now $\xi = \frac{A}{ip} J_1(kr)e^{ipt}$, found by integrating Equation (17) with respect to t.

At $r=a$, $\xi=e$.

Hence $$\frac{A}{ip} J_1(ka)e^{ipt} = \frac{ipA\rho J_0(ka)e^{ipt}}{k\rho_1 h[p_0^2 - p^2 + \alpha^2 + 2i\alpha p]}$$

$$\text{or } \frac{J_1(ka)}{J_0(ka)} = \frac{-p^2\rho}{k\rho_1 h[p_0^2 - p^2 + \alpha^2 + 2i\alpha p]} \tag{20}$$

The R.H.S. (right hand side) of this equation would approach ∞ at $p \longrightarrow p_0$, were it not for the resistance terms, $\alpha^2 + 2i\alpha p$.

Taking these into consideration, and neglecting $p_0^2 - p^2$, the R.H.S. would be,

$$\frac{-p^2\rho}{k\rho_1 h(\alpha^2 + 2i\alpha p)}$$

of which the absolute value is, $\frac{-p^2\rho}{k\rho_1 h}\left(\frac{\sqrt{\alpha^4 + 4\alpha^2 p^2}}{\alpha^4 + 4\alpha^2 p^2}\right) \doteq \frac{-p^2\rho}{k\rho_1 h} \cdot \frac{1}{2\alpha p}$

$$= -\frac{p\rho}{2\alpha k\rho_1 h}, \text{ since } \alpha^4 \text{ is very small compared with } \alpha^2 p.$$

Now $k = \frac{p}{c}$

Hence at $p=p_0$, R.H.S. $\doteq -\frac{p\rho c}{2\alpha\rho_1 hp} = -\frac{\rho c}{2\alpha\rho_1 h}$.

Now the numerator of this fraction is very much greater than the denominator. Hence the R.H.S. is still very great when $p \longrightarrow p_0$, though not $\longrightarrow \infty$.

Since the curve of $\frac{J_1(x)}{J_0(x)}$ against x is very steep at the point where $\frac{J_1(x)}{J_0(x)} \longrightarrow \infty$, it does not change the value of x by any appreciable amount whether we let the R.H.S. of Equation (20) $= \infty$ or only a large number (say >50).

Hence at $p=p_0$, we can neglect the part of the denominator of the R.H.S. of Equation (20) represented by the terms, $\alpha^2 + 2i\alpha p$.

It is only in the neighborhood of $p=p_0$ that the terms $\alpha^2 + 2i\alpha p$ become of importance compared with $p_0^2 - p^2$.

We have shown that the value of x (ka in our equation) is not affected by changes in the denominator when the denominator is small (*i.e.*, in the neighborhood of $p=p_0$). Since only in this neighborhood do the resistance terms become important, and since here they make no appreciable difference, we can neglect these terms for all cases, and have only,

$$\text{R.H.S.} = \frac{-p^2\rho}{k\rho_1 h(p_0^2 - p^2)}$$

Equation (20) now becomes

$$\frac{J_1(ka)}{J_0(ka)} = \frac{-p^2\rho}{k\rho_1 h(p_0^2 - p^2)} = \frac{-p^2\rho}{k\rho_1 h\left(\frac{E'}{\rho_1 a^2} - p^2\right)} = \frac{-p^2\rho}{k\left(\frac{E'h}{a^2} - p^2\rho_1 h\right)} \tag{21}$$

But $k = \frac{p}{c}$ or $p = kc$

Therefore,

$$\text{R.H.S.} = \frac{-k^2c^2\rho}{k\left(\frac{E^1h}{a^2} - k^2c^2\rho_1 h\right)} = \frac{-(ka)c^2a\rho}{h[E^1 - k^2a^2c^2\rho_1]}$$

Let $ka = x$. Then for Equation (21) we have,

$$\frac{J_1(x)}{J_0(x)} = \frac{-xac^2\rho}{h[E^1 - x^2c^2\rho_1]} \tag{22}$$

From Equation (22) we can determine x, which in turn determines the resonant frequency for radial vibrations in the tube, by the following relation,—

$$ka = \frac{p_0 a}{c} = x \qquad \text{or} \qquad p_0 = \frac{cx}{a}$$

$$n = \frac{p_0}{2\pi} = \frac{c_1 x}{2\pi a} \tag{23}$$

Remarks

Equation (23) is, $n = \dfrac{\frac{x}{\pi} \cdot c}{2a}$

Compare this with the result obtained by approximating the boundary conditions,

$$n = \frac{1.22c}{2(a+t)} \tag{18}$$

We now have a variable $\frac{x}{\pi}$ compared with the constant 1.22; and we use the real diameter $2a$ instead of the "effective diameter" $\{d_0 = 2(a+t)\}$, but the form of the equation is unaltered.

The reason for the variable $\frac{x}{\pi}$ is that the resonant frequency (n_0) changes with changing boundary conditions (varying t), and we saw from a consideration of the exact boundary conditions that these conditions are dependent upon frequency.

Part III. Transmission of Sound in Liquids Contained in Cylindrical Tubes. Vibrations Both Longitudinally and Radially

Consider the velocity potential, ϕ, which exists for all cases of fluid motion when no circulation exists. This is obviously the case in sound.

We have the expression, $\ddot{\phi} - c^2\nabla^2\phi = 0$* (24)

Where $c = \sqrt{\frac{K}{\rho}}$ = velocity in the unconfined liquid.

In cylindrical co-ordinates, if ϕ is independent of θ, which is true in purely longitudinal and radial vibrations, we have,

$$\nabla^2\theta = \frac{1}{r}\frac{\partial}{\partial r}\left(r\frac{\partial\phi}{\partial r}\right) + \frac{\partial^2\phi}{dz^2} \tag{25}$$

Substitute in (24),

$$\frac{\partial^2\phi}{\partial t^2} - c^2\left(\frac{\partial^2\phi}{\partial r^2} + \frac{1}{r}\frac{\partial\phi}{\partial r} + \frac{\partial^2\phi}{\partial z^2}\right) = 0 \tag{26}$$

**Reference (2) p. 116, Equation 151a.*

Suppose ϕ is of the form, $\phi = A\,f(r)\,e^{i\omega\left(t-\frac{z}{c_1}\right)}$ where c_1 = phase velocity.

Substitute in (26),

$$-\omega^2 f - c^2\left(\frac{\partial^2 f}{\partial r^2} + \frac{1}{r}\frac{\partial f}{\partial r} - \frac{\omega^2}{c_1^2} f\right) = 0$$

$$\text{or,}\quad \frac{\partial^2 f}{\partial r^2} + \frac{1}{r}\frac{\partial f}{\partial r} + \omega^2\left(\frac{1}{c^2} - \frac{1}{c_1^2}\right) f = 0 \tag{27}$$

Write as, $$\frac{\partial^2 f}{\partial r_2} + \frac{1}{r}\frac{\partial f}{\partial r} + k^2 f = 0 \tag{28}$$

Where, $$k^2 = \omega^2\left(\frac{1}{c^2} - \frac{1}{c_1^2}\right) \tag{29}$$

For k to be real, $\frac{1}{c^2} > \frac{1}{c_1^2}$ or $c_1 > c$. If $c_1 < c$, $\frac{1}{c_1^2} > \frac{1}{c^2}$.

And $k^2 = -\omega^2\left(\frac{1}{c_1^2} - \frac{1}{c^2}\right)$

Or $k = i\alpha$, where $\alpha = \omega\sqrt{\frac{1}{c_1^2} - \frac{1}{c^2}}$ (30)

Hence we have two cases, (A) k real, (B) k imaginary $= i\alpha$.

Case (A)

If k be real, the solution of (28) is, $f = A J_0(kr)$

And hence, $$\phi = A J_0(kr) e^{i\omega\left(t-\frac{z}{c_1}\right)} \tag{31}$$

Let $\dot{\zeta}$ = particle velocity in r direction.
$\dot{\xi}$ = particle velocity in z direction.

$$\dot{\zeta} = -\frac{\partial \phi}{\partial r} = +kA J_1(kr)\, e^{i\omega\left(t-\frac{z}{c_1}\right)} \tag{32}$$

And $$\zeta = \int \dot{\zeta}\, dt = \frac{Ak}{i\omega} J_1(kr)\, e^{i\omega\left(t-\frac{z}{c_1}\right)} \tag{33}$$

Approximate Boundary Conditions for Case (A)

$\zeta = 0$ at $r = 0$, and at $r = a + t$, where a = radius of cylinder, $a + t$ = "effective radius".

These conditions are satisfied if, $J_1\{k(a+t)\} = 0$

$$J_1\{k(a+t)\} = 0, \text{ when } k(a+t) = 1.22\pi \text{ (1st mode) or } k = \frac{1.22\pi}{a+t}$$

But $k = \omega\sqrt{\frac{1}{c^2} - \frac{1}{c_1^2}}$, and $\omega = 2\pi n$, where n = frequency.

Therefore, $$\frac{1}{c^2} - \frac{1}{c_1^2} = \frac{(1.22)^2\pi^2}{(a+t)^2 4\pi^2 n^2} \tag{34}$$

Which leads to, $$c_1 = \frac{nc}{\sqrt{n^2 - n_0^2}} \tag{35}$$

Where $n_0 = \dfrac{1.22c}{2(a+t)}$ = fundamental mode of the radial vibration [see Equation (18)].

The form of the curve resulting from Equation (35) is shown in Fig. 4.

Case (B)

k imaginary ($=i\alpha$).

Equation (28) is now,

$$\frac{\partial^2 f}{\partial r^2} + \frac{1}{r}\frac{\partial f}{\partial r} - \alpha^2 f = 0 \tag{36}$$

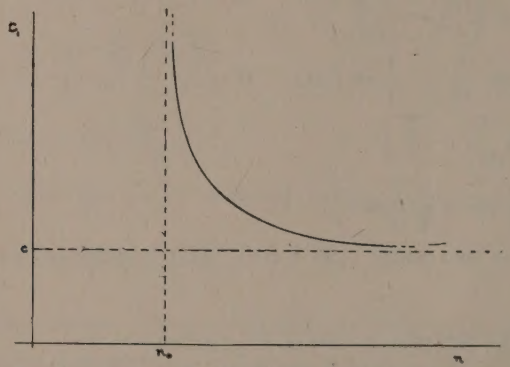

FIG. 4. *Curve of velocity against frequency after first absorption band, using approximate boundary conditions.*

Of which the solution is, $f = I_0(\alpha r)$

Where $I_0(\alpha r) = J_0(i\alpha r) = J_0(kr)$

Hence, $$\phi = A I_0(\alpha r) e^{i\omega\left(t - \frac{z}{c_1}\right)} \tag{37}$$

$$\zeta = -\frac{\partial \phi}{\partial r} = -\alpha I_1(\alpha r) A e^{i\omega\left(t - \frac{z}{c_1}\right)} \tag{38}$$

$$\zeta = -\int \frac{\partial \phi}{\partial r}\cdot dt = \frac{-\alpha}{i\omega} I_1(\alpha r) A e^{i\omega\left(t - \frac{z}{c_1}\right)} \tag{39}$$

Approximate Boundary Conditions for Case (B)

$\zeta = 0$ at $r = 0$ and at $r = a+t$.

Now $I_1(\alpha r) = 0$ for $\alpha r = 0$ and *for no other value* of αr. $\alpha r = 0$ at $r = 0$.

$\alpha r \neq 0$ at $r = a+t$ unless $\alpha = 0$. *i.e.*, $\omega\sqrt{\dfrac{1}{c_1^2} - \dfrac{1}{c^2}} = 0$

$$\omega\sqrt{\frac{1}{c_1^2} - \frac{1}{c^2}} = 0 \text{ if } c_1 = c.$$

This means that when the argument is imaginary, it is zero for all frequencies, and $c_1 = c$. In other words, we have the following situation.

For $n > n_0$, where n_0 is the absorbing frequency, the wave velocity is,

$$c_1 = \frac{cn}{\sqrt{n^2 - n_0^2}}$$

For $n < n_0$, the wave velocity is constant and given by, $c_1 = c$.

This is obviously only a first approximation, as a diminished wave velocity due to lateral expansion of the tube wall is not indicated anywhere in this solution.

Particle Velocities for Case (A) and Case (B)

Case (A) $n > n_0$

$$\xi = -\frac{\partial \phi}{\partial z} = \frac{+i\omega}{c_1} A J_0(kr) e^{i\omega\left(t - \frac{z}{c_1}\right)} \tag{40}$$

This becomes zero for $kr = 0.766\pi$, *i.e.*, for $r = \frac{0.766}{1.22}(a+t)$

And after that it reverses in sign. See Fig. 5.

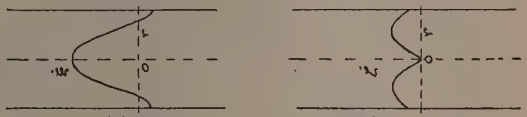

(a) (b)

FIG. 5. *Particle velocities after first absorption band. (a) Longitudinal velocity; (b) radial velocity.*

$$\zeta = -\frac{\partial \phi}{\partial r} = kA J_1(kr) e^{i\omega\left(t - \frac{z}{c_1}\right)} \tag{41}$$

Note that ξ is 90° out of phase with ζ, due to the factor $+i$ by which ξ is multiplied. For $n \to n_0$, $c_1 \to \infty$, and therefore,

$$\xi \left(= \frac{i\omega}{c_1} A J_0(kr) e^{i\omega\left(t - \frac{z}{c_1}\right)} \right) \to 0.$$

This means that for the frequency of radial resonance the wave is propagated with difficulty longitudinally (in the z-direction); that is, there is a great deal of absorption. Also note that the longitudinal wave is not plane.

Case (B)

$$\phi = A I_0(\alpha r) e^{i\omega\left(t - \frac{z}{c_1}\right)} \tag{37}$$

Here $\alpha = 0$, and since $I_0(0) = 1$, we have, $\phi = A e^{i\omega\left(t - \frac{z}{c_1}\right)}$

$$\xi = -\frac{\partial \phi}{\partial z} = \frac{i\omega}{c_1} A e^{i\omega\left(t - \frac{z}{c_1}\right)} \tag{42}$$

ξ is independent of r — it is a plane wave. This is an approximation, true only for low frequencies, as will be discussed later.

Also $$\zeta = -\frac{\partial \phi}{\partial r} = 0 \tag{43}$$

Exact Boundary Conditions Applied

Case (A) k real.

$$\phi = A J_0(kr) e^{i\omega\left(t - \frac{z}{c_1}\right)} \tag{31}$$

$$\zeta = kA J_1(kr) e^{i\omega\left(t - \frac{z}{c_1}\right)} \tag{32}$$

$$\zeta = \frac{Ak}{i\omega} J_1(kr) e^{i\omega\left(t - \frac{z}{c_1}\right)} \tag{33}$$

The conditions are,

(i) At $r=0$, $\zeta=0$; satisfied by Equation (33).

(ii) At $r=a$, $\zeta=e$.

Where $e = \dfrac{\rho\phi}{\rho_1 h[p_0^2 - \omega^2]}$ (5)

And in which expression we neglect terms involving the damping factor (α) for vibration in the tube wall.

Also, $$\phi = Ai\omega J_0(kr) e^{i\omega\left(t - \frac{z}{c_1}\right)} \tag{44}$$

Hence Condition (ii) leads to,

$$\frac{Ak}{i\omega} J_1(ka) e^{i\omega\left(t - \frac{z}{c_1}\right)} = \frac{\rho Ai\omega J_0(ka)\, e^{i\omega\left(t - \frac{z}{c_1}\right)}}{\rho_1 h[p_0^2 - \omega^2]} \tag{45}$$

or, $$\frac{J_1(ka)}{J_0(ka)} = \frac{-\rho\omega^2}{k\rho_1 h[p_0^2 - \omega^2]} \tag{46}$$

Recall that $p_0^2 = \dfrac{E^1}{\rho_1} \cdot \dfrac{1}{a^2}$ (4)

We now have,

$$\text{R.H.S.} = \frac{-\rho\omega^2}{k\rho_1 h\left[\frac{E^1}{\rho_1 a^2} - \omega^2\right]} = \frac{-a}{kah\left[\frac{E^1}{a^2\omega^2\rho} - \frac{\rho_1}{\rho}\right]}$$

From (46) we then get, writing $ka = x$,

$$\frac{J_1(x)}{J_0(x)} = -\frac{a}{h} \frac{1}{x\left[\frac{E^1}{a^2\omega^2\rho} - \frac{\rho_1}{\rho}\right]} \tag{47}$$

Or, $$x\frac{J_1(x)}{J_0(x)} = \frac{-\frac{a}{h}}{\frac{E^1}{a^2\omega^2\rho} - \frac{\rho_1}{\rho}} \tag{48}$$

Now, $$x = ka = a\omega\sqrt{\frac{1}{c^2} - \frac{1}{c_1^2}}$$

And hence, $$c_1^2 = \frac{c^2\omega^2}{\omega^2 - \frac{c^2x^2}{a^2}} \tag{49}$$

Or, since $\omega = 2\pi n$,

$$c_1^2 = \frac{n^2c^2}{n^2 - \frac{x^2c^2}{4\pi^2a^2}} \tag{50}$$

Let $$n_x = \frac{\frac{x}{\pi} \cdot c}{2a} \tag{51}$$

Then, $$c_1 = \frac{nc}{\sqrt{n^2 - n_x^2}} \tag{52}$$

By solving (48) we obtain x, and from (52) we then obtain c_1.

Notice the resemblance between the results obtained for the approximate boundary conditions and those obtained for the exact boundary conditions. The difference is that in the equation for n_x we have a variable $\frac{x}{\pi}$ instead of the constant (1.22) previously obtained for n_0. This occurs because the change in radius of the tube (e) is not constant, but varies with frequency; and therefore the resonant frequency (n_x) for radial vibrations in the liquid also changes.

Case (*B*) k imaginary.

$$\phi = AI_0(\alpha r)e^{i\omega\left(t-\frac{z}{c^1}\right)} \tag{37}$$

$$\xi = -\frac{\partial\phi}{\partial r} = -\alpha I_1(\alpha r)Ae^{i\omega\left(t-\frac{z}{c^1}\right)} \tag{53}$$

$$\zeta = \int \xi dt = -\frac{\alpha}{i\omega} I_1(\alpha r)Ae^{i\omega\left(t-\frac{z}{c^1}\right)} \tag{54}$$

$$\dot{\phi} = i\omega AI_0(\alpha r)e^{i\omega\left(t-\frac{z}{c^1}\right)} \tag{55}$$

The conditions are,

(i) At $r=0$, $\zeta=0$; satisfied by Equation (54).

(ii) At $r=a$, $\zeta=e$, where e is as defined under Case (*A*).

From Condition (ii) we have,

$$-\frac{\alpha}{i\omega} I_1(\alpha a)Ae^{i\omega\left(t-\frac{z}{c^1}\right)} = \frac{\rho i\omega A I_0(\alpha a)e^{i\omega\left(t-\frac{z}{c^1}\right)}}{\rho_1 h[p_0^2-\omega^2]} \tag{56}$$

Or,
$$\alpha\frac{I_1(\alpha a)}{I_0(\alpha a)} = \frac{\rho\omega^2}{\rho_1 h]p_0^2-\omega^2]} \tag{57}$$

Using a somewhat different method of derivation, Korteweg (3) arrived at a result equivalent to Equation (57), and from it obtained his expression for phase velocity. He seems, however, not to have considered the possibility of the argument becoming real ($c_1 > c$), and so missed the second solution represented by Case *A*.

Now
$$p_0^2 = \frac{E^1}{\rho_1 a^2}$$

Hence we have, from (57),

$$\frac{\alpha a I_1(\alpha a)}{I_0(\alpha a)} = \frac{a\rho\omega^2}{h\rho_1\left[\frac{E^1}{\rho_1 a^2}-\omega^2\right]} = \frac{\frac{a}{h}}{\frac{E^1}{a^2\omega^2\rho}-\frac{\rho_1}{\rho}} \tag{58}$$

Or,
$$x^1\frac{I_1(x^1)}{I_0(x^1)} = \frac{\frac{a}{h}}{\frac{E^1}{a^2\omega^2\rho}-\frac{\rho_1}{\rho}} \tag{59}$$

Now,
$$x^1 = \alpha a = a\omega\sqrt{\frac{1}{c_1^2}-\frac{1}{c^2}} \tag{30a}$$

And,
$$\omega = 2\pi n$$

Therefore,
$$c_1 = \frac{cn}{\sqrt{n^2+n_{x^1}^2}} \tag{60}$$

Where,
$$n_{x^1} = \frac{\frac{x^1}{\pi}\cdot c}{2a} \tag{61}$$

Equation (59) is true for all values of ω and x^1, providing x^1 exists and $c_1 < c$, and it gives us an equation for determining x^1 and hence c_1.

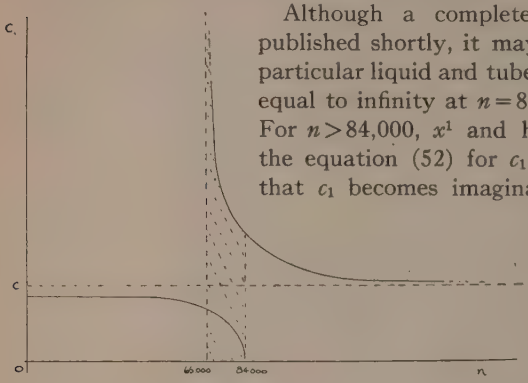

FIG. 6. *Complete velocity-frequency curve for a particular case where the absorbing frequency equals 65000.*

Although a complete experimental paper will be published shortly, it may be mentioned here that for a particular liquid and tube, Case *B* shows that x^1 becomes equal to infinity at $n = 84{,}000$, and at this point $c_1 = 0$. For $n > 84{,}000$, x^1 and hence c_1 are imaginary. From the equation (52) for c_1 in Case *A*, however, we find that c_1 becomes imaginary for $n < 65{,}000$. Hence we see that there is a range (for frequencies between 65,000 and 84,000) where both types of vibration tend to exist. In this range, therefore, both vibrations will be unstable and it will be extremely difficult to measure wave velocities for these frequencies.

The theoretical velocity-frequency curve is shown in Fig. 6. The theoretical frequency of radial resonance for the case mentioned is found from Equations 22 and 23 to be 65,000 cycles. The shaded area shows the region where vibrations are unstable.

Approximation for Low Frequencies

For low frequencies we are obviously dealing with Case *B*.

We had,
$$\alpha a = a\omega\sqrt{\frac{1}{c_1^2} - \frac{1}{c^2}} = \frac{a\omega}{c_1}\sqrt{1 - \frac{c_1^2}{c^2}} \tag{30a}$$

Or,
$$\alpha a = \frac{2\pi a}{\lambda}\sqrt{1 - \frac{c_1^2}{c^2}} \quad \text{where } \lambda = \text{wave-length.}$$

If the frequency be low, $\frac{2\pi a}{\lambda}$ is a small fraction, and we can develop $I_0(\alpha a)$ and $I_1(\alpha a)$ by using only two terms of the series expansion, *i.e.*,

$$I_0(\alpha a) \doteq 1 + \frac{\alpha^2 a^2}{4} = 1 + \frac{x^{1^2}}{4} \tag{62}$$

$$I_1(\alpha a) \doteq \frac{\alpha a}{2}\left(1 + \frac{\alpha^2 a^2}{8}\right) = \frac{x^1}{2}\left(1 + \frac{x^{1^2}}{8}\right) \tag{63}$$

Substituting (62) and (63) in (59), we get,

$$\frac{\frac{x^{1^2}}{2}\left(1 + \frac{x^{1^2}}{8}\right)}{1 + \frac{x^{1^2}}{4}} = \frac{\frac{a}{h}}{\frac{E^1}{a^2\omega^2\rho} - \frac{\rho_1}{\rho}} \tag{64}$$

Which gives, $$\frac{1+x'^2}{4} = \left(\frac{hE'}{2\rho a} - \frac{h\rho_1 a\omega^2}{2\rho}\right)\left(\frac{1}{c_1^2} - \frac{1}{c^2}\right)\left(1+\frac{x'^2}{8}\right) \quad (65)$$

Since $x'^2 = a^2\omega^2\left(\frac{1}{c_1^2} - \frac{1}{c^2}\right)$

But, $$1+\frac{x'^2}{4} \doteq \left(1+\frac{x'^2}{8}\right)^2, \text{ neglecting } \frac{x'^4}{64}$$

Hence we have,

$$1+\frac{x'^2}{8} = \frac{hE'}{2\rho a}\left(\frac{1}{c_1^2} - \frac{1}{c^2}\right)\left(1-\frac{\rho_1 a^2}{E'}\omega^2\right) \quad (66)$$

And finally,

$$c_1^2 = \left(1-\frac{c_1^2}{c^2}\right)\frac{h}{a}\left\{\frac{E'}{2\rho} - \frac{\rho_1 a^2 2\pi^2 n^2}{\rho} - \frac{\pi^2 a^2 n^2}{2}\right\} \quad (67)$$

For ordinary glass, $E' = 6.78\times10^{11}$.

If $n = 5{,}000$, $n^2 = 2.5\times10^7$.

Hence for low frequencies we neglect the second and third terms in the bracket on the R.H.S. of (67) compared with the first term.

Then, $$c_1^2 = \left(1-\frac{c_1^2}{c^2}\right)\frac{hE'}{2\rho a} \quad (68)$$

Or, $$c_1^2 = \frac{c^2}{\frac{2\rho a c^2}{hE'}+1} \quad (69)$$

And since, $c^2 = \frac{K}{\rho}$

We have, $$c_1^2 = \frac{c^2}{1+\frac{2Ka}{hE_1}} \quad (70)$$

This is the expression given by Korteweg (3) and Lamb (4, p. 177, Equation 12; 5, p. 1), as their simple formula.

Taking a particular liquid and tube (the same as previously mentioned), and working out wave velocities from Equations 59 and 60 and from Equation 70, we find the velocity in both cases equal to 1.14×10^5cm./sec. at 1000 cycles. Hence the accurate and approximate formulas give the same results (to at least 1%) at that frequency. At 20,000 cycles there is a slight deviation, as Equations 59 and 60 give a velocity of 1.13×10^5 cm./sec., while Equation 70 gives, of course, the same result as before (since it is independent of frequency). Hence the lateral movement of the tube wall causes a diminution in wave velocity which is practically constant for low frequencies.

An interesting result from the foregoing investigation is that above the absorbing frequency the phase velocity is always greater than the unconfined wave velocity, approaching it asymptotically as the frequency increases. For very high frequencies (very short wave-lengths), the velocity would be practically equal to the value in an infinite medium, however, which is what we should expect.

Particle Velocities

Case A $c_1 > c$

$$\phi = AJ_0(kr)e^{i\omega\left(t-\frac{z}{c_1}\right)} \tag{31}$$

Here the expression for ϕ is the same as was discussed under "Approximate Boundary Conditions". The particle velocities, therefore, are the same as were treated there. It should be added, however, that if we take for an example the same tube and liquid mentioned above, we find that the particle velocity (ξ) becomes zero at $r=a$ for a frequency of 84,000. As the frequency is then lowered to 65,000, the node of particle velocity moves nearer to the axis, with the result that in the centre of the tube the particle velocity (ξ) is 180° out of phase with that in the annulus between the node and the wall of the tube. The situation is then as is shown in Fig. 5. Above 84,000 cycles, ξ is not zero for any value of a.

Case B $c_1 < c$

$$\phi = AI_0(\alpha r)e^{i\omega\left(t-\frac{z}{c_1}\right)} \tag{37}$$

$$\xi = -\frac{\partial\phi}{\partial z} = +\frac{i\omega}{c_1}AI_0(\alpha r)e^{i\omega\left(t-\frac{z}{c_1}\right)} \tag{71}$$

$$\zeta = -\frac{\partial\phi}{\partial r} = -\alpha I_1(\alpha r)Ae^{i\omega\left(t-\frac{z}{c_1}\right)} \tag{53}$$

Fig. 7 shows the way the particle velocities vary with r, *i.e.*, distance from the axis of the tube.

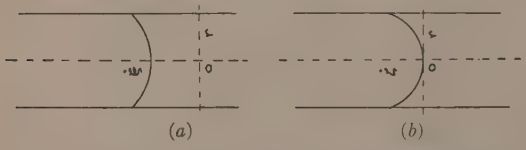

(*a*) (*b*)

FIG. 7. *Particle velocities before first absorption band.* (*a*) *Longitudinal velocity;* (*b*) *radial velocity.*

Note that ζ rises from zero at $r=0$ to a maximum at $r=a$. The particle velocity ξ is a minimum at $r=0$ and increases to a maximum at $r=a$.

For the liquid and tube previously mentioned, if ξ at $r=0$ be represented by unity, then at $r=a$, we have particle velocities as shown in Table I.

TABLE I

PARTICLE VELOCITIES AT WALL OF TUBE FOR VARIOUS FREQUENCIES

n	20000	30000	40000	50000	60000	70000
ξ	1.06	1.17	1.39	2.0	4.2	32.6

These values mean that for audible frequencies (below 20000) the longitudinal wave is sensibly plane, since the velocity at the side of the tube is approximately the same as at the centre. As the frequency approaches the absorbing frequency, however, the wave departs from its plane form; the particle velocity at the boundary tends to become much greater than at the centre.

In the foregoing, viscosity is not taken into account, which will of course tend to reduce the velocity at the wall of the tube, so that the wave will not depart from its plane form as much as would be indicated by our equations.

Since decreased phase velocity in the neighborhood of the absorbing frequency goes hand in hand with increased ξ at the wall of the tube, if ξ, due to viscosity, is prevented from increasing to some extent, then the phase velocity (c_1) will not be diminished as much as would be indicated by our equations.

Higher Modes of Radial Vibration

Although only the fundamental mode of radial vibration has been discussed so far, it is obvious that the higher modes, given by the higher roots of Equation (22), require some mention.

For the tube and liquid already considered, it is found that the second mode occurs at 102,000 cycles. Since the functions $I_0(x^1)$ and $I_1(x^1)$ are not periodic, the type of vibration represented by Case *B* cannot exist except in the range 0 to 84,000 cycles. Above the latter frequency, therefore, it is only Case *A* which need be considered.

If the second mode of radial vibration does not occur, the phase velocity will continue to approach the unconfined value asymptotically. If, however, it does occur, the velocity will be the same as above up to the resonant frequency. At that frequency, the occurrence of the second mode will tend to force it to a very high value again, as did the fundamental vibration at its resonant frequency. Above this frequency, the velocity will again approach the unconfined value, until the third mode is reached, when the situation will be repeated.

There is, however, a practical consideration which will tend to prevent the higher modes from occurring, except for comparatively low fundamentals. We saw, in considering particle velocities, that near the frequency of the fundamental mode the particle velocity (ξ) reversed in phase at a certain distance from the axis of the tube. For the second mode of vibration, there will be two reversals between $r=0$ and $r=a$. For the third mode, three reversals will occur, and so on. Each additional reversal of phase will cause the particles of liquid moving with opposite phase to become closer together. Viscosity will enter into the question, and it is to be expected that these nodes will have to be a certain minimum distance from each other.

Now, the narrower the tube the closer together will the particles moving with opposite phase have to be for a given number of reversals. That is, for a certain wide tube, the requisite minimum distance of one reversal from the other (node to node distance) will allow, say, three of these nodes to occur; in other words, three modes of radial vibration can exist when a longitudinal wave is propagated along the tube. Since these modes are inversely proportional to the diameter of the tube, and the tube is wide, the third mode may have a frequency no higher than the second or even the fundamental mode for a tube that is considerably narrower. With the narrow tube, then, it may be that only the first or second mode can occur, as higher modes would necessitate the nodes of ξ to be closer together than the minimum distance.

The foregoing paragraph may be summarized by saying that for any liquid there will be a maximum frequency above which resonant radial vibrations cannot occur, as viscosity will prevent particles very close together from moving with opposite phase.

Acknowledgment

The writer wishes to thank Dr. R. Ruedy, National Research Laboratories, who obtained for him an abstract of Korteweg's (3) paper, and who checked most of the mathematics.

References

1. Boyle, R. W. and Froman, D. Nature, 126: 602-603. 1930.
2. Crandall, I. B. Theory of vibrating systems and sound. Van Nostrand. 1926.
3. Korteweg, D. J. Ann. Physik, 5: 525-542. 1878.
4. Lamb, H. Dynamical theory of sound. 2d. ed. E. Arnold. 1925.
5. Lamb, H. Mem. Manchester Phil. and Lit. Soc. 42, No. 9. 1898.

ON THE PROPAGATION OF LONGITUDINAL WAVES IN CYLINDRICAL RODS[1]

By R. Ruedy[2]

Abstract

The solution of the velocity equation obtained by Pochhammer on the basis of the mathematical theory of elasticity is determined for the propagation of longitudinal waves of any frequency in a long solid circular cylinder of any diameter. For a given frequency a large number of solutions may be obtained, but when the condition is imposed that for low frequencies the velocity must gradually assume the value found by experiment, a single value is obtained for each frequency. The velocity decreases with increasing frequency, so that, for a cylinder of finite length, the resonance frequencies come closer and closer together. It is also necessary to take into account, however, that in a solid rod longitudinal waves are accompanied by radial vibrations of the particles, and that a cylindrical rod has, regardless of its length, a series of natural frequencies for radial waves, so that for wave-lengths comparable with the diameter of the tube a coupled system of oscillations is set up. The resonant frequencies of such a system depend on the degree of coupling.

Introduction

High mechanical frequencies of vibration produced by taking advantage of piezo-electric effects promise to become an effective tool of investigation. Due to the small wave-length, high frequency vibrations allow acoustic effects to be studied within the confines of the ordinary laboratory. Given strong sources of high frequency waves the metallurgist and the engineer are able to run hysteresis and endurance tests in a much shorter time, even when they have to extend them to several hundred million cycles. As, on the other hand, in the piezo-electric effect, for instance, definite atoms of a group are set in vibration with respect to the rest of the group, a certain amount of chemical activation is to be expected and an influence upon the rate of chemical reaction might be found.

Many of the quantitative expressions given for the propagation and absorption of sound waves in different simple structures, such as rods, tubes or plates, are only valid for waves of moderate frequencies. In view of the simple fact that quartz slabs and bars are now used for maintaining oscillations of over one million cycles per second, constant to within less than fifty cycles, it is desirable to extend the velocity formulas to very high frequencies. As a beginning, the velocity of propagation of the waves in a long circular cylinder was calculated, because this is a simple case and because unpublished work by Boyle seems to show that a discontinuity exists at a certain high frequency.

The Equation for the Velocity of Propagation of Longitudinal Waves

The elementary theory valid for long waves assumes that all the points of a perpendicular cross section are not only in phase, but have the same swinging motion along the axis of the cylinder. On this assumption the square of the

[1] *Manuscript received June 2, 1931.*

Contribution from the National Research Laboratories, Ottawa. This paper was read before Section III of the Royal Society of Canada in May, 1931.

[2] *Junior Research Investigator, National Research Laboratories, Ottawa.*

velocity of propagation of longitudinal waves becomes equal to E/d, where E is Young's modulus and d is the density of the material. As, however, any section of the rod which is expanding along the axis is contracted along the diameter, there arises at the same time a motion of the particles in the direction of the radius. This causes a passing radial increase in density, and therefore, a decrease in the velocity of sound. In the case of uniform elastic solid cylinders the theory gives the following general expression for the propagation of mechanical vibrations (5):

$$\left(2G\,\frac{\partial J_0(h'a)}{\partial a^2} - \frac{p^2 d}{m-1}J_0(h'a)\right)\left(2-\frac{c^2 d}{G}\right) = 4G\,\frac{\partial J_0(h'a)}{\partial a}\,\frac{\partial J_1(k'a)}{\partial a} \Big/ J_1(k'a)$$

where G = modulus of elasticity in shear, $p = 2\pi$ times the frequency f, a = radius of cylinder, c = velocity of propagation of longitudinal waves, $c_0^2 = E/d$,

$$h'^2 = \frac{p^2}{c^2}\left(\frac{c^2}{c_0^2}\,\frac{(m-2)(m+1)}{(m-1)m} - 1\right) = \frac{p^2}{c^2}H'^2, \qquad k'^2 = \frac{p^2}{c^2}\left(\frac{c^2}{c_0^2}\,\frac{2(m+1)}{m} - 1\right) = \frac{p^2}{c^2}K'^2$$

and $2 < m < 5$. The letter m designates the reciprocal of Poisson's ratio; J_0 and J_1 are Bessel's functions of the first kind, of order zero and one. When the assumption is made that f as well as a is very small, the series development of the functions may be stopped after the first or second term, and this leads to the same expressions as are given by the elementary theory (4). For discussing the general case, a more distinct form must be sought for the equation. Replacing the modulus of elasticity in shear by Young's modulus according to the formula $G = \dfrac{mE}{2(m+1)}$ we get

$$\left(1-\frac{c^2}{c_0^2}\,\frac{m+1}{m}\right)\left(\frac{J_1(h'a)}{h'aJ_0(h'a)} - \frac{\dfrac{c^2}{c_0^2}\,\dfrac{(m+1)}{m} - 1}{\dfrac{c^2}{c_0^2}\,\dfrac{(m-2)(m+1)}{(m-1)m} - 1}\right) = \frac{J_1(h'a)}{h'aJ_0(h'a)}\left(1-\frac{k'aJ_0(k'a)}{J_1(k'a)}\right)$$

This equation depends essentially on the ratio c/c_0. Experiment shows that for low frequencies c is smaller than c_0 so that H^2 becomes negative. Writing therefore $ih = h'$ or $H^2 = -H'^2 = 1 - \dfrac{c^2}{c_0^2}\,\dfrac{(m-2)(m+1)}{(m-1)\ m}$ the equation determining the velocity of propagation becomes

$$\left(1-\frac{c^2}{c_0^2}\,\frac{m+1}{m}\right)\left(\frac{iJ_1(iha)}{haJ_0(iha)} + \frac{\dfrac{c^2}{c_0^2}\,\dfrac{(m+1)}{m} - 1}{\dfrac{c^2}{c_0^2}\,\dfrac{(m-2)(m+1)}{(m-1)m} - 1}\right) = \frac{iJ_1(iha)}{haJ_0(iha)}\left(1-\frac{\kappa haJ_0(\kappa ha)}{J_1(\kappa ha)}\right)$$

$$\text{with } \kappa = \frac{K'}{H} = \sqrt{\frac{\dfrac{c^2}{c_0^2}\,\dfrac{2(m+1)}{m} - 1}{1 - \dfrac{c^2}{c_0^2}\,\dfrac{(m-2)(m+1)}{(m-1)m}}}$$

$$ha = \frac{p}{c}Ha$$

The values for the fractions containing Bessel functions are represented in the graph. Restricting for the moment the considerations to the case where h and k' are real and positive, and taking into account that the values for m

vary between from more than 2 to not quite 5, the main features of the solution may be recognized.

1. The solution does not depend on the sign of h; it is therefore sufficient to take the root of H^2 with its positive sign throughout.

2. For values of ha and $k'a$ approaching zero, that is, for very low frequencies, or for very thin cylinders, the equation is satisfied when $c=c_0$. There is no other value for which this happens.

3. The first factor on the left hand side is negative for $c=c_0$, increases to more positive values when c decreases and becomes equal to zero for

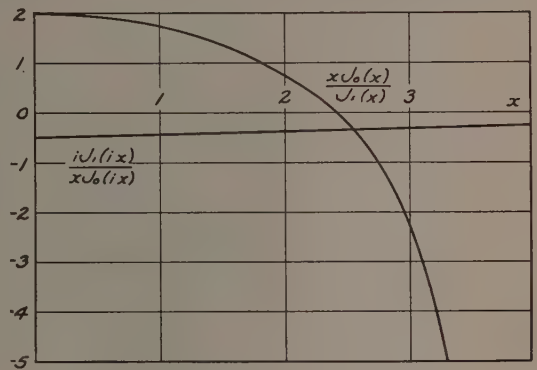

FIG. 1. *Functions used in velocity equation.*

$$\frac{c^2}{c_0^2} = \frac{m}{m+1} < 1$$

On the left hand side evidently $1=\frac{(\kappa ha)J_0(\kappa ha)}{J_1(\kappa ha)}$ or, from the graph $ha\,\kappa \approx 1.85$ and at the same time $\kappa=\sqrt{m-1}$; for instance, for

	m =	8	5	4	3	2.5
	c/c_0 =	0.94	0.91	0.89	0.87	0.85
	κ =	2.64	2	1.73	1.41	1.23
	ha =	0.70	0.93	1.06	1.31	1.50
therefore	$f \approx$	$0.27\frac{c_0}{a}$	$0.27\frac{c_0}{a}$	$0.26\frac{c_0}{a}$	$0.25\frac{c_0}{a}$	$0.27\frac{c_0}{a}$

4. The first term in the second bracket on the left hand side is always negative and varies from -0.5 to $-\infty$ when the independent variable ha varies from zero to infinity. The second term, which is negative for the long waves, the denominator being equal to H'^2, becomes positive for values of $\frac{c^2}{c_0^2} < \frac{m}{m+1} < 1$ and the entire left hand side becomes once more equal to zero when

$$\frac{iJ_1(iha)}{haJ_0(iha)} = \frac{\frac{c^2}{c_0^2}\frac{(m+1)}{m} - 1}{\frac{c^2}{c_0^2}\frac{(m-2)\,(m+1)}{(m-1)m} - 1}$$

The value of κha on the right hand side will again be equal to about 1.85, but the value of ha will be larger than before due to the circumstance that κ decreases when c/c_0 drops to lower values. The exact solution must be found by trial, but the main result is that c/c_0 decreases to below $m/(m+1)$.

5. The lowest velocity for which the equation as written admits of a solution is $\frac{c^2}{c_0^2} = \frac{m}{2(m+1)}$ when K' becomes equal to zero and the values of ha are for

m =	8	5	4	3	2.5
c/c_0 =	0.67	0.65	0.63	0.62	0.6
c_0h =	$7.1f$	$7.7f$	$8.1f$	$8.8f$	$9.6f$

or, as from the velocity equation for $k'=0$ and $h \neq 0$, $\frac{iJ_1(iha)}{haJ_0(iha)} = \frac{1-m}{3m}$,

or	ha ≈	2.7	3.0	3.3	3.8	4.3
and therefore	f ≈	$0.38\frac{c_0}{a}$	$0.39\frac{c_0}{a}$	$0.4\frac{c_0}{a}$	$0.43\frac{c_0}{a}$	$0.45\frac{c_0}{a}$

When c/c_0 continues to decrease beyond this point, the expression for K becomes imaginary, and putting $k'=ik$ the equation may be written

$$\left(1-\frac{c^2}{c_0^2}\,\frac{m+1}{m}\right)\left(\frac{iJ_1(iha)}{haJ_0(iha)}+\frac{\frac{c^2}{c_0^2}\,\frac{m+1}{m}-1}{\frac{c^2}{c_0^2}\,\frac{(m-2)(m+1)}{(m-1)\,m}-1}\right)=\frac{iJ_1(iha)}{haJ_0(iha)}\left(1-\frac{kaJ_0(ika)}{iJ_1(ika)}\right)$$

in which the different terms have the following signs

pos.	neg.	pos.	neg.	neg.
>0.5	<0.3	$>\frac{m-1}{m}$		

As far as the signs are concerned, the modified equation continues to furnish solutions. The left hand side is always positive and remains constantly smaller than unity, whereas the bracket on the right hand side may assume very large values for large ka. In order to satisfy the equation, the expression $\frac{iJ_1(iha)}{haJ_0(iha)}$ must become very small, or iha very large. For extremely large values, for instance, of either f or a, the two sides can become equal only when k is about equal to h, or when c equals zero.

The equation of propagation of longitudinal waves shows, therefore, that the velocity decreases steadily when the frequency, f, increases. This causes a rapid decrease of the wave-length, the rate depending, however, on the diameter of the cylinder. This change influences the rule according to which the higher harmonics would be produced in a bar of quartz and must be considered in explaining deviations from the simple spectrum of overtones that have been observed in the case of quartz crystals (3). Furthermore, because the velocity decreases to below c_0 for rapid vibrations, the fundamental frequency itself of a finite cylinder is lowered. This circumstance may cause the grains of which the metal is composed to act as resonators at much lower frequencies than would be the case for a constant velocity of propagation. In steel the length of the particle size varies from 0.01 to 1 mm., depending on the treatment, so that it does not seem impossible that the resonance frequency of the grains can be attained in ultrasonic experiments. The laws of propagation would then be completely changed, and true anomalous dispersion might be produced.

Motion of Particles

The equation giving the velocity of longitudinal waves in a cylinder involves the assumption that the motion u in the direction of the radius and w along the axis of any particle of the rod is given by the following solution of the general theory:

$$u = [-AhiJ_1(ihr)+C\gamma J_1(kr)]e^{i(\gamma z+pt)}$$
$$w = [+A\gamma iJ_0(ihr)+kCiJ_0(kr)]e^{i(\gamma z+pt)}$$

or

$$u = [-AhiJ_1(ihr)+C\gamma J_1(kr)]\cos(\gamma z+pt)$$
$$w = [-A\gamma J_0(ihr)-CkJ_0(kr)]\sin(\gamma z+pt)$$

where $\gamma = p/c = 2\pi f/c$, z = distance along axis of cylinder, r = distance along radius, t = time, and A and C constants.

The constants A and C have to be chosen so as to conform with experimental conditions, for instance, certain initial or boundary requirements. The condition may be imposed, for instance, that all the points belonging to a certain end section are in phase and have the same amplitude as when they are set in motion by a rigid oscillating piston. In reality, the two components which necessarily make up such a system, cannot always be considered as separate vibrating bodies, but must be treated as a whole. However that may be, as in the equation for w the value of $-J_0(ihr)$ increases with hr whilst that of $-J_0(kr)$ decreases, the condition of w being constant over a whole cross section may be approximately fulfilled in many cases. If it is not realized, a loose contact will be produced between the source of sound and the cylinder and less energy will be transmitted. In the equation for u, if A and C are positive, both terms in the brackets increase on going from smaller to larger distances, r, a feature which might be expected.

When, on increasing the frequency, the velocity falls steadily, the moment arrives when k becomes imaginary. At this point the vibrational motion suffers a sudden change, it becomes equal to

$$u = -AhiJ_1(ihr)\cos(\gamma z+pt)+C\gamma iJ_1(ikr)\sin(\gamma z+pt)$$
$$w = -A\gamma J_0(ihr)\sin(\gamma z+pt)+CkJ_0(ikr)\cos(\gamma z+pt)$$

with $k<h$ or

$$cu/p = -AHiJ_1(ihr)\cos(\gamma z+pt)+CiJ_1(ikr)\sin(\gamma z+pt)$$
$$cw/p = -AJ_0(ihr)\sin(\gamma z+pt)+CKJ_0(ikr)\cos(\gamma z+pt)$$

The point requires further experimental study.

Radial Vibrations

Whereas at sufficiently high frequencies motions w of the particles along the axis are accompanied by strong motions u along the radius, vibrational motions u along the radius alone may exist independently of other types of vibration. The case may therefore occur where the energy of lateral vibrations is used up by radial motions of the particles. The simplest equation for purely radial displacements in a cylinder of finite length is (1)

$$u = U(r)e^{ipt} = AJ_1(gr)e^{ipt}$$

where

$$g^2 = \frac{p^2}{c_0}\sqrt{\frac{(m-2)(m+1)}{(m-1)\ m}}$$

and the boundary conditions for a cylinder of finite radius a give

$$(m-1)gaJ_0(ga)-(m-2)J_1(ga)=0$$

The values of ga satisfying this equation are:

2.0694	8.5758	14.8861	21.1802
5.3958	11.7346	18.0241	24.3251

They determine the resonant frequencies, f_1, f_2 . . . , for radial vibrations in a cylindrical bar:

$$f_1 = \frac{2.0694c_0}{2\pi a}\sqrt{\frac{(m-1)\ m}{(m-2)(m+1)}},$$

$$f_2 = \frac{5.3958c_0}{2\pi a}\sqrt{\frac{(m-1)\ m}{(m-2)(m+1)}},$$

and so on, for the higher modes. The overtones are evidently not harmonic, but tend toward a definite limit, forming finally a broad band of frequencies. For different values of m the first resonant frequencies are

$f_1 \approx$	$0.34\frac{c_0}{a}$	$0.35\frac{c_0}{a}$	$0.36\frac{c_0}{a}$	$0.38\frac{c_0}{a}$	$0.48\frac{c_0}{a}$
for $m =$	8	5	4	3	2.5

that is, frequencies which are only slightly lower than those for which

$$\frac{c^2}{c_0^2} = \frac{m}{2(m+1)}.$$

It is therefore probable that when a longitudinal wave belonging to this region of frequencies is sent through the cylinder, it will set up standing radial waves. The frequency at which the first double system of waves may be expected is higher the thinner the rod. The intensity of the radial motions will be stronger the higher the value of m; the two systems will necessarily react upon each other, forming a system of coupled vibrations. If we assume, as seems probable from the relations governing such a system, that the velocity of propagation of the radial waves is equal to that of the ordinary longitudinal (plus radial component) waves, then very closely

$$\text{radial wave-length} = \frac{2/3\ c_0}{1/3\ c_0}\ a$$

that is, the wave-length of the standing radial waves is determined by the diameter of the rod. In other words this dimension determines an acoustical resonance frequency of the rod, and the properties of the rod with respect to sound waves are governed by resonant frequencies as optical properties are governed by the wave-length of the resonance line. It is indeed in the neighborhood of waves of this length that anomalous dispersion of sound waves has been discovered in cylindrical rods (2).

Acknowledgment

This work was proposed by Dr. R. W. Boyle and thanks are due to him and also to Mr. G. S. Field for suggestions received.

References

1. Airey, J. R. Arch. Math. Phys. 20: 289-294. 1913.
2. Boyle, R. W. and Froman, D. Nature, 126: 602-603. 1930.
3. Giebe, E. and Scheibe, A. Ann. Physik, 9: 93-175. 1931.
4. Muzzey, D. S. Phys. Rev. 36: 935-947. 1930.
5. Pochhammer, L. J. Math., Crelle 81: 324-336. 1876. Summarized by A. E. H. Love, Math. Theory of Elasticity.

RESISTANCE THERMOMETERS FOR THE MEASUREMENT OF RELATIVE HUMIDITY OR SMALL TEMPERATURE DIFFERENCES[1]

By D. C. Rose[2]

Abstract

The instrument described in this paper was designed for the measurement of relative humidity in the slip stream of flying aircraft. As the temperatures to be measured are low, usually between 0° and −10° C., the temperature difference between wet and dry bulb thermometers is sufficiently small that, if mercury thermometers are used, in order to obtain the accuracy required, they would have to be of such fine bore that they could not be read from any distance. As a result wet and dry bulb resistance thermometers have been built connected to a special bridge circuit by means of which the temperature difference can be measured to 0.1° C. or better. The actual dry bulb temperature can be read by a change in the circuit or by a mercury or alcohol thermometer of fairly large bore, which can be read at some distance. In the bridge circuit the two thermometers form two arms of a bridge so that temperature variations in the leads are automatically compensated. A slide wire forms a part of the bridge circuit and the constants are so arranged that a very simple relation gives the difference in temperature of the wet and dry bulbs.

The instrument described in this paper resulted from some investigations being carried out by the author on the atmospheric conditions in the slip stream of flying aircraft. One of the measurements to be made was relative humidity. As the temperatures are rather low, often between 0 and −10° C., the temperature difference between wet and dry bulb thermometers is small enough to require accurate thermometers. If mercury or alcohol thermometers are used the scale divisions should not be more than 0.2° C. apart. Such thermometers necessarily have a small bore and cannot be read from any great distance. In the case in which the author was interested it was found impossible to read precision thermometers which had to be some distance outside the cabin of the aircraft, so it was decided to attempt to use other methods of measuring the temperatures. Methods of measuring relative humidity other than wet and dry bulb thermometers were considered but none seemed as reliable at the low temperatures involved. Hence it was decided to attempt to build satisfactory wet and dry resistance thermometers.

The quantity which must be measured most accurately is the difference between the wet and dry bulb temperatures rather than the actual temperatures. The actual dry bulb temperature can be measured with a thermometer of fairly large bore which can be read from a distance. With this in view the resistance thermometers described here were connected as two arms of a Wheatstone bridge using a 1:1 ratio. The arrangement does not give the temperature of either thermometer but with a very simple type of slide wire forming the other arms of the bridge, the temperature difference between the wet and dry thermometers could be read easily to 0.1 °C. and at the same time the whole apparatus, including the batteries, galvanometer and

[1] *Manuscript received June 6, 1931.*
Contribution from the National Research Laboratories, Ottawa. This paper was read before Section III of the Royal Society of Canada in May, 1931.
[2] *Assistant Research Physicist, National Research Laboratories, Ottawa.*

slide wire, was sufficiently rugged to withstand the vibration in an aeroplane and did not weigh more than a few pounds. Further the apparatus automatically compensates itself for temperature changes in the leads.

The circuit used is shown in Fig. 1. W and D are the wet and dry resistance thermometers (approximately 100 ohms each). It will be seen that the calculation of the results is simpler if the resistances of these two thermometers are the same, but the range of the instrument is increased if they are slightly different. In the apparatus built by the author they happened to be the same, more by accident than by intention. The resistances A and B and the slide wire were simply a Leeds and Northrup "Students Kohlrausch Slide Wire"*.

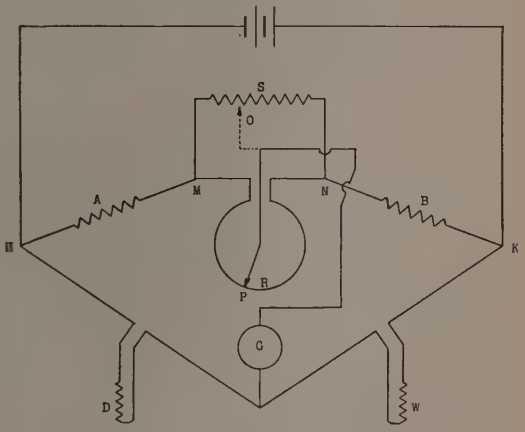

FIG. 1. *Bridge circuit used with resistance thermometers.*

The slide wire has a resistance of 121.4 ohms and the scale reads from 0 to 1000, every five divisions being marked. The resistances of A and B are respectively 546.3 and 546.2 ohms. The purpose of the resistance S is to change the sensitivity of the slide wire. The resistance of the slide wire without S formed too large a portion of the bridge circuit. By varying S a change of 2° C. in the temperature of one of the thermometers could be made to correspond to any number of divisions from a few to 500 on the slide wire.

The process of measuring the temperature differences between D and W is very simple. First the position of the slide for a balance when D and W are at the same temperature must be known. This can be found easily by putting them both in the same temperature bath. If D and W have the same resistance, this position is practically at the centre of the slide wire, as A and B have practically the same resistance. This position will also be independent of S. If D and W have not the same resistance the position of the balance with D and W at the same temperature will depend on S and must be known for whatever value of S is used. The position of this balance is always the same and in the apparatus used by the author remained the same when the whole was dismantled and connected up in the aeroplane. Then with W and D as a wet and dry bulb hygrometer, a balance can be found and the difference in temperature between W and D can be calculated from the equations given below.

Analysis of the Circuit

The circuit shown in Fig. 1 may be treated as a simple bridge circuit by considering a point O on the shunt S at the same potential as the point P on

**Catalogue No. 4261.*

the slide wire. When the bridge is balanced such a point always exists. The introduction of the shunt S in the bridge circuit now means that in place of MP in the simple bridge circuit, the effective resistance of MO and MP in parallel must be used. Hence the resistance of the arm HP is $A+\frac{MP.\,MO}{MP+MO}$ and similarly of the arm KP it is $B+\frac{NP.NO}{NP+NO}$. The conditions for balance are now

$$\frac{D}{W}=\frac{A+\frac{MP.\,MO}{MP+MO}}{B+\frac{NP.NO}{NP+NO}} \tag{1}$$

put this $=\frac{x}{y}$. The quantities observed on the slide wire are MP and PN. The slide wire scale is numbered from 0 to 1000 so that if the reading be divided by 1000, a fraction, θ, of the total resistance of the slide wire is obtained. The resistance $MP=\theta R$ and $PN=(1-\theta)R$. The equation (1) may be reduced to

$$\frac{D}{W}=\frac{x}{y}=\frac{A+C\theta R}{B+C(1-\theta)R}, \tag{2}$$

where $C=\frac{S}{R+S}$, R and S being the resistances of the slide wire and shunt respectively.

The resistances of the thermometers D and W are to a first approximation $D=D_0(1+\alpha t_D)$ and $W=W_0(1+\alpha t_W)$, where D_0 and W_0 are the resistances of the thermometers at some specified temperature in the range of temperatures being measured; α is the temperature coefficient of the resistance of the wire in the thermometers, and t_D and t_W are the differences between the specified temperature and the temperatures observed. The equation may be written

$$\frac{x-y}{y}=\frac{D-W}{W}=\frac{D_0(1+\alpha t_D)-W_0(1+\alpha t_W)}{W_0(1+\alpha t_W)}$$

Assume for the present that $D_0=W_0$, then

$$\frac{x-y}{y}=\frac{\alpha(t_D-t_W)}{1+\alpha t_W}.$$

In practice the quantity αt_W must always be small compared with unity: hence it may be omitted in the denominator and the equation may be written

$$\frac{x-y}{y}=\alpha\,(t_D-t_W)$$

and from (2)

$$=\frac{A+C\theta R-\{B+CR(1-\theta)\}}{B+CR(1-\theta)} \tag{3}$$

and the difference in temperature of the two thermometers may be calculated easily from the known constants of the circuit.

A further approximation which simplifies the calculation may be made. A and B are effectively equal so may be disregarded in the numerator. C is in practice considerably less than 1 otherwise the shunt S is useless. $(1-\theta)$ is considerably less than 1 particularly at the top of the scale. R in the apparatus used was $\frac{2}{9}B$; C was usually between $\frac{1}{6}$ and $\frac{1}{20}$ in all the tests made and if $W_0=D_0$, then $(1-\theta)$ is never more than $\frac{1}{2}$. Hence the term $RC(1-\theta)$ is

never greater than $\frac{2}{9} \cdot \frac{1}{6} \cdot \frac{1}{2} B = \frac{1}{54} B$. Therefore if we neglect this term in the denominator the error involved is less than 2%. Where differences of the order of 2° C. are to be measured, this error is less than possible errors in reading two mercury thermometers even if fairly high precision thermometers are used. The equation now becomes

$$t_D - t_W = \frac{RC(2\theta - 1)}{\alpha B} . \qquad (4)$$

The constant $\frac{RC}{\alpha B}$ may be evaluated for the different values of S used.

The resistance thermometers were made of nickel wire 0.15 mm. in diameter and wound on a hollow ebonite spool. As the wire was bare, a thread (96 to the inch) was turned on the spool to keep it in place. The spool was about $1\frac{1}{4}$ in. long and $\frac{1}{2}$ in. in diameter. It was hermetically sealed in a glass tube filled with a good grade of oil. The oil was added as an insulator and to improve the thermal conductivity between the glass and the wire. This construction of course caused some lag in the resistance wire taking up the temperature of the glass tube, but trials showed that readings could be taken after temperature conditions had been steady for six or seven minutes. The resistance of the thermometers was about 97 ohms and the temperature coefficient of resistance was found to be 0.00284 ohms per ohm per degree between 0 and 20° C.

Actually no attempt was made to make the two resistances exactly the same and when they were sealed up one was slightly higher than the other, but after seasoning they came by accident to the same value so that the balance, when they were at the same temperature, was exactly in the middle of the slide wire. An examination of the above theory shows that there is nothing gained by making them the same If they are different the same formula applies but an additional calculation must be made. The thermometer having the higher resistance should be the wet one and the balance found when the two are at the same temperature, then as the wet thermometer becomes cooler than the dry, the position of balance will move towards the centre of the slide wire scale. A calculation must be made for the difference in temperature required to bring the position of balance to the centre of the scale. This must be added to the difference found when the final reading is taken. There is in fact a slight advantage in having the resistance of the two thermometers slightly different as a greater part of the slide wire scale is usable.

The most suitable value of S depends on the temperature difference to be measured. For differences up to 10° C. a convenient value was found to be about 25 ohms. If S was made smaller than about 5 ohms the position of balance could not be found so accurately, since the galvanometer current was so much reduced. A small resistance box was made for S, having four coils with resistances of 4.38, 6.17, 8.00 and 10.54 ohms. These could be used either individually or in series. The galvanometer was a portable Leeds and Northrup insulation testing set consisting of a portable galvanometer arranged with a telescope and scale and containing a universal shunt, the whole being very conveniently mounted. This was found to be rugged enough for use in

aircraft though if there was excessive vibration the instrument had to be held on the author's knee in order to obtain a good balance. This was not found inconvenient.

In order to check the above theory, readings were taken with the two thermometers in different temperature baths. The following is a set of results:

Balance with both at the same temperature, 500

Balance with one at 17° C. and the other at 7.7° C., 920

Resistance of shunt, S, 20 ohms

$\alpha = 0.00284$ ohms per ohm per °C.

According to formula (4)

$$t_D - t_W = \frac{121.4 \times 0.141 \times 0.840}{0.00284 \times 546.2} = 9.26$$

and as $17.0 - 7.7 = 9.3$, it is seen that the agreement is very good, and one-tenth of a degree was the greatest accuracy hoped for, with the equipment used. Using formula (3) the result would have been about $\frac{1}{3}$% higher making the agreement even better.

A large number of humidity tests were made to try out the instrument in the laboratory. Some of the readings are recorded below. The results are compared with those obtained from wet and dry bulb mercury thermometers placed beside the resistance thermometers both being ventilated by an electric fan.

TABLE I

COMPARISON OF RESISTANCE THERMOMETERS WITH MERCURY THERMOMETERS

Wet bulb temp., °C.	Dry bulb temp., °C.	Balance of bridge	Resistance of S, ohms	$t_D - t_W$ (temp. difference)	
				Formula (4) °C.	Mercury thermometers °C.
10.6	20.3	866	25.00	9.8	9.7
9.3	19.1	835	29.07	10.2	9.8
9.7	19.6	945	18.53	9.2	9.9
11.6	21.0	965	18.53	9.6	9.4
8.9	15.4	814	18.53	6.5	6.5
11.5	20.8	956	18.53	9.4	9.3

In the case of the first three of the above, the room in which the readings were taken was well ventilated by open windows. In the case of the latter three, the windows and doors were closed in order to obtain constant humidity. In view of the difficulty in obtaining constant humidity in a large room containing two sinks as well as a considerable quantity of apparatus the results show very good agreement. Even the proximity of the observer produces a detectable change in the humidity and, as the time lag of the mercury thermometer and the resistance thermometers was very different, great precision could not be obtained unless very special precautions were taken. This time lag in the resistance thermometers seemed unavoidable, as any design of the thermometers which would allow one of them to be kept wet in the usual manner would require the elements well insulated from the water.

Measurements of relative humidity taken in the slip stream of flying aircraft will no doubt be published later. So far the instrument has been tried out on two flights and found to be practical. Its use however is not limited to relative humidity measurements. Wherever temperature differences are required it can be used and by a change-over switch and an additional fixed resistance the temperature of either thermometer could be measured by making the apparatus into an ordinary bridge. If the instrument were to be used in a laboratory the accuracy could be improved a great deal by using precision resistance boxes and a very sensitive galvanometer. It should be easy to measure temperature differences varying from a few degrees to 0.01° C.

It is unlikely that this bridge circuit has never been used before, or that resistance thermometers have never been used for relative humidity measurements but, as far as the author is aware, this combination is new and seems especially well adapted for measurements where small temperature differences are involved.

AN INVESTIGATION OF THE EQUILIBRIA EXISTING IN GAS-WATER SYSTEMS FORMING ELECTROLYTES[1]

By O. M. Morgan[2] and O. Maass[3]

Abstract

The data and theoretical treatment contained in this paper are the continuation of a series of researches instituted to investigate the equilibria existing in certain gaseous-aqueous systems. In this work the vapor pressures and electrolytic conductivities of aqueous solutions of sulphur dioxide, carbon dioxide, and ammonia have been measured with greater precision than ever before over a temperature range from 0 to 25° C. and over a concentration range where their respective vapor pressures do not exceed one atmosphere. From the data thus derived, equilibria relations have been calculated and certain changes have been made in the mode of theoretical procedure involved in this type of calculation.

With regard to the equilibria existing in the three systems, the conclusions drawn may be summarized as follows: Practically all of the ammonia exists in the combined form and practically all the carbon dioxide exists as free carbon dioxide in the aqueous solutions in the temperature range investigated. The amounts of free and combined sulphur dioxide are of the same order of magnitude and the relative amount of combined and free sulphur dioxide can be calculated approximately, the latter increasing markedly with rising temperature. The true dissociation constant can therefore be found for ammonium hydroxide, can be estimated for sulphurous acid, but cannot be calculated for carbonic acid from the available data.

Introduction

Sulphur dioxide, carbon dioxide, and ammonia are very common materials and are widely used in many industries. It is amazing, when a search is made in the literature, to find that the data which are of such economic interest are either lacking or inaccurate. Perhaps the sulphur dioxide-water system has been investigated more thoroughly than the other two.

The solubility of sulphur dioxide in water was determined by Hudson (19) working at approximately atmospheric pressure and temperatures up to 90° C. Sims (44), working at pressures up to 200 cm. and temperatures up to 50° C., measured the vapor pressures with considerable accuracy. Enckell (11) and Oman (39) measured solubilities up to 90° C., Enckell using less exact methods than Oman. Enckell also measured the solubility of sulphur dioxide in other solutions such as calcium bisulphite, sodium sulphate plus hydrochloric acid, and sulphuric acid. Vapor pressure measurements of solutions of sulphur dioxide in water, and in water plus various amounts of bases were made by Smith and Parkhurst (45).

Ostwald (40) and Barth (2) carried out investigations on the conductivity of sulphur dioxide solutions. McRae and Wilson (33) determined partition coefficients of sulphur dioxide between water and chloroform. Walden and Centnerszwer (47) made freezing point determinations. Drucker (10, p. 579) combined the results of the four previous investigations to calculate the so-

[1] *Manuscript received June 9, 1931.*
Contribution from the Physical Chemistry Laboratory, McGill University, Montreal, Canada.

[2] *Assistant Research Chemist, National Research Laboratories, Ottawa, and holder, at the time, of a studentship and fellowship under the National Research Council of Canada.*

[3] *Professor of Physical Chemistry, McGill University.*

called dissociation constant. Kerp and Bauer (23) measured freezing points and conductivities. Fulda (17) gives figures for the dissociation constant at temperatures from 2 to 50° C. These he has calculated from the heat of dissociation data of Thomsen (46) and Berthelot (4). Lindner (28) reviews and discusses these papers and has also made determinations of vapor pressure at 0, 25 and 50° C. on four solutions ranging in concentration from 0.05 to 3.8%. He also made conductivity measurements of the following solutions:— 6.20% at temperatures from 0 to 39.9° C.; 3.24% at temperatures from 12.7 to 56.7° C.; 0.34% at temperatures from 9.5 to 69.9° C.; 0.05% at temperatures from 0 to 70.5° C.

Any other available data on sulphur dioxide have been obtained in this laboratory. C. Maass (31) made vapor pressure and conductivity measurements over all possible concentrations below 27° C.

The range of most interest to those concerned with the sulphite process of cooking wood pulp is that between 0 and 6% concentration and at 100° C. or slightly above. This range has been covered by W. B. Campbell and O. Maass (8) in this laboratory. The apparatus used by these investigators was designed to measure pressures up to four atmospheres and hence did not give precise measurements at the lower pressures. Their reaction chamber was small, which also tended to cut down the precision, and the maximum concentration attained was only 8%. In order to obtain a true measure of the equilibria, as will be seen later, it is necessary to have a comparatively large variation in the water concentration. In the present work concentrations as high as 14% sulphur dioxide were attained which gave approximately twice the variation in the water concentration that was reached by Campbell. Campbell and Maass admit that the values of their equilibria constants are only approximate. The aim of this work was to arrive at a true evaluation of these constants and to investigate the type of equilibria existing at the lower temperatures.

Considerable data are available for carbon dioxide. Bohr (5) working over a temperature range of 0 to 60° C. and over a vapor pressure range of 27 to 140 cm. has determined the Henry's Law constants. Findlay and Creighton (12) measured the solubility of carbon dioxide in water and the effect of fine suspensions on the solubility. Findlay and Williams (15) determined the solubility of carbon dioxide in water at pressures lower than one atmosphere. Findlay and Shen (14) investigated the effect of colloids and fine suspensions on the solubility of carbon dioxide in water. The results were in harmony with Henry's Law. Findlay and Howell (13) measured the vapor pressures of carbon dioxide in pure water and in starch solutions at 25° C. for pressures from 272 to 960 mm. Buch (6) determined the solubility of carbon dioxide in water at temperatures between 17 and 20° C. and calculated the absorption coefficients. Just (20) working at 25° C. determined Henry's Law constant and obtained a value which agreed well with that of Bohr (5) but differed from the rest.

Conductivity data for carbon dioxide are not quite so plentiful. Those given by Knox (24), Pfeiffer (42) and Walker and Cormack (49) are reviewed in a concise manner by Kendall (22) who also supplies considerable data. The

above experimenters worked at temperatures from 0 to 25° C. and concentrations up to 0.08 gm.-mols per litre. The data of Kendall (22) agree very well with those due to Walker and Cormack (49) but do not compare favorably with those of Pfeiffer (42) or Knox (24). Wilke (50) attempts to explain the equilibria of carbon dioxide in water solutions. He determined the dissociation constants by conductivity measurements at various temperatures and showed carbonic acid to be a very weak acid. This acid is shown to be a sensitive compound and is decomposed by slight influences such as the current used for measurement.

Vapor pressures of solutions of ammonia at 0, 20 and 40° C. and up to 3640 mm. have been measured by Neuhausen and Patrick (35). Foote (16), working at 10 and 20° C., determined the vapor pressures up to 1500 mm. As a side issue they investigated the equilibrium in the system ammonia-ammonium nitrate-ammonium thiocyanate with the object of discovering what proportions of these substances were most efficient in absorbing ammonia from gas mixtures. Perman (41, p. 1397) has also covered the lower range of vapor pressures.

Kanolt (21) determined the ionization constant of ammonium hydroxide at 0, 18 and 25° C. Lunden (29, 30) has measured the affinity coefficients of ammonia solutions between 15 and 40° C. and conductivities between 10 and 50° C. in dilute solutions. Noyes and Kato (38) measured the conductivity and determined the ionization up to 156° C. using a steel bomb lined with platinum electrodes which were insulated away from the walls. Burke (7) investigated the ionization of aqueous solutions of ammonia in the presence of urea to find if an ammonia-urea complex were formed. The results showed that such appeared to be the case. Specific conductivity data are also provided by Kohlrausch (25, p. 1078).

The density of ammonia solutions up to 40% concentration and between −15 and 25° C. have been determined by Nichols and Wheeler (36, p. 59) and Baud and Gay (3).

A general summary of the work carried out by other investigators on all three systems shows considerable lack of agreement apart from the total lack of data in certain concentration and temperature regions. One special source of controversy is to be found, not in the accuracy of actual pressure or conductivity measurements, but rather in the determination of the concentration factor. Special emphasis is laid, in the experimental work to be described, on the elimination of all doubt as to the true concentrations, and of true equilibria having been reached between the gaseous and liquid phase. This may have been another source of discrepancies obtained by other investigators.

It would lead too far afield to give a detailed account of all theories that have been put forward in connection with the equilibria existing in the various systems investigated. Due to the fact that the work described in this paper is a continuation of the work begun by C. Maass (31) and Campbell and Maass (8), as far as sulphur dioxide is concerned, it is convenient to overlap their work. On the experimental side this will be done by the comparison of refinements and improvements that have been made. The need for the

extreme precision is brought out by the following review of the theoretical considerations as they have been developed so far. It will be seen that previous data are not adequate in testing it out.

In this theoretical discussion terms peculiar to solutions of sulphur dioxide will be used. This discussion will contain the major number of steps necessary in dealing with gaseous-aqueous equilibria and all the steps necessary for sulphur dioxide as evolved by the above experimenters. However, certain characteristics, depending on the gas under consideration, necessitate minor changes in the mathematical treatment. These peculiarities will be dealt with in discussing the respective systems in later sections.

In aqueous solutions of sulphur dioxide there are three major and one minor equilibria existing. The partial pressure of the sulphur dioxide above the solution is in equilibrium with the uncombined gas in the solution.

$$[SO_2]_{solution} = H[SO_2]_{gas} \tag{1}$$

and since the partial pressure of the gas above the solution is a measure of the concentration of the gas in the vapor

$$[SO_2]_{solution} = Hp \tag{2}$$

where p is the partial pressure of the gaseous sulphur dioxide and H is a constant (Henry's constant).

The sulphur dioxide molecules in the solution are in equilibrium with sulphurous acid and may be represented

$$H_2O + SO_2 \rightleftarrows H_2SO_3 \tag{3}$$

and, applying the mass law,

$$[H_2O]\,[SO_2] = K_1\,[H_2SO_3] \tag{4}$$

The sulphurous acid in solution is ionized to a certain extent and is in equilibrium with its ions

$$H^+ + HSO_3^- \rightleftarrows H_2SO_3 \tag{5}$$

and assuming that the Ostwald dilution law holds in this case,

$$[H^+]\,[HSO_3^-] = K_2\,[H_2SO_3] \tag{6}$$

A further ionization is possible according to the equation

$$H^+ + HSO_3^- \rightleftarrows 2H^+ + SO_3^= \tag{7}$$

but this ionization is so small it may be safely neglected.

The problem now presented is the evaluation of the constants H, K_1, and K_2. Previous investigators have merely calculated the apparent dissociation constant obtained by the assumption that all the sulphur dioxide in the solution is combined with water to form H_2SO_3. That is

$$\begin{aligned}[H^+]\,[HSO_3^-] &= K_a\,([H_2SO_3] + [SO_2]) \\ &= K_a\left(\frac{[SO_2]\,[H_2O]}{K_1} + [SO_2]\right) \\ &= K_a\,[SO_2]\left(\frac{[H_2O]}{K_1} + 1\right),\end{aligned} \tag{8}$$

then since

$$[H^+]\,[HSO_3^-] = K_2[H_2SO_3] = K_2\frac{[SO_2]\,[H_2O]}{K_1}$$

the relation between K_1, K_2, and K_a is

$$K_a = \frac{K_2[H_2O]}{K_1+[H_2O]} \tag{9}$$

The first attempt at the actual evaluation of the constants was made by C. Maass (31) as follows:—

$$C_{H_2O} = [H_2O] + [H_2SO_3] + [HSO_3^-] \tag{10}$$

$$C_{SO_2} = [SO_2] + [H_2SO_3] + [HSO_3^-]. \tag{11}$$

On subtracting (10) from (11)

$$[H_2O] = C_{H_2O} - C_{SO_2} + [SO_2] = C_{H_2O} - C_{SO_2} + Hp \tag{12}$$

$$C_{SO_2} = [SO_2] + \frac{[SO_2]\,[H_2O]}{K_1} + \sqrt{K_a[SO_2]\frac{[H_2O]}{K_1} + 1}$$

$$= Hp\left(1+\frac{[H_2O]}{K_1}\right) + \sqrt{K_a\,Hp\left(1+\frac{[H_2O]}{K_1}\right)},$$

and substituting (12)

$$C_{SO_2} = Hp\left(1+\frac{C_{H_2O} - C_{SO_2} + Hp}{K_1}\right) + \sqrt{K_aHp\left(1+\frac{C_{H_2O} - C_{SO_2} + Hp}{K_1}\right)}. \tag{13}$$

This equation contains two unknowns, H and K_1. The value of K_a was obtained from conductivity measurements. By taking two values of C_{SO_2} at any one temperature and the corresponding pressures it is possible to arrive at the value of H and K_1, and hence K_2, the true dissociation constant. It must be remembered at this point, however, that to get an accurate evaluation of the constants there must be considerable variation in the water concentration, as was mentioned previously. Vapor pressures must also be measured very accurately. For the above reasons C. Maass (31) was able to arrive at only approximate values of the constants. It was found from the calculations that at 15° C. the amount of uncombined sulphur dioxide in the solution amounted to about 20% of the total amount dissolved, whereas at 23° C. the amount of uncombined sulphur dioxide was about 50% of the total, that is, K_1 increased rapidly with temperature. This was for a solution of 5% concentration in each case. The value of the true dissociation constant was found to be approximately 0 02 and did not change much with temperature. It will be shown later from this work that all previous data below 12° C. have been at fault.

Campbell and Maass (8) made a somewhat different use of their data. Sulphurous acid may be assumed to behave as a strong acid, which is reasonable because the organic sulphonic acids as a group are strong acids. They assume

that sulphurous acid is almost completely ionized. Then, instead of considering that water and sulphur dioxide combine to form sulphurous acid which in turn dissociates into its ions, the mechanism may be considered analogous to the formation of NH_4^+ from $NH_3 + H^+$ and the reaction written thus:

$$SO_2 + OH^- + H^+ \rightleftharpoons HSO_3^- + H^+.$$

The extent of the reaction will be determined by the equilibrium expressed as follows:

$$[SO_2]\,[OH^-] = K_3[HSO_3^-]$$

and

$$[H^+]\,[OH^-] = K_w[H_2O]\,.$$

Combining these

$$[SO_2]\,[OH^-] = \frac{[SO_2]K_w\,[H_2O]}{[H^+]} = K_3[HSO_3^-]$$

or

$$H^+[HSO_3^-] = \frac{K_w}{K_3}[SO_2]\,[H_2O]$$

$$= K_b(C_{SO_2} - [HSO_3^-])\,[H_2O] \qquad (14)$$

also

$$[SO_2] = C_{SO_2} - [HSO_3^-] = Hp \qquad (15)$$

Equation (15) may be derived from equation (13) as follows: Equation (13) may be written

$$C_{SO_2} = Hp\left(1 + \frac{[H_2O]}{K_1}\right) + [HSO_3^-] \qquad (13a)$$

If in the first place K_1 is large, or secondly $[H_2O]$ considered to be constant, equation (13) then becomes

$$C_{SO_2} = Hp + [HSO_3^-]$$

or

$$C_{SO_2} - [HSO_3^-] = Hp$$

At high temperatures the first is true and at low concentrations the second is true, so that the data obtained by Campbell and Maass (8) are not adequate to distinguish between equations (13) and (15).

When the data of Campbell and Maass were used and p, the partial pressure of sulphur dioxide, was plotted against the values of $C_{SO_2} - [HSO_3^-]$ a straight line was obtained as was required by equation (15). It must not be concluded though that no sulphurous acid exists as such since the range of dilution in their work at high temperatures is not great enough to affect the proportionality of $[H_2SO_3]$ to $[SO_2]$ when $[H_2O]$ is constant. At any rate it would be too small to be evident in the plot. In this case the two constants instead of three are used to express the equilibria, *i.e.*, H and K_b. K_b, obtained in equation (14), bears a relation to the apparent dissociation constant through the following equations:

$$[H^+]\,[HSO_3^-] = K_a(C_{SO_2} - [HSO_3^-])$$

$$= K_b(C_{SO_2} - [HSO_3^-])\,[H_2O]\,.$$

Hence

$$K_a = K_b\,[H_2O]\,.$$

It may be emphasized again that the measurements at high temperatures will be in accord with equation (15) because the equilibrium given by equation (4) is shifted to the left by rise in temperature as indicated by the data of C. Maass (31). Wright (51) and Baly and Bailley (1) showed by means of absorption spectra that free sulphur dioxide exists in the solution which is in agreement with this idea.

From the above summary of previous work it is seen that measurements of greatest possible precision carried out at temperatures below 25° C. are essential in the determination of the true equilibria. This requires greater refinement of measurement than was used by C. Maass (31) at low concentrations, and over the temperature range not covered by Campbell and Maass (8).

There is another reason for carrying out the work to be described apart from the use in the theory. All three systems investigated are of a particular interest from a commercial point of view. The importance of sulphur dioxide is emphasized in the sulphite cooking of wood pulp, in electrical refrigeration, as a disinfectant and preservative. Carbon dioxide is of importance to the manufacturers of carbonated beverages, while ammonia has numerous uses, the main one at the present time being that of a refrigerant.

The following section will contain a complete discussion of the apparatus and the experimental work with the exception of the respective purifications of each gas studied. Three sections will then be devoted to the presentation of the experimental results obtained for sulphur dioxide, carbon dioxide and ammonia respectively, as well as the theoretical treatment, the corresponding theoretical data, and discussions of the intrinsic value of the data.

Experimental

Apparatus

The apparatus used in the preparation of gaseous-aqueous solutions is illustrated in Fig. 1. The system may be evacuated either by a Hyvac, a water pump, or a Langmuir diffusion pump backed by a Hyvac. C is a metal cylinder containing the gas to be used and F_1, F_2, F_3, and F_4 constitute a fractionating apparatus for the purification of the gas. The pure gas is held in the liquid or solid form, as the case may be, in F_4 by packing it in a Dewar flask containing a dry ice-ether mixture. X is a rough manometer which acts as a safety valve during the successive distillations and also gives a measure of the vapor pressure of the gas which is a check on the rate of distillation.

M_1 is an all glass manometer. The left side is evacuated and the right side is connected to the volume measuring system. It is mounted with an etched mirror scale and by applying pressure or vacuum over the reservoir the mercury is always drawn to the level L_1 for reading. G is a McLeod gauge for the determination of low pressures especially when the manometers are being evacuated. V_1 and V_2 are volumes which have been calibrated carefully to 0.1 cc. The volume of the connecting tubing bounded by stopcocks T_8, T_9, T_{19}, and the level L_1 on manometer M_1 was also calibrated to 0.1 cc. From these calibrations, $V_1 = 587.8$ cc., $V_2 = 175.7$ cc., and V_4 (connecting tubing) $= 90.6$ cc.

V_3 is a small condensation bulb in which the gas was condensed before injection into the conductivity cell. E is a special type of conductivity cell constructed entirely of Pyrex glass. Stirring was effected by the electromagnetic stirrer D operated by the two solenoids B_1 and B_2, the circuit through the former being alternately made and broken by the automatic mercury valve Q, and the latter being in circuit permanently. By varying the current through the solenoids by means of the banks of lamps L_3 and L_4, any length of stroke could be obtained.

Within the cell O_1 and O_2 were platinized platinum electrodes sealed into the Pyrex by the same method as that used by Campbell and Maass (8) and originated by Housekeeper (18). The electrodes were connected to the Wheatstone Bridge through the mercury well and the leads W_1 and W_2. The side arm H

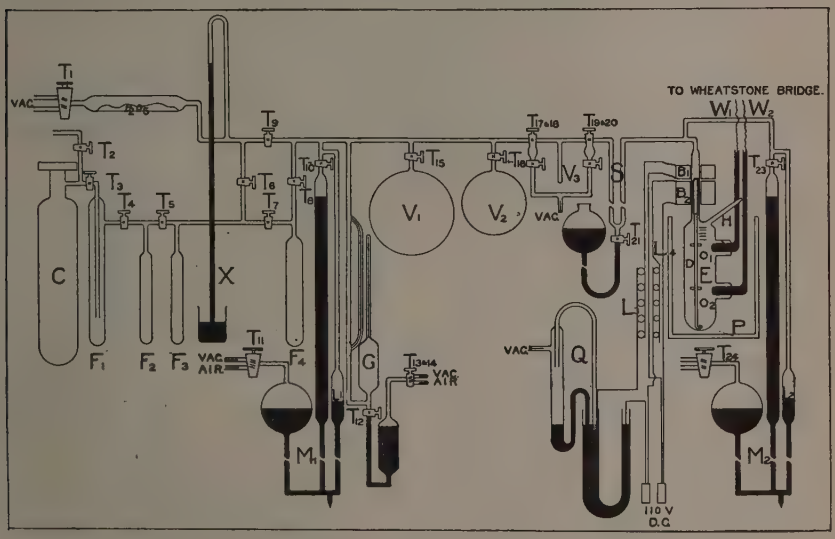

FIG. 1. *Diagram of apparatus.*

was connected to a distillation cell from which the conductivity water was distilled into the cell after a series of freezings and evacuations to rid it of any residual air. The mercury seal S provided a system free from stopcocks during the distillation.

M_2 was a glass manometer similar to M_1 and was used for the measurement of vapor pressures. At low pressures, where the concentration coefficient of the vapor pressure was small, a cathetometer was used for making the readings.

The Wheatstone Bridge consisted of a Leeds and Northrup Kohlrausch slide wire, two banks of Curtiss-wound resistance coils, one reading in steps of 1 ohm from 1 to 1000 ohms, and the other in banks of thousands reading up to 40000 ohms. These resistances were checked against standard coils and were found to be accurate. The slide wire was also calibrated and gave

satisfactory results. A condenser with a maximum capacity of 0.00012 microfarad was shunted across the resistance terminals in order to balance out any capacity that might exist in the cell at low concentrations. This aided in giving better end-points. A Vreeland oscillator, operating on a frequency of 1000 cycles, was used as a source of current. This oscillator gives a pure sine wave with no harmonics. One end of the slide wire was grounded to the plumbing in the laboratory and at no time were any body capacity effects noted. A two stage radio amplifier was used in the phone circuit; this gave much more sensitive end-points and increased the accuracy of the conductivity measurements.

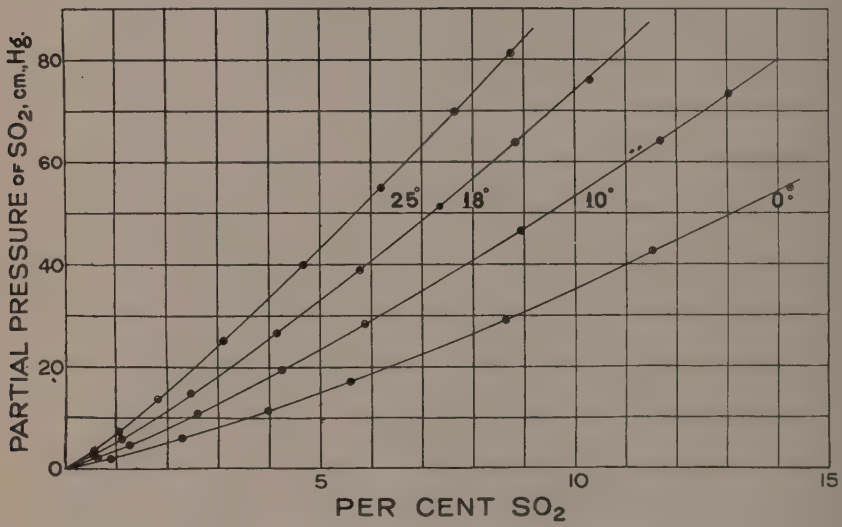

FIG. 2. *Partial vapor pressures of sulphur dioxide solutions.*

The preparation of the solutions and the calculation of the amount of gas in the solution was carried out by the method of Maass and Maass (32).

SULPHUR DIOXIDE

As was indicated in the introduction very accurate data have to be obtained for sulphur dioxide in order to obtain a true insight into the equilibria. For this reason particular care was taken and more time was spent on this system than on the other two.

A cylinder of liquid sulphur dioxide was obtained from the Ansul Chemical Co., in Marinette, Wisconsin. Analysis showed this gas to be very pure but in order to insure the greatest purity possible it was subjected to three consecutive distillations as described in the experimental section. This gave a clear sample of liquid sulphur dioxide. Freezing point and vapor pressure determinations showed it to be extremely pure and it was considered ready for use.

The method of preparing the solutions has been described in the experimental section. In each case the temperature of the conductivity cell was held constant and the concentration was raised by consecutive injections of gas. This was considered to be a more accurate procedure than varying the temperature at one concentration. Time was also saved due to the fact that relatively high concentrations were reached and the greatest time lag was involved in the injection of the gas.

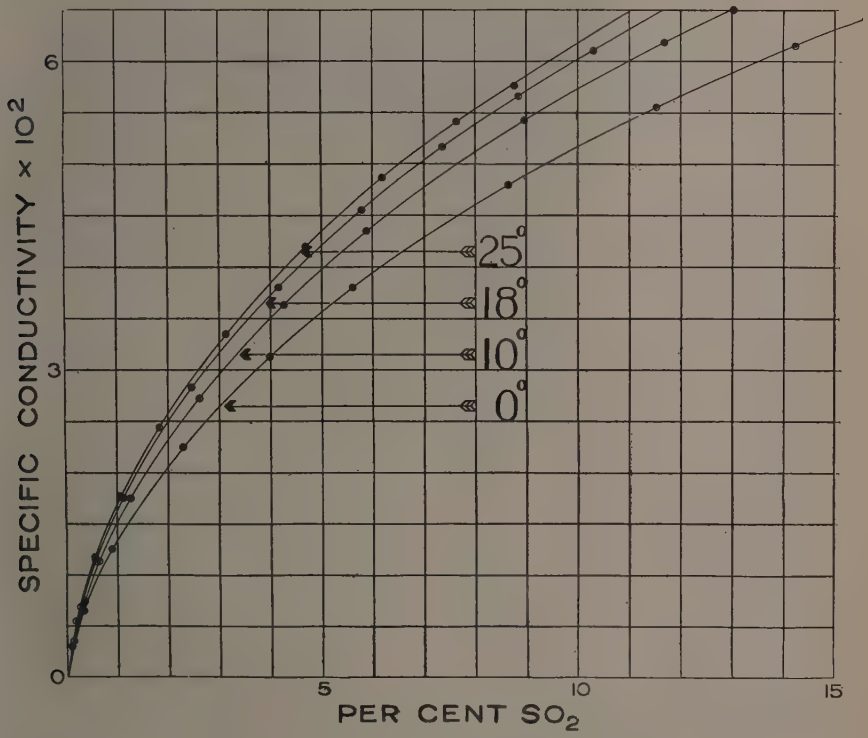

FIG. 3. *Specific conductivity of sulphur dioxide solutions.*

Results

Table I and Fig. 2 and 3 give the experimental data obtained for sulphur dioxide. It should be mentioned here that this is the second set of data for sulphur dioxide that has been obtained by the writer. A set of data was obtained in 1928-29 which was checked by a similar set in 1929-30. The two sets of results were quite gratifying inasmuch as they gave excellent checks. Only slight changes were noted in the 1929-30 conductivity measurements. These latter measurements, however, were taken as being the most nearly correct since a better conductivity apparatus, the one described in the previous section, had been used. There was no noticeable difference in the vapor pressure data.

An inspection of the conductivity and vapor pressure curves shows that they are quite regular within themselves. This is a strong argument in their favor. It was possible to cross check them by taking a certain concentration at say 10° C. and raising the temperature to 18 and 25° C. and taking vapor pressure and conductivity readings. The greatest deviation found by this method of checking was 0.1%. In this way the regularity and accuracy of procedure was proved.

TABLE I

EXPERIMENTAL DATA OBTAINED FOR THE SYSTEM SULPHUR-DIOXIDE WATER

Reading	SO_2 %	Partial pressure of SO_2, cm. Hg.	Specific conductivity	Reading	SO_2 %	Partial pressure of SO_2, cm. Hg.	Specific conductivity
At 0° C. Weight of water used = 116.010 gm.							
1	0.1369	0.17	0.00339	6	5.597	17.30	0.03800
2	0.3374	0.63	0.00650	7	8.630	29.21	0.04804
3	0.8888	1.97	0.01253	8	11.52	41.63	0.05560
4	2.284	6.05	0.02255	9	14.23	55.02	0.06158
5	3.978	11.55	0.03135				
At 10° C. Weight of water used = 115.187 gm.							
1	0.1267	0.35	0.00366	6	4.256	19.52	0.03638
2	0.3414	1.00	0.00748	7	5.872	28.37	0.04355
3	0.6360	2.12	0.01136	8	8.937	46.62	0.05431
4	1.261	4.71	0.01759	9	11.68	64.18	0.06189
5	2.593	10.98	0.02727	10	13.03	73.58	0.06491
At 18° C. Weight of water used = 116.518 gm.							
1	0.0816	0.32	0.00296	6	4.150	26.66	0.03800
2	0.2605	1.10	0.00689	7	5.773	39.01	0.04556
3	0.5563	2.68	0.01143	8	7.340	51.44	0.05169
4	1.103	5.92	0.01757	9	8.831	63.69	0.05667
5	2.458	14.83	0.02832	10	10.30	76.04	0.06108
At 25° C. Weight of water used = 116.416 gm.							
1	0.1735	0.79	0.00545	6	4.672	40.00	0.04201
2	0.5448	3.42	0.01174	7	6.184	55.00	0.04866
3	1.056	7.37	0.01775	8	7.640	69.88	0.05416
4	1.809	13.61	0.02443	9	8.756	81.17	0.05769
5	3.116	25.28	0.03355				

At 25° C. the vapor pressure values obtained by C. Maass (31), and Campbell and Maass (8) are in agreement with themselves but are 2% higher than the values obtained in the present work. There is also an irregularity in the lower pressures amounting to about 1%. At 10° C. the results of C. Maass (31) are even more seriously in error. The apparatus used by these experimenters, as mentioned before, was designed to measure high pressures and for this reason low pressures could not be obtained with as great accuracy.

The conductivity data of C. Maass (31), and Campbell and Maass (8) check to an approximation. However, their results are 0.66% higher than the present values at the higher concentrations and increase in error at the lower concentrations. The deviation may be attributed to the use of a small reaction chamber (20-25 cc), thereby cutting down the accuracy of the determination of the concentration. Higher vapor pressures and conductivities would also point to the presence of some volatile soluble impurity. This latter is not highly probable.

The theoretical treatment of sulphur dioxide as developed to date has been discussed in the introduction. It was quite apparent that over the temperature and concentration range covered in this work that equation (13), as developed by C. Maass (31), was the most rigorous and should be the logical starting point for any further development.

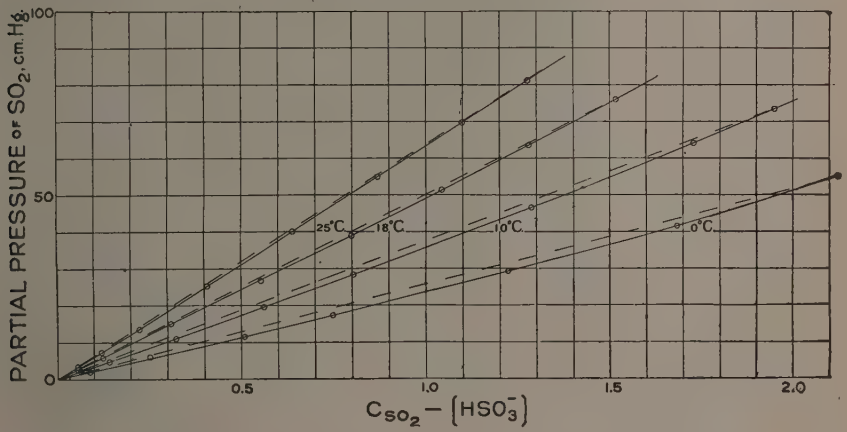

FIG. 4. *Relation of* $C_{SO_2} - [HSO_3^-]$ *to partial pressure of sulphur dioxide.*

The accompanying figure will show that the approximation due to Campbell and Maass (8) does not hold at the lower temperatures and with the more accurate data. When $C_{SO_2} - [HSO_3^-]$ is plotted against the partial pressure of sulphur dioxide above the solution, a decided curvature is noted, which increases with decreasing temperature as shown by the straight dotted lines.

This cannot possibly be due to experimental error, which will be seen from the following figures taken from the above curves drawn on a large scale. At a concentration of one gm.-mol per litre the experimental error would have to be 2 cm. in a measurement of 20 cm. whereas the experimental results are correct to 0.1 mm., or an error of 10% in the estimated value of the concentration, whereas 0.1% is the probable maximum error. Especially when it is seen that all the curves as given by the experimental points have a consistent curvature shown by their continuity, it is realized that the straight line relationship is one which will only hold at high temperatures.

It is possible to predict this curvature from the equation

$$C_{SO_2} = H\not{p}\left(1+\frac{[H_2O]}{K_1}\right) + [HSO_3^-]$$

With increasing temperature K_1 increases rapidly and with increasing sulphur dioxide concentration $[H_2O]$ decreases. The combined effect of these two factors tends to diminish the value of $1+\frac{[H_2O]}{K_1}$ and at an infinitely high concentration and temperature this term would become unity and the equation would become that of a straight line. This proves that had the work of Campbell and Maass (8) been sufficiently accurate they would have obtained curved plots at their lower temperatures and approximations to straight lines at the higher temperatures. However, as has been stated before, their water concentration did not vary enough to warrant this.

In the evaluation of the constants H and K_1 in the present work, equations (10) and (11), due to C. Maass (31), were taken as a starting point.

$$C_{H_2O} = [H_2O] + [H_2SO_3] + [HSO_3^-] \quad (10)$$

$$C_{SO_2} = [SO_2] + [H_2SO_3] + [HSO_3^-] \quad (11)$$

From (11)

$$C_{SO_2} = H\not{p}\left(1+\frac{[H_2O]}{K_1}\right) + [HSO_3^-] \text{ (or } [H^+])$$

$$C_{SO_2} - [H^+] = H\not{p}\left(1+\frac{[H_2O]}{K_1}\right)$$

$$= H\not{p}\left(\frac{1+C_{H_2O} - C_{SO_2} + H\not{p}}{K_1}\right)$$

For convenience let $C_{SO_2} - [H^+] = a$, and $C_{H_2O} - C_{SO_2} = b$

Then

$$a = H\not{p}\left(1+\frac{b+H\not{p}}{K_1}\right) \quad (16)$$

The only unknowns in equation (16) are H and K_1. It was transformed into a quadratic and by inserting values for the other terms, a, b, and $\not{p}$, in two such equations values for H and K_1 were calculated. From this calculation values of H were found to be very small and negative. It was quite obvious that H must be small and positive and that the negative value obtained could be attributed to small experimental errors which were just large enough to transform H from a small positive to a small negative quantity.

After a careful consideration of the situation the following procedure was adopted.

$$a = H\not{p}\left(1+\frac{b+H\not{p}}{K_1}\right) \quad (17)$$

$$A = HP\left(1+\frac{B+HP}{K_1}\right) \quad (18)$$

Equations (17) and (18) represent two points on a sulphur dioxide isothermal. From previous calculations it was concluded that the value of $H\not{p}$ was small

compared with b. Hence, for the time being, Hp was disregarded in the term $b+$Hp and the equations became

$$a = \mathrm{H}p\left(1+\frac{b}{\mathrm{K}_1}\right) \tag{19}$$

$$\mathrm{A} = \mathrm{HP}\left(1+\frac{\mathrm{B}}{\mathrm{K}_1}\right) \tag{20}$$

Divide (19) by (20)

$$\frac{a}{\mathrm{A}} = \frac{p\left(1+\frac{b}{\mathrm{K}_1}\right)}{\mathrm{P}\left(1+\frac{\mathrm{B}}{\mathrm{K}_1}\right)}$$

By letting $\frac{a}{p} = d$ and $\frac{\mathrm{A}}{\mathrm{P}} = \mathrm{D}$ and rearranging it follows that

$$\mathrm{K}_1 = \frac{b\left(\frac{\mathrm{B}}{b} - \frac{\mathrm{D}}{d}\right)}{\frac{\mathrm{D}}{d} - 1} \tag{21}$$

By substituting the value of K_1 obtained in (21) in equations (19) and (20) it was possible to calculate H.

There was considerable incoherent variation in K_1 and it appeared to be very sensitive to small errors in experimental data. This was overcome to a large extent by plotting per cent sulphur dioxide against d for each temperature considered and by inspection picking out pairs of logical d points from which to calculate K_1. An average of the values for K_1 thus obtained at 25 and 18° C., when substituted in equation (16), permitted of a calculation of "a" (*i.e.*, $\mathrm{C}_{\mathrm{SO}_2} - [\mathrm{H}^+]$) within two or three per cent. By trial and error, *i.e.*, by varying slightly the values of H and K_1, the correct values of "a" were obtained within 0.2%. In this way the validity of the constants H and K_1 at 25 and 18° C. was established.

This work was led further afield than was originally expected. At 10° C. the average approximate value of K_1, as calculated from (21), was found to be -2.6, and at 0° C. it was -12.1. Equation (16) may be transformed to

$$\mathrm{K}_1 = \frac{\mathrm{H}pb - \mathrm{H}^2p^2}{a - \mathrm{H}p} \tag{22}$$

In equation (22) H^2p^2 is small with respect to Hpb. H is a constant and at any given concentration and temperature p is a constant, hence an unusually small value of K_1 would be caused by an excessive diminution of the value of b. Since b is the value of the apparent concentration of the water, a low value of b would indicate that water was being removed by some means and would point toward hydrate formation. This is in agreement with the fact that below 12.1° C. a stable heptahydrate forms. In all that has gone before the influence of hydrate formation and hydration of ions on water concentration has been neglected. The influence of the solute on the equilibria, excepting between the various associated water molecules, has also been neglected. It is necessary to assume that these factors are outweighed by those which have been taken into account and emphasis is placed by the authors on the approximate nature of all the calculations. Hydration increases with lower temperature and

evidently becomes very marked at 12.1° C. by the separation of a heptahydrate and is also indicated by the above considerations to be of such an order of magnitude that it cannot be neglected for the 10 and 0° C. data.

In order to determine the extent of the hydrate formation a new equilibrium must be considered, *i.e.*, between the hydrate, the sulphur dioxide, and the water:

$$SO_2 + nH_2O \rightleftharpoons SO_2.nH_2O$$

$$[SO_2]\,[H_2O]^n = \alpha[SO_2.nH_2O] \tag{23}$$

where n is the number of molecules of water in the hydrate. The equilibrium

$$[SO_2]\,[H_2O] = K_1[H_2SO_3]$$

must also be kept in mind.

As a starting point

$$C_{SO_2} = [SO_2] + [H_2SO_3] + [H^+] + [SO_2\ \text{aq.}] \tag{24}$$

$$C_{H_2O} = [H_2O] + [H_2SO_3] + [H^+] + n[SO_2\ \text{aq.}] \tag{25}$$

$$C_{HO_2} - C_{SO_2} = [H_2O] - [SO_2] + (n-1)\,[SO_2\ \text{aq.}]$$

$$b = [H_2O] - [SO_2] + \frac{(n-1)\,[SO_2]\,[H_2O]^n}{\alpha}$$

$$= [H_2O] - Hp + \frac{(n-1)Hp\,[H_2O]^n}{\alpha}. \tag{26}$$

Also from equation (24)

$$C_{SO_2} = Hp + [H^+] + \frac{[H_2O]Hp}{K_1} + \frac{[H_2O]^nHp}{\alpha}$$

and

$$C_{SO_2} - [H^+] = Hp\left(1 + \frac{[H_2O]}{K_1} + \frac{[H_2O]^n}{\alpha}\right)$$

For convenience let $[H_2O] = [x]$, then

$$a = Hp\left(1 + \frac{[x]}{K_1} + \frac{[x]^n}{\alpha}\right) \tag{27}$$

or

$$a - Hp - \frac{[x]Hp}{K_1} = \frac{Hp[x]^n}{\alpha} \tag{28}$$

From (26)

$$b + Hp - [x] = \frac{(n-1)Hp[x]^n}{\alpha} \tag{29}$$

and combining (28) and (29)

$$\frac{b + Hp - [x]}{n-1} = a - Hp - \frac{[x]Hp}{K_1} \tag{30}$$

The value of [x] may be calculated from equation (30) provided that the values of H and K_1 are known at 10° C. Furthermore the numerical value of 7 for n may or may not be legitimate. What equation (30) really represents is that water is removed from active participation in the equilibrium in ways

other than the straightforward H_2SO_3 formation. Whether water is used up in the hydration of the ions is a moot question. Equation (30) in which n is given the somewhat arbitrary value of 7 can therefore only be looked upon as a crude approximation, valuable however in showing that another factor has to be taken into account.

What has been said above has to be borne in mind in all the calculations involving equation (30). All that can be hoped for is that reasonable values of H, K_1 and α will satisfy the experimental results. At higher temperatures also hydrate formation probably has its influence, though the higher the temperature the smaller will be its effect.

The values of H and K_1 were known for 18 and 25° C. and it was a debatable question whether a straight line extrapolation to 10 and 0° C. would be legitimate. On investigating the constants similar to H for inert gases, as given in the literature, it was found that they did not vary with temperature according to a straight line relationship. Reference was made to the apparent H calculated for sulphur dioxide from the relation $H = \frac{a}{p}$. This, of course, exhibited curvature when plotted against temperature. An arbitrary value of H at 10° C. was obtained by calculating a variation of the real H corresponding to the variation of the apparent H. To obtain the corresponding K_1 the ratios of $\frac{H}{K_1}$ were calculated at 18 and 25° C. and were extrapolated to 10° C. Since H had already been determined it was possible to calculate K_1.

Using these values obtained for H and K_1 the corresponding values of [x] at 10° C. were calculated. The values of α were then determined by inserting these approximations in equation (29) and an average value of α was obtained. These values were remarkably constant. Then, by supplying the necessary values in equation (27) it was possible to calculate values of "a" very accurately, there being only an average mean deviation of 0.1% from the experimental values.

The real dissociation constant

$$K_2 = \frac{[H^+]\ [HSO_3^-]}{[H_2SO_3]}$$

was calculated as follows:

$$K_1 = \frac{[H_2O]\ [SO_2]}{[H_2SO_3]} \qquad (4)$$

On rearranging and substituting

$$[H_2SO_3] = \frac{[H_2O]\ [SO_2]}{K_1} = \frac{(b+Hp)\ (Hp)}{K_1}$$

Hence

$$K_2 = \frac{K_1[H^+]^2}{(b+Hp)\ (Hp)}$$

K_2 is calculated only at 18 and 25° C. since the 10° C. calculations, as pointed out above, are the result of only arbitrary approximations.

The theoretical data calculated in connection with this work are presented in Table II for temperatures of 0, 10, 18, and 25° C. C_{SO_2} is the total amount

TABLE II

THEORETICAL DATA CALCULATED FOR THE SYSTEM SULPHUR DIOXIDE-WATER

SO_2, %	Density	C_{SO_2}	C_{H_2O}	Specific cond. $\times 10^3$	$[HSO_3^-]$	a	b	$Ka \times 10^3$	$K_2 \times 10^3$	a(calc.)
At 0° C.										
0.1369	1.0004	0.0213	55.46	3.39	0.0135	0.0078	55.44	23.47		
0.3374	1.0015	0.0523	55.40	6.50	0.0259	0.0263	55.35	25.59		
0.8888	1.0048	0.1393	55.26	12.53	0.0500	0.0893	55.12	28.00		
2.284	1.0127	0.3608	54.92	22.55	0.0900	0.2708	54.56	29.91		
3.978	1.0223	0.6342	54.46	31.35	0.1251	0.5091	53.83	30.74		
5.597	1.0317	0.9005	54.05	38.00	0.1517	0.7488	53.15	30.72		
8.630	1.0488	1.412	53.18	48.04	0.1917	1.221	51.77	30.11		
11.52	1.0604	1.905	52.08	55.60	0.2219	1.683	50.18	29.26		
14.23	1.0663	2.367	50.76	61.58	0.2458	2.123	48.40	28.46		
At 10° C.										
0.1267	1.0001	0.0197	55.43	3.66	0.0117	0.0080	55.41	17.26		—
0.3414	1.0012	0.0558	55.39	7.48	0.0240	0.0318	55.34	18.13		0.0298
0.6360	1.0028	0.0995	55.29	11.36	0.0365	0.0629	55.19	21.13		0.0631
1.261	1.0061	0.1978	55.12	17.59	0.0564	0.1414	54.93	22.55		0.1393
2.593	1.0131	0.4097	54.75	27.27	0.0875	0.3222	54.34	23.78		0.3207
4.256	1.0219	0.6784	54.30	36.38	0.1168	0.5616	53.62	24.29		0.5616
5.872	1.0305	0.9436	53.80	43.55	0.1398	0.8038	52.86	24.32		0.8041
8.927	1.0465	1.459	52.85	54.31	0.1744	1.285	51.39	23.65		1.286
11.68	1.0575	1.926	51.82	61.89	0.1986	1.728	49.90	22.84		1.732
13.03	1.0613	2.156	51.22	64.91	0.2084	1.948	49.07	22.28		1.954
At 18° C.										
0.0816	0.9988	0.0127	55.39	2.96	0.0083	0.0044	55.38	15.53	17.52	
0.2605	0.9997	0.0406	55.35	6.89	0.0192	0.0214	55.31	17.31	27.64	
0.5563	1.0012	0.0868	55.25	11.43	0.0319	0.0549	55.16	18.57	31.29	
1.103	1.0040	0.1727	55.11	17.57	0.0491	0.1236	54.94	19.48	33.58	0.1232
2.458	1.0108	0.3877	54.71	28.32	0.0791	0.3086	54.32	20.27	35.18	0.3069
4.150	1.0195	0.6594	54.19	38.00	0.1061	0.5533	53.53	20.36	35.69	0.5476
5.773	1.0278	0.9255	53.74	45.56	0.1273	0.7982	52.82	20.29	35.46	0.7958
7.340	1.0357	1.186	53.26	51.69	0.1444	1.042	52.08	20.01	35.02	1.042
8.831	1.0432	1.436	52.76	56.67	0.1582	1.278	51.32	19.60	34.43	1.281
10.30	1.0498	1.687	52.28	61.08	0.1706	1.516	50.59	19.20	33.91	1.520
At 25° C.										
0.1735	0.9978	0.0270	55.27	5.45	0.0137	0.0133	55.24	14.08	27.48	
0.5448	0.9996	0.0849	55.20	11.74	0.0295	0.0554	55.12	15.70	29.49	
1.056	1.0010	0.1649	54.96	17.75	0.0446	0.1203	54.80	16.52	31.52	
1.809	1.0059	0.2838	54.81	24.43	0.0613	0.2225	54.53	16.91	32.40	0.2194
3.116	1.0123	0.4918	54.42	33.55	0.0842	0.4076	53.93	17.41	33.18	0.4055
4.672	1.0200	0.7433	53.96	42.01	0.1045	0.6379	53.22	17.45	33.33	0.6379
6.184	1.0275	0.9906	53.47	48.66	0.1222	0.8684	52.48	17.19	32.83	0.8720
7.640	1.0346	1.233	53.04	54.16	0.1360	1.097	51.81	16.86	32.37	1.102
8.756	1.0403	1.420	52.66	57.69	0.1449	1.275	51.24	16.46	31.92	1.273

of sulphur dioxide in the solution expressed in gram-mols per litre. C_{H_2O} is the concentration of the water in the solution also expressed in gram-mols per litre. The density values are those obtained by Campbell and Maass (8). $[HSO_3^-]$ is the concentration of the HSO_3^- ion and is obtained by dividing the specific conductivity by the limiting value given in the following table for the conductivity of H_2SO_3 and multiplying by 1000 to bring it to gram-mols per litre. The values for the limiting conductivity of the HSO_3^- ion were obtained from the formula of Kohlrausch (26).

$$u_t = 44.3\{1+0.0242(t-18)+0.00011(t-18)^2\}$$

using Kerp and Baur's (23) value at 25° C. as revised by Lindner (28). The values for the H^+ ion of course have been well established.

TABLE III

LIMITING CONDUCTIVITIES OF SULPHUROUS ACID

Temp., °C.	H^+	HSO_3^-	H_2SO_3	Temp., °C.	H^+	HSO_3^-	H_2SO_3
0	224.2	26.4	250.6	18	315.0	44.3	359.3
10	275.5	36.0	311.5	25	348.5	49.7	398.2

The values given for a are those of $C_{SO_2} - [HSO_3^-]$ and represent the undissociated sulphurous acid providing that all the sulphur dioxide is combined with water. $C_{H_2O} - C_{SO_2}$ is the b value given and represents the amount of uncombined water assuming that all the sulphur dioxide is combined with water. These assumptions are not true but this mode of tabulation serves as a convenient means in the calculations. The calculation of K_a, K_2 and a has been previously discussed.

The equilibria constants have been obtained more accurately than ever before and fit in with the experimental data within the range of experimental error. The results of previous experimenters have failed to show definitely various fine points which are quite important. For instance, Campbell and Maass (8), Lindner (28), and Kerp and Baur (23) noted that the value of the apparent dissociation constant, K_a, varied with temperature but they did not notice any regular variation with changing concentration. Fig. 5 shows that there is a distinct variation of K_a at all temperatures considered, the rate of

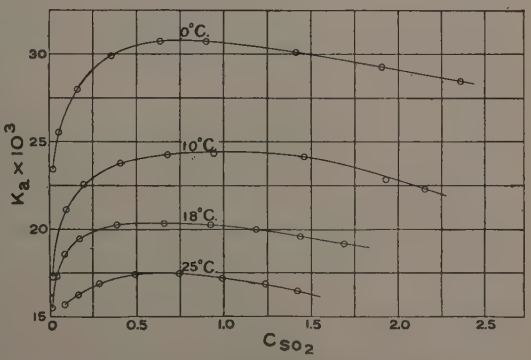

FIG. 5. *Relation of K_a to concentration in the system sulphur dioxide-water.*

increase being greater at the lower concentrations. With increasing temperatures there is decreasing variation. This may be in agreement with the theory evolved above provided that another factor, only important at very low concentrations, is taken into account. This new factor is the secondary dissociation of the sulphurous acid, the additional H^+ ion causing an increase in K_a.

The equilibrium

$$H_2O + SO_2 \rightleftharpoons H_2SO_3$$

has the opposite effect causing a decrease in K_a with rise in concentration as given by the equation

$$K_a = \frac{K_2[H_2O]}{K_1+[H_2O]}$$

Since the secondary dissociation loses its effect with increasing concentration a maximum value of K_a must be reached. Since K_1 increases with rise in temperature the rate of decrease in K_a beyond the maximum concentration should be less at the higher temperatures which was pointed out above. Furthermore it can be predicted that the maximum value of K_a is shifted to a higher concentration with rise in temperature. This variation in K_a is therefore one of the best proofs of the existence of uncombined sulphur dioxide, and also that the amount of free sulphur dioxide increases with rise in temperature.

In the comparison of the observed values of a with those calculated on the basis of equation (16) it is apparent that the poorest agreement is found at the very low concentrations. This is due to the secondary dissociation which has not been taken into account.

The value of K_a reaches a maximum and remains practically constant over a short range of concentration but it then begins to fall off again. For this reason it is illegitimate to strike an average value. The maximum values agree very well with the average values of previous experimenters. Comparison is only possible at 0 and 25° C.

TABLE IV

COMPARISON OF APPARENT DISSOCIATION CONSTANTS

Temperature, °C.	Kerp and Baur	Lindner	Campbell and Maass	This work
0		31.1	31.3	30.7
25	17.4	17.4	17.4	17.4

Dissociation constants do not ordinarily vary to any great extent with temperature. The large variation of K_a proves that it is only an apparent dissociation constant. The values of K_2 at 18 and 25° C., which vary only slightly, prove that it is a true dissociation constant. K_2 varies with the concentration to about the same extent that K_a does. This follows from what has gone before. It is evident that K_2 will always be larger than K_a but will approach it in value when K_1 is small.

Table V contains the values for H and K_1 at the three temperatures investigated.

TABLE V

H AND K_1 AT VARIOUS TEMPERATURES

Temperature, °C.	10	18	25
H	0.01080	0.00870	0.00758
K_1	36.80	39.50	48.51

It will be noted that the value of H decreases and that of K_1 increases with rising temperature. This is what would be expected from the respective equilibria

$$[SO_2] = Hp \qquad (2)$$

and

$$K_1 = \frac{[H_2O]\ [SO_2]}{[H_2SO_3]} \qquad (4)$$

From equation (2) the per cent of uncombined sulphur dioxide can be readily calculated. The values given in Table VI show their order of magnitude.

TABLE VI

COMPARISON OF UNCOMBINED SULPHUR DIOXIDE CONCENTRATION WITH TOTAL SULPHUR DIOXIDE CONCENTRATION

C_{SO_2}, %		2	4	6	8	10
SO_2, %	18° C.	0.626	1.407	2.221	3.071	3.962
	25° C.	0.732	1.608	2.573	3.457	—

The constants H, K_1, and K_2 have not been evaluated for the data at 0° C. It was deemed sufficient proof for the theory to have consistent data at three temperatures. The calculations at 10° C. were very lengthy and it was foreseen that it would take even longer to handle the data at 0° C. since it would necessitate finding values for H and K_1 by trial. The extrapolation of the values of H and K_1 from 10 to 0° C. could not be expected to follow the same ratio as from 18 to 10° C.

After a discussion of the carbon dioxide and ammonia systems the conclusions to be drawn from the sulphur dioxide system will be summed up once more.

CARBON DIOXIDE

An investigation of the equilibria existing in aqueous solutions of carbon dioxide presents essentially different problems from those encountered in sulphur dioxide systems. Sulphur dioxide has a solubility in water sixty times greater than that of carbon dioxide. Sulphurous acid behaves as a strong acid while carbonic acid is apparently very weak and has an extremely small apparent dissociation constant. For these reasons the equilibria must be investigated from a different standpoint as will be seen in this section.

Experimental

The carbon dioxide was generated in a Kipp loaded with very pure marble and dilute hydrochloric acid. The gas was passed through a water wash bottle to remove any acid spray and then through two more wash bottles, one containing alkaline potassium permanganate and the other a solution of sodium carbonate. It was then passed slowly through a large phosphorus pentoxide tube and was condensed with liquid air. This was followed by a triple distillation similar to the one discussed in the experimental section.

The only possible impurity in the gas was a trace of hydrogen chloride. A test was made for this by bubbling a sample of the gas through a solution of silver nitrate. After half an hour no precipitation of silver chloride was noted, which was considered sufficient evidence that no hydrogen chloride was present.

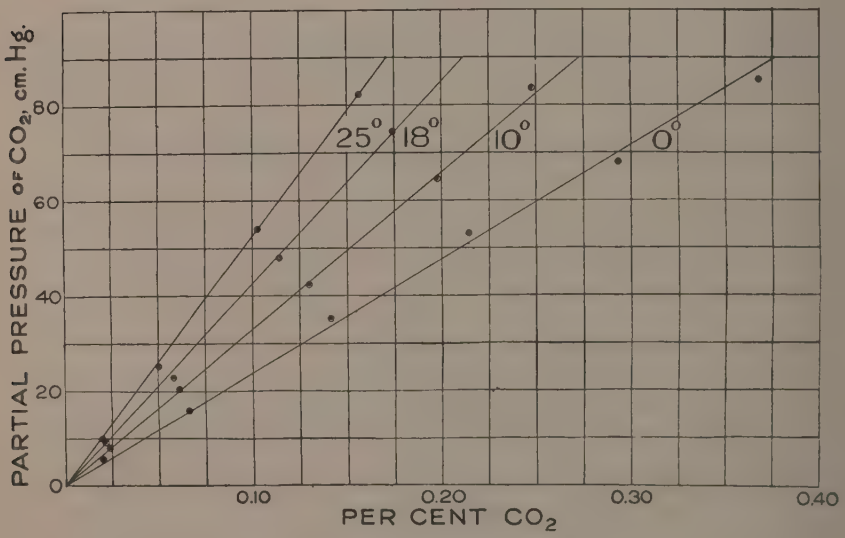

FIG. 6. *Partial vapor pressures of carbon dioxide solutions.*

Due to the fact that carbon dioxide possesses such a small solubility in water every precaution had to be taken in the measurement of the amount of gas injected. The rate of solution was very slow and a long time was necessary to reach equilibrium, usually about 90 min. After completing a run at 0° C. it was decided that much time would be saved if solutions were prepared at 10° C. and after making measurements raise the temperature to 18° and 25° C. since equilibrium was reached more rapidly when the gas was coming out of the solution than when it was going into solution. This procedure was found to be much more satisfactory.

Results

Table VII contains the experimental data and the theoretical data derived from them. The units are the same as those used for sulphur dioxide. Fig. 6 presents the vapor pressure relationships and Fig. 7, the specific conductivity.

It should be stated at this point that the vapor pressure data at 0° C. are inaccurate. The plot in Fig. 6 would indicate that the evacuated arm of the manometer had sprung a leak at some time after a concentration of 0.25% carbon dioxide had been reached since the vapor pressure as measured was too low. Hence the data at 10, 18 and 25° C. only will be considered in the discussion.

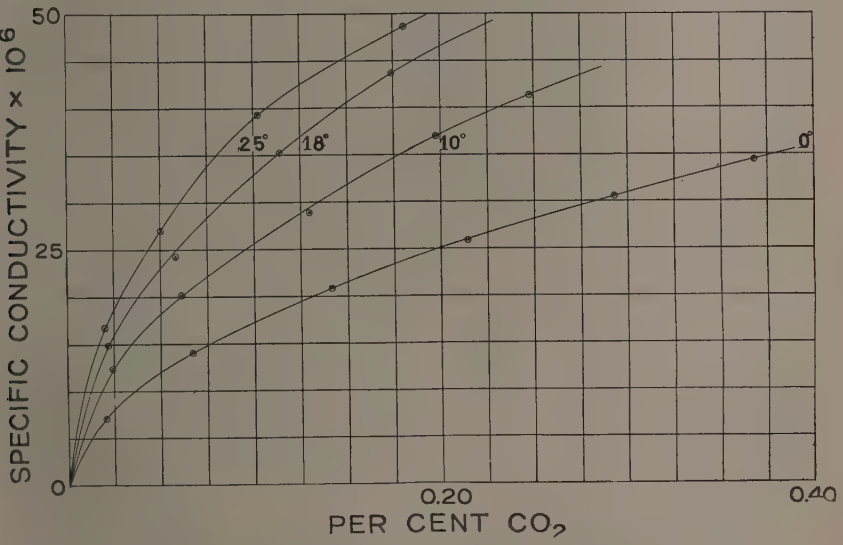

FIG. 7. *Specific conductivity of carbon dioxide solutions.*

The vapor pressure and conductivity data at 10, 18 and 25° C. were consistent within themselves and the curves show the regularity that is to be desired. It will be noticed that the maximum concentration reached at 0° C. was 0.36% as compared with a maximum concentration of 14.2% for sulphur dioxide. In this region of concentration the vapor pressure of both gases is approximately atmospheric. This gives a measure of the relative solubilities.

Since carbon dioxide solutions having vapor pressures of one atmosphere or less are of very low concentration, in every case less than 0.5%, there is only a very slight change in the water concentration, in fact it may be considered as being constant. Hence it has not been possible to treat the equilibria in the same manner as those of sulphur dioxide.

TABLE VII

EXPERIMENTAL AND THEORETICAL DATA FOR THE SYSTEM CARBON DIOXIDE-WATER

CO_2 %	C_{CO_2}	Specific cond. $\times 10^6$	Partial pressure of CO_2, cm. Hg.	$[H^+]$	α	$K_a \times 10^8$	$H \times 10^5$
At 0° C.							
0.0202	0.00458	7.19	5.70	0.000028	0.00456	17.44	80.00
0.0661	0.01503	14.02	16.00	0.000055	0.01497	20.18	93.58
0.1412	0.03208	20.89	35.27	0.000082	0.03200	20.93	90.72
0.2143	0.04870	25.90	53.02	0.000101	0.04860	21.23	92.06
0.2929	0.06656	30.57	68.13	0.000119	0.06640	21.65	97.47
0.3676	0.08354	34.42	85.30	0.000135	0.08341	21.85	97.81
							Av. 91.94
At 10° C.							
0.0240	0.00545	12.30	8.17	0.000038	0.00541	26.87	66.22
0.0611	0.01389	20.18	20.61	0.000062	0.01383	28.30	67.11
0.1297	0.02947	29.89	42.41	0.000092	0.02938	29.22	69.28
0.1975	0.04488	37.00	64.48	0.000115	0.04477	29.39	69.45
0.2475	0.05624	41.34	83.56	0.000128	0.05611	29.27	67.16
							Av. 67.84
At 18° C.							
0.0216	0.00491	14.92	9.23	0.000039	0.00487	32.48	52.82
0.0580	0.01318	24.80	22.98	0.000066	0.01312	33.35	57.10
0.1140	0.02590	35.25	49.14	0.000094	0.02581	34.23	52.52
0.1740	0.03954	43.69	74.45	0.000116	0.03942	34.44	52.94
							Av. 53.84
At 25° C.							
0.0200	0.00454	16.71	9.89	0.000040	0.00450	35.22	45.50
0.0502	0.01141	27.00	25.32	0.000064	0.01135	36.46	44.83
0.1025	0.02329	39.33	54.00	0.000093	0.02320	37.84	42.96
0.1559	0.03542	48.64	82.22	0.000116	0.03530	38.04	42.93
							Av. 44.05

Consider an equation of the form of (13a) in connection with carbon dioxide

$$C_{CO_2} = Hp\left(1 + \frac{[H_2O]}{K_1}\right) + [H^+]. \qquad (31)$$

In this instance the value of H_2O is constant, hence the term $\left(1 + \frac{[H_2O]}{K_1}\right)$ is a constant. Equation (31) is, therefore, that of a straight line. When $C_{CO_2} - [H^+]$ was plotted against the partial pressure of carbon dioxide a straight line relationship was obtained as predicted. This is illustrated in Fig. 8. If concentrations of carbon dioxide as high as 5 to 10% were obtained there would be sufficient change in the water concentration to make the above

approximation illegitimate and a plot, similar to that given in Fig. 8 would show curvature such as is exhibited in Fig. 4 for sulphur dioxide. Such a procedure would necessitate the measurement of vapor pressures up to approximately 100 atmos. Vapor pressures of this order of magnitude have been measured by Sander (43) but with insufficient accuracy for this purpose and no conductivity data at these pressures are available.

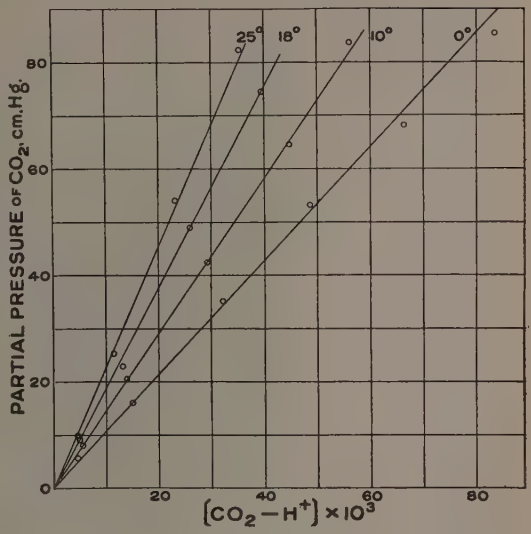

FIG. 8. *Relation of* $C_{CO_2} - [H^+]$ *to partial pressure of carbon dioxide.*

In Table VIII, P_S is the vapor pressure in atmospheres as obtained by Sander (43) experimentally. The column P_H contains the pressures corresponding to the concentrations in the first column calculated using the Henry's Law constant (1.105×10^6) obtained in the present work.

TABLE VIII

COMPARISON OF CARBON DIOXIDE VAPOR PRESSURE DATA DUE TO SANDER WITH THEORETICAL DATA CALCULATED FROM HENRY'S LAW

C_{CO_2}	0.7278	0.8974	1.067	1.199
P_S	25	35	45	53
P_H	18.8	23.1	27.4	30.1

It would be expected that if the values of P_S were plotted against concentration they would exhibit curvature. On the other hand they give a straight line relationship, curvature if any being not discernible. This straight line when extrapolated does not pass through the origin as it theoretically should but meets the pressure axis at a point corresponding to -18 atmospheres. The improbability of Henry's Law holding at these high pressures combined with the peculiar results obtained from extrapolation indicates that Sander's (43) data are inaccurate and show additional reason for continuing this work at higher pressures.

The apparent dissociation constant has been calculated from the relationship

$$K_a = \frac{[H^+]\,[\tfrac{1}{2}CO_3^-]}{C_{CO_2} - [H^+]}.$$

The limiting value of the conductivity of the $\frac{1}{2}CO_3^-$ ion was obtained at the various temperatures from the value given by Kohlrausch (26) at 18° C. by employing the equation

$$T = 60\left\{1 + 0.0270\,(T - 18)\right\}$$

The values are given in Table IX.

TABLE IX

IONIC MOBILITIES OF CARBONIC ACID (KOHLRAUSCH)

Temp., °C.	H^+	$\frac{1}{2}CO_3^-$	H_2CO_3	Temp., °C.	H^+	$\frac{1}{2}CO_3^-$	H_2CO_3
0	224.2	30.8	255.0	18	315.0	60.0	375.0
10	275.5	47.0	322.5	25	348.5	71.3	419.8

The concentration of the H^+ ion was calculated by the same method as HSO_4^- in the previous section.

The constant H calculated from the values of $\frac{a}{p}$ is the reciprocal of the Henry's Law constant given in the International Critical Tables, the value of a in this case being in gram-mols per litre rather than in mol fraction as in the tables.

The vapor pressure data agree very well with those of Bohr (5). This agreement is indicated in the tabulation of Henry's Law constants given in Table X. In this case

$$H_1 = \frac{\text{partial pressure of } CO_2 \text{ in mm. of Hg.}}{\text{mol fraction of } CO_2}$$

TABLE X

HENRY'S LAW CONSTANTS FOR CARBON DIOXIDE

Temperature, °C.		10	18	25
Henry's law constants	Bohr	0.791	1.018	1.243
	Present work	0.797	1.039	1.255

It will be noted that in each case the present work gives a slightly higher value for the constant, the difference being fairly regular.

The conductivity data agree almost perfectly with those of Knox (24) and fairly well with those of Pfeiffer (42), but are constantly higher than those of Kendall (22). This is brought out in Table XI which compares the present work with that of Knox (24) and Kendall (22) at 18° C.

Data at other temperatures where comparison is possible are not tabulated since the same percentage deviation is noted in each case.

A good part of this deviation may be accounted for in Kendall's determination of the carbon dioxide concentration. Due to the fact that it is possible to prepare solutions of only very low concentrations at the pressures here

TABLE XI

SPECIFIC CONDUCTIVITY OF CARBONIC ACID AT 18° C.

C_{CO_2}	Specific conductivity $\times 10^6$		
	Kendall	Knox	Present work
0.0080	17.30	19.56	19.00
0.0188	27.20	29.70	29.69
0.0400		43.77	43.80

considered, a small error in the determination of this concentration would cause a large percentage error. Kendall, using a modification of Pettenkofer's method (48), ran the solution directly from the cell into a bottle containing air free from carbon dioxide. Excess of baryta solution of known concentration was added and the carbon dioxide was determined as barium carbonate. For larger concentrations of carbon dioxide this would be considered by the writers as a sound procedure but in this case it verges on microanalysis. An average concentration of carbon dioxide as determined by Kendall (22) was 0.02 gram-mols per litre. Working with 30 cc. of such a solution, as he did, meant the absolute determination of approximately 0.003 gm. of barium carbonate by titrating the excess of barium hydroxide with hydrochloric acid. Kendall stated that his determinations checked within 0.2% but this would not mean that his determination was correct within that amount as far as the absolute value is concerned. A rough calculation shows that his possible error is in the region of 5%.

In the present work the amount of gas added to the solution was measured by taking pressure and temperature readings of the gas in a calibrated volume before injecting it into the reaction chamber. This combined with vapor pressure readings good to 0.02 cm. permitted of the calculation of the concentration with an accuracy of 0.1%.

A comparison of the conductivity data due to Kendall (22) and those of the present work may also be obtained from Table XII which contains the dissociation constants, maximum values being given in each case.

TABLE XII

DISSOCIATION CONSTANTS OF CARBONIC ACID

Temperature, °C.		18	25
Dissociation constants $\times 10^8$	Kendall	31.4	34.9
	Present work	34.4	38.0

Another point which is not brought out in Kendall's work is the regular variation of K_a with concentration as is shown in Fig. 9. The values of Knox (24), on the other hand, show this variation. This would indicate more

precise measurements in the present work. Kendall also claims that his K_a is a true dissociation constant but previous discussions in this paper have proved that it is only an approximate constant.

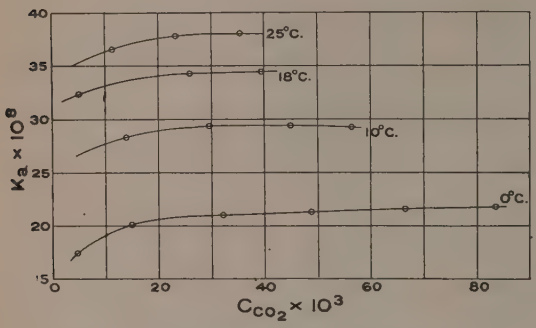

FIG. 9. *Relation of K_a to concentration in the system carbon dioxide-water.*

As has been previously stated, such a small range of concentration permits of only an approximate determination of the equilibrium existing in solutions of carbon dioxide. This work has been merely preliminary and it is hoped that it may be continued by future workers who are interested in this type of research. The value of such data as would be obtained has been previously discussed.

AMMONIA

The system ammonia-water differs in several ways from the two previous systems studied. For vapor pressures of corresponding magnitudes ammonia is two hundred times more soluble in water than is sulphur dioxide. The specific conductivity of ammonia solutions rises sharply to a maximum at low concentrations and then decreases rapidly becoming asymtotic to zero at very

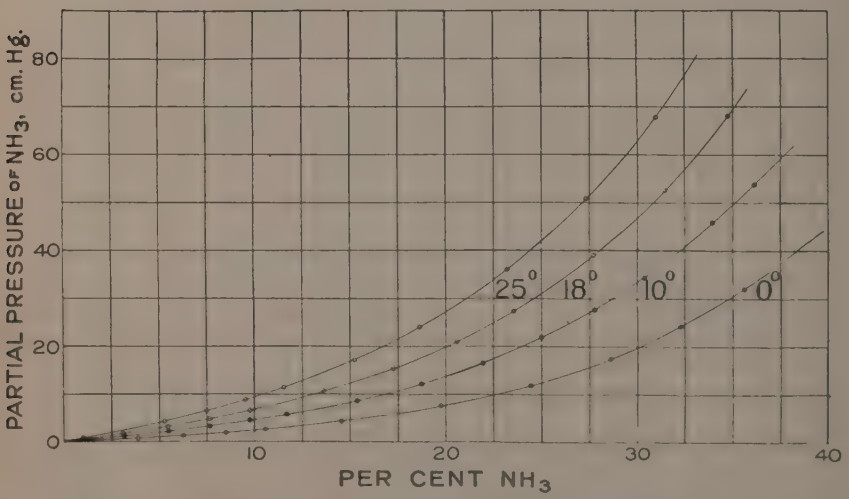

FIG. 10. *Partial vapor pressures of ammonia solutions.*

high concentrations. At the concentrations covered for sulphur dioxide and carbon dioxide the conductivity rose steadily and there was not much indication of a maximum being reached.

A cylinder of liquid ammonia was obtained from the Matheson Company, North Bergen, N.J. Freezing point and vapor pressure determinations showed it to be very pure, there being only a trace of water present. Purification was effected by passing the ammonia, in the gaseous state, through long tubes of

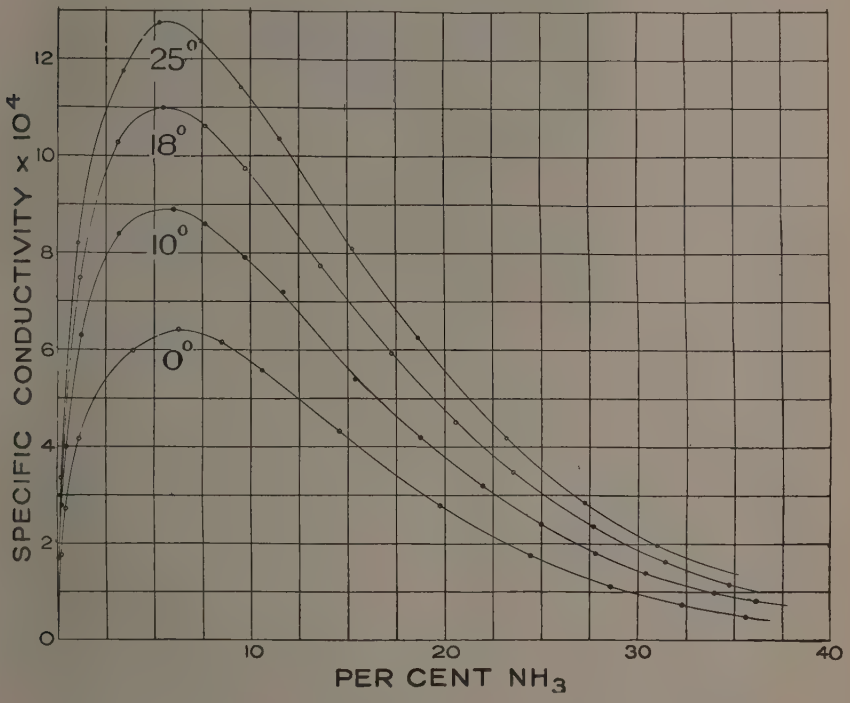

FIG. 11. *Specific conductivity of ammonia solutions.*

lime and condensing it again with a dry ice-ether mixture. The drying process was followed by two fractional distillations, the middle fraction (75%) being retained. The solutions were prepared as previously discussed in the experimental section. The conductivity cell allowing for 100% expansion of the solution was used.

The experimental data are given in Table XIII for temperatures of 0, 10, 18, and 25° C. Fig. 10 and 11 present the vapor pressure and specific conductivity data relationships at the four temperatures. The lower vapor pressures, where the change in pressure with increasing concentration is very small, were measured with a cathetometer. In the calculation of the concentrations the molecular weights of ammonia as found by Carpenter (9)

TABLE XIII

EXPERIMENTAL DATA OBTAINED FOR THE SYSTEM AMMONIA-WATER

NH_3 %	Density	C_{NH_3}	Specific cond. $\times 10^4$	Partial pressure of NH_3, cm. Hg.	NH_3 %	Density	C_{NH_3}	Specific cond. $\times 10^4$	Partial pressure of NH_3, cm. Hg.
At 0° C. Weight of water used = 21.124 gm.									
0.419	0.9984	0.246	2.721	0.15	14.51	0.9482	8.095	4.327	4.46
1.072	0.9958	0.628	4.167	0.29	19.76	0.9324	10.84	2.791	7.75
3.882	0.9847	2.249	5.992	0.70	24.42	0.9191	13.20	1.754	12.05
6.241	0.9759	3.583	6.421	1.43	28.58	0.9078	15.26	1.138	17.71
8.474	0.9682	4.827	6.152	2.00	32.28	0.8983	17.06	0.741	24.38
10.56	0.9610	5.970	5.584	2.72	35.60	0.8900	18.64	0.488	32.18
At 10° C. Weight of water used = 21.525 gm.									
0.213	0.9990	0.125	2.732	0.10	15.35	0.9424	8.511	5.373	8.82
0.448	0.9979	0.263	3.943	0.21	18.72	0.9316	10.26	4.106	12.40
1.221	0.9946	0.714	6.198	0.48	21.95	0.9217	11.91	3.135	16.73
3.162	0.9866	1.835	8.313	1.24	25.00	0.9127	13.42	2.329	22.15
5.475	0.9766	3.149	8.837	2.27	27.78	0.9047	14.79	1.764	28.03
7.626	0.9694	4.349	8.520	3.38	30.38	0.8974	16.03	1.343	34.73
9.705	0.9616	5.491	7.795	4.60	33.92	0.8880	17.72	0.914	46.27
11.68	0.9546	6.560	7.105	5.92	36.12	0.8821	18.74	0.727	54.27
At 18° C. Weight of water used = 21.110 gm.									
0.397	0.9984	0.233	4.500	0.21	17.24	0.9328	9.461	5.837	15.61
1.168	0.9937	0.683	7.382	0.70	20.55	0.9222	11.15	4.407	21.40
3.109	0.9851	1.801	10.18	1.81	23.54	0.9126	12.64	3.376	27.93
5.421	0.9759	3.113	10.90	3.35	27.69	0.9000	14.66	2.261	39.51
7.632	0.9675	4.343	10.51	4.96	31.42	0.8890	16.44	1.529	53.17
9.729	0.9594	5.492	9.641	6.72	34.73	0.8794	17.97	1.069	68.73
13.61	0.9450	7.565	7.643	10.82					
At 25° C. Weight of water used = 21.016 gm.									
0.404	0.9971	0.237	5.290	0.31	11.51	0.9504	6.436	10.35	11.74
1.042	0.9931	0.608	8.207	0.84	15.22	0.9370	8.389	8.100	17.60
3.732	0.9810	2.154	11.76	2.38	18.61	0.9250	10.13	6.254	24.56
5.259	0.9749	3.016	12.75	4.43	23.20	0.9100	12.42	4.193	36.76
7.456	0.9660	4.238	12.36	6.66	27.30	0.8974	14.42	2.857	51.63
9.517	0.9581	5.364	11.42	9.09	30.97	0.8864	16.15	1.965	68.67

were used. The densities given in the above table are those due to Nichols and Wheeler (36). The column C_{NH_3} represents the concentration of ammonia in gram-mols per litre.

As in previous sections the regularity of the data, as exhibited by the plots, is a favorable point. Both the vapor pressure and specific conductivity curves lie in legitimate regions with respect to the different temperatures at which they were obtained.

The best vapor pressure data available with which to compare the present work are those given by Perman (41, p. 1397). Table XIV contains the

comparison of the data. At the higher concentrations Perman's data are slightly higher than those obtained in this work. A higher vapor pressure would indicate either the presence of some volatile impurity in the ammonia, a slight difference in temperature, or incomplete equilibrium. A temperature difference of 0.2° C. would account for this.

TABLE XIV

PARTIAL PRESSURES OF AMMONIA SOLUTIONS AT 10° C.

NH_3, %	4.16	8.26	12.32	15.88	20.54	21.83
Partial pressure of NH_3						
Perman (41)	1.65	3.72	6.42	9.51	14.92	16.98
Present work	1.65	3.72	6.30	9.20	14.50	16.40

On account of the great solubility of ammonia in water the vapor pressures are much lower than those of the two systems dealt with previously. Another reason for such low vapor pressures will be discussed later.

Conductivity data for ammonia are plentiful for dilute solutions but rather scarce for solutions of concentrations greater than 0.1 *N*. Considerable deviation is found in the low concentration data. The chief investigators have been Noyes and Kato (38) and Lunden (29, 30). It has been possible to overlap their range of concentration at only two points in the present work and the agreement there is not good. However, great accuracy is not claimed at the extremely low concentrations in this work since a slight amount of the ammonia injected into the cell at the beginning of a run might be absorbed by the stopcock grease and adsorbed on the glass walls of the system. This amount, though slight, would have a relatively large effect on the first value. The values obtained by Kohlrausch (25, p. 1078) up to concentrations of 30.5% check very well with the present data. Comparisons of the above-mentioned data are given in the following tables.

TABLE XV

SPECIFIC CONDUCTIVITY OF AMMONIA SOLUTIONS $\times 10^4$ (LOW CONCENTRATIONS)

Temp., °C.	C_{NH_3}	Lunden	Noyes and Kato	Present work
18	0.083	—	2.81	2.66
	0.10	3.18	3.10	—
25	0.10	3.70	3.62	3.41

It will be noted from the last column of Table XVI, that the Kohlrausch conductivity curve intersects that of the present work in two places but the difference is never very large. The average mean deviation over the whole range is 0.03 mhos.

TABLE XVI

SPECIFIC CONDUCTIVITY OF AMMONIA SOLUTIONS $\times 10^4$ (HIGH CONCENTRATIONS)

% NH_3	Kohlrausch	Present work	Difference	% NH_3	Kohlrausch	Present work	Difference
0.1	2.51	2.51	—	4.01	10.95	10.76	0.19
0.4	4.92	4.92	—	8.03	10.38	10.48	−0.10
0.8	6.57	6.57	—	16.15	6.32	6.46	−0.14
1.6	8.67	8.52	0.15	30.50	1.93	1.79	0.14

The conditions existing in aqueous solutions of ammonia may be expressed in two equations similar to (10) and (11) for sulphur dioxide.

$$C_{H_2O} = [H_2O] + [NH_4OH] + [OH^-] \tag{32}$$

$$C_{NH_3} = [NH_3] + [NH_4OH] + [OH^-] \tag{33}$$

By following a procedure similar to that used in the previous section an equation of the form of (16) is obtained.

$$a = Hp\left(1 + \frac{b + Hp}{K_1}\right) \tag{34}$$

In this case $a = C_{NH_3} - [OH^-]$ and $b = C_{H_2O} - C_{NH_3}$. On solving (34) for H and K_1, H was found to be extremely small and in some cases negative. In every case it was extremely small compared with the corresponding value of H for sulphur dioxide. This showed that the amount of uncombined ammonia in the liquid phase was negligible. It was borne out by the fact that the vapor pressures were relatively low as compared with those of solutions of sulphur dioxide where there is a considerable amount of uncombined reactant present.

Assuming that the amount of uncombined ammonia was negligible it was necessary to rearrange equation (34) to fit the case, if possible, and to prove that the above assumption was correct. Since H is small, Hp in the term $(b + Hp)$ is negligible compared with b. K_1 is also very small and the value of $\frac{b}{K_1}$ is very large compared with 1. Hence equation (34) becomes

$$a = \frac{Hpb}{K_1}$$

or

$$\frac{a}{b} = \frac{Hp}{K_1} = kp \tag{35}$$

which is the same as

$$\frac{C_{NH_3} - [OH^-]}{C_{H_2O} - C_{NH_3}} = kp \tag{36}$$

Since the value of OH^- is very small (36) may be written

$$\frac{C_{NH_3}}{C_{H_2O} - C_{NH_3}} = kp \tag{37}$$

without affecting the accuracy appreciably.

When $\frac{a}{b}$ was plotted against the partial vapor pressure of the ammonia at each temperature investigated straight lines were obtained as predicted by equation (35). From equation (37) the conclusion may then be drawn that the ratio of the concentration of the ammonia to that of the uncombined water is a constant function of the vapor pressure. It is of course impossible to differentiate between H and K_1 since the constant k gives the ratio of the two. But since a straight line relationship holds it follows that the value for K_1 must be very small, which means that by far the greatest part of the ammonia is combined. Since there is so little free ammonia in the solution the partial vapor pressure will be small in contrast with the two previous systems.

The conclusion drawn above is at variance with the results of Moore (34). Moore, using the partition coefficient of ammonia between water and chloroform, heats of neutralization, and heats of solution, calculated ionization constants for ammonia solutions and from the data thus obtained arrived at the conclusion that at 20° C. the ratio $\frac{NH_3}{NH_4OH}$ was approximately 2. The assumptions made by Moore are not justified and it was pointed out that they were at variance with the partial vapor pressures as registered by ammonia solutions.

Table XVII contains the theoretical data calculated from the experimental data contained in Table XIII. C_{H_2O} represents the water concentration in gram-mols per litre. $[OH^-]$ is the concentration of the OH^- (or NH_4^+) ion, also in gram-mols per litre. The values of a, b, and $\frac{a}{b}$ have been explained already. K_a is the true dissociation constant calculated in a similar manner

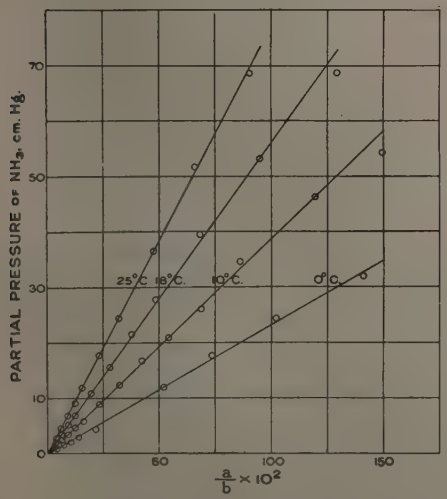

FIG. 12. *Relation of $\frac{a}{b}$ to partial vapor pressure of ammonia.*

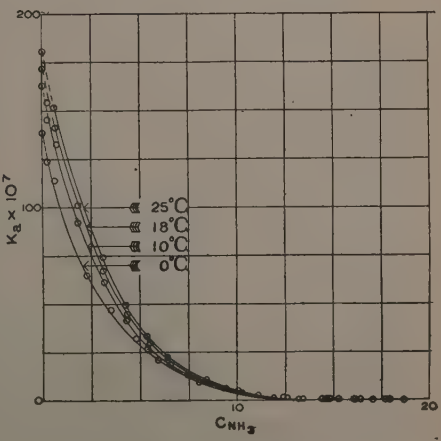

FIG. 13. *Relation of K_a to C_{NH_3} in the system ammonia-water.*

TABLE XVII

THEORETICAL DATA FOR THE SYSTEM AMMONIA-WATER CALCULATED FROM THE EXPERIMENTAL DATA IN TABLE XIII

C_{H_2O}	$[OH^-]\times 10^4$	a	b	$\frac{a}{b}\times 10^2$	$Ka\times 10^7$	C_{H_2O}	$[OH^-]\times 10^4$	a	b	$\frac{a}{b}\times 10^2$	$Ka\times 10^7$
At 0° C.											
55.17	11.29	0.244	54.92	0.445	124.6	45.00	27.74	8.092	36.91	21.93	9.51
54.67	26.71	0.625	54.04	1.157	114.1	41.53	17.89	10.84	30.69	35.33	2.95
52.53	38.41	2.245	50.28	4.465	65.70	38.55	11.24	13.20	25.35	52.07	0.95
50.78	41.16	3.579	47.20	7.580	47.34	35.98	7.29	15.26	20.72	73.64	0.35
49.18	39.44	4.823	44.35	10.87	32.25	33.76	4.75	17.06	16.70	102.1	0.13
47.69	35.80	5.967	41.72	14.30	21.47	31.81	3.13	18.64	13.17	141.6	0.05
At 10° C.											
55.33	13.55	0.124	55.21	0.22	148.2	44.29	26.66	8.508	35.78	23.78	8.35
55.13	19.56	0.261	54.87	0.47	146.4	42.04	20.37	10.26	31.78	32.27	4.04
54.54	30.75	0.711	53.83	1.32	132.9	39.93	15.55	11.91	28.02	42.50	2.03
53.04	41.25	1.831	51.21	3.57	92.92	37.99	11.55	13.42	24.57	54.62	0.99
51.29	43.84	3.144	48.14	6.53	61.13	36.25	8.75	14.79	21.46	68.93	0.51
49.69	42.27	4.344	45.34	9.58	41.12	34.67	6.66	16.03	18.64	86.00	0.28
48.19	38.68	5.487	42.70	12.85	27.26	32.56	4.53	17.72	14.84	119.00	0.12
46.79	35.26	6.566	40.23	16.29	18.95	31.27	3.61	18.74	12.53	149.60	0.07
At 18° C.											
55.20	18.91	0.231	54.97	0.42	154.6	42.85	24.52	9.459	33.39	28.32	6.36
54.50	31.01	0.679	53.82	1.26	141.5	40.66	18.52	11.14	29.51	37.79	3.07
52.97	42.76	1.796	51.17	3.51	101.7	38.73	14.19	12.64	26.09	48.45	1.59
51.23	45.80	3.108	48.12	6.46	67.47	36.12	9.49	14.66	21.46	68.32	0.61
49.60	44.16	4.339	45.26	9.59	44.93	33.84	6.42	16.44	17.40	94.50	0.25
48.06	40.51	5.488	42.57	12.89	29.89	31.86	4.49	17.97	13.89	129.30	0.11
45.31	32.11	7.562	37.75	20.03	13.64						
At 25° C.											
55.11	19.61	0.235	54.87	0.428	163.4	46.68	38.35	6.432	40.24	15.99	22.88
54.53	30.42	0.605	53.92	1.123	152.8	44.09	30.02	8.386	35.70	23.48	10.75
52.42	43.59	2.149	50.27	4.275	88.43	41.78	23.18	10.13	31.65	32.00	5.30
51.26	47.25	3.011	48.24	6.241	74.15	38.79	15.53	12.42	26.37	47.10	1.94
49.62	45.81	4.233	45.38	9.326	49.57	36.21	10.59	14.42	21.79	66.18	0.77
48.11	42.33	5.360	42.75	12.54	33.42	33.95	7.28	16.15	17.80	90.72	0.33

TABLE XVIII

IONIC MOBILITIES OF AQUEOUS AMMONIA (KOHLRAUSCH)

Temp., ° C.	NH_4^+	OH^-	NH_4OH	Temp., °C.	NH_4^+	OH^-	NH_4OH
0	38.43	117.6	156.0	18	64.00	174.0	238.0
10	52.64	148.9	201.5	25	73.92	195.9	269.8

to that used for the apparent dissociation constant for sulphur dioxide and carbon dioxide. In this case it is the true dissociation constant on account of the complete combination of the ammonia with water, the conductivity thus giving a true measure of the fraction of NH_4OH which is ionized.

The ionic mobilities were calculated from the data of Kohlrausch (26) and are given in Table XVIII.

Fig. 12 shows the straight line relationships obtained by plotting partial pressure of ammonia against the values of $\frac{a}{b}$. Fig. 13 indicates the variation of K_a with rising concentration. In Fig. 12 it will be noted that there is a slight wave in the points before and after the value of the concentration where $[OH^-]$ reaches a maximum. This would be expected from equation (36) but the deviation from a straight line is so small that the assumption of almost complete combination of ammonia with water is not invalidated. The values of the constant k are given in Table XIX.

TABLE XIX

VALUES OF CONSTANT k

Temp., °C.	0	10	18	25
k	0.0431	0.0258	0.0178	0.0130

The decrease of k with rise in temperature is to be expected since $k = \frac{H}{K_1}$, since H is bound to decrease and K_1 to increase with rise in temperature. An investigation at high temperatures would therefore be of interest since in that region $\frac{b}{K_1}$ will no longer be extremely large compared to 1.

In Fig. 13 the dotted portions of the curves are the extrapolations to the values given in the literature for very dilute solutions. It will be noted that these extrapolations continue quite regularly from the maximum values of K_a obtained in the present work. A further discussion of K_a will be included in the following section.

Discussion

In the derivations that have been made with regard to existing equilibria the existence of certain assumptions has been indicated and it may be well to emphasize once more that the authors are aware of the approximate nature of their calculations. For instance, there is no doubt that the use of the limiting conductivities used at high concentrations cannot lead to exact results. In the light of existing data it was impossible to do otherwise and that the calculations are warranted is brought out by the agreement between the experimental results and the formulas which were derived. In the following paragraphs further evidence will be offered that these speculations are justified in giving a general insight into the equilibria existing in the systems investigated.

It is evident that in the three systems there is a distinct variation of properties. Carbon dioxide is relatively insoluble, and in solution is ionized only to a slight extent. Sulphur dioxide is more soluble and in solution it is more highly ionized, while ammonia is extremely soluble, slightly ionized, and basic. Due to the wide variation of the properties of these systems, marked differences in the types of equilibria existing would be expected. This has been found to be the case.

Vapor pressure data show that ammonia has the greatest affinity for water, sulphur dioxide is next, and carbon dioxide has the smallest of the three. For this reason it was impossible to reach sufficiently high concentrations of carbon dioxide, with the means at hand, to arrive at a true measure of the equilibrium. Some advance has been made but it will be necessary to proceed to higher concentrations in order to subject it to the type of theoretical treatment used in the cases of sulphur dioxide and ammonia where the change in the water concentration plays an important part.

The relative magnitudes of the affinity of each of these gases for water may be deduced. By multiplying the mol fraction of the gas present in the solutions investigated by the vapor pressure of the pure gas in the liquid state at the same temperature it is possible to calculate the vapor pressure if an ideal solution results. Table XX shows the vapor pressures obtained from this calculation compared with the experimental pressures. C_{gas} is the concentration in gram-mols per litre and the pressures are given in centimetres of mercury.

TABLE XX

COMPARISON OF EXPERIMENTAL AND CALCULATED VAPOR PRESSURES

Gas	C_{gas}	$P_{calc.}$	$P_{meas.}$	$\frac{P_{meas.}}{P_{calc.}}$
CO_2	0.0835	3.93	85.30	21.70
SO_2	0.1393	0.29	1.97	6.79
NH_3	0.2460	1.44	0.15	0.10

It will be noted that $P_{meas.}$ is much greater than $P_{calc.}$ for carbon dioxide and sulphur dioxide and much less for ammonia. This is in good agreement with the data since carbon dioxide was found to be least combined of the three, a smaller amount of uncombined gas was present in the sulphur dioxide solutions, while ammonia, to an approximation, was largely combined.

It should be stated here that the partial vapor pressure above solutions of ammonia is due to NH_3 and not to NH_4OH as might be expected. It has been shown by Carpenter (9) that the amount of combination between ammonia and water in the vapor phase is much below 1%.

On reviewing previous tables it will be seen that the values of K_a, the apparent dissociation constant, decrease with rising temperature in the case of sulphur dioxide and increase in the cases of carbon dioxide and ammonia. It

will be remembered from a previous section that the constants K_a, K_1, and K_2 are connected by the relation

$$K_a = \frac{K_2[H_2O]}{K_1 + [H_2O]}$$

$$= K_2 \frac{1}{1 + \frac{K_1}{[H_2O]}} \qquad (38)$$

The above equation holds in the case of sulphur dioxide where $\frac{K_1}{[H_2O]}$ was shown to have the same order of magnitude as 1. In the case of ammonia where $\frac{K}{[H_2O]}$ is much less than 1, $K_a = K_2$, *i.e.*, the true and apparent dissociation constants are identical. In the case of carbon dioxide, on the other hand, since $\frac{K_1}{[H_2O]}$ is much greater than 1, the equation becomes $K_a = \frac{K_2}{K_1}[H_2O]$, and it is impossible to estimate the true dissociation constant since K_1 could not be determined from the data.

Some light is thrown on the temperature variation of the apparent dissociation constant by the above considerations. From the heat of neutralization data in the literature (27, pp. 1547-1548) the following thermal equations can be derived as holding between 18 and 25° C.

$$NH_4^+ + OH^- = NH_4OH + 1500 \text{ cal.}$$

$$H^+ + HCO_3^- = H_2CO_3 + 3700 \text{ cal.}$$

$$H^+ + HSO_3^- = H_2SO_3 - 2200 \text{ cal.}$$

It follows that the true dissociation constant will increase with rise in temperature for the ammonia and carbon dioxide systems and decrease for the sulphurous acid system. Applying the Van't Hoff isochore to calculate the percentage increase between 18 and 25° C. an increase of 6% is predicted in the case of ammonia. This compares favorably with the 5% increase of the apparent dissociation constant of ammonia, which as stated above, should be the same as the true dissociation constant.

In the case of sulphur dioxide the true dissociation constant is given by the equation

$$K_2 = \frac{[HSO_3^-]}{C_{SO_2} - H_p - [HSO_3^-]}$$

The following table gives these values calculated for various concentrations at 25 and 18° C.

Taking the average as 0.0325 at 25° C. and 0.0348 at 18° C. there is a decrease of between 7 and 8% which agrees favorably with 9% decrease calculated from the thermal data. The apparent dissociation constant decreases by 16% but this is due to the increase in K_1 with rise of temperature. Equation 38 predicts just this result from the values of K_1 for sulphur dioxide.

TABLE XXI

VALUES OF THE TRUE DISSOCIATION CONSTANTS FOR SULPHUR DIOXIDE SOLUTIONS*

18° C.				25° C.			
SO_2 %	K_2	SO_2 %	K_2	SO_2 %	K_2	SO_2 %	K_2
1.103	0.03339	7.340	0.03511	1.809	0.03148	7.640	0.03261
2.458	0.03485	8.831	0.03458	3.116	0.03280	8.756	0.03183
4.150	0.03502	10.30	0.03402	4.672	0.03321		
5.773	0.03531			6.184	0.03310		

**Values of K_2 below 1% sulphur dioxide cannot be determined accurately and hence are not included.*

Consider now carbon dioxide. Where the thermal data predict an increase of 16% in the true dissociation constant, K_2, over the seven degree range, the actual measurements of the apparent dissociation constant show only a 10% increase. However this is to be expected, since K_a is proportional to $\frac{K_2}{K_1}$ and K_1 must increase with rise in temperature and evidently does so to the extent of some 6% over this range.

The above discussion of the variation of the apparent dissociation constant with the temperature is of considerable interest because of the evidence it affords for the following generalizations.

(1) Ammonia, when dissolved in water at ordinary temperatures, is almost completely combined so that the apparent and true dissociation constants are the same.

(2) Sulphur dioxide, in aqueous solution exists partly in the combined state, partly uncombined, to an extent which can be calculated. With rise in temperature the amount of uncombined sulphur dioxide increases rapidly. The true dissociation constant can be calculated approximately.

(3) Carbon dioxide, at ordinary temperatures and pressures, is only slightly combined in its aqueous solutions and becomes decreasingly so with rising temperature. More data at high pressures are necessary to make any estimate of the true dissociation constant.

References

1. BALY, E. C. C. and BAILEY, R. A. J. Chem. Soc. 121: 1813-1821. 1922.
2. BARTH, K. Z. physik. Chem. 9: 176-219. 1892.
3. BAUD, E. and GAY, L. Ann. chim. phys. 17: 398-418. 1909.
4. BERTHELOT, M. Ann. chim. phys. (6) 1: 173. 1884.
5. BOHR, C. Ann. phys. 68: 500-525. 1899.
6. BUCH, K. Soc. Sci. Fennica Commentationes Phys. Math. 2, No. 16, 1-9. 1925.
7. BURKE, W. M. J. Am. Chem. Soc. 42: 2500-2506. 1920.
8. CAMPBELL, W. B. and MAASS, O. Can. J. Research, 2: 42-64. 1930.
9. CARPENTER, G. B. Unpublished thesis, McGill University. 1928.
10. DRUCKER, K. Z. physik. Chem. 49: 563-589. 1904.
11. ENCKELL, J. Papierfabr. 23: 633-636. 1925.
12. FINDLAY, A. and CREIGHTON, H. J. M. J. Chem. Soc. 97: 536-561. 1910.

13. FINDLAY, A. and HOWELL, O. R. J. Chem. Soc. 107: 282-284. 1915.
14. FINDLAY, A. and SHEN, B. J. Chem. Soc. 101: 1459-1468. 1912.
15. FINDLAY, A. and WILLIAMS, T. J. Chem. Soc. 103: 636-645. 1913.
16. FOOTE, H. W. J. Am. Chem. Soc. 43: 1031-1038. 1921.
17. FULDA, W. Arb. Kais. Gesund.-Amt. 30: 81. 1909.
18. HOUSEKEEPER, W. G. J. Am. Inst. Elect. Eng. 42: 954-960. 1923.
19. HUDSON, J. C. J. Chem. Soc. 127: 1332-1347. 1925.
20. JUST, G. Z. physik. Chem. 37: 342-367. 1901.
21. KANOLT, C. W. J. Am. Chem. Soc. 29: 1402-1416. 1907.
22. KENDALL, J. J. Am. Chem. Soc. 38: 1480-1497. 1916.
23. KERP, W. and BAUR, E. Arb. Kais. Gesund.-Amt. 26: 297-300. 1907.
24. KNOX. Ann. phys. 55: 44. 1895.
25. KOHLRAUSCH, F. Landolt and Börnstein, Physikalische-Chemische Tabellen, Vol. 2, 1923.
26. KOHLRAUSCH, F. and HOLBORN, L. Das Leitvermogen der Elektrolyte. 1898.
27. LANDOLT and BORNSTEIN. Physickalische-Chemische Tabellen, Vol. 2. 1923.
28. LINDNER, J. Monatsh. 33: 613-672. 1912.
29. LUNDEN, H. J. chim. phys. 5: 145-185. 1907.
30. LUNDEN, H. J. chim. phys. 5: 574-608. 1907.
31. MAASS, C. Unpublished thesis, McGill University.
32. MAASS, C. E. and MAASS, O. J. Am. Chem. Soc. 50: 1352-1368. 1928.
33. MCRAE, J. and WILSON, W. E. Z. anorg. Chem. 35: 11. 1903.
34. MOORE, T. S. J. Chem. Soc. 91: 1379-1384. 1907.
35. NEUHAUSEN, B. S. and PATRICK, W. A. J. Phys. Chem. 25: 693-720. 1922.
36. NICHOLS and WHEELER. International Critical Tables, Vol. 3. 1926.
37. NOYES, A. A. and coworkers. Landolt and Börnstein, Physikalische-Chemische Tabellen, 5th. ed. Erster Erganzungband. 1927.
38. NOYES, A. A. and KATO, Y. J. Am. Chem. Soc. 30: 335-353. 1908.
39. OMAN, E. Tekn. Tidsckrift. Kemi. 54: 81. 1924.
40. OSTWALD, W. J. prakt. Chem. (2) 32: 314. 1885.
41. PERMAN, E. P., Landolt and Börnstein, Physikalische-Chemische Tabellen, Vol. 2. 1923.
42. PFEIFFER, E. Ann. Phys. 23: 625-650. 1884.
43. SANDER, W. Z. phys. Chem. 78: 513-549. 1912.
44. SIMS. J. Chem. Soc. 14: 1. 1862.
45. SMITH, W. T. and PARKHURST, R. B. J. Am. Chem Soc. 44: 1918-1927. 1922.
46. THOMSEN, J. Thermochem. Unters. 1:169. 1882.
47. WALDEN, P. and CENTNERSZWER, M. Z. physik. Chem. 42: 432-468. 1903.
48. WALKER, J. J. Chem. Soc. 77: 1110-1114. 1900.
49. WALKER, J. and CORMACK, W. J. Chem. Soc. 77: 5-21. 1900.
50. WILKE, E. Z. anorg. allgem. Chem. 119: 365-379. 1922.
51. WRIGHT, R. J. Chem. Soc. 105: 2907-2909. 1914.

THE EFFECT OF TEMPERATURE ON THE EXPRESSION OF FACTORS GOVERNING RUST REACTION IN A CROSS BETWEEN TWO VARIETIES OF *TRITICUM VULGARE*[1]

By J. B. Harrington[2]

Abstract

Two random populations of F_2 plants of the cross Marquillo × Marquis were tested for the reaction of their F_3 seedling progenies to form 21 of *Puccinia graminis tritici* in the greenhouse, at average daily temperatures of 69.7° F. (the warm test) for one population, and 60.6° F. (the cool test) for the other. In both tests Marquis was susceptible and Marquillo was resistant. In the "warm test" ten families of a total of 781 were resistant. In the "cool test" five families of a total of 301 were susceptible. In both cases the results fitted a 63:1 ratio excellently, indicating the operation of three main genetic factors for rust reaction. A genetic hypothesis is proposed that explains the results on the basis of the influence of low temperature in curtailing the action of three susceptibility factors A, B and C carried by Marquis. The results indicate that genetic studies on characters which are easily influenced by environmental conditions should be made under controlled conditions, after ascertaining in advance the general effects of different temperatures, etc., upon the hybrid material to be used.

One of the greatest difficulties in conducting genetic studies on rust reaction has been the influence of environmental conditions, especially temperature and light, upon rust development. Of these two the influence of temperature appears to be of more practical importance, since, with a reasonable duration and intensity of light, rust develops more or less fully. The pronounced influence exerted by temperature on the development of cereal rusts has been pointed out by various investigators, including Peltier (3), Stakman and Levine (6), and quite recently by Gordon (1), Peturson (4) and Johnson (2). The work of these last three investigators is particularly interesting to the geneticist and plant breeder, since it offers at least a partial explanation of many baffling results that have been obtained.

Gordon (1) found that Joanette strain of oats showed a striking difference in its reactions to physiologic forms 1, 3, 4 and 5 of *Puccinia graminis avenae* at a low (57.4° F.) and at a high (75.4° F.) temperature. At the low temperature Joanette strain was resistant to forms 1, 3 and 4, and heterozygous to form 5, but at the high temperature it was heterozygous to forms 1 and 3 and susceptible to forms 4 and 5.

Peturson (4), working with *Puccinia coronata avenae*, obtained equally interesting results. Green Mountain and two other oat varieties were highly resistant to form 7 at 57° F., but fully susceptible at 77° F. Yet the same

[1] *Manuscript received May 7, 1931.*

Contribution from the laboratories of the University of Saskatchewan, Canada, with financial assistance from the National Research Council of Canada. This study forms a part of a co-operative attack on the problem of cereal rust in Canada, carried on jointly by the National Research Council, the Federal Department of Agriculture and the Universities of Manitoba, Saskatchewan and Alberta. The results were reported in full at the meeting of the Associate Committee on Field Crop Diseases at Winnipeg, April 10, 1931.

[2] *Professor of Field Husbandry, University of Saskatchewan.*

varieties were quite susceptible to form 4 at both temperatures. Other varieties were susceptible to both forms at both temperatures.

Results obtained by Johnson (2) with *Puccinia graminis tritici* also demonstrated that physiologic forms do not behave identically with respect to temperature. Johnson showed that Mindum and two other durum wheats which give at average greenhouse temperatures an X type reaction to ten different forms of rust were more or less resistant at low temperatures and more or less susceptible at high temperatures. For Mindum the temperature range necessary to give the difference between resistance and susceptibility varied from 7° to 13° F. for the different forms. He also found that when these varieties were infected by physiologic forms, to which they are normally resistant, there was practically no difference observable in the rust reactions obtained at the two different temperatures. Similarly, in the case of forms to which these wheats are normally susceptible, there was no difference to be seen in the ultimate rust reactions at the high and low temperatures.

The plant breeder works largely with hybrid material and he wonders, in connection with this last piece of work, what the reaction of hybrids would be when the parent varieties were (a) of the X reaction group, and (b) of the group that reacted the same whether the temperature was high or low. A striking example in answer to the last question was furnished by the results obtained from a hybrid population used in the rust research breeding work at the University of Saskatchewan.

Experimental Procedure

A random population of 781 F_2 plants of the cross Marquillo × Marquis was tested by means of F_3 seedling progeny to physiologic form 21 of *Puccinia graminis tritici* in the greenhouse during October and November 1926, at a temperature that was kept as close to 70° F. as was possible without the use of automatic controls. The average temperature during the period from the first inoculation, October 17, until seven days after the last inoculation, November 9, was 69.7° F. For convenience this test will be referred to as the "warm test". The average daily hours of sunshine was 4.0 and the average daily outdoor temperature was 32.7° F., the minimum being 12.6° F. and the maximum 49.3° F. The outside temperatures were not low enough at any time to cause a coating of ice or snow to remain on the greenhouse glass. The temperature and sunshine data are shown graphically in Fig. 1.

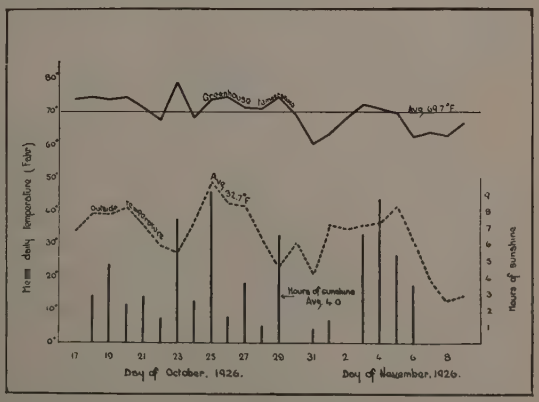

FIG. 1. *Greenhouse and outside temperature and hours of sunshine for the "warm test".*

A further test of 301 F_3 families from the same random lot of F_2 material (kept in reserve since 1926) was made during December 1930 in the same greenhouse with conditions as nearly as possible similar to those of 1926, excepting that the temperature was kept close to 61° F., the average temperature being 60.6° F. for the period of test, December 2 to 15. For convenience this test will be called the "cool test". The average daily hours of sunshine was 3.6; the average daily outdoor temperature was 23.8° F. with the minimum at 6.3° F. and the maximum at 30.6° F. As in the 1926 test, the outside temperatures were not low enough to cause a coating of ice on the greenhouse glass. The hours of sunshine averaged almost the same in the two tests, but as the sun in December gives a lower light intensity than in October or early November, supplementary artificial light was furnished in 1930 from 5 p.m. to 11:30 p.m. each night, by means of 200-watt Mazda lamps, each illuminating one square yard of greenhouse bench. It is considered by the writer, from frequent inspection of the infected seedlings in each test, that the general light environment in the 1926 test was fairly comparable to that of the 1930 test. The 1930 temperature and sunshine data are given in Fig. 2.

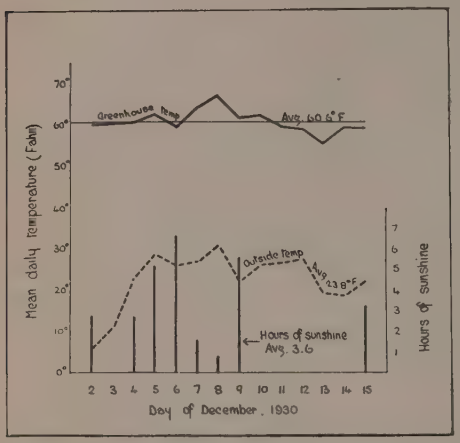

FIG. 2. *Greenhouse and outside temperature and hours of sunshine for the "cool test".*

Results

The results obtained from the two tests are given in Tables I and II. It is quite clear from Table I that susceptibility was dominant in the "warm test". Only ten families of a total of 781 were resistant. It is similarly clear from Table II that resistance was dominant in the "cool test". Five families were susceptible in a total of 301. The parent varieties, however, gave practically the same results regardless of the temperature, Marquis being susceptible in both tests and Marquillo resistant in both. These varietal behaviors are in full agreement with those obtained by Johnson (2) working with Mindum and Speltz Marz.

Perhaps the simplest and most satisfactory genetic analysis of the data consists in treating each set of results from the point of view of the fully recessive class as compared with all other classes. This is done in Table III. The X^2 test for the "warm test" results show an excellent fit to a 63:1 ratio ($P = 0.73$). If the susceptible F_2 plants (about 50) which were discarded in the field were included, the fit should still be very good ($P = 0.59$). The "cool

test" results showed an exceedingly good fit to a 63:1 ratio (P = 0.89). Thus, although the two sets of results are almost complete opposites from the point of view of resistance and susceptibility, they agree in indicating the operation of three main genetic factors for rust reaction.

TABLE I

DISTRIBUTION OF 781 F_2 PLANTS* OF THE CROSS MARQUILLO × MARQUIS, ACCORDING TO THE REACTION OF THEIR F_3 SEEDLING PROGENY TO FORM 21 IN THE GREENHOUSE AT A TEMPERATURE OF APPROXIMATELY 70° F. (WARM TEST)

Material	Distribution of F_2 plants according to the classes determined by the reaction of F_2 seedlings					Number of F_3 families
	R**	HR	H and I	HS	S	
Marquis					15	
Marquillo	13					
F_2	11	29	91	261	389	781

This was not a complete random sample with respect to rust reaction, since approximately 50 of the most susceptible plants were discarded in the field.

***R, resistant; HR heterozygous resistant; H, heterozygous; I, intermediate; HS, heterozygous susceptible; S, susceptible.*

TABLE II

DISTRIBUTION OF 301 F_2 PLANTS OF THE CROSS MARQUILLO × MARQUIS, ACCORDING TO THE REACTION OF THEIR F_3 SEEDLING PROGENY TO FORM 21 IN THE GREENHOUSE AT A TEMPERATURE OF APPROXIMATELY 61° F. (COOL TEST)

Material	Distribution of F_2 plants according to the classes determined by the reaction of F_3 seedlings					Number of F_3 families
	R*	HR	H and I	HS	S	
Marquis					20	
Marquillo	18					
F_2	209	68	14	5	5	301

See footnote of Table I.

TABLE III

COMPARISON OF THE RESULTS OF THE TWO TESTS AND THE PROBABLE FIT TO A 63:1 GENETIC RATIO IN EACH CASE

Test	Distribution of F_2 plants according to the F_3 reactions			X^2	P	Fit to a 63:1 ratio
	R	H	S			
"Warm test"	11		770*	0.12	0.73	Excellent
"Cool test"		296	5	0.02	0.89	Excellent

The addition of the very susceptible plants discarded in the field would augment this number by approximately 50, making $X^2 = 0.31$ and $P = 0.59$, which still shows an excellent fit.

Discussion of Results

The extreme difference in the results obtained from practically identical F_2 populations tested at different temperatures in the greenhouse to the same form of rust is of both genetic and economic interest. The F_2 populations are reasonably large in each case and arose from seed taken from the same bag, the population for the "warm test" being grown in 1926 and the population for the "cool test" in 1930. Both populations were normal in growth and similar in the character "plant height" for which they were studied. The F_3 families of each population were tested in the same greenhouse with the same equipment, and all environmental factors that were under the control of the technician who looked after the material were kept as nearly as possible the same, with the exception of temperature. The temperature in 1926 averaged 69.7° F., whereas in 1930 it averaged 60.6° F.

The amount and intensity of light in the two tests were not the same, owing to the tests being made in different years and at slightly different times of year. However, it does not seem probable that the light differences were responsible to any large extent for the great differences in rust reaction that occurred. The writer has frequently found that moderate differences in light intensity and duration did not cause large differences in the reactions of varieties or hybrids in seedling tests.

There were some distinct variations in the average daily greenhouse temperatures in the 1926 test due to unavoidable circumstances. Since the average difference of 9.1° between the "warm test" and the "cool test" brought about such great differences in the reactions of F_3 families, it might be thought that the two day duration of approximately 65° between October 30 and November 1 in the "warm test" would detrimentally affect the hybrid seedling reactions. This influence, if any, should be revealed by a fluctuation characterized by an increase in the proportion of resistant families for that portion of the test. No such variation in the results was found, as the analysis in Table IV shows. This table gives the rust classes of the F_3 families in each test according to the incubation periods as summarized by weekly groups.

TABLE IV

DISTRIBUTION OF F_3 FAMILIES OF BOTH TESTS BY RUST CLASSES ACCORDING TO THE INOCULATION DATES AS SUMMARIZED INTO WEEKLY GROUPS

Inoculation dates	R	HR	H and I	HS	S
Oct. 17–23, 1926	3	4	10	39	52
Oct. 24–31, 1926	2	7	18	72	125
Nov. 1– 8, 1926	4	20	62	146	206
Dec. 2– 9, 1930	115	20	36	3	3
Dec. 7–14, 1930	94	8	18	2	2

Genetic Considerations

A genetic hypothesis to explain the difference between the two sets of results is proposed as follows: Considering that three main genetic factors

govern rust reaction in the cross Marquillo × Marquis, let these be called A, B and C. Then either Marquis or Marquillo may be considered to have the constitution AABBCC. As susceptibility was dominant in Marquillo × Marquis hybrids when grown in the field and was also dominant in the "warm test" in the greenhouse, the constitution AABBCC may logically be assigned to Marquis and aabbcc to Marquillo. Let A, B and C be factors which when all are present in the homozygous condition cause susceptibility whether the temperature is around 61° or around 70° F. Then in either test Marquis and one sixty-fourth of the F_3 families would appear equally susceptible. When these factors are completely absent no susceptibility develops, whether the temperature approximates either 61° or 70°. Then Marquillo and one sixty-fourth of the F_3 families would be resistant in both tests.

Let these factors be such that their action in causing susceptibility is greatly reduced or curtailed at moderately low temperatures as compared with their action at moderately high temperatures. Then, when one or more of them is present in single or double dose in a warm greenhouse test, more or less susceptibility is evident, depending upon the dosage and perhaps upon differential effects of the different factors. But when a test is made in a cool greenhouse, little susceptibility occurs unless four or five doses of A, B and C are present, and full susceptibility occurs only when each factor is present in double dose (homozygous) with a total of six doses concerned. In the "warm test" the complete heterozygote AaBbCc would be about as susceptible as any individual carrying four, five or six doses, viz: AaBBCC, but in the "cool test" the AaBbCc individuals would show very little susceptibility.

This is a fairly simple hypothesis, having as its chief feature the radical curtailment of the action of the susceptibility factors when the temperature is low.* The hypothesis carries the implication that one or two doses of A, B or C produces as much susceptibility at 70° F. as four or five doses would at 61° F. The hypothesis explains the results satisfactorily. This is brought out graphically in Fig. 3, where the rust class distribution for each

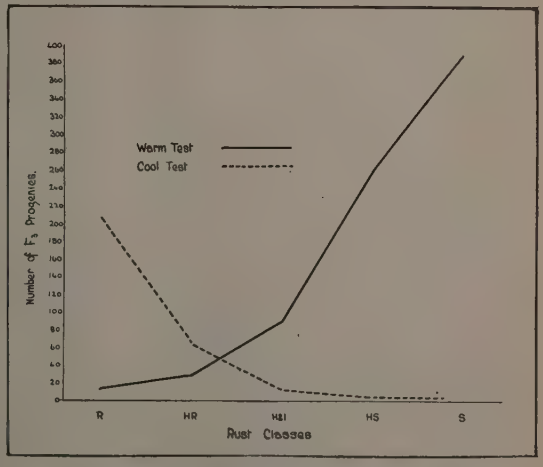

FIG. 3. *Distribution of Marquillo × Marquis F_2 plants according to the reaction of F_3 seedling progeny at different temperatures.*

**Whether the temperature exerts a direct effect on the parasite or on the host or on both, or whether complicated indirect actions are involved, is not known. For the time being the expression "curtailment of action of the susceptibility factors" seems to be appropriate.*

test is shown. The hypothesis is supported indirectly by both pathological and genetical findings in which lowered temperatures have been found to result in lowered pathogenic activity. The present experiment, however, is the first reported case, as far as the writer knows, where the influence of temperature appeared to be responsible for the reversal of the proportions in a genetic ratio.

A somewhat similar, though much less striking, case of the effect of different environments upon similar hybrid populations was reported recently by Quisenberry (5) in connection with the inheritance of winter hardiness. He had seed of the same group of F_3 families sown at St. Paul, Minn., and at Moccasin, Montana. At St. Paul the winter conditions were more severe than at Moccasin and approximately three times as many hybrid lines were tender than were hardy. At Moccasin the opposite was true.

The results of these studies clearly indicate that genetic studies on characters which are easily influenced by environmental conditions should be made under controlled conditions, after ascertaining in advance the general effects of different temperatures, light conditions, etc., upon the hybrid material to be used.

It is of interest to consider the effect of results such as those reported here upon the usual designations attached to factors. For example, should factors A, B and C be called dominant factors for susceptibility when they produce very little susceptibility at 61° F? Should they be called dominant for susceptibility when 209 of a total of 301 F_2 plants show (as in the cool test) as high resistance as Marquillo which possesses none of these factors? While such questions tend to place the terms "resistant" and "susceptible" in a rather precarious position, it is nevertheless true that these terms are generally used to refer to performance under ordinary field conditions. Perhaps confusion may be avoided by referring to such factors as "field susceptibility factors" rather than as "susceptibility factors".

There is one further genetical point that might be considered here. It is possible that in some crosses one or more of the genetic factors controlling rust reaction might be quite susceptible to temperature influences and the other controlling genetic factors be free from such influences. In such a case a genetic analysis, even with controlled conditions, might prove to be very difficult. It is easy to see why the disturbing factor just mentioned, together with the uncontrolled conditions in a field nursery, might make exact genetic analysis of field results an impossibility.

Breeding Considerations

The same F_3 families that were tested in the greenhouse in October and November 1926 were grown in the field nursery in 1927, where there was a uniformly heavy epidemic. The nursery results were closely like those obtained in the greenhouse from seedlings tested at approximately 70° F. to form 21. The use of form 21 in the greenhouse was particularly appropriate, since it is a prominent form in western Canada and appeared to be the most prevalent form in the nursery during the 1927 epidemic. In addition to

form 21, forms 15, 17, 29, 30 and 36 were found in this nursery.* The relationship for F_2 plants between the reaction of their F_3 seedling progeny to form 21, and the reaction of maturing F_3 progeny in the nursery to the mixture of forms including form 21, was determined by use of the contingency surface. The coefficient of contingency was 0.69 ± 0.062, indicating a strong positive relationship.

While no relationship between the "cool test" and field results has been obtained, it is apparent that there would be no positive correlation but probably a strong negative one if the field results were secured under conditions such as characterized the 1927 crop season. This point is extremely significant, because the "warm test" proved to be highly effective in the selection of resistant hybrids and made possible the reduction of 4,200 field harvested hybrid lines to only 419 during the winter months, whereas the "cool test" would have had a negative value in this regard, for it would have been deceiving.

The importance of this work to the practical breeder can hardly be overestimated. The present results suggest that wherever greenhouse, or indeed field nursery, results on reactions to pathogenes are to be used as deciding factors in the selection of hybrid plants or lines, all possible information should be obtained at a very early stage in the breeding project (preferably by means of a small experimental F_2 population) on the effects of different temperatures with respect to reactions to representative or leading physiologic forms of the pathogene used. This information would be the basis for making controlled tests under conditions that would promote the greatest effectiveness in making selections.

References

1. Gordon, W. L. Effect of temperature on host reactions to physiologic forms of *Puccinia graminis avenae*, Erikss. and Henn. Sci. Agr. 11: 95-103. 1930.
2. Johnson, T. A study of the effect of environmental factors on the variability of physiologic forms of *Puccinia graminis tritici*, Erikss. and Henn. Dom. Can. Dept. Agr. Bull. 140, n.s. 1931.
3. Peltier, G. L. A study of the environmental conditions influencing the development of stem rust in the absence of an alternate host. II. Infection studies with *Puccinia graminis tritici*, Form III and Form IX. Nebraska Agr. Exptl. Sta. Research Bull. 25. 1923.
4. Peturson, B. Effect of temperature on host reactions to physiologic forms of *Puccinia coronata avenae*. Sci. Agr. 11: 104-110. 1930.
5. Quisenberry, K. S. Inheritance of winter hardiness, growth habit and stem-rust reaction in crosses between Minhardi winter and H-44 spring wheats. U.S. Dept. Agr. Tech. Bull. 218. 1931.
6. Stakman, E. C. and Levine, M. N. Effect of certain ecological factors on the morphology of the Urediniospores of *Puccinia graminis*. J. Agr. Research, 16: 43-72. 1919.

The writer is indebted to Doctors Newton and Johnson of the Dominion Rust Research Laboratory, Winnipeg, for identifying these cultures and for supplying pure cultures for greenhouse studies.

THE RELATIONSHIP BETWEEN ENDOSPERM DEVELOPMENT AND MORPHOLOGIC CHARACTERS IN THE F_2 GENERATION OF A *T. DICOCCUM* X *T. VULGARE* CROSS[1]

By J. B. Harrington[2]

Abstract

The relationship between the degree of plumpness of F_2 seeds and the type of the resulting F_2 plants was studied in the cross Vernal (*T. dicoccum*) × Marquis (*T. vulgare*). A random sample of F_2 seeds was divided into three classes based upon kernel plumpness, *viz.* plump (Class A), slightly shrunken (Class B), and shrunken (Class C). In these there were by number 55.5, 41.0 and 3.5% of seeds respectively. Emergence of F_2 plants in the field was 64, 58 and 36% for Classes A, B and C. The F_2 plants were studied for 13 morphological characters. Comparing the populations for all characters combined, Class A was more *dicoccum*-like than Class B, and Class B much more *dicoccum*-like than Class C. The proportion of *vulgare*-like character was 16, 20 and 32% for Classes A, B and C, respectively. Considering the character of the individual plants, the ratios of *dicoccum*-like to *vulgare*-like were 12.1:1, 5.3:1, and 2.2:1 for classes A, B and C, respectively. Furthermore, the *vulgare*-like plants of classes A and B were less *vulgare*-like than those of Class C. There were present, however, in Classes A and B some plants that were fully as *vulgare*-like as any in Class C. These results indicate that, in an interspecific wheat cross, the breeder should give special attention to the shrunken F_2 seeds if he has very limited nursery space and a large amount of seed; whereas if he has plenty of space for a large population, special care of shrunken F_2 seeds does not seem warranted.

It has been commonly observed that wide interspecific crosses in wheat give rise to F_2 seed that varies greatly in endosperm development. These seeds are all produced by F_1 plants that are about as uniform as the plants of either parent variety, providing the latter were reasonably pure when the cross was made. The F_2 seeds vary in endosperm development from badly shrunken individuals carrying little or no food supply to individuals that are fully as plump as the seed of either parent variety. When this seed is sown in a nursery under ordinary field conditions, most of the very shrunken individuals fail to produce plants. Since cytological evidence indicates that an unbalanced chromosome condition may cause a shrunken endosperm which is known to affect plant characters, it is important to determine the relationship between endosperm development and plant type in wide wheat crosses. Such a determination should show the significance of the field elimination of individuals with shrunken endosperms.

The present investigation was made for the purpose of studying the relationship between the degree of plumpness (as indicating endosperm development) of F_2 seeds and the type of the resulting F_2 plants in interspecific wheat crosses.

[1] *Manuscript received May 26, 1931.*

Contribution from the laboratories of the University of Saskatchewan, Canada, with financial assistance from the National Research Council of Canada. This study forms a part of a co-operative attack on the problem of cereal rust in Canada, carried on jointly by the National Research Council, the Federal Department of Agriculture and the Universities of Manitoba, Saskatchewan and Alberta. The results were reported in full at the meeting of the Associate Committee on Field Crop Diseases at Winnipeg on April 9, 1931.

[2] *Professor of Field Husbandry, University of Saskatchewan.*

FIG. 1. *Vernal × Marquis F_2 seed. A—random sample; B—plump (Class A); C—slightly shrunken (Class B); D—shrunken (Class C).*

It was decided to limit the study to an emmer × common cross, since such crosses have been worked with extensively both genetically and cytologically. The cross Vernal (*T. dicoccum*) × Marquis (*T. vulgare*) appeared to be highly desirable for this study, for it had been studied recently by Thompson and Hollingshead (4), Harrington (1) and by Harrington and Smith (2). These studies furnished a background of cytological and genetical information. In addition, this cross was being used in the writer's project for the attainment of desirable rust resistant wheat, and much nursery, greenhouse and laboratory data were available.

Procedure

A random sample of several hundred F_2 seeds from the cross Vernal (Sask. 1289)* × Marquis (Sask. 1221)* was divided into three classes based upon kernel plumpness as follows: (1) plump, (2) slightly shrunken, (3) shrunken. The sample consisted of 55.5% plump seeds, 41.0% slightly shrunken and 3.5% shrunken. Fig. 1 illustrates the random sample and its three component parts. Eighty seeds of each plumpness group were sown in the nursery in May 1929 in rows one foot apart and spaced six inches apart in the rows. Percentage emergence was recorded for the three classes of F_2 and the parent variety checks. At maturity the separate groups were harvested by pulling the plants.

A laboratory study was made of the plants with respect to characters in which the parent varieties differed markedly. These were as follows:

Spike form (width ratio of lateral side to dorsi-ventral side)
Spike compactness (average length of ten central internodes)
Stem hollowness (taken 2 cm. below the collar)
Stem thickness (taken 2 cm. below the collar)
Lower width of rachis segment
Rachis hairiness (marginal)
Glume adherence
Glume shape (length *vs.* width)
Glume shoulder width
Keel sharpness (angle shown by cross section of lower half)
Awning
Seed character (considering kernel length and width, cheek angularity and crease width and depth).

A full description of the parent variety stocks and of the F_1 was published by the writer (1) in 1930. Only the classes "slightly shrunken" and "shrunken" were studied morphologically, owing to the general similarity between the plants of the groups "plump" and "slightly shrunken".

The results from the 1929 study were so interesting that it was thought worth while to repeat the work in 1930 using F_2 seed from the same lot as was used in 1929. This was done in the same manner as in 1930, but the number of seeds sown was larger, as follows: 100 plump, 125 slightly shrunken, 155 shrunken. The increase in number for the slightly shrunken and shrunken

**These parental variety stocks were known to be highly uniform.*

classes was to offset the poorer stands expected from these classes. The harvested plants of all three classes were studied morphologically. For convenience the three groups of plants from plump, slightly shrunken and shrunken seed, respectively, will be referred to hereafter as Class A, Class B and Class C.

Results

Seedling Emergence

The seedling emergence for both studies is shown in Table I. The percentage germination for the classes "plump" and "slightly shrunken" are fairly similar and not much lower than that for the parent varieties. Evidently slight shrunkenness of the seed is not a serious limiting factor to the survival of F_2 seedlings. On the other hand, the stand from shrunken seeds was very poor in both tests, averaging only 35.5%.

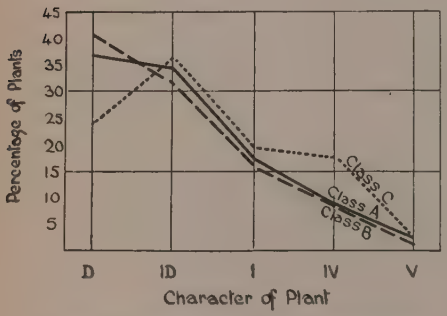

FIG. 2. *Spike form in Vernal × Marquis F_2.*

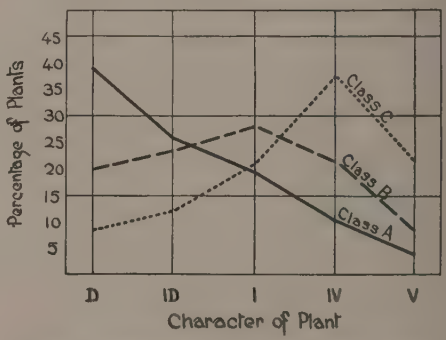

FIG. 3. *Rachis width in Vernal × Marquis F_2.*

TABLE I

COMPARATIVE DATA ON SEEDLING EMERGENCE

Year of study	Percentage emergence				
	Marquis	Vernal	F_2 plants from seeds that were:		
			Plump Class A	Slightly shrunken Class B	Shrunken Class C
1929	77	75	64	60	37
1930	66	60	64	56	34

Comparison of Classes A, B and C for Morphologic Characters

The results of the laboratory study of 1929 material showed that Class B was more *dicoccum*-like than Class C with respect to eleven of the twelve characters used and that, conversely, Class C was more *vulgare*-like than Class B for nine of the twelve characters.

Essentially the same results were obtained in the 1930 study as in the previous work as far as the comparison between Class B and Class C is concerned. In addition there were the Class A results. As expected from the superficial

examination in the field in 1929, Classes A and B were found not to differ much. Nevertheless the data reveal a definite tendency for Class A to be more *dicoccum*-like and Class B more *vulgare*-like for most of the characters studied. Comparing Classes B and C, it was found that Class B was more *dicoccum*-like than Class C for every character, and that Class C was more *vulgare*-like than Class B for ten of the twelve characters. Descriptions of random groups of plants from each plumpness class of the 1931 material are given in Table II.

TABLE II

DESCRIPTION OF A RANDOM PORTION OF THE VERNAL × MARQUIS F_2 PLANTS FROM EACH OF THE THREE PLUMPNESS CLASSES STUDIED IN 1930

Plumpness class	Line No.	Spike form	Spike compactness	Stem hollowness	Rachis articulation	Rachis width	Stem thickness	Glume adherence	Rachis hairiness	Shoulder width	Glume length-width ratio	Keel sharpness	Awning	Seed character*
A	62	D**	D	D	ID	ID	I	ID	D	D	D	D	D	
A	63	ID	IV	I	D	ID	I	ID	D	D	D	D	I	
A	64	V	V	I	V	IV	ID	V	V	D	ID	IV	D	
A	65	D	D	D	ID	D	D	IV	ID	D	D	ID	D	
A	66	D	D	ID	D	ID	I	ID	D	I	I	D	IV	
A	67	ID	D	D	ID	IV	V	I	D	I	I	I	V	
A	68	I	D	IV	ID	I	IV	IV	D	D	D	V	ID	
A	69	ID	D	D	ID	D	ID	D	ID	ID	D	D	V	
A	70	I	V	I	D	I	IV	I	IV	I	ID	V	V	
A	71	I	D	ID	D	I	ID	I	D	ID	D	IV	D	
A	72	D	D	D	ID	ID	I	I	D	I	I	I	V	
A	73	ID	D	D	ID	ID	ID	ID	D	D	D	D	V	
A	74	D	D	ID	ID	D	ID	V	D	ID	I	I	ID	
A	75	D	D	D	ID	IV	IV	IV	ID	D	ID	I	V	
A	76	ID	D	ID	D	D	D	D	D	ID	D	D	V	
A	77	I	D	I	ID	I	I	I	ID	D	I	I	V	
A	78	ID	D	IV	D	V	IV	D	I	IV	IV	ID	IV	
A	79	ID	D	ID	ID	D	D	I	D	ID	I	IV	IV	
A	80	I	D	ID	ID	ID	I	I	ID	ID	IV	ID	ID	
A	81	IV	D	ID	I	ID	I	I	D	D	I	ID	D	
B	108	D	D	IV	D	IV	IV	D	IV	IV	I	ID	IV	IV
B	109	ID	D	ID	ID	ID	ID	IV	D	D	D	D	I	ID
B	110	I	D	ID	ID	D	ID	IV	I	D	ID	I	ID	IV
B	111	D	D	IV	IV	I	I	IV	I	ID	I	D	D	I
B	112	I	D	I	IV	I	ID	I	ID	ID	I	ID	I	IV
B	113	D	D	ID	D	D	D	I	D	D	D	D	D	ID
B	114	IV	V	IV	ID	IV	V	I	ID	D	D	I	D	IV
B	115	V	V	IV	V	V	IV	V	IV	D	ID	IV	D	IV
B	116	ID	D	ID	D	I	I	D	D	ID	ID	D	D	ID
B	117	ID	D	D	ID	IV	I	I	D	D	ID	D	IV	ID

**Seed character was not recorded for Class A plants.*

***D = dicoccum-like; V = vulgare-like; I = intermediate; ID = intermediate between D and I; IV = intermediate between I and IV.*

TABLE II—*Continued*

Plumpness class	Line No.	Spike form	Spike compactness	Stem hollowness	Rachis articulation	Rachis width	Stem thickness	Glume adherence	Rachis hairiness	Shoulder width	Glume length - width ratio	Keel sharpness	Awning	Seed character
B	118	I	D	IV	I	I	IV	IV	V	D	D	V	D	ID
B	119	D	D	ID	I	ID	D	I	D	D	D	I	D	ID
B	120	IV	D	IV	ID	I	I	V	I	D	ID	V	ID	ID
B	121	D	D	ID	IV	D	D	ID	D	D	D	ID	V	D
B	122	ID	I	D	D	ID	D	I	ID	ID	ID	I	D	ID
B	123	I	D	ID	I	IV	V	IV	D	D	D	V	I	ID
B	124	D	D	ID	IV	I	I	ID	D	ID	ID	D	IV	I
B	125	D	IV	I	D	ID	D	D	D	ID	D	D	D	D
B	126	ID	D	ID	I	D	ID	I	ID	ID	I	ID	IV	I
B	127	ID	D	I	D	D	I	ID	D	I	I	I	V	IV
C	158	ID	ID	I	D	V	IV	ID	V	IV	IV	ID	D	I
C	159	ID	ID	IV	ID	D	I	I	I	I	I	IV	IV	D
C	160	I	D	V	V	IV	IV	V	ID	I	I	I	V	IV
C	161	I	D	V	IV	V	V	IV	ID	IV	V	IV	D	V
C	162	ID	D	D	ID	ID	D	ID	D	D	D	ID	V	ID
C	163	D	D	D	ID	ID	I	IV	D	D	D	D	IV	ID
C	164	I	I	I	ID	IV	IV	I	IV	ID	ID	ID	D	I
C	165	D	D	ID	D	D	D	ID	ID	D	D	D	D	D
C	166	IV	IV	I	I	I	V	IV	ID	ID	I	IV	IV	IV
C	167	I	D	IV	I	IV	V	I	ID	IV	IV	I	IV	I
C	168	ID	D	I	IV	I	D	V	D	D	ID	I	IV	I
C	169	D	D	I	IV	I	I	I	D	IV	IV	I	IV	I
C	170	ID	D	I	D	ID	ID	ID	D	I	I	D	V	ID
C	171	V	IV	IV	IV	I	IV	V	ID	ID	I	V	IV	IV
C	172	ID	ID	I	I	IV	ID	IV	ID	ID	ID	I	IV	ID
C	173	IV	D	IV	ID	V	V	IV	V	V	V	I	IV	I
C	174	D	D	IV	ID	V	V	I	D	I	V	I	V	IV
C	175	ID	I	IV	ID	I	ID	IV	I	ID	D	ID	I	†
C	176	IV	D	I	I	I	I	ID	I	ID	ID	I	D	ID
C	177	I	D	ID	ID	D	D	V	D	D	D	IV	ID	D

†*Sterile*

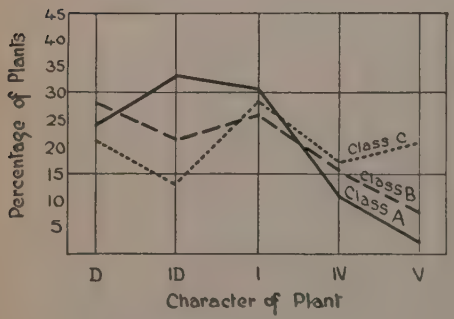

FIG. 4. *Stem thickness in Vernal × Marquis F_2.*

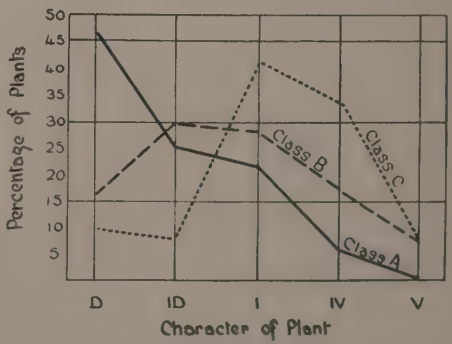

FIG. 5. *Stem hollowness in Vernal × Marquis F_2.*

TABLE III

DISTRIBUTION OF THE 46 VERNAL × MARQUIS F_2 PLANTS FROM *plump* SEEDS (CLASS A) WITH RESPECT TO EACH MORPHOLOGIC CHARACTER

Character	Character categories				
	D	ID	I	IV	V
Spike form	17	16	8	4	1
Spike compactness	40	0	1	1	4
Stem hollowness	21	12	10	3	0
Rachis articulation	14	23	6	1	2
Rachis width	18	12	9	5	2
Stem thickness	11	15	14	5	1
Glume adherence	6	8	12	15	5
Rachis hairiness	30	11	3	1	1
Shoulder width	27	13	5	1	0
Glume shape	23	12	9	2	0
Keel sharpness	16	8	9	5	8
Awning	15	7	2	6	16

TABLE IV

DISTRIBUTION OF THE 90 VERNAL × MARQUIS F_2 PLANTS FROM *slightly shrunken* SEEDS (CLASS B) WITH RESPECT TO EACH MORPHOLOGIC CHARACTER

Character	Character categories				
	D	ID	I	IV	V
Spike form	37	29	15	8	1
Spike compactness	58	8	10	5	9
Stem hollowness	14	27	26	16	7
Rachis articulation	28	19	23	15	5
Rachis width	18	21	25	19	7
Stem thickness	26	20	23	14	7
Glume adherence	22	18	25	15	10
Rachis hairiness	40	22	11	8	9
Shoulder width	51	22	13	3	1
Glume shape	37	34	15	3	1
Keel sharpness	32	21	18	10	9
Awning	25	8	17	28	12
Seed character	17	31	22	19	1

Since the results of the 1929 work and of the duplicate study made in 1930 agree reasonably well, they may be combined for the purpose of summarization. This has been done in Tables III, IV, and V. The results on four important species differentiating characters are presented graphically in Fig. 2 to 5. In Fig. 6 the proportion of *vulgare*-like character that occurred in each plumpness class is shown for both 1929 and 1930. This graph illustrates quite clearly (1) the close agreement between the results of the two studies and (2) the distinct relationship between endosperm development and plant character. The 1930 study wherein all three classes were studied shows 16, 20 and 32% of *vulgare*-like* character for the Classes A, B and C, respectively.

**Categories IV and V were taken collectively as showing vulgare-like character.*

TABLE V

DISTRIBUTION OF THE 61 VERNAL × MARQUIS F_2 PLANTS FROM *shrunken* SEEDS (CLASS C) WITH RESPECT TO EACH MORPHOLOGIC CHARACTER

Character	Character categories				
	D	ID	I	IV	V
Spike form	15	22	12	11	1
Spike compactness	24	10	15	7	5
Stem hollowness	6	5	25	20	5
Rachis articulation	17	18	12	10	4
Rachis width	5	7	13	23	13
Stem thickness	13	8	17	10	13
Glume adherence	8	13	14	15	11
Rachis hairiness	22	16	9	5	9
Shoulder width	17	18	13	11	2
Glume shape	11	15	20	9	6
Keel sharpness	14	16	18	6	7
Awning	14	6	5	23	13
Seed character	5	17	17	7	2

Character of Individual Plants with Respect to Classes A, B and C

The foregoing analysis of the results has been upon the basis of population characteristics and tendencies, but it is also important to consider the data from the viewpoint of individual plant character. This was done by taking ID and D as indicating *dicoccum*-like character and IV and V as representing *vulgare*-like character. Category I, being a neutral class, was not considered. A determination was made of the relative proportions of *dicoccum*-like and *vulgare*-like plants in each plumpness class for the 1929 and 1930 studies. The combined results are shown in Table VI. The average ratio of *dicoccum*-like to *vulgare*-like plants was 12.1 to 1.0 for Class A, 5.3 to 1.0 for Class B and 2.2 to 1.0 for Class C.

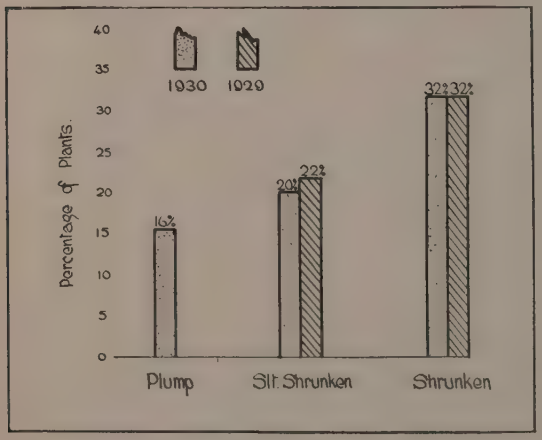

FIG. 6. *Proportion of vulgare-like character in a dicoccum × vulgare F_2 from seeds having different degrees of endosperm plumpness.*

It is apparent from these results that the ratio of *dicoccum*-like to *vulgare*-like plants depends upon the plumpness of the F_2 seed,—the plumper the seed the more *dicoccum*-like the resulting plants.

Since the *vulgare*-like plants are not equally *vulgare*-like it is of interest to examine the character of these plants to determine the relationship between

the degree of *vulgare*-ness and the plumpness of the F_2 seeds. In Table VII the data on the *vulgare*-like plants are summarized according to the three plumpness classes, and in each case the ratio of D plus ID to IV plus V determined. These ratios are 1.0 to 1.9 for Class A, 1.0 to 2.0 for Class B and 1.0 to 2.8 for Class C. It is evident that the *vulgare*-like plants of Class A were less *vulgare*-like than those of Class B, and much less *vulgare*-like than those of Class C.

The questions then arise: Are the *vulgare*-like plants of Classes A and B *all* less *vulgare*-like than those of Class C, or, if not, are they consistently unlike *vulgare* in certain characters and in that way different from the Class *C vulgare*-like plants? Examination of the data from all of the *vulgare*-like plants showed that both of these questions could be answered in the negative. Some of the most *vulgare*-like plants in the study were in Class B and the *dicoccum* resemblances that existed in the *vulgare*-like plants appeared to be distributed at random.

TABLE VI

THE DETERMINATION OF THE PROPORTION OF *vulgare*-LIKE F_2 PLANTS FROM F_2 SEEDS HAVING DIFFERENT DEGREES OF ENDOSPERM PLUMPNESS
RESULTS FROM THE RANDOM F_2 GROWN IN 1929 AND 1930

Basis of classification of F_2 plants	Distribution of F_2 plants according to F_2 seed plumpness					
	Class A (plump)		Class B (sl. shrunk)		Class C (shrunken)	
	No. of plants	Ratio of *dicoccum*-like to *vulgare*-like plants	No. of plants	Ratio of *dicoccum*-like to *vulgare*-like plants	No. of plants	Ratio of *dicoccum*-like to *vulgare*-like plants
Plants classified as D, ID or I for all of the 12 characters	9		8		2	
Plants classified as V, IV or I for all of the 12 characters	0		0		1	
Plants classified as D or ID for at least two more characters than as IV or V	41	13.6 : 1.0	67	5.6 : 1.0	33	2.2 : 1.0
Plants classified as V or IV for at least two more characters than as ID or D	3		12		15	
Plants classified as D or ID for more characters than as IV or V	42	10.5:1.0	73	4.9 : 1.0	40	2.2 : 1.0
Plants classified as V or IV for more characters than as ID or D	4		15		18	
Average ratio for last two sets of determinations*		12.1 : 1.0		5.3 : 1.0		2.2 : 1.0

**The numbers in the first set of determinations are too small to be accurate.*

TABLE VII

THE RELATIONSHIP BETWEEN F_2 SEED PLUMPNESS AND THE DEGREE OF *vulgare*-LIKE CHARACTER IN THE *vulgare*-LIKE F_2 PLANTS

Plumpness class	No. of *vulgare*-like F_2 plants	Character categories					Ratio of *dicoccum*-like to *vulgare*-like character
		D	ID	I	IV	V	
A	4*	10	5	7	12	14	1.0 : 1.9
B	15	23	25	46	59	38	1.0 : 2.0
C	18	25	20	61	70	56	1.0 : 2.8

**This number is small owing to no Class A plants being studied in 1929.*

Discussion and Conclusions

The fact that the shrunken F_2 seeds of the cross *T. dicoccum* × *T. vulgare* tend to give plants that are more *vulgare*-like than those from plump or slightly shrunken seeds is of considerable interest to the plant breeder. If he has very limited field space in which to grow an F_2 population from an interspecific cross and has a large amount of seed available, it would appear advisable not to select the plumpest portion of the seeds but rather the shrunken portion. The low viability of the shrunken seeds might be compensated for by sowing at a heavier rate. At the same time, all possible care to insure emergence and further growth of the young seedlings should be taken. Seedlings from shrunken seeds might even be started in a greenhouse.

On the other hand, if the breeder is not especially limited as to nursery space and has only a reasonably large supply of seed, which is usually the case, the findings of this study indicate that he need give no special attention to the shrunken seeds. This is apparent from the calculation made in Table VIII. These calculations were made for the purpose of obtaining figures that would represent the values of the three plumpness classes in terms of comparable *vulgare*-like plants. The final value for each class was arrived at by multiplying together the figures in the 2nd, 3rd, 4th and 5th columns and bringing the resulting figures to a percentage basis. The method used is logical and takes fully into account the different quantitative and qualitative attributes of the

TABLE VIII

A VALUATION OF THE IMPORTANCE OF SHRUNKEN F_2 SEEDS IN THE CROSS VERNAL EMMER × MARQUIS

Plumpness class	Proportion in random sample, %	Emergence in field, %	*Vulgare*-like plants		Percentage values
			Proportion, %	Ratio V & IV : D & ID	
A	55.5	64.0	7.6	1.9 : 1.0	37.2
B	41.0	58.0	15.9	2.0 : 1.0	54.9
C	3.5	35.5	31.3	2.8 : 1.0	7.9

three classes. The shrunken seeds gave proportionately a much higher number of *vulgare*-like plants than either the plump or the slightly shrunken seeds, and these *vulgare*-like plants averaged nearly 50% higher in number of *vulgare* characters than those from the other classes. But these advantages are much more than balanced by the very low proportion of shrunken seeds to start with and the low emergence in the field. Consequently under ordinary field conditions the expectation of comparable *vulgare*-like plants from the shrunken seeds would be only one-twelfth of that from the plump and slightly shrunken seeds. That is to say, the results demonstrate that the shrunken seeds in the cross studied were of relatively little importance.

If the breeder has only a small amount of F_2 seed the situation is different, because the plants from shrunken seeds are in general more heterozygous than those from plump seeds. A given lot of plants from shrunken seeds should yield progeny with a greater proportion of diversity in character combinations than a similar number of plants from plump seeds. Owing to this fact every feasible means should be used to get the shrunken seeds to produce plants *in cases where the total amount of F_2 seed is very limited.* In such cases rigid selection of plants would not be made until the F_3 generation.

The results of the present study are of particular interest in connection with the method used by McFadden (3) on the cross Yaroslav (*T. dicoccum*) × Marquis (*T. vulgare*), a cross not unlike the one used in the present study. McFadden stated that he used a Clipper seed cleaner vigorously upon all the threshed seed obtained from the F_3 population* grown *en masse* in his nursery. He added that the grading process and strong air blast removed practically all of the light weight seed. He then used for his next year's nursery only the plump, well-developed grains. It is apparent that he discarded a very large proportion of the shrunken seeds, yet he was remarkably successful and produced the well-known highly rust resistant bread wheat varieties, Hope and H-44.

Genetically and cytologically the appearance of a much larger proportion of *vulgare*-like plants from the shrunken seed than from the plump or slightly shrunken seeds is to be expected. Thompson and Hollingshead (4) showed clearly for a *dicoccum* × *vulgare* cross, similar to the one used by the writer, that after the F_1 generation surviving individuals with unbalanced chromosome conditions were more or less abnormal in various characters. Of these the ones that approached either a 28- or a 42-chromosome condition were the least abnormal. Now the number of hybrids approaching the 28-chromosome condition was much larger than the number that approached *vulgare* in chromosome constitution. This is to be expected, since chromosome loss or elimination is found to occur frequently in such a cross and the restitution of hybrids with 42 or nearly 42 chromosomes is much less likely to occur than the restitution of hybrids with 28 or nearly 28 chromosomes. Therefore, since the plumper seeds have the closest approach to a balanced chromosome condition, they should give a larger proportion of *dicoccum*-like plants than of

**No seed or plant selection was made in F_2 owing to the very limited size of the population.*

vulgare-like plants. Conversely, the shrunken seeds should yield a relatively higher proportion of *vulgare*-like plants. Of course, *some* plump seeds should give rise to *vulgare*-like plants and *some* shrunken seeds should give *dicoccum*-like plants. The results fitted these expectations quite satisfactorily.

References

1. HARRINGTON, J. B. The relationship between morphologic characters and rust resistance in a cross between emmer (*Triticum dicoccum*) and common wheat (*T. vulgare*). Can. J. Research, 2: 295-311. 1930.
2. HARRINGTON, J. B. and SMITH, W. K. The inheritance of reaction to black stem rust of wheat in a *dicoccum* × *vulgare* cross. Can. J. Research, 1: 163-188. 1929.
3. MCFADDEN, E. S. A successful transfer of emmer characters to *vulgare* wheat. J. Am. Soc. Agron. 22: 1020-1034. 1930.
4. THOMPSON, W. P. and HOLLINGSHEAD, L. Preponderance of *dicoccum*-like characters and chromosome numbers in hybrids between *Triticum dicoccum* and *Triticum vulgare*. J. Genetics, 17: 283-307. 1927.

WALLROTHIELLA ARCEUTHOBII, A PARASITE OF THE JACK-PINE MISTLETOE[1]

By E. Silver Dowding[2]

Abstract

Arceuthobium, the host of *Wallrothiella Arceuthobii*, has been found in British Columbia, Alberta, Manitoba, and Ontario and *Wallrothiella Arceuthobii* has been found in Manitoba and Alberta.

Arceuthobium fruits become infected in Canada in the spring, about a week after fertilization. The fungus and the infected fruits then increase in size, and they attain their maximum development by the summer of the following year.

The ascospores are not violently discharged into the air. The spores ooze out into water when the perithecia are wet.

The mature perithecium is made up of two compartments, the lower compartment containing the asci, and the upper compartment into which the ascospores are discharged and where they collect.

It is suggested that insects are agents which disperse the ascospores.

Ascospores sown in *Arceuthobium* decoction commence to germinate, but growth ceases after the germ tube has reached the length of about one millimetre.

Attempts to inoculate the stigmas of healthy Arceuthobium with "sprout-mycelium" have so far been unsuccessful.

I. Introduction

Arceuthobium is a mistletoe, allied to Viscum and Loranthus, which parasitizes certain conifers. Several species of the genus, in their turn, are parasitized by a fungus known as *Wallrothiella arceuthobii* (Pk.) Sacc. Arceuthobium is dioecious and the male and female plants are usually found growing on the same tree. The fungus attacks the pistillate flowers only and therefore occurs exclusively on the female plants.

The writer has paid special attention to *W. arceuthobii* as it grows on *Arceuthobium americanum* on *Pinus banksiana* in western Canada.

Arceuthobium americanum, when occurring on *P. banksiana*, is commonly known as the jack-pine mistletoe. This mistletoe induces abnormal branching of the infected jack pines resulting in the formation of "witches' brooms." In the field it is not difficult to find these brooms, for they stand out clearly against the sky (Plate I, Fig. 1 and 2).

To find *W. arceuthobii* one must first find "witches' brooms" like those just described. When these have been discovered, one must examine the fruits of the female mistletoes. If the fruits have been parasitized by the fungus, the fungus can readily be recognized as a black stroma protruding from their apices. The protruding part of each stroma is more or less hemispherical, is about 1 mm. in length and 1.5 mm. in width, and exhibits about forty papillae which are the protruding necks of as many perithecia (Text-fig. 1, 3, 4).

The jack-pine mistletoe severely damages the pines which it attacks, in that it checks their growth and renders their timber valueless for commercial purposes. At Victoria Beach, Lake Winnipeg, in certain stands of *Pinus*

[1] *Manuscript received May 15, 1931.*
Contribution from the Department of Botany, University of Manitoba, Winnipeg, Canada.

[2] *Research worker on Dermatophytes, University of Manitoba, and holder, at the time, of the Hudson's Bay Research Fellowship.*

banksiana, it was observed that at least four-fifths of the fruits of the mistletoe were parasitized by *Wallrothiella*. Since parasitized fruits never produce viable seeds, it is clear that the fungus is one of the agencies which serves to restrict the spread of the mistletoe in North America.

Wallrothiella arceuthobii was discovered in 1873, in New York State by Peck (11) who named it *Sphaeria arceuthobii*. In 1900 it was observed in the Upper Peninsula of Michigan by Wheeler (13), in 1915 in Montana and Idaho by Weir (12), and in 1929 in Alberta, Canada, by the author. These records of collections from such widely separated localities seem to indicate that *W. arceuthobii* is widely distributed throughout the northern part of North America and that possibly it occurs there from the eastern to the western coast.

Weir (12) reports that *Wallrothiella arceuthobii* has been observed in the United States of America on the following five species of *Arceuthobium:*

A. pusillum (Peck) Kuntze on *Picea mariana*,

A. americanum (Nutt.) Kuntze on *Pinus murrayana*,

A. douglasii (Engelm.) Kuntze on *Pseudotsuga taxifolia*,

A. douglasii var. *abietina* Engelm. on *Abies grandis* and *A. lasiocarpa*.

A. douglassii var. *microcarpa* Engelm. on *Picea engelmanni*.

In this paper an attempt will be made to extend our knowledge of the distribution, life history, and ecology of *Wallrothiella arceuthobii* as it occurs on the jack-pine mistletoe in Canada.

II. Distribution in Canada

Dr. E. H. Moss first drew the writer's attention to *Wallrothiella* on *Arceuthobium* fruits collected from pines in central Alberta. During the last three years the author has taken every opportunity to examine the various species

TABLE I

AREAS IN CANADA FROM WHICH ARCEUTHOBIUM HAS BEEN COLLECTED

Locality	Mistletoe	Host tree	Infection by *W. Arceuthobii*
1. Mt. Garibaldi, near Vancouver	*A. tsugensis*	*Tsuga heterophylla*	Uninfected
2. Tunnel Mt., Banff, Alberta	*A. americanum*	*Pinus murrayana*	Uninfected
3. Assiniboine River, from Whitecourt to Ft. Assiniboine	*A. americanum*	*P. banksiana*	Uninfected
4. North of Edmonton between N. Saskatchewan River and Athabasca River	*A. americanum*	*P. banksiana*	Infected
5. Grand Rapids at the mouth of the Saskatchewan River	*A. americanum*	*P. banksiana*	Uninfected
6. Victoria Beach on the S.E. shore of Lake Winnipeg	*A. americanum*	*P. banksiana*	Infected
7. Near Lake Temagami, eastern Ontario	*A. pusillum*	*P. mariana*	Uninfected

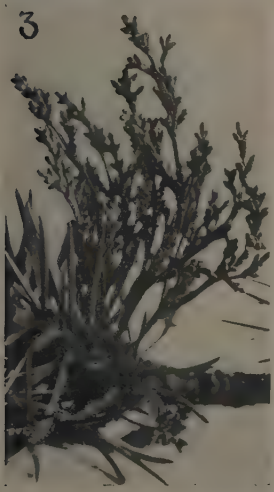

The trees illustrated are Pinus banksiana. The mistletoe is Arceuthobium americana. FIG. 1. *Pine in central Alberta, infected with Arceuthobium. The infected limb shows enormous hypertrophy.* FIG. 2. *Pines in central Manitoba infected with Arceuthobium. The trees are dwarfed and abnormally compact in habit.* FIG. 3. *A pine branch infected with female plants of Arceuthobium whose fruits are in turn infected with Wallrothiella. (Natural size.).* FIG. 4. *Female branch of Arceuthobium bearing flowers and fruits. The fruits are parasitized by Wallrothiella. Three times natural size.* FIG. 5. *Healthy Arceuthobium flowers growing on a "witches' broom" of a pine have been inoculated with the mycelium of Wallrothiella and tied into bags.*

of *Arceuthobium* in Canada for possible infection in order to determine the northern range of *Wallrothiella arceuthobii*. Areas in British Columbia, Alberta, Manitoba, and Ontario, where coniferous trees were severely infected with the jack-pine mistletoe, were visited and the mistletoe was examined. Fruits were discovered infected with *Wallrothiella* in Alberta and in Manitoba.

Seven areas in Canada from which *Arceuthobium* has been collected are listed in Table I, together with the name of the host trees and the presence or absence of *Wallrothiella arceuthobii*.

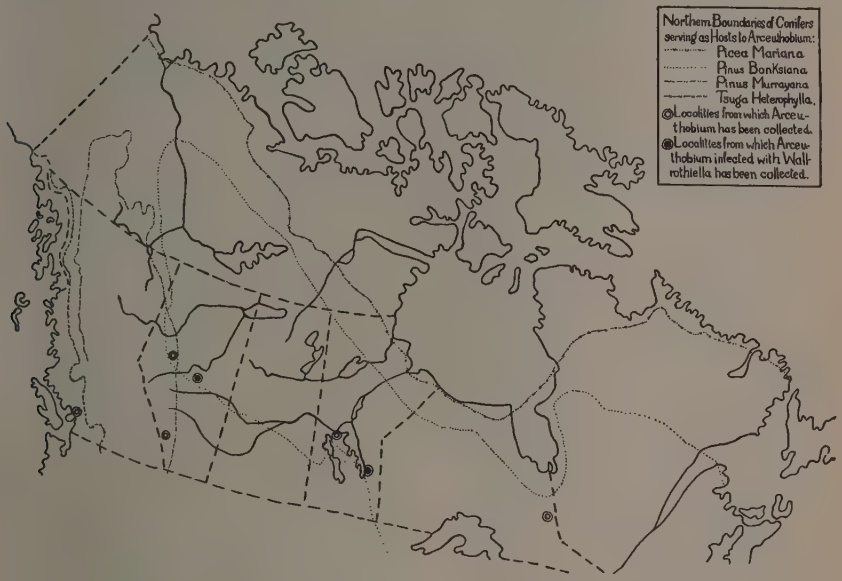

Map showing the distribution of Arceuthobium and of Wallrothiella in Canada.

The accompanying map of Canada shows the limits of distribution of conifers that serve as hosts of *Arceuthobium* as recorded in the Atlas of Canada (1) and it shows the localities from which healthy *Arceuthobium* and *Arceuthobium* infected with *Wallrothiella arceuthobii* were collected.

Although *Wallrothiella arceuthobii* has been collected from only two districts in Canada, central Alberta and central Manitoba, these districts are so widely separated (they are about eight hundred miles apart) that it seems probable that the range of the fungus in Canada is from the eastern to the western coast.

In central Alberta, where in 1927 field observations were made (3), the pines that were infected with mistletoe were growing on sandy ridges separated either by sloughs or by muskegs. The mistletoe growing on trees which bordered the depressions were the ones that were most frequently infected by *Wallrothiella*. In central Manitoba the infected trees that supported

Wallrothiella were growing on a low sandy peninsula of Lake Winnipeg. Further, Weir (12) states that he finds the fungus most frequently "in damp river bottoms or on the borders of swamp areas." From all these observations we may conclude that damp low-lying localities near water are most favorable for the growth of *Wallrothiella*.

III. Life History

The fungus invades the gynaeceum of *Arceuthobium vaginatum* via the stigma. In western Canada this invasion takes place in the spring soon after pollination.

On May 8, a visit was made to a forest of mistletoe-infected *Pinus banksiana* in Alberta, when it was found that the male flowers of the mistletoe were open and exposing their pollen. Some female flowers were collected and afterwards sectioned by the paraffin method. The sections showed pollen tubes in the stylar canals. Hence on or before May 8 pollination must have been taking place.

TEXT-FIG. 1–4. *Wallrothiella arceuthobii on Arceuthobium americanum, collected in June.* TEXT-FIG. 1. *Infected female branch of Arceuthobium: a, flowers; b, fruit; c, fruit bearing Wallrothiella perithecia. Twice natural size.* TEXT-FIG. 2. *Female flowers of Arceuthobium: The perianth has been removed to show the stigma which is covered with spores of Wallrothiella. Five times natural size.* TEXT-FIG. 3. *Fruit of Arceuthobium infected with Wallrothiella. Five times the natural size.* TEXT-FIG. 4. *Stroma, cut from an infected fruit to show the perithecia. Magnification, 18.*

On May 24 fertilized female flowers were collected and afterwards sectioned by the paraffin method. The sections showed a small embryo contained within the nucellus and fungal tissue in the interior of the upper part of the stigma (Text-fig. 7).

The facts recorded above seem to indicate that a pollen-tube succeeds in fertilizing the ovum before the fungus has destroyed the stigma.

The fact that the pistillate flowers of *Arceuthobium* become pollinated and fertilized before they are attacked by *Wallrothiella arceuthobii* is greatly to the advantage of the fungus. Before fertilization, the flowers of *Arceuthobium* are extremely small—less than 1 mm. long—and, if they were to become infected by *Wallrothiella* at this time, the stroma of the fungus would not be able to attain its normal length of 2 mm. and its width of 1.5 mm. As soon as fertilization has been accomplished, the ovary is stimulated to grow and soon becomes 3 mm. long and many times its original size. After thus having enlarged and having become

a focus for food supply, it is very well fitted to meet all the demands made upon it by the fungus. After fertilization the infected fruit increases in size not only during the ensuing summer, but also during the summer of the next year. Throughout both summers the fungus continues its growth in the fruit, and thus the growth of the fruit and that of the fungus keep pace with one another.

After the fungus has entered the stigma, the hyphae grow down the style and enter the ovary wall (Text-fig. 6). Here they spread laterally to the vascular tissue of the perianth (Text-fig. 7 and 8). Other hyphae then grow down the central axis of the fruit in the form of a slender column (Text-fig. 8). During the spring of the second year this column replaces all the central tissue of the fruit including the embryo and grows downwards until it reaches the abscission layer of the peduncle (Text-fig. 8). In the previous autumn and during the following spring the aerial portion of the stroma comes to project as a black knob at the top of the fruit (Text-fig. 8). In this knob some forty perithecia are developed (Text-fig. 1, 3, and 4). In June, the mouths of the perithecia become distended and reveal large numbers of free ascospores (Text-fig. 4). The ascospores are dispersed from the mouths of the perithecia from early in June until late in August.

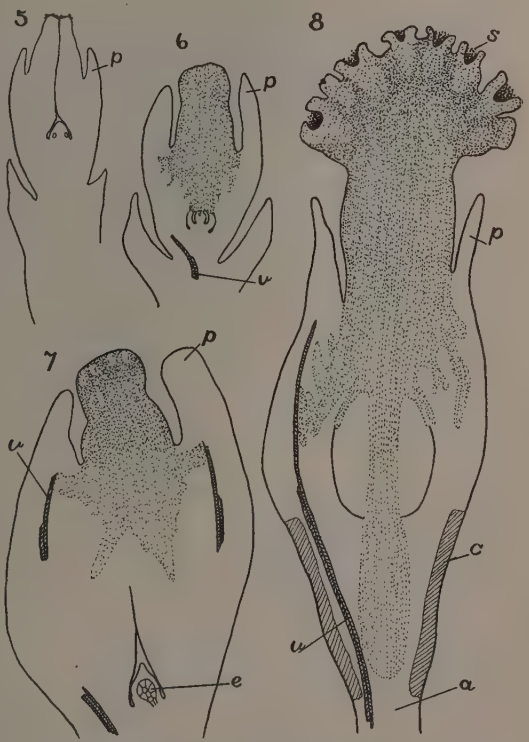

TEXT-FIG. 5–8. *Longitudinal sections of flowers and fruits of Arceuthobium americanum infected by Wallrothiella arceuthobii: p, perianth; v, vascular tissue; e, embryo; s, spores; c, collenchyma; a, abscission layer. Magnification, 14.* TEXT-FIG. 5. *Flowers bearing spores on stigma collected May 8, 1928.* TEXT-FIG. 6. *Flower with stigma replaced by fungal tissue collected June 3, 1928.* TEXT-FIG. 7. *Fruit with stigma replaced by fungal tissue. Collected July, 1928.* TEXT-FIG. 8. *Fruit completely infected with Wallrothiella, collected June 3, 1929.*

The female flower of *Arceuthobium* was described in 1888 by Johnson (8), in 1915 by Heinricher (6), and in 1931 by the author (4). It consists of a bipartite perianth which is fused to the ovary for two-thirds of its length (Text-fig. 5-8) and a gynaeceum which develops one seed in its ovary and which terminates in a hollow knob-shaped stigma. Heinricher (7) has observed that

in Austria the female flowers of *A. oxycedri* secrete an oily drop into the hollow stigma. The hollow stigma of some of the female flowers of *A. americanum* collected by the author in Manitoba in May had a glistening drop exuding from it, and doubtless this drop corresponds to that observed by Heinricher. The stigmatic secretion of *Arceuthobium* flowers may well be a suitable medium for the germination not only of pollen grains derived from the male flowers but also of ascospores of *Wallrothiella*.

The normal fruits of *Arceuthobium* violently expel their seeds to a distance of many yards (3); but abnormal fruits infected with *Wallrothiella* never discharge seeds but fall to the ground a little later than the time (September) when the normal fruits explode.

IV. The Discharge and Dispersal of the Ascospores

Experiments set up with a view to finding out whether or not the ascospores are violently shot into the air were made upon material collected in the summer and examined: (1) after being kept dry until the following January; (2) in the laboratory within a few hours of its being collected; and (3) in the field immediately after being collected. Two types of experiments were set up: (1) with a Van-Tieghem cell and (2) with a cover-glass only.

(1) A tiny branch (8 mm. long) bearing infected fruits of *Arceuthobium* was placed in a Van-Tieghem cell (Text-fig. 9) so that the stromata at the top of the fruits looked upwards toward the cover-glass. To hold the branch in the required position a copper-wire support was employed. The perithecia in the stromata were 1-3 mm. from the cover-glass. After the experiment was set up the cover-glass was examined microscopically at intervals up to 48 hr. No spores were deposited by the perithecia on the under side of the cover-glass. This result goes to show that the perithecia cannot shoot their ascospores upwards to a height of 1-3 mm.

(2) Pieces of the stroma of infected fruits were sliced off and placed on a slide so that the perithecia looked upwards, and then a cover-glass was rested on the top of the perithecia. No spores became deposited on the under side of the cover-glass.

From the results of the two series of experiments just described we may conclude that the perithecia of *Wallrothiella arceuthobii* are unable to discharge their ascospores violently.

If a mature stroma is placed in water in a beaker for four minutes, is then removed, set on a slide in air, and examined with the low power of the microscope, bubbles of air can be seen emerging from the mouths of the perithecial cavities, and bearing ascospores in the films of water which envelop them (Text-fig. 10).

If a dry stroma collected in the summer, either immediately after having been collected or some months later, is set in water for a few minutes and is then lightly touched to white paper, it leaves a black spore-deposit on the surface of the paper.

The two observations just recorded go to show that the ascospores of the fungus are readily set free from a stroma as soon as this is wetted.

Peck (11) states that the asci of *Wallrothiella* are fugaceous, so that at first it was thought that, when the perithecia are ripe, the walls of the asci disintegrate and the ascospores thus liberated within the perithecial cavities escape from the mouths of these cavities when the stroma is wetted. That this view is not entirely correct is shown by the observations now to be recorded.

An immature perithecium, collected during the autumn or winter previous to spore dispersal, consists of a peridium four or five layers of hyphae thick which encloses a single chamber containing asci and paraphyses (Text-fig. 11). The mouth of the perithecium at this stage appears to be closed or almost so.

An examination of the perithecia in a stroma collected in the spring a year after the fungus has entered the fruit shows that the hyphae at the mouths of the perithecia have grown upwards, outwards, and then somewhat inwards so as to form a wide-open *antechamber* communicating with the original and older *perithecial cavity* by a narrow neck (Text-fig. 12).

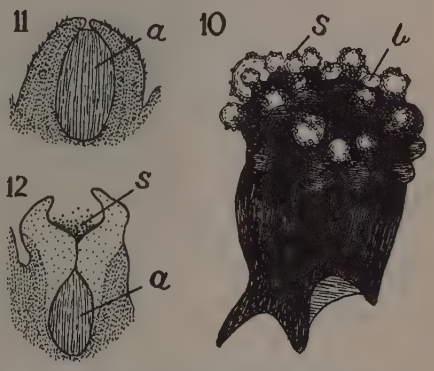

TEXT-FIG. 9–12. *Wallrothiella arceuthobii, illustrating spore emergence: b, air bubbles; s, spores; a, asci.* TEXT-FIG. 9. *Fungus on Arceuthobium arranged in Van Tieghem cell in an attempt to obtain a spore deposit upon the cover slip. Reduced to one-half the natural size.* TEXT-FIG. 10. *Diagram of stroma soaked in water. Bubbles of air are escaping from the perithecia bringing spores out with them. Magnification, 8.* TEXT-FIG. 11. *Diagram of longitudinal section of perithecium collected in February, showing single compartment containing asci. Magnification, 35.* TEXT-FIG. 12. *Diagram of longitudinal section of perithecium collected in June, showing the lower compartment containing asci and the upper compartment containing spores. Magnification, 35.*

In a ripe perithecium, as shown in sections made by the paraffin method, the perithecial cavity always contains intact asci, and presumably also discharged asci, but never any free spores, whereas the antechamber contains free spores only (Text-fig. 4 and 12).

The observations recorded above suggest that the asci in the perithecial chamber discharge their spores into the antechamber. The means by which this is brought about is obscure. As experiments already recorded have shown, there is no reason to suppose that the asci violently shoot away their spores. It therefore seems probable that the walls of the asci become diffluent and that by their swelling they carry the spores upwards through the perithecial neck into the antechamber. An ascus has been observed greatly swollen and pressing its apex against the base of the perithecial neck. This observation seems to indicate that the asci successively discharge their eight ascospores, one ascus following another in pressing up to the base of the neck.

A stroma less than one year old, as already explained, has no antechamber. Its asci are all intact and none of them has as yet discharged its ascospores.

If such a stroma is placed in water for some minutes, no spores are discharged. In a mature stroma the perithecia have their antechambers filled with discharged spores. It is only from such perithecia that spores ooze out when the stroma is wetted.

The spores when dry stick together and to any substratum they may be on. Since they are not shot into the air, it is unlikely that they are dispersed by the wind. It seems not unlikely that the same insects which pollinate the flowers of *Arceuthobium* transfer the ascospores to the stigmas of the flowers. The author, in May, has seen small flies hovering over the flowers of *Arceuthobium* and ants swarming over the infected pine branches; and Mr. H. J. Brodie, whilst visiting Lake Winnipeg in August, 1930, to collect material for the writer wrote to me as follows: "I spent a considerable time in watching the movements of the ants. Each ant would crawl out to the tip of a pine needle and back to its base, repeating this operation several times on each branch tip. . . . . I have seen the ants crawling over *Arceuthobium*." Further observations are required to determine exactly whether or not ants and other insects visit the spore-filled antechambers of the perithecia and actually transport the spores from an infected fruit to a healthy flower.

Rain might splash the spores about on a single pine tree and so perhaps occasionally bring about fresh infections in the same tree. However this agency could not spread the fungus from tree to tree in a loose pine stand.

V. Asci and Ascospores

As a preliminary step in attempting to germinate the ascospores, a mature stroma that had been soaked in sterile water was rubbed on a sterile slide so as to break open the perithecia. A mucilaginous smear of fungal material was thus obtained. Microscopical examination of the smear showed that it consisted of asci, ascospores, fragments of the stroma, and sometimes foreign spores (Text-fig. 13). If a stroma is kept damp for some days, foreign spores are frequently obtained in the smear, particularly those of *Cladosporium herbarum* which are easily recognized by their amber color (Text-fig. 13).

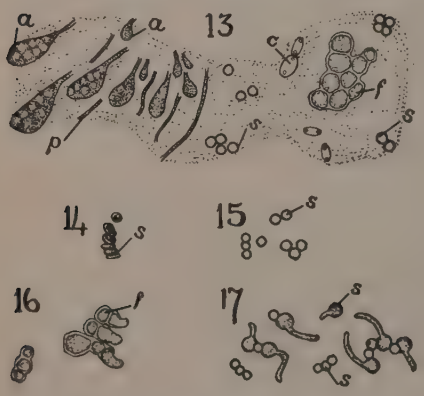

TEXT-FIG. 13–17. *Wallrothiella arceuthobii. All the material was obtained by making a smear with a wet stroma upon a glass slide: a, asci, upside down; p, paraphyses; s, ascospores; f, fragment of stroma; c, conidia of Cladosporium. Magnification, 230.* TEXT-FIG. 13. *A typical smear from a stroma containing asci of various ages, paraphyses, fragments of the stroma Wallrothiella, ascospores, and contamination consisting of conidia of Cladosporium.* TEST-FIG. 14. *Ascospores in dry condition.* TEXT-FIG. 15. *Ascospores in water.* TEXT-FIG. 16. *Fragment of the stroma germinating in nutrient medium.* TEXT-FIG. 17. *Ascospores germinating in nutrient medium.*

Asci of various stages of development can be found in a smear from the stroma, mixed with extremely fine paraphyses. They are club-shaped, tapering below into a slender stalk, and about 25 μ long and 10 μ wide. They correspond in outline to the arrangement of the spores within. The eight spores are usually arranged in

two columns, a long column of six and a short column of two beside the longer column, so that the ascus wall is slightly extended on one side where the separated pair of spores lie (Text-fig. 13).

The ascospores are dark-colored owing to the spore wall containing a black pigment. When wet, the spores are globose (Text-fig. 15) but when dry they collapse to flattened discs. The dry spores cohere in such a way as to resemble a pile of coins (Text-fig. 14). The spores are 4 to 6 μ in diameter and, when dry, they flatten out to 2 μ in thickness.

Repeated trials were made to germinate the ascospores. The spores were sown in water, potato agar, malt agar, and pine decoction. Some were unheated, others were heated to temperatures varying from 30° to 75° C. All attempts made during the winter failed. In the spring, large quantities of fresh *Arceuthobium* plants were obtained. A decoction of *Arceuthobium* was made and the ascospores were sown in hanging drops of this medium in Van-Tieghem cells. A group of ascospores was selected and drawn with the camera lucida just after sowing. It was re-examined after 24 hr. and the identical spores that had been drawn were found to have swollen and to have commenced to germinate (Text-fig. 17). The germ tubes attained a length of about one millimetre but, unfortunately, they could not be induced to grow any further.

VI. Cultivation of Wallrothiella from the Stroma

For culturing the stroma, fresh material was used because stored material sometimes became grown over with molds. The fresh stroma was steeped for a minute in 1% corrosive sublimate, washed in sterile water, and planted in a hanging drop of sterile water or potato agar. Within a few hours, stout vigorous hyphae appeared all over the surface of the stroma (Text-fig. 18), which gave rise to large quantities of yeast-like sprout cells (Plate 2, Fig. 2 and 3).

The stroma is so darkly pigmented and composed of such fine closely interwoven hyphae that even in the thinnest stroma section that it is possible to cut by hand the germinating hyphae can never be traced back to definite hyphae of the parent stroma, so that there was the possibility that the growth in the medium arose from foreign spores lodged in the crevices of the stroma.

In two sets of observations, now to be recorded, evidence was obtained which seems to show conclusively that the sprout-mycelium originated from the tissue of the stroma and not from foreign spores.

(1) A fragment of stroma was planted in a hanging drop of nutrient medium and, when a halo of hyphae had grown out into the medium, the tissue was fixed. It was then dehydrated, embedded in paraffin, sectioned 8 μ thick, and stained. The sections showed that the germinating hyphae could actually be traced back into the stroma tissue (Text-fig. 19).

(2) The stroma of *Wallrothiella* at a level where it emerges from the mistletoe fruit, is hollow. Attention was directed to the sterile inner surface of the cavity upon which no foreign spores could possibly be lodged. A large number of sections of the stroma that were cut at the level of the cavity were planted

in a hanging drop of nutrient medium, and one slice of stroma was eventually found in which the first hypha to grow took its origin from the inner surface of the cavity (Text-fig. 20; Plate 2, Fig. 1). This hypha was watched over a period of several hours, and it was seen to elongate, to become septate, and to give rise to an abundance of sprout cells (Text-fig. 21).

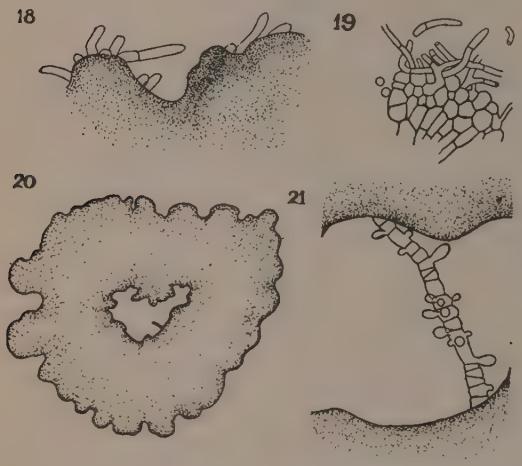

TEXT-FIG. 18–21. *Wallrothiella arceuthobii. Diagrams of germination of the stroma.* TEXT-FIG. 18. *Portion of the stroma sown in nutrient medium 24 hr. previously, showing outgrowth of hyphae. Magnification, 150.* TEXT-FIG. 19. *Paraffin section of stroma illustrated in Text-fig. 18., showing the connection of the germinating hyphae with the stroma tissue. Magnification, 150.* TEXT-FIG. 20. *Section of the stroma sown 24 hr. previously in nutrient medium, showing the development of a hypha from the inner surface of the cavity. Magnification, 65.* TEXT-FIG. 21. *The hypha shown in Text-fig. 20, two days later, showing formation of cross-walls and commencement of sprouting. Magnification, 150.*

The sprout cells of the *Wallrothiella* mycelium give rise by budding to more sprout cells. In a liquid medium the sprout cells bud so rapidly that a white precipitate of yeast-like cells collects at the bottom of the medium. Budding is common in the early phase of many fungi. Martin (10) has recorded that the phenomenon has been observed in the following genera: *Dermatium*, *Fumago*, *Polyspora*, *Exobasidiopsis*, *Microstroma*, *Spaceloma*, and others.

When the mycelium is older, the walls become darkly pigmented and the formation of sprout cells gives way to the formation of thick-walled conidia which clothe the hyphae in a brown sheath. The hyphae secrete sheaths of mucilage, and as the culture dries out the mucilage cements the mycelium to the substratum in which condition it can retain its vitality for at least six months. The mycelium shows a remarkable resemblance to *Dermatium pullulans*.

Brefeld (2) in 1891 describes a similar type of mycelium in a species closely related to *Wallrothiella*, *Sphaerulia intermixta*. In this species the ascospores give rise to a sprout-mycelium. After the exhaustion of the nutrient medium the sprout cells change to multicellular brown gemmae. Their ability to germinate is not injured by drying for eighteen months.

Gaümann and Dodge (5), who quote Brefeld's account, remark that "sprouting" has not been reported elsewhere in the group and that the results were probably based on impure cultures.

Strong evidence has been brought forward to show that the sprout-mycelium obtained in my cultures from stroma sections belongs to *Wallrothiella*. To establish the connection beyond any doubt it would be necessary to germinate the ascospores in pure cultures, and obtain a mycelium which would become a sprout-mycelium or to induce the sprout-mycelium obtained from a stroma to produce *Wallrothiella* perithecia.

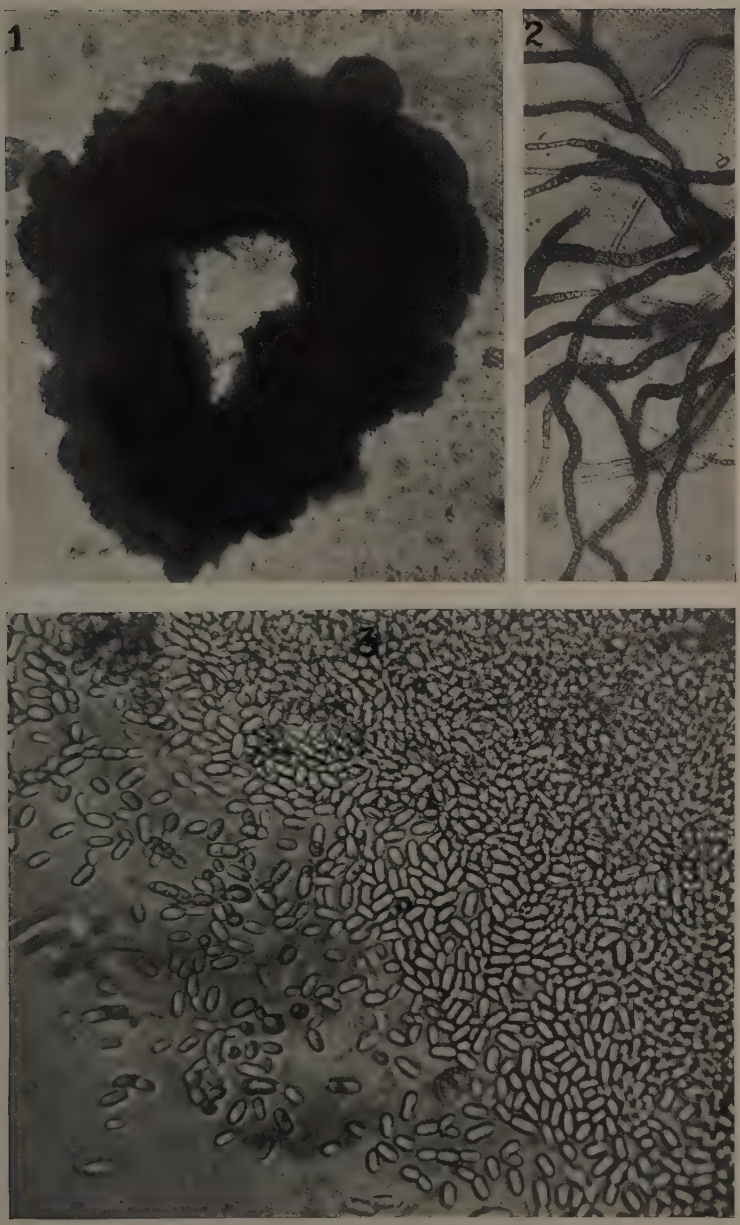

All figures are those of Wallrothiella arceuthobii. FIG. 1. *Section of the stroma of Wallrothiella which was sown in potato-agar 24 hrs. previously. A hypha has grown out from the inner surface of the cavity (an arrow points to it). Magnification, 45.* FIG. 2. *Mycelium grown in potato-agar from Wallrothiella stroma. Magnification, 150.* FIG. 3. *Sprout cells in water, developed from mycelium of Wallrothiella. Magnification, 150.*

VII. Inoculation Experiments

The sprout-mycelium obtained from the stroma of *Wallrothiella* was inoculated upon healthy stigmas of *Arceuthobium*.

The first material to be used as a host in the inoculation experiment was *A. tsugensis*. This mistletoe was collected attached to *Tsuga heterophylla* and sent from Vancouver by Mrs. G. Smith to the laboratory where it was kept in water. The sprout-mycelium obtained from a stroma and growing in artificial culture was smeared on the stigmas of the mistletoe and the plants were kept for a month. The inoculations were not successful. This experiment was not regarded as conclusive because the cuticle on the stigma of *A. tsugensis* was about three times as thick as the cuticle on the stigma of *A. americanum* so that *A. tsugensis* may quite possibly be resistant to the fungus.

The following spring *A. americanum* growing on jack pine on the shore of Lake Winnipeg was used as a host. Inoculation experiments were made in the field upon plants which were left attached to the pine trees during the course of the experiment. Trees were selected for the inoculations on which there was no *Wallrothiella*. The sprout-mycelium was smeared over healthy stigmas, and the branches of inoculated fruits were covered by paper bags. In this way several hundred fruits were inoculated. Controls of fruits that had not been inoculated were also tied in bags. (Plate 1, Fig. 5).

In the following autumn the trees were re-examined and it was found that the experiments had been interfered with. Squirrels had torn most of the bags, with the exception of one, which covered about fifty fruits that had been inoculated. None of the fruits that had not been interfered with had become infected with *Wallrothiella*.

At the time of the second visit to the trees, fresh plants were inoculated with mycelium, and these are to be examined in the autumn of 1931.

Acknowledgment

This investigation was carried out in the Botanical Department of the University of Manitoba during the writer's tenure of the Hudson's Bay Research Fellowship, 1929-30. The expenses involved in collecting material were defrayed by a grant from the Royal Society. The author desires to acknowledge with her best thanks the generous assistance given her by Professor A. H. Reginald Buller.

References

1. Atlas of Canada, Dept. of the Interior, Canada. 1906.
2. Brefeld, O. Unters. Ges. Geb. Mykol. 10: 157-378. 1891.
3. Dowding, E. S. J. Ecol. 17: 82-105. 1929.
4. Dowding, E. S. Botan. Gaz. 91: 42-54. 1931.
5. Gäumann, E. A. and Dodge, C. W. Comparative morphology of fungi, McGraw-Hill. 1928.
6. Heinricher, E. Sitzb. Akad. Wiss. Wien. Abt. 1. 124 Bd. 3 & 4 heft. 181-230. 1915.
7. Heinricher, E. Sitzb. Akad. Wiss. Wien. Abt. 1. 124 Bd. 6 & 7 heft. 481-504. 1915.
8. Johnson, T. Ann. Botany, 2: 137-160. 1888.
9. MacDougal, D. T. Minnesota Botanical Studies, 2: 169-173. 1898-1902.

10. MARTIN, G. H. Phytophathology, 19: 1117-1123. 1929.
11. PECK, C. H. N.Y. State Museum of Natural History. 27th Ann. Rep. 1874-1876. Report of the Botanist, 73-116. 1874.
12. WEIR, J. R. J. Agr. Research, 4: 369-378. 1915.
13. WHEELER, C. F. Mich. Agr. Coll. Exptl. Bull. 186: 17-28. 1900.

THE EPITHALASSA OF THE STRAIT OF GEORGIA

SALINITY, TEMPERATURE, pH AND PHYTOPLANKTON[1]

By A. H. Hutchinson[2] and C. C. Lucas[3]

Abstract

The investigation was initiated in order to determine the extent of the Fraser River's effect on temperature, salinity, currents, and fish food, probable factors in the direction of salmon migrations. A correct valuation of the Fraser River in these respects has necessitated a survey of the Strait of Georgia waters and an estimate of the relative importance of water entering the Strait from other sources, from the sea through the passes and from other rivers. It is believed that the data presented may have a potential economic value as a basis for a further knowledge of the habits of fish, the establishment of oyster beds, the development of clam beaches and of crab and shrimp industries and the location of summer resorts. Conclusions regarding the interrelations of salinity, temperature, pH, tidal movements and phytoplankton, may be of scientific interest.

The following conclusions discussed in the paper may be emphasized: (1) The Strait of Georgia is a great basin, connected with the sea by narrow passes, which receives water from a number of large rivers, notably the Fraser River. (2) The river water is conserved during the summer and forms a marked upper layer, epithalassa, which is characterized by low salinity and high temperature. The increase in temperature as compared with sea water may amount to 10° C. or 18° F. (3) Throughout the greater part of the region this epithalassa has a stability which is sufficient to resist tidal and wave movements. (4) Since time is a factor, the heating effect of the sun, insolation, upon the epithalassa becomes most evident at regions some distance from the river mouth. In the case of a large river, as the Fraser, this distance may exceed ten miles. (5) Abundant fish food in the form of plankton is present and the amount is greatest at the regions where the most complete mixing of the river and of the sea water takes place. Evidently each water source contributes certain conditions or factors favorable for plankton growth. Further investigation to determine the exact nature of these conditions is in progress. (6) Mass movements of the epithalassa accompany tidal changes, resulting in variations of salinity, temperature and plankton at any point according to the source of the translocated water and the phase of the tide.

Introduction

The original problem which gave the primary impetus to the present investigation was the feasibility of diverting the migrations of salmon by closing Canoe Pass, the most southerly outlet of the Fraser River. This necessitated a general survey of the area and an estimate of the relative effect of this river in comparison with the other rivers entering the Strait of Georgia; a study of the effect of tides and other influences upon the salinity, temperature, pH, phosphate, silicate, nitrogen content, and plankton, including zooplankton and phytoplankton of the Strait of Georgia; and in turn the effect of physical and chemical conditions and the distribution of fish food upon marine organisms including fish and shellfish.

Fraser (7) and Cameron and Mounce (3) published accounts previously with reference to physical and chemical conditions at a number of regions, especially in the vicinity of the Pacific Biological Station, Departure Bay, Nanaimo.

[1] *Manuscript received March 23, 1931.*
Contribution from the Department of Botany, University of British Columbia, Vancouver, Canada, with financial assistance from the National Research Council of Canada.

[2] *Professor of Botany, University of British Columbia.*

[3] *Professor of Chemistry, Brandon College.*

Thompson (14), Gran and Thompson (8), Thompson and Van Cleve (16), Thompson and Wright (17) and Thompson, Miller, Hitchings and Todd (15) have been investigating the Puget Sound and San Juan region of neighboring waters with headquarters at the Puget Sound Biological Station, Friday Harbor.

At the Pacific Biological Station, Departure Bay, Nanaimo, Dr. Clemens, Director of the Station, has taken charge of a drift-bottle study of currents. Clemens (5, 6) and Williamson (19, 20) have published several papers on salmon migrations; Campbell (4), on Zooplankton; and Hutchinson, Lucas and McPhail (9, 10, 12, 13) on temperature, salinity, pH, silicate, phosphate and phytoplankton of the Strait of Georgia. The work is being continued by Carter, Fleming and Beal.

This account is limited to a consideration of the temperature, salinity, pH and phytoplankton of the Strait of Georgia and neighboring waters to a depth of 50 yards (45.7 metres) during the summer months.

Constant use has been made of Tide Tables of the Pacific Coast of Canada (1), British Admiralty Charts and the B.C. Pilot (2), and data have been obtained from Johnston's account of the sedimentation of the Fraser River delta (11).

Acknowledgment is made of numerous valuable articles on oceanographic conditions in other regions. A review of these does not fall within the scope of the present account, although conditions in other parts of the world have thrown much light upon the problem under consideration.

Methods and Measurements

The methods used are described in earlier papers (9, 10, 12, 13); these are in accord with the methods recommended by the "Conseil Permanent International pour l'exploration de la mer." The metric system is used except in the determination of distance where miles* and yards** are the units. The investigation was started when a yard meter only was available for the cable measurements and for the sake of uniformity this unit has been retained. Temperature is expressed as degrees centigrade; salinity as grams of total halide expressed as chloride per litre, and plankton as volumes of centrifuged plankton material from 100,000 volumes of sea water.

General Description of the Strait of Georgia

The Straight of Georgia, situated between the southern portion of Vancouver Island and the mainland of British Columbia and the State of Washington is a great basin 140 miles long and of width varying from 20 to 30 miles. It is connected with the Pacific Ocean by several narrow passes. Boundary Pass and Rosario Strait at the south open into the Strait of Juan de Fuca; and Discovery Pass at the north continues to Seymour Narrows and Johnston Strait (Chart 1). A double chain of elongated islands parallel the southerly portion of Vancouver Island to form Stuart and Trincomali Channels. Active, Porlier and Gabriola Passes, between these islands, furnish additional extremely

**1 mi. = 1.60 kilometres; **1 yard = 0.914 metres.*

constricted outlets. Texada Island, 30 miles long, is situated opposite Jervis Inlet and is accompanied by a smaller island, Lasqueti, located near mid-channel. At the north a number of circuitous channels connect indirectly with Johnston Strait and the Pacific Ocean. One known as the Hole-in-the-Wall has a very descriptive name (Chart 1).

Tides

The tides are most unusual. The chief flood enters through Juan de Fuca Strait and continues to the north end of the Strait of Georgia, especially on the east side where its effect passes through Sutil Channel and to Toba and Bute Inlets; another flood enters through Johnston Strait and Discovery Pass at the north, and affects the northwest portion of the Strait of Georgia especially along the shore of Vancouver Island. The latter flood precedes the former by approximately two hours. They result in eddies and turbulence which is marked southward to Texada Island. The tide which enters the Strait of Juan de Fuca floods one hour longer through Rosario Strait on the Washington side than through Haro Strait, toward Vancouver Island. The result is a great swirl which affects the area from Boundary Pass to Boundary Bay. This swirl was examined on August 17, 1929. At slack tide, a calm area extended with its centre two miles off East Point, Saturna Island, for a distance of two miles in every direction and was delimited by a circle of turbulence easily discerned from the centre and traversed at its southerly and northerly extremities during our cruise. The region of marked turbulence apparently increases in diameter toward mid-tide until it reaches the Point Roberts-Boundary Pass line.

The remarkable phenomenon of a tidal current which persists for the complete 24 hr. in a single direction, southeastward, was observed July 18, 1929, in Tumbo Channel, three miles N.E. of East Point, Boundary Pass. Since this small channel, two miles long, opens directly at each end to the Strait of Georgia one would not expect tidal currents to be marked; at midtide, however, a sixty-foot boat at anchor was nearly capsized. Similarly the "B.C. Pilot" records that "close along the southeast side of East Point the stream always sets northeastward."

Tidal currents are increased in complexity by fiords such as Burrard, Jervis, Toba, Bute and Saanich Inlets and Howe Sound, which vary in length from 40 to 80 miles, attain a depth in some cases of 300 fathoms (548 m.) and are limited by shallow and often narrow mouths.

These unusual tidal conditions are superimposed upon the well-known characteristic of the tides of Juan de Fuca, Puget Sound and the Strait of Georgia, namely, the inequality of alternate daily tides; the one fluctuates in height by approximately twelve feet, the other by one-quarter of that amount (1, 2, B.C. Pilot, Tide Tables).

Rivers Flowing into the Strait of Georgia

The Fraser River has a minimal average annual discharge of 80 million acre-feet; one-fifth of this amount is discharged during the months of October to

April while 64 million acre-feet of water is contributed during the summer period, May to September (11, 12, 18).

It is estimated that this water would occupy the upper portion of the basin of the Strait of Georgia in the part most directly affected or northward to 49°25′ to a depth of 80 ft. if not removed. The Squamish River, during the same period, discharges on the average about one-twelfth that amount; the

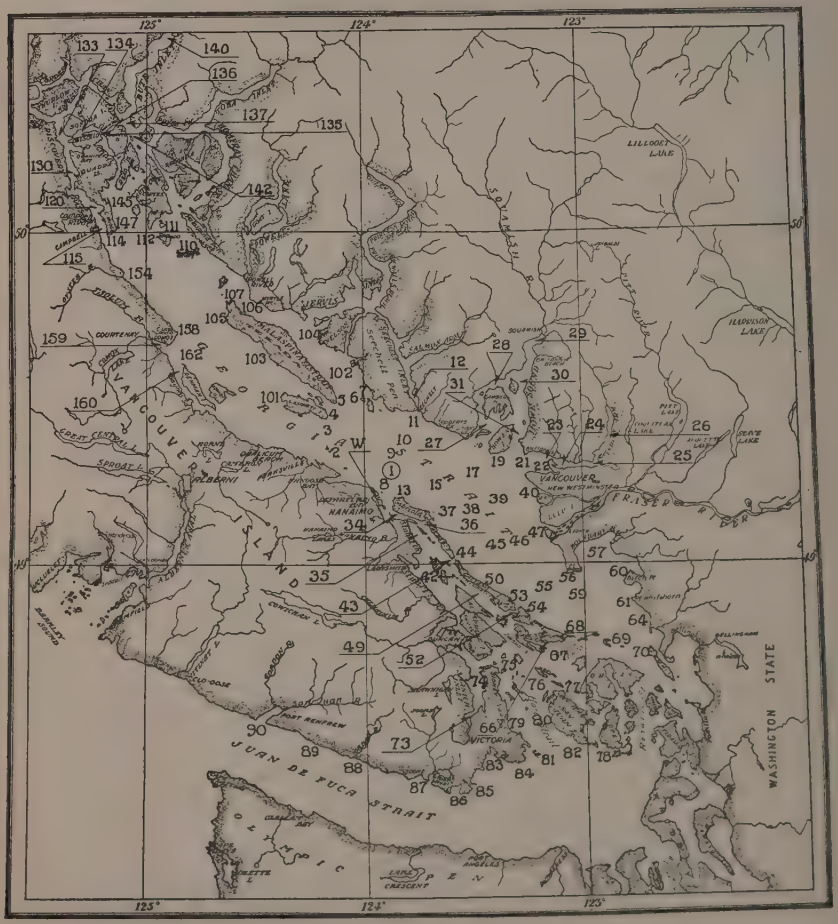

CHART 1. *Stations, Strait of Georgia.*

Nanaimo River less than one one-hundredth on the average; and a number of smaller rivers a proportion which has an effect on salinity of local significance only. The rivers flowing into Jervis, Bute and Toba Inlets, although relatively small and of undetermined discharge have a decided effect upon the waters not only within the limits of their respective inlets but also upon the neighboring regions of the Strait of Georgia.

TABLE I

SURFACE SALINITY, TEMPERATURE, PLANKTON AND pH ON LINE WESTWARD FROM THE FRASER RIVER MOUTH

Reference No.	Station	Location	Date	Time	Tide	Temp., °C.	Chlorine, grams per litre	pH	Plankton, volumes per 100,000
1	35	N. 49°6′, W. 123°47′	July 10, 1928	1:00 p.m.	E 1	18.8	12.33	8.55	45.0
2	35	Stuart Channel, Northern part	July 16, 1927	8:30 a.m.	E 1	19.30	13.58	—	17.5
3	35a		July 14, 1926	12:30 p.m.	E 5	19.9	14.50	8.5	41.0
4	35		Aug. 13, 1926	3:00 p.m.	F 3	17.9	15.12	8.50	36.0
5			July 29, 1926	11:15 a.m.	E 3	17.3	15.23	8.4	26.0
6	35a		July 29, 1926	9:10 a.m.	E 1	16.6	15.33	8.4	50.0
7	35b		July 29, 1926	10:40 a.m.	E 2	16.1	15.48	8.4	67.0
8	42a	N. 48°56′, W. 123°42′	July 14, 1926	1:30 p.m.	E 6	20.6	14.80	8.5	50.0
9	42	Stuart Channel S.	July 29, 1926	12:07 p.m.	E 4	17.20	15.38	—	—
10	35e	N. 49°5′, W.123°38′	June 25, 1927	2:50 p.m.	E 1	14.50	13.81	—	87.0
11	35d	Trincomali Ch. N.	June 16, 1927	2:30 p.m.		14.95	14.12	8.52	—
12	43b	N. 48°59′, W. 123°36′	July 11, 1928	6:30 p.m.	F 6	20.35	7.28	8.45	—
13	43	Near Porlier Pass	July 16, 1927	7:40 p.m.	F 6	13.60	13.77	—	32.5
14	43	Trincomali Ch.	June 25, 1927	2:50 p.m.	E 1	15.00	14.18	8.50	75.0
15	43a		July 12, 1928	8:00 a.m.	F 2	14.4	14.68	8.35	62.0
16	44b	N. 49°13′, W. 123°31′	July 11, 1928	6:10 p.m.	E 6	20.7	5.78	8.45	—
17	44	Near Porlier Pass	July 15, 1927	3:20 p.m.	F 3	19.20	6.17	8.40	1.2
18	44	Str. of Georgia	July 11, 1928	6:20 p.m.	F 1	20.4	6.52	8.42	—
19	44a		July 30, 1926	5:35 p.m.	F 3	19.0	6.83	8.35	8.4
20	44		July 16, 1926	4:20 p.m.	F 2	20.0	8.12	8.55	—
21	44		Aug. 6, 1926	4:05 p.m.	F 4	17.80	13.48	8.70	32.0
22	45	N. 49°4′, W. 123°29′	July 19, 1929	1:06 p.m.	F 3	17.75	4.74	7.88	0.7
23	45a	Str. of Georgia	July 11, 1928	5:20 p.m.	E 6	19.7	7.63	8.47	—
24	45	W. of mid-channel	July 11, 1928	5:45 p.m.	E 6	19.70	7.84	8.45	4.0
25	45c		July 28, 1928	10:11 p.m.	F 2	19.1	8.51	8.50	—
26			July 28, 1928	10:00 a.m.	F 2	18.1	12.09	8.64	—
27	45c		July 28, 1928	10:11 a.m.	F 2	18.2	12.28	8.67	—
28	45		Aug. 6, 1926	5:00 p.m.	F 5	18.20	12.52	8.65	32.0
29	46a	N. 49°5′, W. 123°24′	July 11, 1928	4:50 p.m.	E 5	19.10	1.81	8.25	0.2
30	46	Str. of Georgia	July 11, 1928	5:03 p.m.	E 6	20.1	2.83	8.25	0.2
31	46	E. of mid-channel	Aug. 6, 1926	6:00 p.m.	E 1	18.0	10.97	8.55	9.0
32	47	N. 49°6′, W. 123°20′	July 30, 1927	3:36 p.m.	F 3	18.48	0.115	8.02	1.2
33	47	Str. of Georgia	June 23, 1927	5:08 p.m.	E 5	15.0	0.29	7.80	0.7
34	47	Near lightship	July 11, 1928	4:36 p.m.	E 5	18.50	1.74	8.23	1.2
35	47		July 12, 1926	10:00 a.m.	E 3	17.4	4.17	8.5	—
36	47		Aug. 11, 1926	2:53 p.m.	F 2	18.30	4.86	8.30	1.2
37	47a		July 12, 1926	9:30 a.m.	E 2	17.0	8.72	8.45	6.0
38	47b		July 12, 1926	10:15 a.m.	E 3	16.9	11.33	8.5	—

The temperatures of these rivers, as they enter the Strait, vary greatly according to their sources and the time of the year. In January the Fraser River at New Westminster has a mean temperature of 4° C.; in April, 6.5 to 7.3° C.; in May, 7.3 to 10° C.; in June, 10 to 15° C.; in July, 15 to 17.5° C. and in August, 16 to 17.5° C. In contrast the surface temperature near the head of Howe Sound on July 9, 1927, was 9.5° C. and on August 6 it was 11.9° C. On September 19, 1928, the surface temperature near the entrance of Comox River was 16.6° C. The three rivers cited are typical of three classes; the first, those of great length which are snow-fed primarily but which become warmed by insolation on their way to the sea, such as the Fraser River; second, glacial streams with their sources near the coast, such as those flowing into Howe Sound and Jervis, Toba and Bute Inlets; and third, those which are relatively short and which are fed by mountain or upland lakes. The rivers on the eastern slope of Vancouver Island, namely Campbell, Oyster, Comox, Qualicum, Englishman, Nanaimo, Chemainus and Cowichan are included in this class. The primary effect upon the temperature of the Strait is evidently dependent upon the factors of volume and temperature.

Surface Salinity, Temperature, Plankton and pH on a Line West from the Fraser River

Stuart Channel

Stations 35 and 42 received water of high salinity from the Strait of Juan de Fuca through Sansum Narrows and Trincomali Channel to the south; sea water mixed with Fraser River water through Dodds Narrows and Porlier Pass and fresh water from the Chemainus River chiefly. The chlorinity shows a variation during July and August from 12.33 to 15.48 gm. per litre. The low values in early July are obviously the result of the flood water of the Chemainus River which occurs in May and June. The variation is not great either from month to month or with the tides; the mid-flood water on August 13 differed from the mid-ebb of July 29, by only 0.6 gm. Cl per litre. The temperature varied from 16.1 to 20.6° C. during this period and showed the evidence of a stable upper layer warmed by insolation. The plankton is consistently abundant and the pH high (8.4) as a result of the utilization of carbon dioxide by the phytoplankton.

Trincomali Channel

The variations in salinity and temperature are less than in Stuart Channel; for instance, there is little tidal variation (cf. 14.18 gm. Cl for the ebb and 13.77 for the flood). The salinities are intermediate between the extremes of Stuart Channel while the temperatures are uniformly lower, 13.7 to 14.6° C. This water is subject to marked tidal currents and the resulting turbulence. The two substations 43 (a) and 43 (b), situated a mile apart, the former in Trincomali Channel and the latter in the adjacent waters of the Strait of Georgia outside Porlier Pass, show a decided difference in both temperature and salinity (14.4° compared with 20.35° C. and 14.68 gm. Cl compared with 7.28 gm. Cl).

The evidence points to the barrier effect of passes on the escape of surface fresh water from the Strait of Georgia. The phytoplankton quantity and the pH are similar to those of Stuart Channel.

Strait of Georgia

The surface samples on a line across the Strait of Georgia from Porlier Pass to the lightship at the mouth of the Fraser River show a gradation from a minimal chlorinity of 5.78 gm. Cl per litre at Station 44 (Table 1) on the ebb tide to 0.29 at station 47. This tide carries the Fraser River water, which was taken northwestward by the flood, southward again to the westerly stations. The chlorinity values for the flood are affected by the sea water entering through the Straits and had maximum values during July and August of 13.5 gm. Cl at station 44 and 4.9 gm. Cl at station 47 (Table I). A very sudden change in salinity occurs within two miles of the lightship. On July 12, 1926, at 10:00 a.m. a sample was taken: chlorinity, 4.17; temperature, 17.4° C. Fifteen minutes later, less than two miles distant the values were: chlorinity, 11.33 gm. Cl; and temperature, 16 9° C. Lines of separation between the turbid water from the Fraser River and the blue water of the Strait are often very evident, and as previously recorded several similar lines may be observed frequently, forming arcs the radii of which are greatest northwestward from the Fraser River mouth.

The temperature of the surface water does not vary entirely with chlorinity along the Porlier Pass to the lightship line. On the ebb it was highest, 20.7° C., at the most distant station, that is, at 44, and decreased to 17.5° C., the usual summer temperature of the Fraser River, as the lightship was approached. The water carried northwestward by the flood tide and finally southward to station 44 by the ebb becomes warmed by insolation. The lower temperature near the river mouth is further shown in June; for instance, on June 23, 1927 the chlorinity was 0.29 and the temperature, 15.0° C. The flood tide on the other hand was characterized during July and August by a higher temperature at the lightship (*e.g.*, 15.06 and 15.08° C.) than at more distant points, especially at the last of this phase (for instance, 13.62° C. at station 46, Aug. 6, 1926). The colder water from Juan de Fuca is increased in temperature on the flood tide in proportion to its degree of mixing with the warmer Fraser River water as well as by solar heating and consequently time and distance become factors.

The surface plankton at the lightship is scarcely measurable and the pH is correspondingly low (*e.g.*, 7.8 and 8.0) at station 46, two and one-half miles distant, and the greatest recorded surface phytoplankton quantity is 9.0 units with a pH of 8.55; and at stations 45 and 44, *i.e.*, at distances of five and seven miles the plankton had increased to 32.0 units at the optimum conditions. The pH at these points, respectively, was 8.65 and 8.70. The greatest plankton abundance occurs at a chlorinity 12.5 to 13.5 gm. Cl per litre north of the Fraser River; that is, where the mixing of river and sea water is most complete. The very high pH at these points is explained by two considerations: (1) the rapid photosynthesis carried on by the abundant phytoplankton in the more

TABLE II

TEMPERATURE, SALINITY, pH AND PLANKTON AT 10 YARDS (9.14 METRES) ON A LINE WESTWARD FROM THE FRASER RIVER MOUTH

Reference No.	Station	Location	Date	Time	Tide	Temp., °C.	Chlorine, grams per litre	pH	Plankton, volumes per 100,000
39	35e	N. 49°6′, W. 123°46′	July 10, 1928	2:54 p.m.	E 2	13.13	14.70	8.25	22.5
40	35b	Stuart Channel N.	Aug. 2, 1928	10:22 a.m.	E 3	13.57	—	8.20	—
41	35		July 29, 1927	10:44 a.m.	E 5	13.84	14.91	8.23	5.80
42	35		July 29, 1926	10:24 a.m.	E 2	12.10	16.19	—	18.5
43	42	N. 48°50′, W. 123°42′ Stuart Channel S.	July 29, 1926	11:45 a.m.	E 3	12.58	16.20	7.95	1.3
44	43	N.48° 59′, W. 123°36′	Aug. 6, 1926	8:44 a.m.	E 3	15.18	14.61	8.35	18.0
45	43	Trincomali Ch. N.	July 29, 1927	1:32 p.m.	F 2	11.32	15.24	8.25	55.0
46	44	N. 49°2′, W. 123° 31′	July 30, 1927	5:56 p.m.	F 5	16.42	13.89	8.62	22.5
47	44	Near Porlier Pass	Aug. 6, 1926	3:56 p.m.	F 3	17.15	14.41	8.30	—
48	44	Str. of Georgia	July 16, 1926	4:15 p.m.	F 2	13.90	15.87	8.30	—
49	45	N. 49°3′, W. 123°27′ Str. of Georgia	Aug. 6, 1926	4:45 p.m.	F 4	16.45	14.74	8.50	8.0
50	45	W. of mid-channel	July 11, 1928	5:32 p.m.	E 6	13.67	14.77	8.30	12.5
51	46	N. 49°5′, W. 123°24′	Aug. 6, 1926	5:50 p.m.	F 6	13.62	15.78	8.20	—
52	47	N. 49°6′, W. 123°20′	July 11, 1928	4:18 p.m.	E 5	14.14	14.46	8.39	22.5
53	47	Near lightship	Aug. 11, 1926	2:31 p.m.	F 2	16.62	15.06	8.40	10.0
54	47	Str. of Georgia	July 30, 1927	3:14 p.m.	F 3	13.43	15.08	8.28	27.5
55	47a		Aug. 12, 1926	9:16 a.m.	E 2	16.15	15.12	8.45	—

TABLE III

TEMPERATURE, SALINITY, pH AND PLANKTON, AT 6 YARDS (5.5 METRES) ON A LINE WESTWARD FROM THE FRASER RIVER MOUTH

Reference No.	Station	Location	Date	Time	Tide	Temp., °C.	Chlorine, grams per litre	pH	Plankton, volumes per 100,000
56	35	N. 49°6′, W. 123°46′	July 29, 1927	10:49 a.m.	E 5	14.45	14.78	8.38	81.9
57	35a	Stuart Ch. N.	July 29, 1926	10:28 a.m.	E 2	12.75	16.32	8.10	—
58	42a	N. 48°56′, W. 123°42′	July 14, 1926	2:35 p.m.	F 1	18.65	14.91	8.5	—
59	42	Stuart Ch., S.	July 29, 1926	11:58 a.m.	E 3	13.12	15.82	—	5.0
60	43	N. 48°59′, W. 123°36′	Aug. 6, 1926	8:45 a.m.	E 3	15.50	14.62	8.85	20.0
61	43	Trincomali Ch. N.	July 29, 1927	1:37 p.m.	F 2	14.33	14.74	8.30	70.0
62	44	N. 49°2′, W. 123°31′	July 30, 1927	6:00 p.m.	F 5	17.23	13.27	8.90	100.0
63	44	Str. of Georgia	Aug. 6, 1926	4:00 p.m.	F 3	17.68	13.78	8.50	—
64	45	N. 49°3′, W. 123°27′	July 11, 1928	5:36 p.m.	E 6	14.80	14.20	8.42	45.0
65	45	Str. of Georgia	Aug. 6, 1926	4:49 p.m.	F 4	17.02	14.38	8.50	24.0
66	46	N. 49°5′, W. 123°24′	Aug. 6, 1926	5:58 p.m.	F 6	16.09	14.71	8.40	—
67	47	N. 49°6′, W. 123°20′	July 11, 1928	4:27 p.m.	E 5	17.64	10.57	8.42	30.0
68	47	Near lightship	July 30, 1927	3:18 p.m.	F 3	16.20	14.02	8.06	1.46
69	47a	Str. of Georgia	Aug. 12, 1926	9:20 a.m.	E 2	16.96	14.57	8.45	—
70	47		Aug. 11, 1926	2:35 p.m.	F 2	17.22	14.73	8.40	22.0

TABLE IV

SURFACE SALINITY, TEMPERATURE, pH AND PLANKTON ON A MID-CHANNEL LINE THROUGH HARO STRAIT, STRAIT OF GEORGIA AND DISCOVERY PASSAGE

Reference No.	Station	Location	Date	Time	Tide	Temp., °C.	Chlorine, grams per litre	pH	Plankton, volumes per 100,000
71	82a	N. 48°27′, W. 123°3′	July 15, 1926	4:54 p.m.	F 4	13.00	16.98	8.15	8.0
72	80	Haro Strait	July 15, 1926	5:40 p.m.	F 6	13.00	16.52	8.25	35.0
73	80	N. 48°32′, W. 123°12′	July 15, 1926	6:35 p.m.	E 1	11.95	17.35	8.05	17.0
74	77	Haro Strait	Aug. 17, 1929	11:45 a.m.	F 3	12.70	16.59	7.82	1.5
75	77	N. 48°37′, W. 123°4′	Aug. 16, 1929	2:33 p.m.	F 4	13.60	16.60	7.95	0.5
76	77a		July 15, 1926	2:55 p.m.	F 3	13.50	16.77	8.10	3.6
77	77a		July 15, 1926	11:50 a.m.	E 3	13.00	16.78	8.05	3.6
78	77		July 15, 1926	12:20 p.m.	E 4	13.20	16.79	8.10	7.2
79	77		Aug. 17, 1929	10:45 a.m.	F 2	11.70	17.25	7.80	1.5
80	76	Haro Strait N. 48°38′, W.123°15′	July 15, 1926	10:10 a.m.	E 2	13.40	16.42	8.15	35.0
81	76		June 24, 1927	6:08 p.m.	E 5	11.00	16.42	8.20	25.0
82	68b	Boundary Pass	July 27, 1928	2:00 a.m.	E 3	17.00	13.22	8.62	50.0
83	68a	N.48°46′, W. 123°3′	July 15, 1928	2:42 p.m.	E 1	14.00	13.84	—	17.5
84	68		July 13, 1928	1:28 p.m.	F 5	14.20	14.00	8.22	16.2
85	68b		July 26, 1928	12:30 p.m.	E 3	15.10	14.43	8.40	7.50
86	68b		July 26, 1928	11:21 a.m.	E 2	16.30	14.49	8.40	50.0
87	68	Boundary Pass	Aug. 13, 1926	8:00 a.m.	F 6	12.10	16.38	8.25	17.0
88	68	N. 48°46′, W. 123°3′	July 25, 1927	8:51 a.m.	F 1	10.02	16.64	8.08	20.0
89	68s3		Aug. 17, 1929	12:20 p.m.	F 2	13.10	16.30	7.90	1.0
90	68s2		Aug. 17, 1929	12:25 p.m.	F 2	12.70	16.49	7.90	2.0
91	68s1		Aug. 17, 1929	12:30 p.m.	F 2	12.90	16.44	7.90	2.0
92	68		Aug. 17, 1929	12:45 p.m.	F 2	15.20	15.32	8.02	1.5
93	68n1		Aug. 17, 1929	12:50 p.m.	F 2	17.20	13.37	8.25	1.5
94	68n3		Aug. 17, 1929	1:02 p.m.	F 3	18.90	12.05	8.30	1.5
95	68n4		Aug. 17, 1929	1:18 p.m.	F 3	18.80	11.40	8.40	1.0
96	68		Aug. 17, 1929	1:35 p.m.	F 3	19.30	12.18	8.40	0.5
97	57	S.E. Active Pass	July 29, 1927	6:23 p.m.	F 6	19.46	8.88	8.70	1.5
98	54	Strait of Georgia	July 19, 1929	11:45 a.m.	F 2	16.93	11.05	8.10	0.7
99	54	N. 48°54′, W. 123°15′	July 30, 1926	4:05 p.m.	F 2	17.20	12.62	8.35	28.0
100	54		July 17, 1929	11:00 a.m.	F 3	16.24	13.79	8.60	2.0
101	54		July 19, 1929	11:45 a.m.	F 2	16.93	11.05	8.10	0.7
102	54		July 18, 1929	8:15 a.m.	F 1	15.00	14.96	7.98	0.4

103	55	Strait of Georgia	Aug. 12, 1926	1:10 p.m.	E 6	17.00	13.54	8.50	64.0
104	55	N. 48°56′, W. 123°11′	July 28, 1928	8:15 a.m.	E 6	17.00	13.74	8.70	—
105	55(5)		July 28, 1928	8:30 a.m.	E 6	16.9	13.96	8.65	—
106			July 28, 1928	8:45 a.m.	E 6	16.2	14.15	8.66	—
107	55(5)		July 28, 1928	7:55 a.m.	E 6	15.90	14.55	8.47	60.0
108	53	N. 48°55′, W. 123°16′	July 19, 1929	12:02 p.m.	F 2	17.18	11.60	8.05	—
109	53	Strait of Georgia	July 16, 1926	2:20 p.m.	F 1	19.8	12.03	8.60	0.7
110	53a	N.E. of Active Pass	Aug. 11, 1926	6:25 a.m.	F 6	16.6	12.89	8.50	—
111	50	Strait of Georgia	July 15, 1927	4:20 p.m.	F 4	19.10	5.27	8.65	0.5
112	50a	E. of Galiano Island	Aug. 11, 1926	4:10 p.m.	F 4	—	6.57	8.50	20.0
113	50	N. 48°58′, W. 123°23′	July 30, 1926	4:50 p.m.	F 2	17.80	8.50	8.35	27.0
114	50b		Aug. 12, 1926	7:00 a.m.	F 6	16.8	8.66	8.45	—
115	50		July 19, 1929	12:15 p.m.	F 3	17.25	10.01	8.22	—
116	50		July 16, 1926	3:30 p.m.	F 1	19.5	11.08	8.55	0.7
117	50b		Aug. 11, 1926	4:35 p.m.	F 4	18.	11.67	—	40.0
118	50		Aug. 17, 1929	4:00 p.m.	F 5	19.10	14.45	8.40	0.5
119	45c	Strait of Georgia	July 28, 1928	10:15 a.m.	F 2	20.0	1.15	8.03	—
120	45a	5 miles N.E. Porlier P.	July 11, 1928	5:20 p.m.	E 6	19.7	7.3	8.47	—
121	45	N. 49°4′, W. 123°27′	July 11, 1928	5:45 p.m.	E 6	19.70	7.84	8.45	4.0
122	45c		July 28, 1928	10:12 a.m.	F 2	19.1	8.51	8.50	—
123	45c		July 28, 1928	10:10 a.m.	F 2	18.2	12.28	8.67	—
124	45		Aug. 6, 1926	5:00 p.m.	F 5	18.20	12.52	8.65	32.0
125	46a	Op. Fraser River	July 11, 1928	4:50 p.m.	E 6	19.10	1.81	8.25	—
126	46	Strait of Georgia	July 11, 1928	5:03 p.m.	E 6	20.1	2.83	8.25	—
127	46	N. 49°5′, W. 123°24′	Aug. 6, 1926	6:00 p.m.	E 1	18.0	10.97	8.55	1.90
128	40a	Strait of Georgia	June 23, 1927	3:40 p.m.	E 3	17.6	1.25	7.85	0.5
129	40	N. 49°11′, W. 123°20′	June 23, 1927	4:12 p.m.	E 4	16.2	1.38	8.00	—
130	40	N.W. Fraser River	Aug. 11, 1926	1:28 p.m.	E 6	20.0	2.64	8.00	2.4
131	40a		Aug. 11, 1926	1:43 p.m.	F 1	20.5	3.26	8.10	—
132	37	Strait of Georgia	July 28, 1928	10:15 p.m.	F 2	20.0	1.15	8.03	—
133	37	E. of Gabriola Pass	July 28, 1928	10:30 p.m.	F 2	19.5	5.78	8.50	—
134	37	N. 49°9′, W. 123°33′	July 28, 1928	10:44 p.m.	F 2	19.0	7.70	8.58	—
135	14	Strait of Georgia	July 4, 1927	9:20 a.m.	E 2	15.80	9.75	8.38	5.6
136	14a	N.W. Entrance Island	July 11, 1928	11:31 a.m.	F 3	19.4	9.90	8.42	—
137	14	N. 49°13′, W. 123°25′	July 11, 1928	11:05 a.m.	F 3	19.5	10.23	8.50	30.0
138	14		July 12, 1927	11:15 a.m.	E 3	17.75	12.94	8.40	5.0
139	14		Aug. 10, 1926	11:58 a.m.	E 6	18.30	13.68	8.80	48.0
140	14		July 19, 1929	2:15 p.m.	F 4	15.96	14.50	8.22	—
141	14		Aug. 17, 1929	7:25 p.m.	E 1	19.40	14.53	8.25	4.0

TABLE IV—*Continued*

Reference No.	Station	Location	Date	Time	Tide	Temp., °C.	Chlorine, grams per litre	pH	Plankton, volumes per 100,000
142	15a	Strait of Georgia	July 11, 1927	11:53 a.m.	F 5	19.7	8.98	8.45	—
143	15	N.E. Entrance Island	July 11, 1927	11:42 a.m.	F 4	19.5	10.24	8.42	20.0
144	15	N. 49°14′, W. 123°21′	July 4, 1927	9:40 a.m.	E 2	15.70	10.92	8.38	7.5
145	15		July 6, 1927	4:55 p.m.	F 4	17.2	11.18	—	6.5
146			July 26, 1929	12:15 p.m.	E 4	17.10	13.89	8.30	—
147	16	Strait of Georgia	July 11, 1928	12:14 p.m.	F 5	20.1	8.90	8.52	12.5
148	16	N. 49°14.5′, W. 123°37′	July 26, 1929	1:02 p.m.	E 5	17.40	12.30	8.20	—
149	9	N. 49°21′, W. 123°50′	Aug. 4, 1926	4:36 p.m.	F 6	20.00	12.01	8.90	60.0
150	10	N. 49°23′, W. 123°48′	Aug. 4, 1926	4:00 p.m.	F 6	19.00	12.61	8.85	65.0
151	1	Strait of Georgia	June 21, 1927	11:34 a.m.	E 2	18.60	8.08	8.30	0.5
152	1	N. 49°19′, W. 123°52′	Aug. 1, 1928	12:07 p.m.	F 1	18.80	9.70	8.70	1.0
153	1		Aug. 4, 1926	5:35 p.m.	E 1	19.0	12.18	8.60	60.0
154	1		Aug. 18, 1927	8:21 a.m.	F 5	20.30	12.57	8.65	22.5
155	1		Oct. 21, 1926	—	—	11.38	13.96	8.10	—
156	1		July 10, 1929	11:45 a.m.	E 4	14.89	14.64	8.6	1.0
157	1		June 29, 1929	11:23 a.m.	E 2	15.40	14.65	8.5	1.0
158	1		Sept. 20, 1928	1:39 p.m.	E 2	13.60	15.03	8.2	—
159	1		Dec. 18, 1928	—	—	6.79	15.64	—	—
160	1		Oct. 23, 1928	—	—	10.04	15.92	8.1	—
161	1		Mar. 31, 1927	—	—	7.8	16.24	7.8	—
162	1		Feb. 3, 1927	—	—	7.2	16.41	8.0	—
163	1		Feb. 9, 1927	11:50 a.m.	E 6	7.20	16.58	7.98	—
164	1		Apr. 25, 1929	11:23 a.m.	E 2	15.40	14.65	8.5	1.0
165	1		Mar. 24, 1929	12:15 p.m.	F 1	8.32	16.84	7.85	0.2
166	1		Mar. 2, 1929	11:00 a.m.	E 2	7.20	16.97	7.75	0.4
167	2e	N. 49°20′, W. 124°9′	June 27, 1927	12:30 p.m.	F 3	16.90	10.31	8.30	15.0
168	2e		June 27, 1927	12:00 p.m.	F 2	15.80	11.52	8.28	21.2
169	2b		June 28, 1927	8:10 p.m.	E 2	16.60	11.82	8.45	8.2
170	2	Strait of Georgia	Aug. 11, 1928	9:35 a.m.	F 2	17.8	12.12	8.45	2.5
171	2	Off Ballenas Island	July 30, 1926	11:22 a.m.	F 3	18.00	12.82	8.55	58.0
172	2a	N. 49°20′, W. 124°9′	July 30, 1926	2:40 p.m.	F 6	17.97	13.28	8.55	38.0
173	2b		July 23, 1926	6:40 a.m.	E 6	16.85	13.92	8.55	0.5
174	2W		Aug. 8, 1929	4:00 p.m.	E 3	18.00	14.64	8.30	1.5
175	2		Aug. 6, 1928	12:00 p.m.	E 2	15.4	14.90	8.48	4.0

176	3	Strait of Georgia	June 28, 1927	7:10 p.m.	E 1	16.20	13.50	8.40	12.5
177	3	S. Lasqueti Island	Aug. 6, 1928	1:00 p.m.	E 4	17.6	13.67	8.57	0.5
178	3	N. 49°23′, W. 124°11′	July 30, 1926	4:50 p.m.	E 1	17.0	14.45	8.45	6.2
179	3w		Aug. 8, 1929	6:00 p.m.	E 5	18.80	15.49	8.30	1.0
180	101	Strait of Georgia	June 28, 1927	5:25 p.m.	F 6	16.35	12.44	8.40	7.5
181	101s	N.W. Lasqueti Island	Aug. 11, 1928	8:45 a.m.	F 1	17.5	12.90	8.43	0.5
182	101s	N. 49°35′, W. 124°30′	Aug. 6, 1928	1:50 p.m.	E 5	17.7	13.82	8.50	2.5
183	101n		Aug. 11, 1928	7:35 a.m.	E 6	16.1	14.44	8.22	5.0
184	101n	N. 49°35′, W.124°30′	Aug. 6, 1928	2:45 p.m.	F 1	16.8	14.80	8.47	2.5
185	101w		Aug. 8, 1929	7:00 p.m.	E 5	19.80	15.33	8.30	3.0
186	103	W. Texada Island	June 28, 1927	3:10 p.m.	F 4	14.90	14.80	8.28	7.5
187	103	N. 49°40′, W. 124°35′	Aug. 6, 1928	3:25 p.m.	F 1	16.3	14.99	8.45	2.5
188	105	N.W. Texada Island	Aug. 6, 1928	6:15 p.m.	F 4	18.3	13.36	8.67	4.5
189	105	N. 49°45′, W.124°42′	June 28, 1927	1:12 p.m.	F 3	16.70	13.80	8.52	2.5
190	162		Aug. 10, 1928	12:40 p.m.	F 5	18.4	13.04	8.40	2.5
191	162		Aug. 9, 1929	11:57 a.m.	E 4	16.74	15.55	8.40	0.5
192	154		Aug. 10, 1928	11:30 a.m.	F 4	17.7	13.68	—	16.0
193	154		Aug. 9, 1929	2:50 p.m.	F 1	16.21	15.75	8.42	1.5
194	153		Aug. 9, 1928	6:20 p.m.	F 1	16.9	15.0	—	1.0
195	152		Aug. 9, 1928	6:05 p.m.	F 1	18.2	14.74	—	—
196	151		Aug. 9, 1928	5:50 p.m.	F 1	18.1	14.25	—	—
197	150		Aug. 9, 1928	5:35 p.m.	F 1	19.1	14.42	—	—
198	149		Aug. 9, 1928	5:20 p.m.	E 6	19.9	12.83	—	5.0
199	114	N. 49°59′, W. 125°10′	Aug. 7, 1928	10:05 a.m.	E 1	18.0	13.55	8.60	2.5
200	115	N. 50°0′, W. 125°13′	Aug. 6, 1929	10:25 a.m.	E 1	17.8	13.56	8.55	4.0
201	115		Aug. 9, 1929	5:49 p.m.	F 3	15.20	16.00	8.32	5.0
202	116		Aug. 7, 1928	10:35 a.m.	E 1	17.7	13.76	8.60	4.0
203	120	Discovery Passage Quathiaski Cove	Aug. 8, 1928	5:00 a.m.	F 2	14.4	15.17	—	12.5
204	120	N. 50°1′, W. 125°22′	Aug. 7, 1928	1:00 p.m.	E 4	13.0	15.77	8.27	5.0
205	120		Aug. 7, 1928	7:01 p.m.	F 3	12.6	15.93	8.22	6.2
206	120		Aug. 7, 1928	9:00 p.m.	F 5	11.3	16.30	8.00	7.5
207	120n.1.		Aug. 10, 1929	8:00 a.m.	F 6	10.54	16.71	7.78	0.5
208	130	Discovery Passage Plumper Bay	Aug. 8, 1928	11:20 a.m.	E 1	12.0	16.04	8.10	0.5
209	130	N. 50°10′, W. 125°22′	Aug. 8, 1928	4:30 p.m.	F 1	11.2	16.34	8.08	5.0
210	133	N. 50°17′, W. 125°27′	Aug. 9, 1928	9:40 a.m.	F 5	11.8	16.16	8.13	2.5
211	133		Aug. 10, 1929	11:41 a.m.	E 2	10.45	16.79	7.80	0.5

intense light near the surface and the consequent lowering of the carbon dioxide content and, (2) the relatively small buffer action of these diluted waters because of the lower concentration, particularly of bicarbonates.

Temperature, Salinity, pH and Plankton at 10 Yards (9.14 Metres) Depth on a Line Westward from the Fraser River Mouth

The salinity at 10 yards (9.14 metres) shows much less variation either with distance from the river or as a result of tides. In all cases there is evidence of rather complete mixing of river and sea water; the lowest recorded chlorine values are about 14.0 and occurred on the late flood at station 44. At this distance of seven miles the effect of the fresh water is shown at a greater depth. This fact is emphasized by the relatively high salinity at a depth of 10 yards at the Fraser River mouth (average Cl = 15+). In Trincomali Channel there is a greater variation at 10 yards than in Stuart Channel. The reverse of this is the case at the surface. Apparently more water enters Porlier Pass from the 10 yards than from the surface level. This furnishes further evidence for the conservation of the fresh water in the Strait of Georgia (cf. 9, 10, 12).

The temperature is relatively uniform in Stuart Channel at 10 yards as compared with Trincomali Channel; summer records show the extremes of 12.12 and 13.84° C. in the former and 11.32 and 15.18° C. in the latter. The relatively high salinity at the lightship is accompanied by a somewhat lower temperature, but the difference in temperature is proportionately less since the water from the region of Point Roberts has been considerably warmed by radiation.

The plankton quantity is also much more uniformly high at the 10 yards level, a circumstance which is apparently related to the high degree of mixing. The pH is considerably lower even with a high plankton content. At station 43 with a plankton record of 55.0 units the pH is 8.25. At the greater depth photosynthesis is less rapid and the buffer action is greater due to the higher concentration of bicarbonates.

The values at six yards are intermediate and will be discussed under the description of Fig. 17 and 18.

Surface Salinity, Temperature, pH and Plankton on a Mid-channel Line Through Haro Strait, Strait of Georgia and Discovery Passage

Haro Strait

In Haro Strait the surface salinity during the summer ordinarily varies less than a gram per litre. On July 15, 1926, samples were taken before and after the passing of a tide-rip; the values were, before the eddy, chlorinity 16.52 gm. Cl per litre and temperature 13.00° C.; after the eddy, chlorinity 17.35 gm. Cl per litre and temperature 11.95° C. The column of water as a whole shows relatively little change in temperature and salinity, in fact the surface salinity after the eddy was somewhat higher than that at 50 yards, before the eddy. It would appear that the column is very unstable and readily inverted by

tidal currents. A similar result from the turbulence of a water column of nearly uniform density is shown for station 77. The greatest variations recorded were for two points, one in an open area and the other in a narrow passage (ref. No. 74, 79). On July 15, 1926, the chlorinities were the same, 16.42 gm., while the temperatures were 13.40° C. and 11.00° C., respectively. The samples were collected exactly an hour apart. Temperature increases to some extent with increased insolation but much less than in areas where there is a stable epithalassa.

Ordinarily there is a small quantity of phytoplankton on the flood tide coming from Juan de Fuca (0.5 to 3.6 units), while on the ebb the currents carry material from the Sidney and Swanson channels to give values as high as 35.0 units. The pH on the flood varies from 7.8 to 8.1 and may attain 8.25 on the ebb when the phytoplankton is abundant. Again high salinity is accompanied by considerable buffer action and a relatively stabilized pH.

Boundary Pass

The dividing line between the area of sea water dominance and that diluted by the river occurs at or near East Point, Boundary Pass; there is a change of position of several miles according to the phase of the tide, however. According to the authors' records the summer chlorinity range at station 68 was 13.22 to 16.64 gm. Cl and the corresponding temperatures were 17.0° C. and 10.02° C., the first reading in each case being on the mid-ebb, the latter on the mid-flood, July 27, 1928, and July 25, 1927, respectively. A series of samples collected over a distance of five miles, two miles south of East Point to three miles northwest, on August 17, 1929, showed a chlorinity change from 16.49 to 11.40 gm. Cl and temperatures from 12.70° C. to 18.80° C. and in a distance of 200 yards when opposite East Point the changes were 16.44 to 15.32 gm. Cl and 12.90° C. to 15.20° C.

The ebb waters whose chlorinity shows evidences of mixing are characterized by high plankton content (20 units). The end of the recorded flood period also brings phytoplankton from the Boundary Bay region because of the nature of the tidal swirl described above (Table IV, 84, 87). The early flood, however, has a low plankton value (0.5 to 2.0 units). Again, the highest pH, 8.62, was obtained for the water with most abundant phytoplankton, while on the flood tide the pH readings were repeatedly 7.90.

The Strait of Georgia, Southern Portion

A comparison of the salinities at stations 54 and 55 gives further evidence of the effect of the tidal swirl in Boundary Bay. Although station 55 is several miles nearer the Fraser River the salinity is generally higher (13.54 to 14.55 gm. Cl); there is a lower temperature (17.00 to 15.90° C.) and high plankton (60.0) and pH values (8.50 to 8.70) on the ebb, while at station 54 the flood, which might be expected to give high salinity values and low temperature, gives values which are relatively the reverse (Table IV, 98-104). Station 55 is within the Boundary Bay swirl while station 54 is westward beyond its immediate influence and within the area of the more direct influence of the Fraser River.

Station 53 is situated approximately the same distance from Active Pass as station 54; the former in a northeasterly direction, the latter southeasterly. The maximum temperature recorded for station 54 is 17.20° C. and for station 53 is 19.8° C.; similarly the chlorinity for the former is 14.96 gm. Cl and for the latter 12.89 gm. Cl. It would appear that the more saline water of lower temperature emerging with the flood through Active Pass is carried somewhat southward. This is in accord with the observation that the ebb tide is stronger on the western side of the Strait while the flood tide is stronger on the eastern side. On Aug. 17, 1927, more direct evidence was obtained from a series of surface samples collected on the flood tide along the east side of Saturna, Mayne, Galiano, Valdes and Gabriola Islands. Opposite the mid-point of Mayne Island the temperature was 19.30° C., the chlorinity 12.72 gm. Cl; at station 54 the readings were 18.73° C. and 13.76 gm. Cl; at station 53, 20.40° C. and 13.80 gm. Cl. A similar effect was observed opposite Porlier and Gabriola Passes.

Westward from the Fraser River

Remarkably low salinities are found on the ebb tide on a line westward from the Fraser River mouth and extending across the Strait of Georgia practically to Gabriola and Valdes Islands. At station 45 which is five miles from the lightship at the margin of the delta a reading of 1.15 gm. Cl was obtained near the beginning of the flood (Table IV, 119). The early flood entering along the east side forces the river water before it; a similar effect is seen at station 50 (Table IV, 111). The maximum summer chlorinity observed at this station 45 was 12.52 gm. Cl near the end of the ebb tide (Table IV, 124).

At station 40, near the north outlet of the Fraser River the lowest salinity was shown at the mid-ebb; at station 46 it occurred at the end of the ebb and at station 50 at the beginning of the flood; that is, the time factor enters since the more distant points are affected later as indicated by the phase of the tide.

The surface temperatures during July and August show consistently high values between 18.0 and 21° C. westward from the river. At station 45 chlorinity variations of 10.37 gm. Cl were recorded while the temperature variation was not more than 1.80° C.

The surface plankton is very low where the chlorinity is less than 12.0 gm. Cl. However, relatively high plankton values are found associated with chlorinities only slightly higher, for instance:— at station 45 at the end of the flood, when the chlorinity was 12.52, a sample containing 32 plankton units was collected.

The pH is uniformly high with abundant plankton (8.4-8.8) and in a number of cases it may be as high as 8.55, (Table IV, 127), with low plankton content. In such instances, however, it is found that there is high phytoplankton content at depths of two and four yards and the diffusion of carbon dioxide to these regions and wind action may account in part for this seeming anomaly.

North of the Fraser River

The effect of the river on both temperature and salinity is greater on the east side of the strait and it diminishes rapidly from mid-channel westward on a line

from Burrard Inlet to Nanaimo; the maximum chlorinity recorded at station 16 is 12.30 gm. Cl and the minimum 8.90 gm Cl, while five miles west at station 14 the extremes are 14.53 and 9.75 gm. Cl. The highest temperature at station 16 was 20.1° C. and at station 14 it was 19.5° C. As mentioned above the temperature increases with distance from the Fraser River since time is a factor in insolation, but this effect is overcome when the epithalassa is disturbed by mixing as a result of tidal or wind movements.

Farther north, the effect of the Fraser is carried farther westward as shown by the salinity at station 1, which is more than 25 miles northwest of the Fraser River mouth and which showed a minimal chlorinity in June 1927 of 8.08 gm. Cl and a maximal temperature in August 1927 of 20.30° C. (Fig. 8). The effect is most marked at the last of the flood or the beginning of the ebb.

The maximum phytoplankton is found at the last of the flood also, and occurs at the surface (20-65 units). One of the highest pH values was obtained at station 10 on Aug. 4, 1926, at the last phase of the flood tide, namely, pH 8.85, with plankton, 65 units. Frequently the change in plankton quantity is sudden, especially near the limits of an area of abundance. At station 2a, Ballenac Islands, on August 3, 1926, the phytoplankton changed from 19.0 to 38.0 units during a half-hour, shortly before the high water slack. A very small decrease in chlorinity from 13.48 to 13.28 gm. per litre was recorded.

The seasonal variation at station 1 is indicated in Table I, 155-168. The direct effect of atmospheric temperature and radiation on the surface water temperature is apparent and the high winter salinity may be noted also. These data are discussed in earlier papers (9, 12) and graphs are given to illustrate seasonal changes.

The Texada Island Region

At station 3, off the southern end of Lasqueti Island, the salinity varied from 13 to 15.50 gm. Cl. The epithalassa is however of sufficiently low density to be fairly stable and consequently the temperature is maintained during the summer at 16.2 to 18.8° C. (Table IV, 176-179). Station 101 had a similar temperature and somewhat higher chlorinity while at station 103, off the mid-point of Texada Island the chlorinity was relatively uniform, 14 80-14.49 gm. Cl, and the temperature was lower, 14.90 to 16.3° C. This area is beyond the immediate effect of the Fraser River and is within the sphere of influence of the cold saline waters from Discovery Passage at the north. At station 105 near the north end of Texada Island the salinity was lower, 13.36-13.80 gm. Cl, and the temperature was higher, 16.70 to 18.3° C., due to the effect of river water from northern inlets, especially Toba and Bute, which extend southward, particularly on the eastern side of the Strait.

The plankton quantity was low; at stations 101 and 103 readings of 7.5 units were obtained. The pH values were higher than might be expected, namely, 8.2 to 8.6. However, this may be accounted for by the proximity of phytoplankton either at lower levels or of laterally situated areas. North of the Fraser the salinity which is associated with optimal phytoplankton conditions varies from 11.0 gm. Cl, to 13.5 gm. Cl; that is, in the areas of

TABLE V

SALINITY, TEMPERATURE, pH AND PLANKTON, AT 6 YARDS (5.5 METRES) ON A MID-CHANNEL LINE THROUGH HARO STRAIT, STRAIT OF GEORGIA AND DISCOVERY PASSAGE

Reference No.	Station	Location	Date	Time	Tide	Temp., °C.	Chlorine, grams per litre	pH	Plankton, volumes per 100,000
212	80	N. 48°32′, W. 123°12′	July 15, 1926	6:20 p.m.	F 6	12.35	17.10	8.15	—
213	76	N. 48°38′, W. 123°3′	July 15, 1926	10:54 a.m.	E 1	12.1	16.59	8.10	—
214	68		July 13, 1928	1:17 p.m.	F 5	13.18	14.13	8.20	12.5
215	68		Aug. 13, 1926	7:53 a.m.	F 6	11.72	16.52	8.20	6.0
216	68a		June 25, 1927	9:04 a.m.	F 1	9.96	16.73	8.05	2.50
217	68b		June 27, 1928	2:10 a.m.	F 3	16.40	13.74	8.53	60.0
218	68b		July 26, 1928	4:48 p.m.	E 2	15.17	14.47	8.35	45.0
219	68b		July 26, 1928	11:02 a.m.	F 3	14.38	14.15	8.25	15.0
220	54	N. 48°54′, W. 123°15′	July 17, 1929	7:32 p.m.	E 3	14.62	14.62	8.25	0.5
221	54		July 17, 1929	10:46 a.m.	F 2	12.90	15.34	8.10	0.2
222	54		July 30, 1926	4:04 p.m.	F 2	13.38	15.73	8.30	30.0
223	54		July 17, 1929	4:26 p.m.	E 1	10.75	16.51	7.75	0.5
224	55	N. 48°56′, W. 123°11′	Aug. 12, 1926	1:01 p.m.	E 6	15.37	14.52	8.48	—
225	53	N. 48°55′, W. 123°16′	July 16, 1926	2:07 p.m.	E 6	13.98	16.01	—	—
226	50	N. 48°58′, W. 123°23′	July 16, 1926	3:22 p.m.	F 1	13.9	15.81	8.28	—
227	45	N. 49°4′, W. 123°28′	July 11, 1928	5:35 p.m.	E 6	14.80	14.20	8.42	45.0
228	45		Aug. 6, 1926	4:49 p.m.	F 4	17.02	14.38	8.50	48.0
229	46	N. 49°5′, W. 123°24′	Aug. 6, 1926	5:58 p.m.	F 6	16.09	14.71	8.40	—
230	16		Aug. 10, 1926	2:10 p.m.	F 2	13.70	15.71	8.40	12.0
231	17	N. 49°15′, W. 123°33′	July 11, 1928	12:52 p.m.	F 6	16.17	11.24	8.35	5.0
232	17		July 8, 1927	1:34 p.m.	F 6	14.08	14.48	8.40	5.0
233	17		July 26, 1929	2:32 p.m.	F 1	13.20	15.40	8.15	—
234	8	N. 49°17′ W. 123°54′	Aug. 4, 1926	7:15 p.m.	E 3	16.53	14.82	—	—

235	1	N. 49°19′, W. 123°52′	Aug. 1, 1928	11:51 a.m.	F 1	16.60	14.39	8.60	—
236	1	10 mi. N.W. Departure	Aug. 18, 1927	8:37 a.m.	F 5	16.54	15.00	8.65	20.0
237	1	Bay	Aug. 4, 1926	5:38 p.m.	E 1	13.82	15.18	8.20	25.0
238	1		June 16, 1927	2:25 p.m.	—	11.35	15.69	8.20	—
239	1		Mar. 31, 1927	—	—	7.6	16.31	—	10.0
240	1		Dec. 17, 1926	—	—	7.7	16.68	8.0	—
241	10	N. 49°26′, W. 123°48′	Aug. 4, 1926	3:53 p.m.	F 6	13.60	15.29	8.25	64.0
242	2a		July 30, 1926	2:09 p.m.	F 5	16.42	14.42	8.35	0.5
243	2	N. 49°20′, W. 124°9′	July 23, 1926	6:27 a.m.	E 6	16.4	15.31	8.2	—
244	3	N. 49°24′, W. 124°12′	July 30, 1926	4:40 p.m.	E 1	15.55	15.10	—	2.0
245	3a		Aug. 3, 1926	7:10 p.m.	E 4	16.35	15.25	—	—
246	4	N. 49°28′, W. 124°10′	Aug. 4, 1926	7:51 a.m.	E 5	16.57	14.67	—	40.0
247	101	N. 49°28′, W. 124°29′	June 28, 1927	5:36 p.m.	F 6	15.17	13.60	8.48	25.0
248	103	N. 49°35′, W. 124°32′	June 28, 1927	3:53 p.m.	F 4	13.37	15.62	8.23	2.0
249	105	N. 49°41′, W. 124°43′	Aug. 6, 1928	4:36 p.m.	F 2	17.96	13.99	8.60	2.5
250	105	N.W. Texada Island	June 28, 1927	1:12 p.m.	F 3	14.66	14.12	8.32	20.0
251	107	N. 49°48′, W. 124°42′	June 28, 1927	11:37 p.m.	F 1	14.55	15.27	8.30	7.5
252	162	N. 49°39′, W. 124°48′	Aug. 10, 1928	12:34 p.m.	F 5	17.71	13.62	8.30	2.5
253	162	E. Comox Spit	Aug. 9, 1929	11:36 a.m.	E 4	15.81	15.58	8.30	0.5
254	110	N. 49°58′, W. 124°50′	Aug. 7, 1928	2:00 a.m.	E 5	17.8	13.23	8.40	6.2
255	110	N. Savary Island	Aug. 6, 1928	11:05 p.m.	E 1	17.7	13.52	8.50	5.0
256	110		Aug. 6, 1928	7:16 p.m.	F 5	17.59	13.66	8.55	6.0
257	110 n.e.		Aug. 12, 1929	9:33 a.m.	F 3	14.36	15.78	8.35	—
258	154	N. 49°54′, W. 125°5′	Aug. 9, 1929	2:30 p.m.	F 6	12.03	16.37	7.94	4.0
259	114	N. 49°59′, W. 125°10′	Aug. 9, 1929	5:31 p.m.	F 2	13.99	16.13	8.30	5.0
260	120	N. 50°1′, W. 125°14′ Quathiaski Cove	Aug. 8, 1928	4:50 a.m.	F 1	14.2	15.22	—	9.0
261	120	Discovery Pass	Aug. 7, 1928	11:38 a.m.	E 2	12.17	16.00	8.21	7.5
262	130	N. 50°10′, W. 125°22′	Aug. 8, 1928	11:12 a.m.	E 1	11.69	16.15	8.10	6.0
263	130	N. Seymour Narrows	Aug. 8, 1928	7:32 p.m.	F 2	11.42	16.30	8.10	5.0
264	133	N. 50°17′, W. 125°27′	Aug. 9, 1929	11:23 a.m.	E 2	10.20	16.85	7.82	1.0

primary mixing of river and sea water. The greater part of the area west of Texada Island has a higher salinity, the mixing has been completed and there is little phytoplankton. It is notable, however, that even small streams flowing into this region are accompanied by a very abundant plankton. The rivers entering at Courtenay, protected as they are by Comox Spit and Denman Island, give conditions which support plankton measuring 50+ units and the rivers entering at Qualicum and Parksville have similar effects, although less extensive, partly because of the unprotected shore line.

Northern Part of the Strait of Georgia

Water from two sources enters the northern part of the Strait, one through Discovery Passage and the other through Bute and Toba Inlets. The former source has high salinity and low temperature and enters at the western limit, while the latter has low chlorinity and high temperature during the summer period and enters the eastern area. Between is a region of turbulence which is increased by the meeting of the tidal flood currents, the one from the south and the other from the north. The tide from the south continues through Sutil Channel and into Bute and Toba Inlets, that is, for more than 60 miles. The tidal current through Discovery Passage may attain 12 knots. In part at least the mass of water which accumulates at the northwestern region of the Strait of Georgia may account for the well-known general eastward drifts in this region.

Certain eddy regions occur where there is practically no tidal change. At station 110, Savary Island, Aug. 6-7, 1928, a twelve-hour series of samples was collected with a constant temperature of 17.8° C. except for one reading, 17.5° C., and the variation to a depth of 10 yards was not more than 0.4° C. Similarly the chlorinity to the same depth was constantly within the limits 13.26 to 13.65. The plankton at the surface remained between 5.0 and 6.0 units, and the pH at 8.35 to 8.40. The conditions at this station were the most nearly constant observed in the Strait of Georgia.

Conditions on the west side of the Strait are illustrated by records at station 162, off Cape Lazo, 25 miles from the entrance to Discovery Passage, which had a temperature 18.4° C. and chlorinity 13.04 gm. Cl on the flood tide and shows the effect of the Fraser River while on the ebb the characters of the water from Discovery Passage become apparent with temperature 16.74° C. and chlorinity 15.55 gm. Cl. The line of separation between waters from the south and from the north evidently shifts on either side of this station from one phase of the tide to another. At station 115 the low chlorinity and high temperature, 14.56 gm. Cl and 17.8° C., occurred on the ebb and the reverse on the flood, 16.00 gm. Cl and 15.20° C. The water of low salinity comes from Sutil Channel and that of high from Discovery Passage. Tides of the same phase have reverse effects on opposite sides of the separating line according to the source of the flood waters, from the south or from the north.

A series taken at the beginning of the flood, Aug. 9, 1928, from the mouth of Sutil Channel, station 149, in a direction southwesterly to station 153, a dis-

tance of eight miles, showed a temperature change from 19.9 to 16.9° C. and a chlorinity change from 12.83 to 15.0 gm. Cl. A westerly series would show a similar change within a much less distance.

Discovery Passage

The temperature and chlorinity are relatively uniform. At Quathiaski Cove, which is nearly opposite Campbell River, the chlorinity varied only from 15.17 to 16.71 gm. Cl and the temperature from 14.40 to 10.54° C. at the surface during a 24-hr. series. The river water which enters is so distributed by the turbulence that its effect is dissipated. An eight-hour series showed a change of chlorinity from 15.77 to 16.30 gm. Cl, accompanied by a pH change from 8.27 to 8.00 with constant or slightly increased phytoplankton.

At station 130 north of Seymour Narrows a 24-hr. series showed a temperature variation of 11.2 to 12.0° C. and chlorinity 16.04 to 16.34 gm. Cl, and at station 133, at the entrance to Okisallo Channel, a temperature 10.45 to 11.8° C. and chloride 16.16 to 16.79 gm. Cl were recorded. The plankton was sparse, 0.5 units on the ebb with a pH from 7.80 to 8.15. It may be noted that while the surface salinity is lower than that sometimes found in Haro Strait, (cf. 16.79 and 17.35 gm. Cl), the temperature is lower than in Haro Strait during the summer, (cf. 10.45 and 12.40° C., using the maximal readings for chlorinity and the minimal for temperature).

Salinity, Temperature, pH and Plankton at a Depth of 6 Yards (5.5 Metres) on a Line Through Haro Strait, Strait of Georgia and Discovery Passage

The readings at six yards (5.5 metres) give a fair estimate of the depth of the epithalassa. At the time of the flood waters of the Fraser River, June 27, 1928, chlorinity at station 68 was 13.74 at six yards depth, on the mid-flood, while August 13, 1926, it was 16.73 gm. Cl. This is in agreement with observations recorded by Thompson (15) who reports that at certain periods water of decidedly low salinity is found as far south as the entrance to San Juan Passage. This low salinity water of June 27, 1928 also had a high temperature, 16.40° C., and an exceptionally high plankton content of 65 units, and pH of 8.53. The evidence would indicate that the source was the region eastward, as explained before, and not southward as one might at first suppose. The early flood moves from the south as indicated by the sample taken at six yards on June 25, 1927, when the chlorinity was 16.73 gm. Cl, the temperature was 9.96° C., the plankton 2.5 units and the pH 8.05. Station 54 shows something of the same effect of the swirl off the Boundary Bay. On July 17, 1929, the beginning of the ebb gave a high chlorinity, 16.51 gm. Cl; low temperature, 10.75° C.; low pH 7.75; and plankton, 0.5 units, having apparent characteristics of sea water.

The regions which show the most marked characteristics at depth of six yards are found westward and northward of the Fraser River mouth. At station 45, Aug. 6, 1926, the temperature was 17.02° C. and chlorinity 14.38 gm. Cl, and at station 17, July 11, 1928, was 16.17° C. and 11.24 gm. Cl.

TABLE VI

SURFACE TEMPERATURE, SALINITY, pH AND PLANKTON ON A LINE FROM SNAKE ISLAND, NANAIMO, TO VANCOUVER

Reference No.	Station	Location	Date	Time	Tide	Temp., °C.	Chlorine, grams per litre	pH	Plankton, volumes per 100,000
265	13	N. 49°13′, W. 123°52′	July 11, 1928	9:42 a.m.	F 2	18.3	9.98	8.5	20.0
266	13b	S.E. Snake Island.,	July 11, 1928	10:10 a.m.	F 3	18.2	11.17	8.50	—
267	13c		July 11, 1928	10:21 a.m.	F 3	19.2	10.30	8.50	—
268	14	N. 49°13′, W. 123°45′	July 11, 1928	10:05 a.m.	F 3	19.5	10.23	8.50	30.0
269	14a		July 11, 1928	11:31 a.m.	F 3	19.4	9.90	8.42	25.0
270	15	N. 49°14′, W. 123°41′	July 11, 1928	11:42 a.m.	F 4	19.5	10.24	8.42	20.0
271	15a		July 11, 1928	11:53 a.m.	F 5	19.7	8.98	8.45	—
272	16	N 49°15′, W. 123°37′	July 11, 1928	12:03 p.m.	F 5	19.6	8.91	8.42	12.5
273	16a		July 11, 1928	12:14 p.m.	F 5	20.1	8.90	8.52	—
274	17	N. 49°15′, W. 123°34′	July 11, 1928	1:02 p.m.	F 6	20.5	8.34	8.33	10.0
275	17a		July 11, 1928	1:12 p.m.	F 6	20.45	7.26	8.40	—
276	18	N. 49°16′, W. 123°30′	July 11, 1928	1:23 p.m.	F 6	20.80	7.05	8.30	2.5
277	19	N. 49°16′, W. 123°25′	July 11, 1928	1:45 p.m.	E 1	21.75	8.18	8.35	5.0
278	19a		July 11, 1928	1:56 p.m.	E 1	21.4	7.48	8.38	—
279	20	N. 49°17′, W. 123°21′	July 11, 1928	2:46 p.m.	E 2	22.10	7.50	8.40	7.5
280	20b		July 11, 1928	2:46 p.m.	E 2	23.20	6.13	8.32	—
281	20c		July 11, 1928	2:56 p.m.	E 2	23.70	4.63	8.27	0.2
282	40	N. 49°12′, W. 123°20′	July 11, 1928	3:15 p.m.	E 2	22.5	3.15	8.20	0.2
283	40		July 11, 1928	3:16 p.m.	E 2	22.0	1.77	8.20	—
284	20	N. 49°17′, W. 123°21′	July 6, 1928	3:05 p.m.	F 1	20.5	4.60	—	1.0
285	21	N. 49°17′, W. 123°18′	July 6, 1928	2:40 p.m.	F 1	18.0	2.51	—	1.0
286	23	N. 49°18′, W. 123°8′	July 6, 1928	2:14 p.m.	F 1	16.95	4.32	8.25	1.0
287	24	N. 49°18′, W. 123°5′	July 6, 1928	11:48 a.m.	E 5	15.24	9.05	8.25	2.0
288	24		Aug. 11, 1926	7:50 a.m.	E 1	15.3	13.38	8.25	10.0

The chlorinity mentioned for station 17, which is 20 miles north of the river mouth, is the lowest recorded for this depth. In this area the upper six yards are fairly uniform while between the depths of six and ten yards there is a rapid increase in salinity and decrease in temperature.

Northward there is a very narrow normal range of chlorinity, 14.0 to 15.6 gm. Cl, while the temperature varies from 13.2 to 16.6 ° C. At the north and south ends of Texada Island however, stations 101 and 105, the chlorinity is low, 14.0 and 13.6 gm. Cl. It would appear that some distance from the sources of fresh water, namely, Bute and Jervis Inlets, the six yard level attains a low salinity as in the case near the Fraser cited above. At Savary Island, station 101, and off Cape Lazo the effect of the river water emerging from the inlets at the north is even more marked. The temperatures were 17.71 and 17.8° C. respectively, while the chlorinities were 13.62 and 13.23 gm. Cl.

Temperature, Salinity, pH and Plankton on a Line from Snake Island, Nanaimo, to Vancouver (Table VI)

This series of surface samples was collected July 11, 1928. There may be noted a *gradual increase of temperature* from 18.2° C. at Snake Island to Station 20, located two miles west of the entrance of Burrard Inlet, where the temperature was 23.70° C., while at station 40, opposite the north arm of the Fraser River, a somewhat lower temperature of 22.0° C. was observed. On July 6, 1928, a series from the entrance of Burrard Inlet, station 20, to Vancouver Harbor showed a sudden decrease in temperature at the Narrows, that is, from 18.0 to 15.24° C. This series shows that the maximum temperature is attained about 20 miles from the Fraser River after insolation has had time to intensify its effect and beyond there is a gradual decrease, which may be shown by the salinity to result from mixing with colder sea water. The temperatures also indicate that very little surface river water goes through the passes. As explained in a previous paper by Lucas (12) and Hutchinson (9) there is a "piling up" at the narrows and a "sliding back" of the upper, less saline layer.

In general the chlorinity decreased from 11.17 to 1.77 gm. Cl from Snake Island across the Strait to the north arm of the Fraser River. The most notable feature, however, was the occurrence of successive crests of higher salinity at distances of ten to twelve miles; in each case there was a rather abrupt increase to the high salinity followed by a gradual decrease eastward, for instance, 8.98, 11.17, 10.30, 10.23, 9.90 gm. Cl for the first wave; followed by 9.90, 10.24, 8.98, 8.91, 8.90, 8.34, 7.26, 7.05 gm. Cl for the second wave; and 7.05, 8.18, 7.48, 7.50, 6.13, 4.63, 3.15, 1.17 gm. Cl for the third wave. On a calm day corresponding regions of successively less turbidity may be seen as one proceeds from the river across the Strait. These have abrupt western limits and are chiefly the result of the water carried north and westward by successive tides. These tidal "waves" are longer northwestward than westward from the river.

The surface plankton showed a single crest on this line at station 14, 25 miles from the river mouth, with 30 units of phytoplankton. There was a gradual decrease toward the river with a scarcely measurable value of 0.2 at station 40, and there was a correspondingly gradual change in pH from 8.50 to 8.20, as the salinity and the amount of plankton decrease.

TABLE VII

SURFACE SERIES, STRAIT OF GEORGIA TO HEAD OF HOWE SOUND (Aug. 9, 1927)

Station	Time	Tide	Temp., °C.	Chlorine, grams per litre	pH	Plankton, volumes per 100,000
21	10:20 a.m.	F 3	17.40	4.49	8.22	1.2
31	11:10 a.m.	F 3	17.0	4.34	8.41	3.0
30	2:20 p.m.	F 6	16.00	2.64	7.85	0.5
29	4:22 p.m.	E 2	9.50	0.03	7.55	0.2
30	6:14 p.m.	E 5	15.60	2.09	—	0.5
31	7:12 p.m.	E 6	17.80	4.55	8.45	—

Surface Series

Strait of Georgia to the Head of Howe Sound (Table VII)

The temperature decreases gradually along a line from the mouth of Howe Sound to station 30, ten miles or less from the head, that is, from 17.40 to 16° C. and then decreases rapidly to the mouth of the Squamish River which is fed by glaciers; the temperature on August 9, 1927 was 9.50° C. The first series was taken on the flood tide and the second on the ebb of the same day with approximately the same values for the same station, which would indicate that there is relatively little tidal effect in a sound with a wide mouth, as in this case; other data support this opinion.

The salinity varied from 4.49 gm. Cl at the mouth of the Sound to 0.03 gm. Cl at the head; these values are lower than others obtained at other times in the

TABLE VIII

SURFACE SERIES, DEPARTURE BAY TO BOUNDARY PASS VIA TRINCOMALI CHANNEL (Aug. 16, 1929)

Station	Time	Tide	Temp., °C.	Chlorine, grams per litre	pH	Plankton, volumes per 100,000
35	8:55 a.m.	F 1	17.40	15.10	8.65	10.0
35g	9:15 a.m.	F 1	17.00	15.20	8.65	9.5
43n	9:45 a.m.	F 1	16.90	15.15	8.30	5.5
43s	10:20 a.m.	F 2	15.00	15.40	8.00	1.5
49	10:05 a.m.	F 2	16.90	15.08	8.60	13.5
52g	11:45 a.m.	F 3	16.41	15.28	8.42	19.0
52k	12:30 p.m.	F 3	14.80	15.81	8.22	1.5
68c	1:05 p.m.	F 3	12.20	16.98	7.90	2.0
68d	1:40 p.m.	F 4	12.20	16.95	8.00	—

same area. The plankton was very low in quantity at the surface. The pH showed the direct effect of the presence or absence of sea salts, pH 7.55 for chlorinity 4.49 gm. Cl.

Further study of this area is being conducted.

Stuart Channel to Boundary Pass, via Trincomali Channel and Plumper Sound (Table VIII)

During this series two marked crests in temperature, plankton and pH may be noted. In Stuart Channel the values are high; temperature, 17.40° C.; pH, 8.65; and plankton, 10 units, with a correspondingly low chlorinity, 15.10 gm. Cl. There is a gradual change to station 43s, a mile south of Porlier Pass, where the values are: 15.0° C.; pH, 8.00; plankton, 1.5 units; and chlorinity, 15.40 gm. Cl. Then an abrupt change to station 49, opposite the mid-point of Galiano Island with readings; 17.90° C.; pH, 8.60; plankton, 13.5 units; and chlorinity, 15.08 gm. Cl; and finally a gradual change through Plumper Sound to Boundary Bay with records of 12.20° C.; pH, 8.00; 2.0 or less units of plankton and 16.98 gm. Cl. The relation of these characteristics is most evident; temperature, plankton and pH decrease with an increase of chlorinity in this area while a decrease in chlorinity is accompanied by increase of the other characteristics. It may be noted that these readings were taken beginning with the first of the flood tide and continuing past mid-tide. The regions of low chlorinity are north of Porlier and Active Passes respectively, and the river water which entered during the preceding ebb is carried northward by the flood; the areas of high chlorinity are composed essentially of water, such as comprises the great mass within these channels, originating from Haro and Juan de Fuca Straits.

TABLE IX

SURFACE SERIES, SOUTH OF BOUNDARY PASS TO STRAIT OF GEORGIA (AUG. 17, 1929)

Station	Time	Tide	Temp., °C.	Chlorine, grams per litre	pH	Plankton, volumes per 100,000
68s3	11:45 a.m.	F 1	12.70	16.59	7.82	1.5
68s2	12:20 p.m.	F 1	13.10	16.30	7.90	1.0
68s2	12:25 p.m.	F 1	12.70	16.49	7.90	1.0
68	12:30 p.m.	F 2	12.90	16.44	7.90	2.0
68n1	12:45 p.m.	F 2	15.20	15.32	8.02	—
68n2	12:50 p.m.	F 2	17.20	13.73	8.25	—
68n3	1:02 p.m.	F 3	18.90	12.05	8.30	1.5
68n4	1:18 p.m.	F 3	18.80	11.40	8.40	1.0
68n5	1:35 p.m.	F 3	19.30	12.18	8.40	0.5

South of Boundary Pass to the Strait of Georgia (Table IX)

This series has been mentioned previously but a number of additional facts may be deduced. The boat, "A. P. Knight" travels about eight knots, consequently the total distance represented in the table is about sixteen miles and within six miles the change took place from typically Juan de Fuca or

sea water to Strait of Georgia water, showing the effect of the Fraser River. The most notable change occurred in less than two miles off East Point, namely: temperature, 12.90 to 17.20° C.; chlorinity, 16.44 to 13.73 gm. Cl; and pH, 7.90 to 8.25.

TABLE X

SURFACE SERIES, JOHNSTON STRAIT TO BUTE INLET (AUG. 10, 1929)

Station	Time	Tide	Temp., °C.	Chlorine, grams per litre	pH	Plankton, volumes per 100,000
133	11:41 a.m.	E 2	10.45	16.79	7.80	0.5
134	12:40 p.m.	E 3	10.80	16.71	7.82	0.5
135	1:52 p.m.	E 4	10.57	16.57	7.79	1.0
136	2:30 p.m.	E 6	13.70	11.43	8.08	3.0
137	2:55 p.m.	F 1	16.90	5.18	8.50	1.0
138	5:10 p.m.	F 3	14.00	2.90	8.05	0.5
140	7:41 p.m.	F 5	16.22	2.31	7.70	0.2

TABLE XI

SURFACE SERIES, JOHNSTON STRAIT TO BUTE INLET (AUG. 9, 1928)

Station	Time	Tide	Temp., °C.	Chlorine, grams per litre	pH	Plankton, volumes per 100,000
133	9:40 a.m.	F 5	11.8	16.16	8.13	2.5
134	10:00 a.m.	F 5	11.6	15.95	8.08	2.5
135	10:30 a.m.	F 5	11.2	16.16	8.08	5.0
137	12:25 p.m.	F 6	14.0	5.35	8.45	5.0

Johnston Strait to Bute Inlet (Tables X and XI)

On August 9, 1928, and August 10, 1929, surface series from Johnston Strait, station 133, through Okisollo Channel, and through the Hole-in-the-Wall to Bute Inlet were collected, the former on the flood tide and the latter on the ebb. The most marked feature is the sudden change in chlorinity and temperature as one passes through the Hole-in-the-Wall, a distance of four miles; *e.g.*, chlorinity from 16.57 to 5.18 gm. Cl and temperature from 10.57 to 16.90° C. At Orford Bay, 20 miles up the inlet, the temperature was 16.22° C. and the chlorinity 2.31 gm. Cl. Although glacial water enters the inlet, especially at the head, the stability of the epithalassa makes possible a high surface temperature due to insolation.

The temperature was higher by more than 1° C. and the salinity lower by 0.6 gm. Cl on the flood as compared with the ebb in Okisollo Channel. It would appear that less saline water is carried from Johnston Strait, probably from the Salmon and other neighboring rivers; or it may be that the water column observed on the ebb had become more uniform due to turbulence in the narrow passes.

There is little surface plankton, 0.5 to 1.5 units, the chlorinities being extremely high. The pH shows a maximum with intermediate salinity as previously described.

Bute Inlet to Sutil Channel and the Strait of Georgia to Comox Harbor (Tables XII and XIII)

This series was collected during the ebb, August 11, 1929. The effect of the tide is illustrated by comparison of the surface data at station 137, at the mouth of Bute Inlet, with those at the beginning of the flood on the preceding day (cf. Table X). On the early flood the temperature was 16.90° C. and the chlorinity, 5.18 gm. Cl, while on the early ebb the values were 12.42° C. and 11.97 gm. Cl. Since the readings were taken shortly after the turn of the tide, they represent the effect of the previous phase to a great extent. There is a gradual increase in salinity from the mouth of Bute Inlet through Sutil Channel to the Strait of Georgia, namely, from 11.97 to 15.60 gm. Cl. The effect of the saline water entering through Discovery Passage is evident. There is a rapid decrease in salinity from the mouth of Sutil Channel eastward to Savary Island, that is, from station 147 to 110; the change is 15.60 to 13.78 gm. Cl.

The gradual increase in salinity is accompanied by a rapid increase in temperature from 12.42 to 21.20° C.; that is, the heating effect of insolation more than counterbalances the cooling effect of ocean water which enters through Discovery Passage with a temperature approximately 12.5° C. On the other hand there is a lowered temperature opposite Calm Channel, station 142, which may be due to colder waters entering from the not distant glacial sources of Bute Inlet, or may be caused chiefly by the turbulence due to the meeting of currents, bringing colder water from a lower depth. The temperature at this point for two successive years, 1928 and 1929, Tables XI and XII, was more than 2° C. lower than at points two miles either north or south.

Although there was very little surface phytoplankton the depth samples which were taken indicate that the increasing pH, from 8.25 to 8.62, was the result of a corresponding increase of diatoms and peridinians immediately below the surface.

Sutil Channel to Comox Harbor (Table XIII)

The series began at the entrance of Calm Channel then to Sutil Channel, continued through Sutil Channel south across the northern part of the Strait of Georgia to Cape Lazo and finally inside Comox Spit. From station 142 to 147 the series duplicated that of Table XII except that it was taken one day later in the same month of the preceding year and at an earlier part of the ebb tide. In Sutil Channel the salinity is lower and the temperature higher showing the effect of the river water which has been warmed through insolation. The temperatures were 14.0 to 20.4° C. and the chlorinities, 8.77 to 12.98 gm. Cl. The higher salinity at station 145 is probably due to sea water which has entered through Okisollo Channel. A similar and more marked increase in salinity, in this case accompanied by a decrease in temperature, is evident at station 157 as a result of the water which flows through Discovery Passage; the changes are from 20.2 to 16.8° C. and from 12.98 to 15.30 gm. Cl.

While crossing Comox Spit the chlorinity is decreased from 15.30 to 15.03 gm. per litre; the temperature increased from 16.8 to 18.2° C. Although the waters from the Comox and Tsolum Rivers lower the chlorinity of the waters protected by Denman Island less than 0.3 gm. Cl per litre, this change is accompanied by a remarkable increase in plankton from 4.0 units to 25.0 units with a corresponding increase in pH. The temperature near the entrance of the River is 16.6° C., or 1.6° C. less than in the bay where sufficient time has made possible the heating effect of insolation on the surface water.

Surface Isohalines for the Strait of Georgia and Neighboring Waters during July and August at Flood Tide

Chart 2 is an attempt to put into graphical form the average surface chlorinity conditions during the months of July and August. It is recognized that it is difficult to represent a dynamic situation dependent upon many variable factors in a static chart. Moreover although many samples have been collected over this extensive area the diagram attempts to summarize only the data collected to date. In fact, a number of areas are being investigated in greater detail at present. The survey is admittedly general.

TABLE XII

SURFACE SERIES, BUTE INLET TO STRAIT OF GEORGIA (AUG. 11, 1929)

Station	Time	Tide	Temp., °C.	Chlorine, grams per litre	pH	Plankton, volumes per 100,000
137	11:51 a.m.	E 1	12.42	11.97	8.25	—
137s1	12:15 p.m.	E 1	13.70	12.48	8.24	—
137s2	12:30 p.m.	E 2	16.30	11.39	8.30	0.3
142	2:01 p.m.	E 5	14.42	13.14	8.42	—
143	3:30 p.m.	E 6	16.80	13.48	8.50	—
147	4:30 p.m.	E 6	18.80	15.60	8.62	—
110	4:25 p.m.	F 1	21.20	13.78	8.60	—

TABLE XIII

SURFACE SERIES, SUTIL CHANNEL TO COMOX HARBOR

Station	Date	Time	Tide	Temp., °C.	Chlorine, grams per litre	pH	Plankton, volumes per 100,000
142	Aug. 9, 1928	3:05 p.m.	E 2	14.0	8.77	—	2.5
143	Aug. 9, 1928	3:35 p.m.	E 3	18.0	9.95	—	5.0
144	Aug. 9, 1928	3:50 p.m.	E 3	19.0	9.88	—	5.0
145	Aug. 9, 1928	4:20 p.m.	E 3	20.4	13.40	—	2.5
147	Aug. 9, 1928	4:50 p.m.	E 5	20.2	12.98	—	2.5
157	Aug. 9, 1928	7:50 p.m.	F 3	16.8	15.30	—	4.0
160	Aug. 9, 1928	9:23 p.m.	F 5	18.2	15.03	8.45	25.0
159	Aug. 10, 1928	10:38 a.m.	F 3	16.6	15.0	8.28	21.0

(a) Salinities of the Area Dominated by the Fraser River

The greater part of the southern portion of the Strait of Georgia is dominated as to salinity by the Fraser River during the summer months when the mass of fresh water contributed is the greatest and when the low specific gravity of the warmer, less saline water provides conditions for a stable epithalassa. The

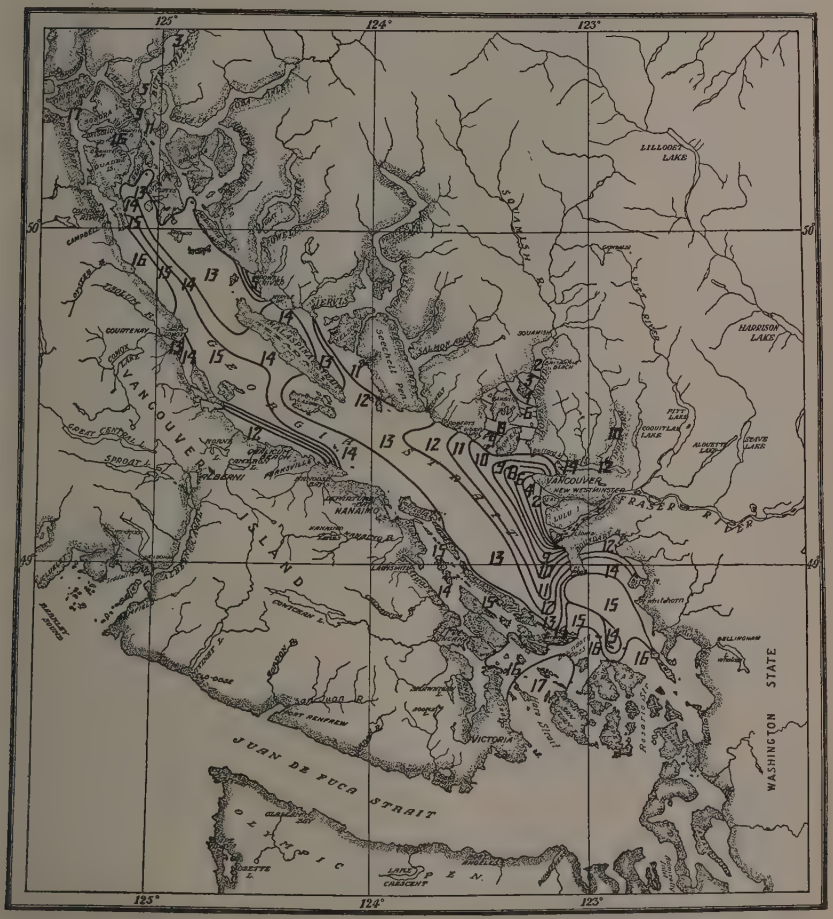

CHART 2. *Salinity, Strait of Georgia.*

surface water as it enters has a chlorinity less than 1.0 gm. About this centre the isohalines form an irregular fan-shaped figure, the radii being least westward and southeastward, greater southwestward and greatest northwestward; the distances are approximately 10, 20 and 40 miles for chlorinity 12.0 gm. Cl. The northwest and southeast tidal movements explain these phenomena.

The region with a chlorinity of 13.0 gm. occupies nearly one-half the total region extending from a narrow tip at the east of Saturna Island to Lasqueti and Texada Islands as an ever widening area. The region with chlorinity 14.0 gm. Cl forms what may be regarded as the transition region from that dominated by the Fraser River to those controlled by other factors; it extends first as a narrow fringe along Saturna, Mayne, Galiano, Valdes and Gabriola Islands, and as a wider area northward to the central point of Texada Island. In June, these isohalide areas extend farther because of the high water of the Fraser (12).

(*b*) *Salinities of the Areas Dominated by Rivers Fed by Glacial Streams*

The most notable of those studied are Bute Inlet and Howe Sound.

Bute Inlet. At Orford Bay which is only half the distance up Bute Inlet the chlorinities are as low as 3.0 gm. Cl. This was the most distant observation. There is a gradual increase through Sutil Channel and at the mouth the chlorinity is 13.0 gm. Cl. A similar condition obtains southward on the east side of the Strait of Georgia to the north end of Texada Island a distance of 40 miles; the total distance from the head of the inlet is more than 100 miles (160 km.). Toba Inlet is probably similar and contributes to the general effect within the Strait of Georgia, but has not been investigated.

Howe Sound. The Squamish River with its tributary the Cheakamus River lowers the chlorinity at the head of Howe Sound to less than 2.0 gm. per litre and its influence is shown, especially on the ebb tide, to the mouth of the sound where its effect merges with that of the Fraser River. The total distance is 25 or 30 miles. Although the water discharge of the Squamish River is probaby greater than that of the rivers flowing into Bute Inlet, the influence is less evident partly because the Sound has less length and has a wide mouth and partly because of the proximity of a greater factor, the Fraser River. Further investigation of this area is being conducted.

Indian Arm. The chlorinity of Indian Arm, Burrard Inlet, is lowered by the Indian River to the extent of 4.0 gm. Cl per litre at four miles from the head although the river is small. Vancouver Harbor has a much higher chlorinity than English Bay or the waters of Indian Arm. The primary effect of the Indian River does not pass the Second Narrows and that of the Fraser is held back by the First Narrows, or Lion's Gate, due to the "piling up" of sea water and the "sliding back" of surface river water as described above. The high chlorinity (14+gm. Cl) along the north shores of Stanley Park is such that the kelps, as *Nereocystis*, and animals such as starfish, sea urchins and tube worms thrive, while in English Bay and neighboring waters there is a paucity of marine forms. The small streams Capilano, Seymour and Lynn which enter at the narrows become thoroughly mixed with the sea water and do not form a definite epithalassa.

Jervis Inlet. This inlet receives a number of streams whose effect is such that at the mouth the chlorinity is 11.00 gm. Cl and at the junction of the area of its influence and that of the Fraser River, that is, toward the southern portion of Texada Island, the combined effect gives a chlorinity 12.0 gm. per litre.

Powell River. This river empties into the open Strait. The chlorinity of 5.0 gm. per litre at its mouth changes within a distance of two miles seaward to the general chlorinity of 13.0 gm. Cl.

(*c*) *Salinities of the Areas Dominated by Rivers Fed by Upland Lakes*

The rivers of the east coast of Vancouver Island are relatively small and are fed by lakes, consequently the quantity of their water supply although small is more uniform. The effect of the Chemainus River is the most marked chiefly because it flows into a protected area, namely, Stuart Channel; consequently the river water is conserved. The Comox and Tsolum Rivers have a similar effect on Baynes Sound, between Denman Island and Vancouver Island. In each case the chlorinity of these considerable bodies of water is lowered at the surface by 1.0 to 2.0 gm. Cl per litre.

The Horne, Qualicum and Englishman Rivers in the Qualicum Beach area affect only the area near the shore because of the more open nature of the shore line. However, Denman and Hornby Islands offer some protection from tidal currents.

Campbell River enters Discovery Passage near Seymour Narrows and although it has considerable volume its effect cannot be detected easily at Quathiaski Cove on the opposite shore. The turbulence due to tidal currents causes immediate mixing.

Similarly the Cowichan River has little effect beyond the limits of Cowichan Bay. A special study of Saanich Arm and Cowichan Bay is being made by Carter.

The influence of the Serpentine and Nicomekl Rivers is marked over the tide flat area only. Because of the importance of this region for oyster beds a separate investigation is being conducted by Elsey.

(*d*) *The Salinities of Areas Dominated by Sea Water*

The sea water which enters through Juan de Fuca Strait has a chlorinity 17.0 or more gm. Cl per litre; it enters by Rosario Strait and Boundary Pass into the Strait of Georgia and is evident until at the Point Roberts-Saturna Island line it has a halide value of 14.0 gm. Cl. This may be regarded as the line of transition between the dominance of the sea and of the river. The effect of the current through Rosario Strait extends farther since the current continues one hour longer. An area of lower chlorinity is situated near Sucia Island and is the result of the tidal swirl of the Boundary Bay region which apparently surrounds small areas of river water and at the flood of the river may carry them southward through Boundary Pass. Ordinarily however the river water is conserved in the Strait because of the "piling up" effect at the passes on the ebb tide.

The water from Haro Strait also enters Swanson Channel (chlorinity, 16.0 gm. Cl), and continues through Trincomali Channel with chlorinity 15.0 gm. Cl and another branch flows into Saanich Inlet. The narrow neck of water dominated by the sea, extending through Trincomali Channel more than 30 miles and separated from Georgia Strait by islands interrupted by

narrow passes, has a chlorinity 2.0 gm. Cl per litre greater than adjacent waters. This gives an excellent example of the closure to fresh water effected by constricted passes.

The sea water from Johnston Strait which enters through Discovery Passage has a lower salinity (16+gm. Cl) than that from the south through Juan de Fuca. Its effect on the waters of the Strait of Georgia is limited chiefly to the western portion as far south as Cape Lazo (chlorinity, 16 gm. Cl); while the area of 15-gm. chlorinity extends beyond Hornby Island. There is an eastward drift, especially at the north, where this area of influence comes in contact with that dominated by the rivers of Bute and Toba Inlets.

Surface Isotherms, Strait of Georgia

Chart 3

The chart represents the average surface temperature near the final phase of the flood tide during the months of July and August.

Area Dominated by the Fraser River

This area is situated with its centre 20 miles north of the river's mouth and has the form of a triangle. The northern angle extends nearly to Texada Island, the southern to Saturna Island and the eastern to the entrance of Burrard Inlet; more than four-fifths of the area is north of the main channel of the river. The surface river water meets a barrier at the southern passes and floats northward, propelled by the current of the flood tide on the east side of the strait, and southward on the west side carried by the final phases of the flood and by the ebb. The river water has an average summer temperature slightly greater than 16° C. as it enters the strait; it becomes warmed by insolation to 22° C. or higher as it approaches the centre of its distribution, and gradually decreases to 18° C. as it becomes mixed with the waters from the north; this transition area extends along the west shores of Mayne, Galiano, Valdes, and Gabriola Islands, and northward to surround Texada Island.

Areas Dominated by Rivers of Glacial Origin

These have much lower temperatures near the mouths. At the head of Howe Sound the temperature is 10° C. and there is a rapid increase due to radiation until the waters of the Squamish combine with those of the Fraser to make possible the high temperature, 22° C. Indian Arm, Burrard Inlet, has a higher temperature near its head, 14° C.; since it receives a small stream only the epithalassa is not very stable and the maximum temperature is 16° C. The rivers flowing into Bute Inlet lower the temperature at its head very materially; at Orford Bay more than 20 miles from the head the temperature varies from 10 to 15° C. according to the tide; at the mouth of the inlet it is 17° C. and becomes 19° C. at the mouth of Sutil Channel. This temperature is maintained to the north end of Texada Island. In the eddy about Savary Island a temperature of 21° C. is attained.

Areas Dominated by Rivers Originating from Upland Lakes

These areas receive river water which has been warmed previously to some extent and which enters at a temperature approximately 17° C. Provided

this is conserved by barriers it soon becomes warmed to 20° C. Cowichan Bay, Stuart Channel, Qualicum Beach, Baynes Sound, and Boundary Bay are included in the group of areas so affected.

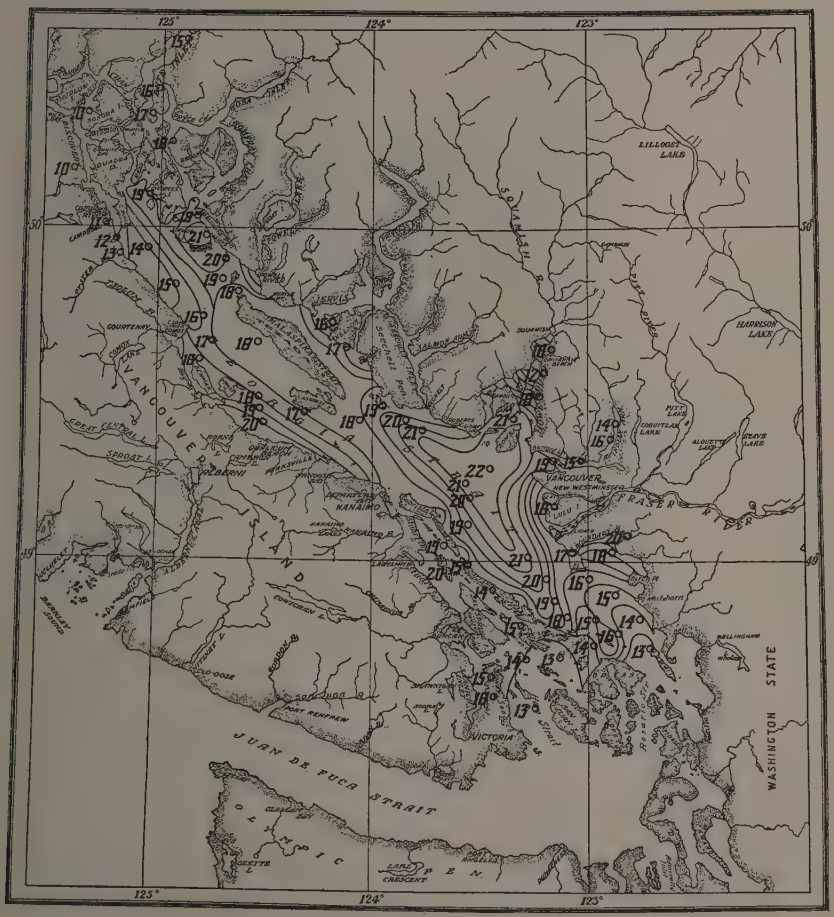

CHART 3. *Temperature, Strait of Georgia.*

Areas Dominated as to Temperature by the Sea Water

These are similar in outline to the salinity areas. The waters of Haro and Rosario Straits, with a temperature 13° C. extend their influence to the Point Roberts-Saturna Island line where the mixing with the Fraser water produces a temperature of 16° C. A long neck extends up Trincomali Channel which maintains a temperature of 15° C. even to Porlier Pass.

The water entering by Discovery Passage has a lower temperature than that entering at the south, namely, 10° C., and it affects the western side of the Strait of Georgia as far south as Cape Lazo, at 16° C., and to the Ballenacs Islands, at 17° C.

In general the temperature depends upon the time and degree of insolation as well as the temperature of the source. The time during which heating may continue depends upon the stability of the epithalassa. The temperature, although often related to chlorinity, is not necessarily an expression of the salinity. Starting with a source such as the Fraser River or Bute Inlet the temperature increases with increased chlorinity until its maximum is reached and from that point it decreases with increased chlorinity. Although the chlorinity of Saanich Arm (station 74) is high even near its head, the temperature reaches 18° C. or higher since it is subject to very minor currents only at its upper reaches. Ladysmith Harbor (station 42) is similarly affected.

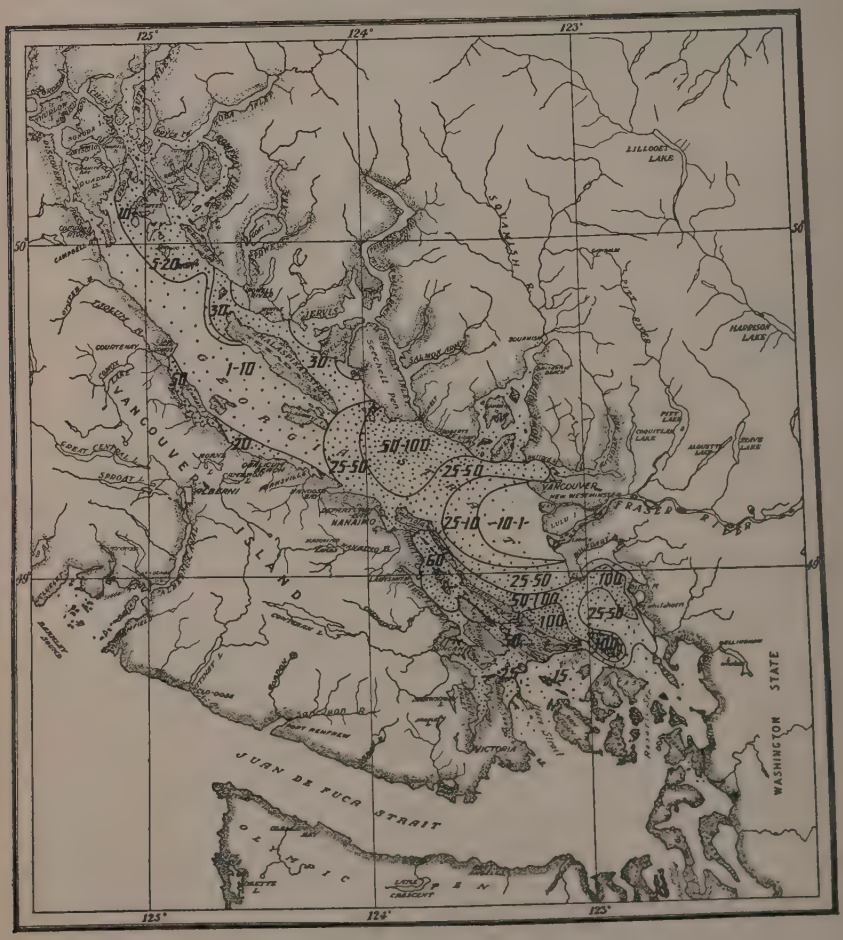

CHART 4. *Phytoplankton, Strait of Georgia.*

TABLE XIV

Chlorine, Strait of Georgia, S.W. (Fig. 1)

Station	133	130	120	114	154	105	103	3	1	14	44	54	68n	685	76	80
Date	9/7/29	8/7/28	7/7/28	9/7/29	9/7/29	6/7/28	28/5/27	3/7/26	4/7/26	10/7/26	30/6/27	30/6/26	13/6/28	13/6/26	15/6/26	15/6/26
Tide	E 2	F 3	F 3	F 1	F 2	F 4	F 6	F 6	F 1	F 5	F 2	F 5	F 6	F 6	F 6	F 6
Depth	Chlorine, grams per litre															
Yards / Metres																
0 / 0	16.79	16.00	15.93	16.00	15.75	13.80	14.80	14.60	12.81	13.68	12.68	12.62	14.00	16.38	16.42	16.52
2 / 1.8	16.79	16.10	15.95	16.05	15.83	13.86	14.89	14.66	14.08	13.74	13.81	14.63	14.10	16.44	16.41	17.07
4 / 3.7	16.76	16.20	15.94	16.12	16.40	13.96	15.17	14.82	14.85	15.47	13.77	15.16	14.14	16.54	16.61	17.10
6 / 5.5	16.85	16.30	15.90	16.13	16.37	14.12	15.62	15.10	15.18	15.49	13.77	15.73	16.50	16.51	16.59	—
10 / 9.1	16.88	16.36	16.03	16.40	16.54	15.37	16.09	15.83	15.53	16.08	13.89	15.80	16.50	16.64	16.59	17.16
20 / 18.2	16.92	16.42	—	16.48	16.58	16.33	16.59	16.18	16.27	16.31	14.97	16.40	16.65	16.65	16.71	17.17
30 / 27.4	16.94	—	—	16.71	16.80	16.57	16.68	16.39	16.38	16.43	16.17	16.52	—	—	16.94	17.20
50 / 45.7	16.98	—	—	16.85	16.85	—	16.73	16.51	16.62	16.80	16.50	16.77	—	—	17.18	17.31
100 / 91.4	17.00	—	—	17.88	17.25	—	16.99	16.97	16.80	17.09	—	—	—	17.45	17.38	17.98

TABLE XV

Chlorine, Strait of Georgia, N.E. (Fig. 2)

Station	137	142	144	110	107	104	7	10	17	40	47	48	56	61	64	70	78
Date	9/7/28	11/7/29	9/7/28	11/7/29	28/5/27	27/5/27	13/7/29	4/7/26	26/6/29	11/7/26	12/7/26	12/7/26	12/7/26	12/7/26	12/7/26	12/7/26	15/6/26
Tide	F 6	E 3	E 3	F 3	F 2	E 2	F 4	F 6	F 1	F 1	F 2	E 1	E 2	F 1	F 5	F 6	F 3
Depth	Chlorine, grams per litre																
Yards / Metres																	
0 / 0	5.35	13.14	9.88	14.71	12.16	9.54	12.68	12.61	11.11	2.64	4.86	9.84	13.62	15.39	15.20	16.01	17.14
2 / 1.8	8.80	14.00	—	15.32	12.18	9.46	12.78	—	13.09	—	13.79	14.25	13.67	15.41	15.67	15.91	17.14
4 / 3.7	10.58	15.83	—	15.53	13.78	9.73	13.09	14.38	14.01	—	14.26	14.71	14.04	15.41	15.67	16.00	17.28
6 / 5.5	11.68	15.90	13.55	15.78	15.27	12.61	13.65	15.29	15.40	—	14.73	14.95	14.99	15.60	15.96	16.01	17.18
10 / 9.1	14.53	16.10	—	16.12	15.24	16.13	15.87	16.03	15.69	—	15.06	15.81	15.82	16.06	15.89	16.08	17.29
20 / 18.2	15.60	16.40	—	16.52	16.22	16.58	16.00	16.32	16.48	—	15.93	16.43	16.48	—	16.44	16.48	17.28
30 / 27.4	15.83	16.45	—	16.74	16.50	16.71	16.70	—	16.87	—	16.30	16.51	16.79	—	16.59	16.68	17.20
50 / 45.7	—	—	—	—	—	16.73	—	—	17.06	—	16.50	—	—	—	—	—	17.29
100 / 91.4	16.78	17.15	—	17.25	—	16.76	—	—	17.22	—	17.03	—	—	—	—	—	—

The Distribution of the Surface Phytoplankton in the Strait of Georgia

Chart 4

The unit of plankton quantity used is volumes of phytoplankton in 100,000 volumes of sea water as determined by the net and centrifuge method (9).

The regions of maximum surface phytoplankton content related to the Fraser River have their respective centres 35 miles northward from the river mouth, opposite Seechelt and Departure Bay; 15 miles southward on the Boundary Bay-Mayne Island line, and westward in Trincomali Channel, especially near the passes. The northern area coincides with the chlorinity area 10.5 to 13.5 gm. Cl while the southern and western regions are found where the chlorinity is between 14.5 and 16.5 gm. Cl. The chlorinity may not be a limiting factor directly but these regions are characterized in each case by the most complete mixing of sea water and river water and evidently each contributes some essential condition or factor necessary for the rapid growth of phytoplankton. Near the Fraser River mouth the surface plankton cannot be measured by the centrifuge method while in the maximal areas the quantity may exceed 100 volumes in 100,000 of sea water as determined by the centrifuge method, or a litre of compacted diatoms from a cubic meter of sea water. According to the light conditions, instruments can be seen to a depth of one or two yards only. The phytoplankton area north of the river contains species of *Chaetoceros* chiefly during the summer months and those neighboring Boundary Bay and in Trincomali Channels have in addition a large *Sceletonema* proportion. The smaller rivers have correspondingly small areas of abundant phytoplankton near their mouths. The areas of maximal plankton are near the small rivers to which they are related presumably because optimal mixing is obtained at a short distance. Also, if the mixing area is restricted, as in the cases of Baynes Channel and Stuart Channel there is an abundant flora, while a more extended phytoplankton area results in less density, provided the river water supply is of the same order of magnitude, as in the cases of Bute Inlet, Sutil Channel and the northeastern portion of the Strait of Georgia.

Isohalide Vertical Section

(*a*) *Haro Strait, Boundary Pass, Southwest Strait of Georgia and Discovery Passage* (*Fig. 1, Table XIV*)

(*b*) *Rosario Strait, Northeast Strait of Georgia, Sutil Channel and Bute Inlet* (*Fig. 2, Table XV*).

In so far as is possible the data illustrated are for the months of July and August and were taken on the flood tide. Fig. 1 and 2 were drawn from the data recorded in Tables XIV and XV.

Fig. 1 and 2 show that the region under consideration is a great basin and that to a depth of 30 yards (27.5 metres) and in many places to 50 yards (45.7 metres) the Strait of Georgia has a chlorinity lower than the surface water either in the Strait of Juan de Fuca or in Johnston Strait, during the months of July and August, as is indicated by the isohalide line, 16.5 gm. Cl.

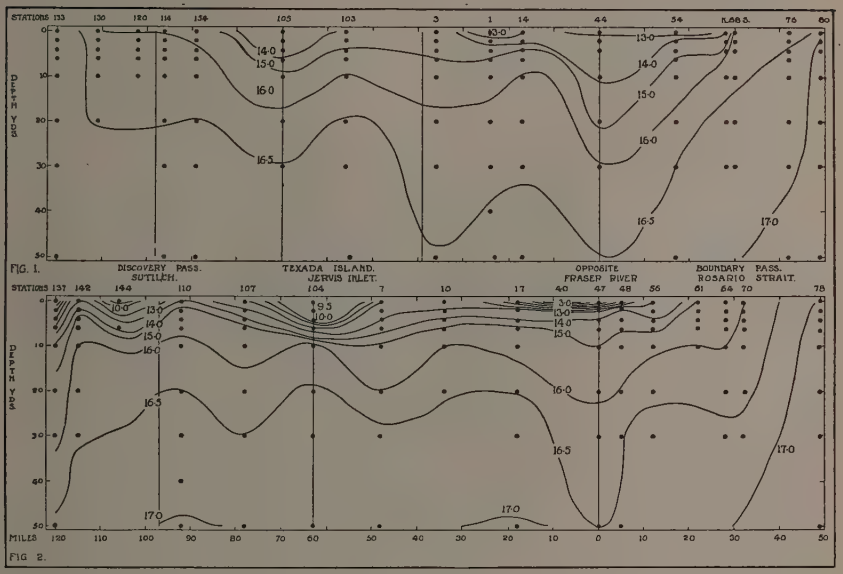

FIG. 1 AND 2. *Salinity as chloride, Strait of Georgia.*

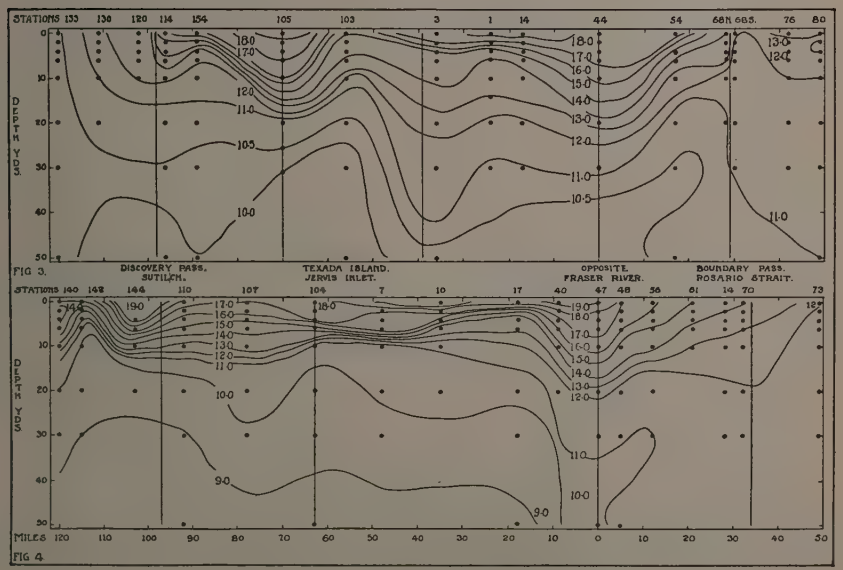

FIG. 3 AND 4. *Temperature, Strait of Georgia.*

The line 16.0 gm. Cl has an average depth of 15 yards (13.7 metres); the line 15.0 gm. Cl extends the full length of the Strait, 130 miles, except near the entrance of Discovery Passage and ordinarily attains a depth varying from 5 to 10 yards (4.5-9.0 metres); the line, 14.0 gm. Cl, extends the complete distance from 18 miles south of the Fraser River on the northeastern side of the Strait of Georgia to its northern limit and onward through Sutil Channel to Bute Inlet, with the possible exception of a small area near Jervis Inlet; its most extreme depths are seven yards near the mouth of Jervis Inlet and nine yards near the mouth of Bute Inlet. On the southwestern side the line, 14.0 gm. Cl, is limited to the region from 25 miles south of the Fraser River to 30 miles north, and to that region westward from the north end of Texada Island which is affected by the waters from Bute, Toba, and Jervis Inlets, and is at the region of their fusion. It may be noted that the depth of the last-mentioned region is five yards (4.5 metres) while that at the Fraser River mouth is two yards (1.8 metres); on the other hand the depth at a point opposite the Fraser River, 15 miles westward, is 11 yards (10 metres). It is evident that the depth to which the effect extends depends upon at least two factors, namely, the extent of the water source and the distance from the source. On this basis may be explained the fact that although the northeastern side of the Strait of Georgia receives a greater supply of river water and has a proportionately low surface and near surface salinity in general (Fig. 2), still, the southwestern side shows a lower salinity at the depths between 30 and 50 yards (27.4 to 45.7 metres), Fig. 2.

It may be noted that Rosario and Haro Straits have a greater salinity than Discovery Passage, as indicated by the line 17 gm. Cl.

Region Dominated by the Fraser River

This region is characterized by a decided lowering of the salinity in a region which extends directly across the Strait of Georgia; moreover, the salinities from 14.0 to 16.5 gm. Cl attain a greater depth at station 44, 15 miles west of the Fraser River mouth, than at the lightship, at the limit of the river's delta. Similarly this region extends from north to south for a distance somewhat greater than 20 miles. An east-to-west vertical section of this area is described later. The rapid change in salinity, especially near the surface, at Boundary Pass is evident from the chart, (Fig. 1, station 68), and this may be contrasted with the gradual transition northward from the Fraser River.

Region Dominated by Jervis Inlet

The region dominated by Jervis Inlet waters at the mouth is most evident near the surface and results in a chlorinity of 10 gm. Cl to a depth of 5 yards (4.5 metres) and is noticeable to 8 yards (7.3 metres) where the chlorinity is 15.0 gm. Cl. Below 10 yards (9.1 metres), on the contrary, the salinity is greater than at either station 107, 17 miles north, or station 7, 13 miles south. In fact, it appears that the waters from Jervis Inlet affect the salinity at a greater depth northward and southward, that is, from depths of 10 to 30 yards (9.1 to 27.4 metres) at the stations mentioned, situated at the north and south

ends respectively of Malaspina Strait, than at the mouth of Jervis Inlet itself (Fig. 2). Moreover, it appears that the low chlorinity water has its effect to depths between 10 and 50 yards (9.1 and 45.7 metres) at station 3; that is, at the region westward from the south end of Texada Island (Fig. 1), and it may also flow around the north end of Texada Island at the lower depths and combine with the waters from Bute and Toba Inlets to produce low salinity water at station 105 (Fig. 1). In this instance as in that of the Fraser the effect reaches its greatest depth near its distance limit. The chlorinities between 10 and 30 yards (9.1 and 27.4 metres) depth at station 105 are similar to those at station 107. The chlorinities at station 103 are generally the highest of any in the Strait, in contrast with the low chlorinities at stations 3 and 105. The two latter are influenced by waters from Jervis Inlet; the former, although nearer, is separated by Texada Island.

Region Dominated by Bute Inlet

This region extends beyond 50 yards (45.7 metres) depth at the mouth of the inlet as indicated by the line 16.5 gm. Cl (Fig. 2). At Savary Island (station 110) the effect of the eastward drift from Discovery Passage modifies the chlorinity, while the river water reaches the lower depth of 30 yards (27.4 metres) at the north end of Texada Island, station 107. The combined effects of the rivers from Jervis, Bute and Toba Inlets reinforce the local stream, Powell River. To determine the relative values of these rivers as sources of the marked chlorinity depression between 15 and 30 yards (13.7 and 45.7 metres) depth would require more data than are available at present. The salinities at the mouth of Bute Inlet are generally lower at corresponding depths than is the case at station 45, the region of maximum depth effect of the Fraser River. This circumstance is due probably to the retention of the fresh inlet water by the passes. The increase in salinity at station 142 may be due to turbulence in the passes near this point or to the undetermined salinity of the water which issues from Toba Inlet through Calm Channel at the ebb tide.

Transition Regions—Strait of Georgia to Sea Water

Discovery Passage

Discovery Passage receives the Campbell River eight miles south of Seymour Narrows through which the tidal current often exceeds 10 knots; on the flood some river water enters also from the Sutil Channel region. The almost uniform salinity from the Oyster River mouth through Discovery Passage to station 133, and especially the small variation of 16.0 to 16.5 gm. Cl between the depths, surface to 20 yards (18.3 metres), may be explained by the complete mixing of this river water with the sea water (Fig. 2).

Southern Portion of the Strait of Georgia

This is a region beyond the Point Roberts-Saturna Island line, (stations 56 to 70, Fig. 2), where the variation between the surface and 25 yards (22.8 metres) depth is from 15.0 to 16.0 gm. Cl except at the surface near station 56. In this transition region between the sea water and the area dominated by the river the most abundant phytoplankton is located.

TABLE XVI

Temperature, Strait of Georgia, S.W. (Fig. 3)

Station	133	130	120	114	154	105	103	3	1	14	44	54	682	685	76	80
Date	9/7/29	8/7/28	7/7/28	9/7/29	9/7/29	6/7/28	28/5/28	3/7/26	4/7/26	10/7/26	30/6/27	30/6/26	13/6/28	13/7/26	15/6/26	15/6/26
Tide	E 2	F 3	F 3	F 3	F 1	F 2	F 4	F 6	F 6	F 1	F 5	F 2	F 5	F 6	F 6	F 6
Depth	Temperature, °C.															
Yards / Metres																
0 / 0	10.45	11.82	12.40	15.20	16.21	18.1	14.90	17.00	19.0	18.30	17.53	17.20	14.00	12.10	13.40	13.0
2 / 1.8	10.40	11.79	12.55	14.95	14.88	17.97	14.73	16.99	17.52	17.53	17.62	15.27	13.55	11.95	12.55	11.75
4 / 3.7	10.38	11.79	12.48	14.78	12.18	18.08	14.37	15.08	15.10	15.90	17.40	14.60	13.44	11.73	12.25	11.80
6 / 5.5	10.20	11.42	12.19	13.99	12.03	17.96	13.37	15.55	13.82	14.86	17.23	13.38	13.18	—	12.10	12.35
10 / 9.1	10.19	11.09	12.03	12.01	11.37	17.90	11.34	14.30	13.20	13.62	16.42	12.62	11.68	11.70	12.00	12.00
20 / 18.2	10.18	11.03	—	11.81	10.87	10.85	10.20	12.32	11.13	11.64	13.82	10.75	10.92	11.60	11.80	11.62
30 / 27.4	10.15	—	—	10.49	10.38	10.02	9.75	11.53	10.58	11.01	11.21	10.10	—	11.48	11.38	11.57
50 / 45.7	10.15	—	—	9.76	10.02	—	9.33	10.38	—	—	—	10.92	—	—	10.95	11.08
100 / 91.4	10.00	—	—	8.73	8.45	—	8.40	9.28	9.40	—	—	9.66	—	9.95	9.70	9.40

TABLE XVII

Temperature, Strait of Georgia, N.E. (Fig. 4)

Station	140	142	144	110	107	104	7	16	17	40	47	48	56	61	64	70	73
Date	9/7/28	11/7/29	9/7/28	11/7/29	28/5/27	27/5/27	13/7/29	4/7/26	26/6/29	11/7/26	12/7/26	12/7/26	12/7/26	12/7/26	12/7/26	12/7/26	15/6/26
Tide	F 6	E 3	E 3	F 3	F 2	E 2	F 4	F 6	F 1	F 1	F 2	E 1	E 2	F 1	F 5	F 6	F 3
Depth	Temperature, °C.																
Yards / Metres																	
0 / 0	14.0	14.42	19.0	18.00	16.22	17.80	19.00	19.00	18.40	19.00	18.30	17.00	16.3	14.9	14.5	13.50	12.40
2 / 1.8	13.65	13.95	—	16.23	16.37	17.56	17.21	—	14.97	—	17.86	16.50	15.78	14.41	13.94	13.28	11.75
4 / 3.7	14.17	10.39		15.63	15.43	17.34	16.97	15.73	14.76	—	17.97	16.02	15.56	14.18	13.69	13.09	11.75
6 / 5.5	13.32	10.20	19.0	14.36	14.55	14.35	16.57	13.60	13.20	—	17.22	16.00	14.93	13.66	13.92	13.00	11.38
10 / 9.1	12.28	9.41	—	12.40	13.26	10.35	10.72	11.60	12.19	—	16.62	13.41	14.16	12.70	13.92	12.92	11.38
20 / 18.2	9.94	9.06		9.68	10.75	9.60	10.62	10.75	10.18	—	12.60	11.33	11.30	—	11.82	11.96	11.38
30 / 27.4	9.52	9.00	—	9.02	9.98	2.94	9.88	—	9.60	—	11.37	—	11.07	—	11.61	11.48	11.18
50 / 45.7	—	—	—	8.22	—	8.81	—	—	8.96	—	10.92	—	—	—	—	—	11.18
100 / 91.4	8.75	8.38	—	7.86	—	8.38	8.65	—	—	—	10.18	—	—	—	—	—	—

Region Dominated by Waters from the Sea

The region dominated by waters from the sea entering through Juan de Fuca Strait and Johnston Strait may be taken as having a salinity greater than 16.5 gm. Cl. This includes the Strait of Georgia below the depth of 50 yards (45.7 metres) and in many places that below 30 yards (27.4 metres). There is a rapid depression of the transition region from the surface between stations 76 and 80 in Haro Strait to the 50 yard (45.7 metre) level at station 44, opposite the Fraser River. At the north, the effect of the sea predominates below the 30 yard (27.4 metre) level southward to Lasqueti Island on the west and to Burrard Inlet on the east side of the Strait.

Isotherm Vertical Section

(*a*) *Haro Strait, Southwest Strait of Georgia and Discovery Passage (Fig. 3, Table XVI)*

(*b*) *Rosario Strait, Northeast Strait of Georgia, Sutil Channel and Bute Inlet (Fig. 4, Table XVII)*

In the regions dominated by river water there is a remarkable parallelism between the general configuration of the isotherms and the isohalines. Among the most significant parallelisms are:— (1) The increased temperature of the regions dominated by the Fraser River, particularly at stations 47 and 44; by the waters from Jervis Inlet at station 104, near the surface, and stations 3, 105 and 107 at greater depths; by the Bute and Toba Inlet waters at stations 137 and 144 near the surface, and at stations 137, 110 and 107 at greater depths. (2) The more gradual decrease of temperature with increased depth on the southwest side of the Strait as compared with the northeast side explained by the descent of the warmed, less saline waters as the distance from river sources is increased. (3) There is a pronounced parallelism between the isotherm, 12° C., and the isohaline, 16 gm. Cl, which is of sufficient exactness to place it within the limits of an experimental error.

This parallelism does not exist to the same extent at the surface or in the regions which are dominated by sea water. Between five yards (4.6 metres) and the lower limit of river dominance the controlling factor in the temperature control is the proportion of warmer river water and of colder sea water, which chiefly is expressed by the chlorinity. The layer of river water proper is of such stability that at the mouth of the Fraser River it is found in the upper four yards (3.6 metres); here the chlorinity at 4 yards (3.6 metres) is 13.0 gm. Cl. The river water which penetrates beyond this level has remained at the surface for a time sufficient to be warmed to a temperature which is practically uniform. The heating effect is correspondingly constant. The temperature of the surface water, on the other hand, is an expression involving a number of factors, chiefly: (1) the temperature of the river at its mouth; (2) the amount of insolation, which depends upon solar intensity and time, (the time is greater at greater distances from the source); and (3) the proportion of the river and sea water (which may be determined from the chlorinity). The great differences between the temperatures at the mouth of the Fraser

River, near the head of Howe Sound, at the entrance of Powell River and in Bute Inlet, locations where the salinities are similar, may be explained on the basis of the temperature of the source and the time of exposure to radiation.

The isotherm vertical section within the *region dominated by the sea water* has a number of important features:— (1) The sea water which enters Discovery Passage, station 133, has a temperature of 10.45° C. at the surface and 10.15° C. at 50 yards (45.7 metres) depth. (2) The sea water entering at Haro Strait and Rosario Strait has a temperature which ordinarily is 12.40° C. at the surface and 11.08° C. at 50 yards (45.7 metres) depth. (3) The temperature of the water entering the Strait of Georgia from the Strait of Juan de Fuca is 2 0° C. at the surface and 1.0° C. at 50 yards (45 7 metres) in excess of the temperature of the water entering from Johnston Strait. (4) The water at the 50-yard (45.7 metre) depth, from Burrard Inlet northward, on the northeast side of the Strait of Georgia, has a temperature 1.0° C. lower than station 133, in Discovery Passage, and 2.0° C. lower than station 80, Haro Strait, at the same level. (5) The warming effect of the sea water at the lower depths in the Strait of Georgia results in a *divergence of the isotherms from the direction of the isohalide lines in the regions dominated by sea water.* (6) In July and August the warming effect of the water entering through Haro and Rosario Straits is evident at the 50-yard (45.7 metre) level nearly as far north as the Fraser River. An earlier paper (10) drew attention to the seasonal increase in temperature and chlorinity at station 1 from May until November. This may be explained by the gradual encroachment of water from Haro Strait. The probability for the validity of this explanation is evident from the configuration of the isotherms in Fig. 6 and 7. At 50 yards (45.7 metres) depth there is a difference of 2.0° C. in 20 miles distance: at station 44 the temperature is 10.9° C.; at station 17, 10.9° C.

It would appear that the central portion of the Strait of Georgia is dominated by the water from the inlets to a depth of 50 yards (45.7 metres) at least, since the isotherms parallel the isohalide lines to this depth. *The temperatures in the Strait opposite the mouths of Jervis and Toba Inlets are relatively low and the chlorinities high, below the 10-yard (9.1 metre) level.* This would suggest that these Inlets contain a depth layer of similar characteristics which is undisturbed by the surface waters and is not dominated by the rivers. Although the inlets mentioned have not been investigated, others which are similar provide evidence in this direction. Saanich Arm at a depth of 100 yards (91.4 metres) had a temperature of 9.10° C. and a chlorinity of 17.35 gm. Cl, on July 12, 1928; Bute Inlet had a temperature of 7.64° C. and a chlorinity of 17.40 gm. Cl, on August 10, 1929. The temperatures were lower and the salinities higher than in the Strait of Georgia at the same depth. On this basis the occurrence of the inlets along the northeast side of the Strait of Georgia would explain the lower temperatures and higher chlorinities, below the 20-yard (18.3 metre) level, on the northeast as compared with southwest side of the strait.

TABLE XVIII

SALINITY AND TEMPERATURE AT VARIOUS DEPTHS (FIG. 5-16)

Fig.		5	6	7	8	9	10	11	12	13	13	14	14	15	15	15	15	16	16
Station		47	68s	137	29	44	64	110	31	7	17	68	68	52	52	17	17	7	7
Date		11/7/26	13/7/28	9/7/26	9/6/27	30/6/27	28/6/28	11/7/29	9/6/27	13/7/29	11/6/28	27/6/28	27/6/28	15/6/27	15/6/27	26/6/29	11/6/28	13/7/29	13/9/29
Tide		F 2	F 6	F 6	E 2	F 5	F 3		F 4	F 4	F 6	F 1	E 2	F 6	E 6	E 6	F 6	F 4	E 4
Depth																			
Yards	Metres	Chlorinity in grams chlorine per litre																	
0	0	4.86	16.38	5.35	0.04	12.68	13.44	14.71	4.34	12.68	8.34	14.34	13.97	16.90	7.87	11.11	8.34	12.68	13.28
2	1.8	13.79	16.44	8.80	0.07	13.81	13.78	15.32	7.20	12.78	8.95	16.30	14.32	16.70	9.01	13.09	8.95	12.78	13.78
4	3.7	14.26	16.54	10.58	13.41	13.77	14.12	15.53	14.16	13.09	9.60	16.50	14.39	16.76	11.49	14.01	9.60	13.09	14.11
6	5.5	14.73	—	11.68	14.90	13.77	14.07	15.78	14.60	13.63	11.24	16.77	14.47	16.74	13.10	15.40	11.24	13.63	14.23
10	9.1	15.06	16.51	14.53	15.61	13.89	14.77	16.12	15.34	15.87	14.04	16.77	14.47	16.73	14.47	15.69	14.04	15.87	15.38
20	18.2	15.93	16.64	15.60	16.33	14.97	15.07	16.52	16.50	16.60	15.75	16.80	14.90	16.89	16.48	16.48	15.75	16.60	16.60
30	27.4	16.30	16.65	15.83	16.37	16.17	15.62	16.74	16.55	16.70	—	17.00	15.45	—	—	16.87	—	16.70	—
50	45.7	16.50	17.00	16.30	—	—	—	17.00	16.80	16.90	—	17.30	—	—	—	17.06	—	16.90	—
		Temperature, °C.																	
0	0	18.30	12.10	14.0	9.50	17.53	16.50	17.45	17.00	17.63	20.5	14.8	16.00	10.50	16.70	18.40	20.50	17.63	16.90
2	1.8	17.86	11.95	13.65	9.46	17.62	15.78	16.23	16.03	17.60	19.83	11.8	15.50	10.42	16.01	14.98	19.83	17.69	16.80
4	3.7	17.97	11.73	14.17	10.59	17.40	15.36	15.63	11.59	17.31	19.17	11.3	15.30	10.34	14.54	14.76	19.17	17.31	17.00
6	5.5	17.22	—	14.32	9.96	17.23	15.35	14.36	11.03	17.01	16.17	11.00	15.17	10.36	13.32	13.20	16.17	17.01	17.10
10	9.1	16.62	11.70	12.28	9.07	16.42	14.08	12.40	10.52	12.81	13.63	10.80	15.15	10.36	12.27	12.19	13.63	12.81	14.90
20	18.2	12.60	11.60	9.94	8.65	13.82	13.33	9.68	10.10	10.31	11.04	10.70	14.15	10.28	10.37	10.18	11.04	10.31	10.31
30	27.4	11.37	11.48	9.52	8.60	11.21	12.53	9.02	9.84	9.88	—	10.68	13.13	—	—	9.60	—	9.88	—
50	45.7	10.92	10.60	9.03	—	—	—	8.60	9.40	9.40	—	10.60	—	—	—	8.96	—	9.40	—

Salinity- and Temperature-depth Curves

(*Fig. 5-16, Table XVIII*)

The configuration of the temperature- and salinity-depth curves, especially in the upper 30 yards (27.4 metres), is dependent primarily upon the sources of the water.

Fraser River Mouth

Fig. 5 illustrates the conditions *at the Fraser River mouth.* The salinity increases rapidly from the surface to a depth of two yards (1.8 metres), then gradually to a depth of 30 yards (27.4 metres). There is a gradual decrease

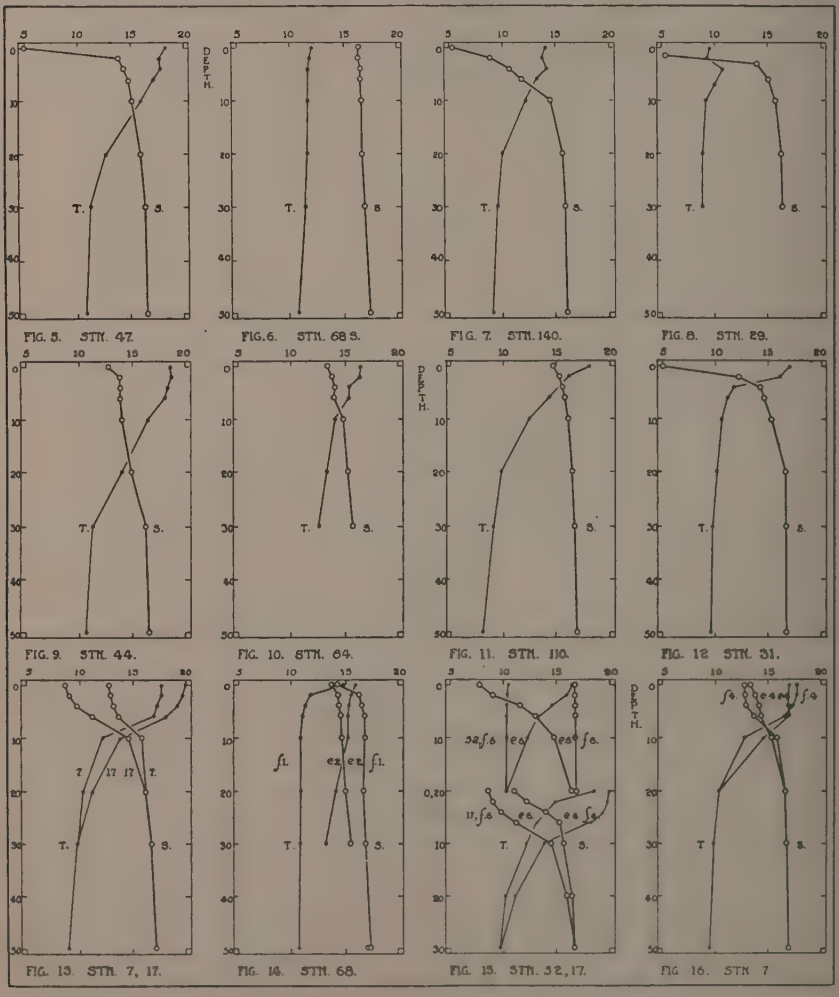

FIG. 5–16. *Temperature- and salinity-depth curves, Strait of Georgia.*

in temperature from the surface to 30 yards (27.4 metres) depth. This results in the class of configuration which may be known for convenience as the "X" type. It represents the conditions where the Fraser River is dominant and at the same time is meeting the water from the Haro and Rosario Straits. Fig. 9 represents similar conditions at station 44, which is 15 miles westward from the lightship at the river's mouth. The curves are very similar below the two-yard (1.8 metres) level. At station 64 the same type of curve is evident (Fig. 13) although modified by sea water of the type shown in Fig. 6.

Haro Strait

The conditions in Haro Strait, where the sea water dominates, are illustrated by Fig. 6. The surface has high salinity and low temperature. The change both in temperature and salinity is very uniform and gradual from the surface to a depth of 50 yards (45.7 metres). This may be known as the "H" type of configuration. It is characteristic of the waters of Haro and Rosario Straits and of Trincomali Channel at the south, and of Discovery Passage and Okisollo Channel at the north.

Regions near Rivers of Glacial Origin

These regions have salinity-temperature curves of the "n" type as illustrated in Fig. 7, 8, 11, 12. Near a river such as the Squamish there is at the surface low salinity and low temperature. The salinity increases rapidly with increased depth to four yards (3.6 metres); from this level downward there is a decrease in the rate of salinity increase. At greater distances from the river the curve maintains its general characteristics but tends to be modified toward a more uniform rate of salinity increase with depth. At greater distances from the supply (Fig. 12 and 7) of glacial water the surface temperature is increased by radiation; the near-surface decrease in temperature with depth is rapid, while toward lower depths the rate of decrease in temperature becomes less, giving graphically the upward loop of the "n" configuration. Howe Sound, (Fig. 8 and 12) and Bute Inlet (Fig. 7) illustrate these conditions.

Regions at a Considerable Distance from a River Supply

These show conditions illustrated by Fig. 15 or conforming to the *"U" type.* Insolation has decreased the already low specific gravity of the surface water to produce a very stable epithalassa at the upper levels, that is, to 6.0 yards (5.5 metres) depth. The decrease in temperature and the increase in chlorinity which is only slight to the depth of six yards (5.5 metres), is rapid from six yards to 10 yards (9.1 metres) and is gradual from 10 to 30 yards (9.1 to 27.4 metres) depth. Conditions at stations 7 and 17 are illustrated but the graph represents the conditions at many others, notably stations 15-20, 8-11, 3-7, 104, 105, 144, etc.

The Effect of Tides on the Configuration of the Temperature and Chlorinity Depth Curves (Fig. 14-16, Table XVIII)

At station 68, Boundary Pass, a 24-hr. series of samples was collected, July 27, 1928, with the results as shown in Fig. 14. The beginning of the ebb gave the "X" curve which is characteristic of the waters northeastward from

this station, and as illustrated in Fig. 10, while the early flood tide gave the "H" type of configuration of the waters in Haro Strait as shown in Fig. 6. The slight modifications in the upper two yards (1.8 metres) are accounted for by the fact that the samples were collected in a bay adjacent to the pass proper, and a small eddy allowed surface water to collect.

In Active Pass (station 52), which connects the Strait of Georgia, opposite the Fraser River, with Trincomali Channel another 24-hr. series was collected. As illustrated in Fig. 15 the last phase of the flood brought water from Trincomali Channel which had a temperature-chlorinity curve of the "H" type while the ebb tide gave conditions represented by the "X" curve, characteristic of the Fraser River region (cf. Fig. 6 and 9 with Fig. 15, station 52).

Fig. 15 also illustrates a change of conditions from the flood to the ebb at station 17, but not on the same day. The ebb brings water from Howe Sound which shows the "n" configuration (cf. Fig. 12) while the flood brings water from the Fraser which gives the "u" curve indicating water from a point some distance from a river supply (cf. Fig. 13).

The tidal variation is less at station 7 (Fig. 16) than at the other regions illustrated. Water from the Fraser is brought northward by the flood and that from Jervis Inlet is brought southward by the ebb. Both have the "u" shaped curve of water subjected to insolation (cf. Fig. 13); the degree of its expression is greater however in the case of the Fraser River water at the flood. It is evident from the cases cited that there is considerable mass movement of water due to the tides, and that the body of water which is transported maintains its individuality to such an extent that it may be identified at any phase of the tide by its temperature-chlorinity configuration.

Chlorinity, Temperature and Phytoplankton, Vertical Sections, on a Line Westward from the Fraser River

TABLE XIX

TEMPERATURE, STRAIT OF GEORGIA, FRASER RIVER TO PORLIER PASS AND STUART CHANNEL (FIG. 17)

Station		35	43	44	45	46	47
Date		29/7/27	29/7/27	30/7/27	6/8/26	30/7/27	29/7/27
Tide		E 6-F 1	F 2	F 5	F 4	F 4	F 3
Depth		Temperature, °C.					
Yards	Metres						
0	0	16.37	15.64	17.53	18.20	18.58	18.48
2	1.8	16.11	16.23	17.62	17.50	17.56	17.82
4	3.7	15.92	14.27	17.40	17.30	17.33	17.72
6	5.5	14.45	14.33	17.23	17.12	17.16	16.20
10	9.1	13.84	11.33	16.42	16.45	16.08	13.43
20	18.2	12.20	11.62	13.82	15.28	13.02	11.33
30	27.4	—	11.56	11.21	12.03	10.94	10.97

The data represented in Fig. 17, 18, 19, were obtained on the flood tide of two successive days, with the exception of those for station 45.

Isotherms (*Fig. 17*)

The isotherms demonstrate: (1) that the heating effect at the Fraser River mouth is limited to the upper 10 yards (9.1 metres); (2) that westward there is a rapid increase in the depth of the heating effect and that the maximum depth is reached in mid-channel; (3) that on the western side of the strait there is a decrease in the isotherm depths and as Porlier Pass is entered the temperature below 10 yards (9.1 metres) depth is less than 12° C. while at the surface it is 15.6° C.; (4) the water in Trincomali Channel, station 43, has much lower temperatures at corresponding depths than in Stuart Channel, station 35. This difference is due to the insolated river water which enters Stuart Channel from Chemainus and other rivers and which is retained by barriers.

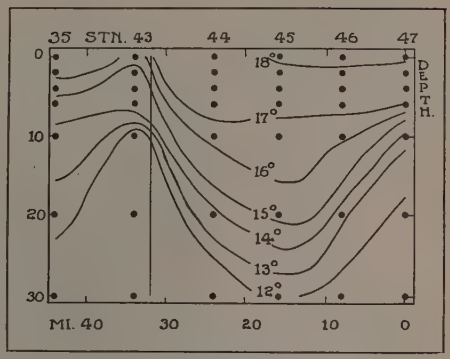

FIG. 17. *Temperature-depth curves, Strait of Georgia.*

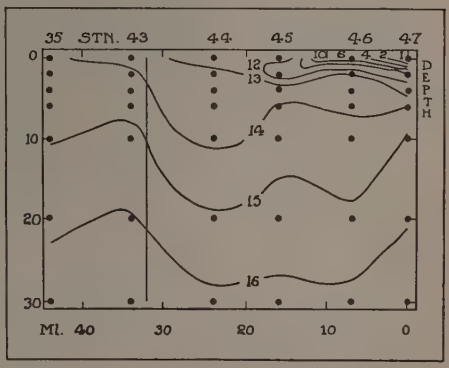

FIG. 18. *Salinity-depth curves, Strait of Georgia.*

Isohalines (*Fig. 18*)

The isohalines may be compared with the isotherms and the following features noted. (1) The relatively constant temperature, 18.58 to 17.53° C., near the surface is not entirely paralleled by the chlorinity; there are tidal waves, one of which is evident at station 45 especially from the fact that the chlorinity at two yards (1.8 metres) depth is less than that at the surface, 12.00 gm. Cl as compared with 12.52 gm. Cl. The cooling effect associated with increase in the salinity may be obviated by the greater insolation made possible by

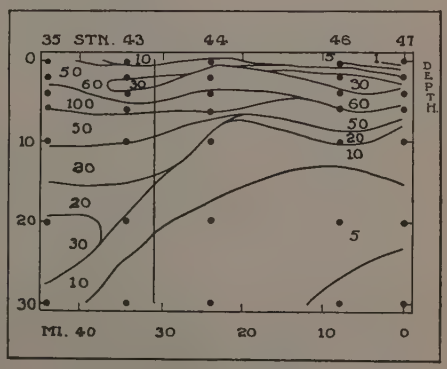

FIG. 19. *Phytoplankton-depth curves, Strait of Georgia.*

the time factor. At station 45 the near-surface temperature is higher than at station 46 although the chlorinity is greater also. Again the time factor of insolation and of mixing may account for the conditions. (2) Generally, there is a parallelism between chlorinity and temperature, that is, generally the temperature is related to the factor which expresses the degree of mixing of warmer, insolated river water and of colder sea water.

TABLE XX

SALINITY, STRAIT OF GEORGIA, FRASER RIVER TO PORLIER PASS AND STUART CHANNEL (FIG. 18)

Station		35	43	44	45	46	47
Date		29/7/27	29/7/27	30/7/27	6/8/26	30/7/27	29/7/27
Tide		E 6-F 1	F 2	F 5	F 4	F 4	F 3
Depth		Chlorinity,—grams per litre					
Yards	Metres						
0	0	14.30	13.62	12.68	15.52	5.18	0.12
2	1.8	14.34	14.30	13.81	12.00	13.69	11.31
4	3.7	14.47	14.49	13.77	13.73	13.73	12.95
6	5.5	14.78	14.74	13.77	14.38	13.80	14.02
10	9.1	14.91	15.24	13.89	14.74	14.17	15.08
20	18.2	15.68	16.11	14.97	15.23	15.18	15.90
30	27.4	—	16.12	16.17	16.22	16.22	16.57

TABLE XXI

PHYTOPLANKTON, STRAIT OF GEORGIA, FRASER RIVER TO PORLIER PASS AND STUART CHANNEL (FIG. 19)

Station		35	43	44	45	46	47
Date		29/7/27	29/7/27	30/7/27	6/8/26	30/7/27	29/7/27
Tide		E 6-F 1	F 2	F 5		F 14	F 3
Depth		Phytoplankton, volumes per 100,000 volumes of sea water					
Yards	Metres						
0	0	45	10	10	—	7	0.1
2–0	1.8–0	54	60	50	—	30	10
4–2	3.7–1.8	90	30	65	—	30	70
6–4	5.5–3.7	95	70	110	—	60	—
10–6	9.1–5.5	58	55	22	—	50	27
20–10	18.2–9.1	20	21	13	—	9	12
30–20	27.4–18.2	33	9	7	—	6	5

TABLE XXII

SALINITY AND PHYTOPLANKTON AT DEPTH (FIG. 20-27)

Fig.		20	20	21	21	22	22	23	23	24	25	25	26	26	27	27
Station		47	47	45	61	46	44	52g	64	54	52d	52d	1	10	68b	68b
Date		30/6/27	11/7/26	6/7/26	12/7/26	30/6/27	30/6/27	16/6/27	27/6/28	29/6/27	15/6/27	15/6/27	4/7/26	4/7/26	26/6/28	26/6/28
Tide		F 3	F 2	F 5	F 3	F 4	F 5	F 5	E 3	F 6	E 2	F 4	E 1	F 6	E 2	F 3
Depth																
Yards	Metres	Chlorine in grams per litre														
0	0	0.11	4.86	12.52	15.39	5.18	12.68	14.96	13.44	8.88	10.68	16.43	12.18	12.61	14.18	14.49
2	1.8	11.31	13.79	12.62	15.41	13.69	13.81	15.02	13.78	9.50	11.23	16.32	14.08	—	14.26	14.55
4	3.7	12.95	14.62	13.73	15.41	13.73	13.77	15.29	14.12	10.97	11.20	16.41	14.85	14.38	14.26	14.66
6	5.5	14.02	14.73	14.38	15.60	13.80	13.77	15.74	14.07	10.82	12.30	16.40	15.18	15.29	14.36	14.75
10	9.1	15.08	15.06	14.74	16.06	14.17	13.89	15.80	14.77	11.58	16.06	16.43	15.53	16.03	14.37	14.92
20	18.2	15.90	15.93	15.23	16.68	15.18	14.97	16.20	15.07	15.74	16.12	16.46	16.27	16.32	14.72	15.38
30	27.4	16.57	16.30	16.22	16.69	16.22	16.17	16.20	15.62	16.02	—	—	16.38	—	16.03	15.75
		Phytoplankton, volumes per 100,000 volumes of sea water														
0	0	1.2	0.5	32.0	65.0	7.5	10.0	40.0	80.0	1.5	2.5	18.0	60.0	65.0	65.0	50.0
2–0	1.8–0	10.0	—	—	75.0	30.0	50.0	38.0	40.0	25.0	10.0	14.0	—	—	90.0	30.0
4–2	3.7–1.8	—	30.0	40.0	—	30.0	65.0	15.0	35.0	16.0	8.0	—	30.0	60.0	60.0	30.0
6–4	5.5–3.7	70.0	—	—	56.0	60.0	110.0	18.0	34.0	4.0	15.0	8.0	—	10.0	28.0	15.0
10–6	9.1–5.5	27.0	22.0	8.0	10.0	50.0	22.0	9.0	22.0	105.0	5.0	—	8.0	—	35.0	12.0
20–10	18.2–9.1	12.0	10.0	4.0	4.0	9.0	13.0	3.0	12.0	22.0	2.0	5.0	—	2.0	20.0	17.0
30–20	27.4–18.2	5.0	5.0	3.0	3.0	6.0	7.0	3.0	7.0	15.0	1.0	—	0.5	—	20.0	14.0

Phytoplankton

The vertical section which shows the phytoplankton regions according to quantity demonstrates the following. (1) That the surface phytoplankton near the river mouth, station 47, is minimal and that it increases toward station 35, in other words, there is an increase in phytoplankton with increase of chlorinity, which expresses the degree of mixing. (2) That near the river mouth the maximal phytoplankton is found between two and four yards (1.8 and 3.6 metres) depth while at stations more distant it occurs at the four- to six-yard (3.6 to 5.5 metre) level; again these levels express the regions of blending of the sea and river waters. (3) That abundant plankton is found at even greater depths in regions where mixing has been possible at such depths because of the relative instability of the column, as at stations 43 and 35. (4) That tidal waves of phytoplankton are much more marked than those of either temperature or chlorinity. In Trincomali Channel near Porlier Pass depth phytoplankton reversals occur as for instance 10, 60, 30, 70 units of phytoplankton for the regions, surface, 2-0, 4-2, 6-4 yards (1.8-0, 3.6-1.8, 5.5-3.6 metres). In conclusion, the optimum conditions for the growth of phytoplankton are not in the waters of high or of low chlorinity and not necessarily in regions of intermediate chlorinity, but rather in regions where mixing is taking place, that is, where chlorinity changes are taking place. The temperature seems to have an effect upon the occurrence of species but within the limits of summer variation found in the Strait of Georgia no direct relation between phytoplankton quantity and temperature has been observed.

Phytoplankton-chlorinity Depth Curves

(*Fig. 20-27; Table XXI*)

Region Dominated by the Fraser River

The region dominated by the Fraser River, Fig. 20, 22, 24, 26, representing stations 47, 46, 44, 54, 1, 10, has the following characteristics: (1) At the surface there is a chlorinity less than 10 gm. Cl and a phytoplankton quantity less than 1.0 unit. (2) At station 47 in July there is a rapid transition of chlorinity from 11.0 to 15.0 gm. Cl between the depths of 2 and 10 yards (1.8 and 9.1 metres); in this region abundant phytoplankton is present and the maximum is at 4-6 yards (3.6-5.5 metres). The transition is less rapid in August and there is less abundant phytoplankton. (3) At stations 44 and 46 the region with chlorinities from 13.0 to 15 gm. Cl occurs between the depths 2 and 20 yards (1.8 and 18.3 metres) and throughout this region there is abundant plankton, with the maximum at a depth of 6 yards (5.5 metres). The similarities in the salinity curves are accompanied by corresponding similarities in plankton curves. (4) At station 54 (Fig. 24) the chlorinity is below 10.0 gm. Cl to a depth of 2 yards (1.8 metres) and in this region there is a minimal amount of phytoplankton. The transition from 10.0 to 15.0 gm. Cl occurs between the depths 2 yards (1.8 metres) and 20 yards (18.3 metres) and again this region has abundant plankton with a maximum at 10 yards (9.1 metres). (5) The phytoplankton maximum increases in depth at greater distances

from the river; that is, at the region where the chlorinity transition reaches a lower level. (6) The quantity of phytoplankton of regions near the Fraser River is represented by a "loop" curve; the type is "sub-surface maximal".

Regions Beyond the Centre of Dominance of the Fraser River

In these regions, particularly northward, the "U" type of chlorinity-temperature curve generally maintains, but at the last of the flood the direct influence of the river is shown as an "X" curve, as shown in Fig. 26. At this phase of the tide the plankton quantity is the greatest (13). Two very similar instances are shown at stations 10 and 1. In each case the surface chlorinity is between 12.0 and 13.0 gm. Cl and, in contrast with stations where the surface chlorinity is below 10.0 gm. Cl, the maximum of phytoplankton is at the surface. There is a rapid transition between the surface and 10 yards (9.1 metres) from 12.0 to 16.0 gm. Cl and at the latter depth a minimal phytoplankton flora is present. Again, the region of mixing is the region of phytoplankton growth.

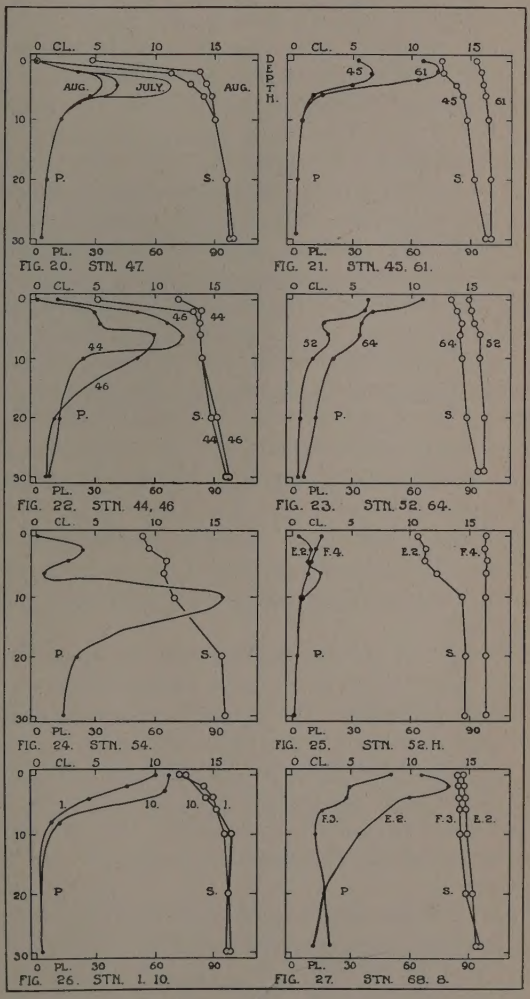

FIG. 20–27. *Phytoplankton- and salinity-depth curves, Strait of Georgia.*

At regions beyond the centre of surface dominance of the Fraser River, southward, and where the sea water dominates at lower depths, the characteristic Fraser River phytoplankton "loop" or "sub-surface maximum" curve gives place to the "diagonal" curve or "surface maximum" type.

Transition conditions between these two types are shown at stations as remote from one another as 45 and 61. At station 45, Fig. 21, the flood tide

brings water from Boundary and Porlier Passes; the surface chlorinity is 12.52 gm. Cl and at 10 yards (9.1 metres) depth it is 14.74 gm. Cl. There is a high phytoplankton quantity at the surface, 32 units, somewhat higher at 2-4 yards (1.8-3.6 metres), 40 units, and a rapid decrease to the 10 yard (9.1 metre) depth. Similarly at station 61 where the effect of the Fraser River is most marked at the last of the ebb or early flood tide. The tendency toward dominance of the sea water is shown by the salinity line approaching the "H" type in regions where the phytoplankton curve is of the "diagonal" or "surface maximum" type.

The similarity between the curves for station 52, near Active Pass in Trincomali Channel, and for station 64, north of Rosario Strait, is evident in Fig. 23. There is a gradual transition of chlorinity from the surface to the 20-yard (18.3 metre) level, accompanied by an abundant surface flora and a gradual decrease to the same level. The plankton quantity is greater in the instance which has the lower general chlorinity, that is, which is intermediate between sea and river water.

The relation of phytoplankton quantity to tides is illustrated by Fig. 22, 23, 24, 25 and 27.

At Active Pass a 24-hr. series of samples showed extremes of phytoplankton and of chlorinity at mid-ebb and mid-flood (Fig. 25). At the mid-ebb the salinity was of the Fraser River "X" type, and the phytoplankton showed the Fraser River "loop" type with a maximum at 6 yards (5.5 metres), while on the flood the water from Trincomali Channel gave the "H" chlorinity curve and the "diagonal line" phytoplankton curve with the maximum at the surface.

Another 24-hr. series at Boundary Pass gave the transition in phytoplankton types from that of Haro Strait to that of the southern portion of the Strait of Georgia (Fig. 27). The variation in salinity is very small as compared to the changes in plankton quantity which show the proportion of 1:2; other phases of the tide showed greater differences in chlorinity, for instance, at the last of the flood and the beginning of the ebb, Fig. 14. However, the greatest phytoplankton quantity occurred at mid-tide when an intermediate chlorinity between 14.0 and 15.0 gm. Cl indicated the maximal mixing of the sea and river water.

In a number of instances *tidal effects* on salinity are shown in the diagrams by *reversals* in the general trend of the curve such as between the 4- and 6-yard (3.6 and 5.5 metre) levels (Fig. 23). These indicate regions of contact of waters resulting from opposite phases of the tide, evident in the form of tidal waves which in some cases are very pronounced. At station 64 there is a decrease and at 52 an increase between the levels mentioned. These chlorinity reversals are accompanied by plankton reversals similarly of an opposite kind at the two stations. Other instances of parallel plankton and chlorinity reversals are evident in Fig. 24, and 25 for stations 54 and 52. Chlorinity reversals which are difficult to measure because they are practically within the limit of experimental error may be accompanied by a twofold or threefold

increase in plankton quantity (station 54, Fig. 24). A reversal, 10.97, 10.82, 11.58 gm. Cl, at 4, 6 and 10 yards (3.6, 5.5 and 9.1 metres) depth was accompanied by plankton quantities 16, 4, 105, at corresponding depths.

The Time Factor in Phytoplankton Quantity

From the preceding description and from the figures, it is apparent that even at the same time of the year and with similar chlorinities the phytoplankton quantity may show great variations. At the stations adjacent to the Fraser River illustrated in Fig. 20, 22, 24, the maximal plankton quantity occurs at chlorinities between 12.0 and 14.0 gm. Cl in each case. As the distance from the river increases the depth of the phytoplankton maximum increases and there is also an increase in the total phytoplankton quantity. The distance of the river's effect from its mouth, the depth to which mixing has extended and the amount of phytoplankton growth in a mixing area show parallel increases which are dependent upon the time factor. Also the most abundant surface phytoplankton is found at the most distant areas of complete mixing (Chart 4). The time factor is difficult to determine and consequently no quantitative data can be given at present. The nature of the diatom growth curve would enter into the equation. The general evidence points to the importance of the time factor and experimentation in this field should yield interesting results.

Acknowledgment

The writers wish to express their appreciation of the facilities provided by the Biological Board of Canada at the Pacific Biological Station, and by the University of British Columbia.

References

1. Anderson, F. Tide Tables, Pacific Coast of Canada, Dept. Marine and Fisheries. 1926–1930.
2. British Columbia Pilot, v. 1. Hydrographic Dept., Admiralty, London. 1923.
3. Cameron, A. T. and Mounce, I. Some physical and chemical factors influencing the distribution of marine flora and fauna in the Strait of Georgia. Contr. Can. Biol. n.s. 1: 41-70. 1922.
4. Campbell, M. H. A preliminary quantitative study of the zoöplankton in the Strait of Georgia. Trans. Roy. Soc. Can. 23, III: 1-28. 1929.
5. Clemens, W. A. Suggestions as to the standardization of plankton methods. Proc. Third Pac. Sci. Congress, Tokyo, 183-184. 1928.
6. Clemens, W. A. and Williamson, H. C. Migrations of Pacific salmon. Proc. Fourth Pac. Sci. Congress, Java, 3: 453-458. 1929.
7. Fraser, C. M. Temperature and specific gravity variations in the surface waters of Departure Bay, B.C. Contr. Can. Biol., 1918-1920: 35-48. 1921.
8. Gran, H. H. and Thompson, T. G. The diatoms and physical and chemical conditions of the sea water of the San Juan Archipelago. Publ. Puget Sound Biol. Sta. 7: 169-204. 1930.
9. Hutchinson, A. H. A bio-hydrographical investigation of the sea adjacent to the Fraser River mouth. Trans. Roy. Soc. Can. 22, V: 293-310. 1928.
10. Hutchinson, A. H., Lucas, C. C. and McPhail, M. Seasonal variations in the chemical and physical properties of the waters of the Strait of Georgia in relation to phytoplankton. Trans. Roy. Soc. Can. 23, V: 177-188. 1929.

11. JOHNSTON, W. A. Sedimentation of the Fraser River delta. Geol. Survey of Canada, Memoir, 125. 1921.
12. LUCAS, C. C. Further oceanographic studies of the sea adjacent to the Fraser River mouth. Trans. Roy. Soc. Can. 23, V: 29-68. 1929.
13. LUCAS, C. C. and HUTCHINSON, A. H. A bio-hydrographical investigation of the sea adjacent to the Fraser River mouth. Trans. Roy. Soc. Can. 21, V: 485-520. 1927.
14. THOMPSON, T. G. The standardization of silver nitrate solution used in chemical studies of sea water. J. Am. Chem. Soc. 50: 681-685. 1928.
15. THOMPSON, T. G., MILLER, R. C., HITCHINGS, G. H. and TODD, S. P. Studies of the sea water near the Puget Sound Biological Station during the summer 1927. Publ. Puget Sound Biol. Sta. 7: 65-100. 1929.
16. THOMPSON, T. G. and VAN CLEVE, R. Determination of the chlorinity of ocean waters. Report, International Fisheries Com. 3: 1-14. 1930.
17. THOMPSON, T. G. and WRIGHT, C. C. Ionic ratios of the waters of the north Pacific ocean. J. Am. Chem. Soc. 52: 915-920. 1930.
18. WEBB, C. E. Water Resources Paper No. 51. Surface water supply of Canada; Pacific Drainage; British Columbia and Yukon territory, climatic year 1924-1925. Dept. of Interior, Canada. 1927.
19. WILLIAMSON, H. C. Contr. Can. Biol. and Fisheries, n.s. 3: 265-306. 1927.
20. WILLIAMSON, H. C. Contr. Can. Biol. and Fisheries, n.s. 4: 453-470. 1929.